Investigations on whole cell biocatalysts with application in beverage production and aroma composition

Dissertation
zur Erlangung des Doktorgrades
der Naturwissenschaften

vorgelegt beim Fachbereich 08 – Biologie und Chemie
der Justus-Liebig-Universität
in Gießen

von
Felix Marcel Rainer Graf
aus Kelkheim / Ts.

Frankfurt am Main (2023)

Vom Fachbereich 08 – Biologie und Chemie der Justus-Liebig-Universität als Dissertation angenommen.

Dekan:

Prof. Dr. Thomas Wilke

Justus-Liebig-Universität Gießen, Abteilung für Tierökologie und Systematik

Gutachter:

Prof. Dr. Holger Zorn

Justus-Liebig-Universität Gießen

Institut für Lebensmittelchemie und Lebensmittelbiotechnologie

Prof. Dr.-Ing. Dirk Holtmann

Karlsruher Institut für Technologie

Institut für Bio- und Lebensmitteltechnik

Parts of this work are published in scientific journals:

Graf, F.M.R.; Buchhaupt, M.: Comparative Investigations on Different *β*-Glycosidase Surrogate Substrates. Fermentation 2022, 8, 83. https://doi.org/10.3390/fermentation8020083

Graf, F.M.R., Weber, H. E., Buchhaupt, M.: Investigation of non-*Saccharomyces* Yeasts With Intracellular *β*-Glycosidase Activity for Wine Aroma Modification. Journal of Food Science 2022, 87, 4868– 4877. https://doi.org/10.1111/1750-3841.16355

Graf, F.M.R., Buchhaupt, M.: Engineering Volatile Thiol Formation in Yeast. Journal of Applied Microbiology 2022; lxac078, https://doi.org/10.1093/jambio/lxac078

Acknowledgements

The practical part of this thesis was conducted at the DECHEMA Research Institute in the working group microbial biotechnology between January 2018 and December 2021. I would like to express my sincere gratitude for the funding provided by the State of Hesse within the LOEWE project AROMAplus.

I would also like to thank

Dr. Markus Buchhaupt for his trust in me and for providing me with the topic, although I had not been working in the laboratory for quite a long time. Despite the special circumstances during our collaboration, we were always able to maintain a constructive working relationship. The results described could only be achieved through our fruitful collaboration.

Prof. Dr. Holger Zorn for taking over the initial review and for his valuable input during our project meetings.

Prof. Dr.-Ing. Dirk Holtmann for his spontaneous commitment as second reviewer and his conscientious interaction with his colleagues.

All remaining and former members of the microbial biotechnology working group. The fewer we became, the more we grew together.

Dr. Hendrik Schewe for his help at all times of the day and his support with the analytics.

All employees of the DECHEMA research institute, regardless of their professional assignment, for the friendly working atmosphere. I would especially like to mention the members of the DECHEMA band, with whom I was able to spend many great hours, even though it sometimes took me quite an effort.

My family and especially my parents, who encouraged me and made it possible for me to go down that road.

My friends, who provided the necessary compensation for long lab days with devotion.

And Lisa, who has had my back at all times during the past years.

This work is dedicated to my two nephews, whom I was sadly never able to hold in my arms.

1 Table of Contents

1.1 List of Abbreviations

3MH	3-Mercaptohexanol
3MHA	3-Mercaptohexanyl acetate
4MMP	4-Mercapto-4-methylpentan-2-one
4-MUG	4-Methylumbelliferyl-*β*-D-Glucopyranoside
Aesculin (Esculin)	6-O-(-D-Glucosyl)aesculetin
AU	Arbitrary unit
Arbutin	Hydroquinon-*β*-D-glucopyranosid
BCA	Bicinchoninic acid
BLAST	Basic Local Alignment Search Tool
Cys-3MH	3-Mercaptohexanol-cysteine conjugate
ddH_2O	Double-distilled water
DMSO	Dimethyl sulfoxide
DTNB	5,5-Dithio-bis-(2-nitrobenzoic acid)
GC-MS	Gas chromatography mass spectrometry
G418	Geneticin
Glut-3MH	3-Mercaptohexanol-glutathione conjugate
GST	Glutathione-*S*-transferase
HGU	Hochschule Geisenheim University
ITS	Internal transcribed spacer
KanMX	Kanamycin A selection marker
L	Liter
NCBI	National Center for Biotechnology Information
NEB	New England Biolabs
NIST	National Institute of Standards and Technology

PDMS	Polydimethylsiloxan-Sorbens
pNPG	4-Nitrophenyl-*β*-D-glucopyranoside
SC-medium	Synthetic complete medium
SCD-Medium	Synthetic complete dextrose medium
SIM	Selected Ion Monitoring
SMC	S-Methyl- L-cysteine
SMC-medium	S-Methyl-L-cysteine medium
TNB^{2-}	Ionized dianion of DTNB
YPD	Yeast extract Peptone Dextrose
YPD-Medium	Yeast extract Peptone Dextrose Medium

1.2 List of Figures

1.3 List of Tables

2 Abstract

In the presented work, investigations of enzyme activities related to the processing of fruits, especially grapes, and the release of aroma-relevant molecules from musts during fermentation are described. For this purpose, among other investigations, a library of more than 2000 yeasts isolated at Hochschule Geisenheim University was screened with respect to their *β*-glycosidase, pectinase, peptidase and *β*-lyase activities. Co-fermentation of yeasts with high activities of the mentioned enzyme classes is an attractive alternative to the application of enzyme preparations in winemaking.

While no relevant pectinase activities were detected in the isolates studied, high peptidase activities were identified for some *Metschnikowia pulcherrima* isolates, resulting in greater decreases in the protein signal of musts compared to a selected commercial preparation of the same species.

To test organisms for the presence of *β*-glycosidase activities and to be able to characterize this enzyme activity, four different surrogate substrates are currently mainly used. In another part of the present work, the properties and applicability of these compounds (arbutin, esculin, pNPG and 4-MUG) are compared and the advantages and disadvantages of their use are discussed. All four substrates were found to be suitable for photometric assays. 4-MUG was found to be the most suitable for the intended work due to its high sensitivity, high robustness and ease of use. A direct comparison of these compounds has not been described to date and will facilitate selection for screening approaches and other applications. In addition, the study of the accumulation of the product of hydrolysis of 4-MUG is described, which may provide indications to the localization of *β*-glycosidases.

Following the identification of 4-MUG as the most suitable surrogate substrate, the aforementioned strain library was assayed for *β*-glycosidase activity. The activity in the supernatant and after cell disruption, as well as the activity of whole cultures at pH 7 and pH 3 were evaluated. Several cell lysates showed high activity, which strongly decreased under wine-typical conditions. Similar results were obtained for the activity in supernatants, with only one strain of the species *Rhodotorula mucolaginosa*, already known for *β*-glycosidase activity, showing high activity at low pH values.

Currently, most of the known *β*-glycosidases identified with the above mentioned surrogate substrates are secreted enzymes. These enzymes are easy to find and characterize, but intracellular enzymes with interesting properties may have been previously overlooked. By studying yeasts with cell-associated *β*-glycosidase activity, the use of whole cells as flavor-enhancing catalysts in winemaking or the processing of other fruit juices should be further established as an alternative to the addition of enzyme preparations, which is currently the

predominant practice. Such an approach using whole cells could not only have the advantage of protecting the enzymes against low pH values, but could also lead to different selectivity profiles, as substrate and product transport through the cell membrane is required and whole cells may additionally influence the final flavor composition. The screening identified four yeast strains whose whole cells showed high *β*-glycosidase activity even at low pH values. Subsequent comparative analyses of the aroma composition in the headspace of assays with whole cells and cell lysates after combination with glycoside extracts indicated a specific influence of intact cells on the released aroma compounds. The highest *β*-glycosidase activity in must was measured in the experiments with a strain of the species *Nakazawaea ishiwadae*.

Another part of the work presented deals with volatile thiols, which are potent flavor and fragrance compounds found in many fruits and can impart tropical aroma sensations such as passion fruit, guava or blackcurrant. Since these thiols are also characteristic for some wine varieties such as Sauvignon Blanc, their biosynthetic pathways were intensively researched and strategies have been developed to increase their concentrations in winemaking. These include the use of yeast strains with a pronounced ability to release thiols from precursors present in the must. A key enzyme activity for this release, among other enzymes and transporters, is the yeasts' *β*-lyase activity encoded, for example, by the *IRC7* gene. In this context, the compound SMC has been described as a *β*-lyase surrogate substrate that can be used to evaluate the thiol-releasing ability of certain microorganisms, since SMC cleavage is the only way for the cell to assimilate nitrogen. In the presented work, SMC was used as a screening tool to identify yeasts with potentially high thiol-releasing ability. In addition, the use of SMC as a tool for targeted evolutionary approaches aimed at introducing high thiol-releasing activity into microorganisms is demonstrated.

SMC-based growth screening and subsequent testing identified two strains of the species *Pichia kudriavzevii* and *Wickerhamomyces anomalus* with promising thiol-release properties. Furthermore, the directed evolution approach resulted in mutants of four different yeast strains with improved growth in SMC medium. The experiments described could enable the application of an adaptive evolutionary approach to improve thiol release from natural precursors in non-*Saccharomyces* yeasts and established yeast strains for wine and beer production, which could have very broad applications.

Furthermore, in the work described, a thiol synthesis pathway comprising the corresponding plant and the yeast enzymes was introduced into a laboratory yeast strain, optimized for higher productivity, and characterized in terms of the biosynthetic diversity. In addition to genome integration of the *Escherichia coli* gene *tnaA*, which encodes an enzyme with high *β*-lyase activity, a glutathione synthetase and glutathione-*S*-transferases were overexpressed. Up to 8.9 µg L^{-1} 3-mercaptohexan-1-ol could be formed with the strain from externally added

(E)-2-hexen-1-ol. Well-characterized thiols such as 2-methyl-2-butanthiol, 3-mercapto-3-methylbutan-1-ol, and 8-mercapto-*p*-menthan-3-one could be formed by feeding the yeast cells with the corresponding alcohol, alkenol, aldehyde or ketone precursors. In addition, several previously undescribed thiol compounds could be synthesized. This concept allows the discovery of thiols with interesting odor properties and could be optimized for a biotechnological production process in the future. Furthermore, the selectivity of yeast- and wine-based glutathione-*S*-transferases for specific substrates can be analyzed using the described system.

2.1 Zusammenfassung

In der vorliegenden Arbeit werden Untersuchungen von Enzymaktivitäten beschrieben, die im Zusammenhang mit der Verarbeitung von Früchten, insbesondere von Trauben, und der Freisetzung von aromarelevanten Molekülen aus Mosten während der Fermentation stehen. Hierfür wurde unter anderem eine Bibliothek von über 2000 Hefen, die an der Hochschule Geisenheim isoliert wurden, in Hinblick auf ihre *β*-Glykosidase-, Pektinase-, Peptidase- und *β*-Lyase-Aktivitäten durchmustert. Die Co-Fermentation von Hefen mit hohen Aktivitäten der genannten Enzymklassen ist eine attraktive Alternative zur Anwendung von Enzympräparaten in der Weinherstellung.

Während bei den untersuchten Isolaten keine relevanten Pektinase-Aktivitäten festgestellt werden konnten, wurden für einige *Metschnikowia pulcherrima* Isolate Peptidase-Aktivitäten identifiziert, die in Vergleichsversuchen in Most stärker ausgeprägt waren als die Peptidase-Aktivitäten von einem ausgewählten kommerziellen Präparat der gleichen Spezies.

Um Organismen auf das Vorhandensein von *β*-Glykosidase-Aktivitäten zu testen und diese Enzymaktivität charakterisieren zu können, werden zur Zeit hauptsächlich vier verschiedene Surrogatsubstrate verwendet. In einem weiteren Teil der vorliegenden Arbeit werden die Eigenschaften und die Anwendbarkeit dieser Verbindungen (Arbutin, Esculin, pNPG und 4-MUG) verglichen und die Vor- und Nachteile bei der Verwendung diskutiert. Alle vier Substrate wurden als geeignet für photometrische Tests befunden. 4-MUG stellte sich aufgrund der hohen Empfindlichkeit, der hohen Robustheit und der einfachen Anwendung als am besten für die angestrebten Arbeiten geeignet heraus. Ein direkter Vergleich dieser Substanzen ist bislang nicht beschrieben und wird die Auswahl für Screening-Ansätze und andere Anwendungen in Zukunft erleichtern. Darüber hinaus wird die Untersuchung der Akkumulation des Produktes der Hydrolyse von 4-MUG beschrieben, die Hinweise auf die Lokalisierung der untersuchten *β*-Glykosidasen geben könnte.

Im Anschluss an die Identifizierung von 4-MUG als das am besten geeignete Surrogat-Substrat wurde die genannte Stammbibliothek mit Hinblick auf *β*-Glykosidase-Aktivität untersucht. Hierbei wurde die Aktivität im Überstand und nach dem Zellaufschluss, sowie die Aktivität von intakten Zellen bei pH 7 und pH 3 bewertet. Mehrere Zelllysate zeigten eine hohe Aktivität, die jedoch unter weintypischen Bedingungen stark abnahm. Ähnliche Ergebnisse ergaben sich für die Aktivität in den Überständen, wobei nur ein Stamm der Art *Rhodotorula mucolaginosa*, die bereits für *β*-Glykosidase-Aktivität bekannt ist, eine hohe Aktivität bei niedrigen pH Werten aufwies.

Zur Zeit handelt es sich bei den meisten bekannten *β*-Glykosidasen, die mit den oben genannten Surrogatsubstraten identifiziert wurden, um sekretierte Enzyme.

Diese Enzyme sind leicht zu finden und zu charakterisieren, aber intrazelluläre Enzyme mit interessanten Eigenschaften könnten bisher übersehen worden sein. Durch die Untersuchung von Hefen mit zellassoziierter *β*-Glykosidase-Aktivität soll die Verwendung ganzer Zellen als aromaverbessernde Katalysatoren bei der Weinherstellung oder der Verarbeitung anderer Fruchtsäfte im Vergleich zur derzeit vorwiegend praktizierten Zugabe von Enzympräparaten stärker etabliert werden. Ein solcher Ansatz mit ganzen Zellen könnte nicht nur den Vorteil des Schutzes der Enzyme gegen niedrige pH-Werte haben, sondern auch zu unterschiedlichen Selektivitätsprofilen führen, da der Substrat- und Produkttransport durch die Zellmembran erforderlich ist und ganze Zellen die endgültige Aromazusammensetzung zusätzlich beeinflussen können. Bei der durchgeführten Durchmusterung konnten vier Hefestämme identifiziert werden, deren ganze Zellen auch bei niedrigen pH-Werten eine hohe *β*-Glykosidase-Aktivität zeigten. Anschließende vergleichende Analysen der Aromazusammensetzung im Kopfraum von Assays mit ganzen Zellen und Zelllysaten nach der Kombination mit Glykosidextrakten deuten auf einen spezifischen Einfluss intakter Zellen auf die freigesetzten Aromastoffe hin. Die höchste *β*-Glykosidase-Aktivität in Most wurde bei einem Stamm der Art *Nakazawaea ishiwadae* identifiziert.

Ein weiterer Teil der vorgestellten Arbeit befasst sich mit flüchtigen Thiolen, die als potente Geschmacks- und Duftstoffe in vielen Früchten vorkommen und tropische Aromeneindrücke wie Passionsfrucht, Guave, oder schwarze Johannisbeere vermitteln können. Da diese Thiole auch für einige Weinsorten wie Sauvignon Blanc charakteristisch sind, werden ihre Biosynthesewege intensiv erforscht und Strategien zur Steigerung ihrer Konzentrationen bei der Weinherstellung entwickelt. Dazu gehört die Verwendung von Hefestämmen mit ausgeprägter Fähigkeit zur Freisetzung von Thiolen aus im Most vorhandenen Vorstufen. Eine wesentliche Enzymaktivität für diese Freisetzung ist neben anderen Enzymen und Transportern die zum Beispiel vom *IRC7*-Gen kodierte *β*-Lyase-Aktivität der Hefen. Die Verbindung SMC wurde in diesem Zusammenhang als *β*-Lyase-Surrogatsubstrat beschrieben, das zur Einschätzung der Thiol-Freisetzungsfähigkeit bestimmter Mikroorganismen verwendet werden kann, da die SMC-Spaltung für die Zelle die einzige Möglichkeit ist Stickstoff zu assimilieren. In der vorliegenden Arbeit wird diese Verwendung von SMC als Screening-Tool zur Identifizierung von Hefen mit potenziell hoher Thiol-Freisetzungsfähigkeit genutzt. Darüber hinaus wird die Verwendung von SMC als Werkzeug für gezielte Evolutionsansätze demonstriert, die auf die Einführung einer hohen Thiol-Freisetzungsaktivität in Mikroorganismen abzielen.

Im Rahmen eines SMC-basierten Wachstumsscreenings und anschließender Tests wurden zwei Stämme der Arten *Pichia kudriavzevii* und *Wickerhamomyces anomalus* mit vielversprechenden Eigenschaften zur Thiol-Freisetzung identifiziert.

Ein Ansatz der gerichteten Evolution führte darüber hinaus zu Mutanten von vier verschiedenen Hefestämmen mit verbessertem Wachstum in SMC-Medium. Die beschriebenen Experimente könnten die Anwendung eines adaptiven evolutiven Ansatzes zur Verbesserung der Thiol-Freisetzung aus natürlichen Vorläufern in nicht-*Saccharomyces*-Hefen und etablierten Hefestämmen für die Wein- und Bierproduktion mit sehr breiter Anwendung ermöglichen.

Darüber hinaus wurde in den beschriebenen Arbeiten ein Thiol-Syntheseweg, der die entsprechenden Pflanzen- und Hefeenzyme umfasst, in einen Laborhefestamm eingebracht, im Hinblick auf eine höhere Produktivität optimiert und hinsichtlich seiner biosynthetischen Vielfalt charakterisiert. Neben der Genomintegration des *Escherichia coli* Gens *tnaA*, das für ein Enzym mit hoher *β*-Lyase-Aktivität kodiert, wurden eine Glutathionsynthetase und Glutathion-*S*-Transferasen überexprimiert. Bis zu 8,9 µg L^{-1} 3-Mercaptohexan-1-ol konnte mit dem Stamm aus extern zugegebenem *(E)*-2-Hexen-1-ol synthetisiert werden. Zudem konnten gut charakterisierte Thiole wie 2-Methyl-2-butanthiol, 3-Mercapto-3-methylbutan-1-ol und 8-Mercapto-*p*-menthan-3-on durch Fütterung der Hefezellen mit den entsprechenden Alkohol-, Alkenol-, Aldehyd- oder Ketonvorläufern gebildet werden. Darüber hinaus konnten mehrere bisher unbeschriebene Thiolverbindungen synthetisiert werden. Dieses Konzept ermöglicht die Entdeckung von Thiolen mit interessanten Geruchseigenschaften und könnte in Zukunft für einen biotechnologischen Produktionsprozess optimiert werden. Darüber hinaus kann mit dem beschriebenen System die Selektivität von Hefe- und Wein-basierten Glutathion-*S*-Transferasen für bestimmte Substrate analysiert werden.

3 Introduction

Wine is a complex mixture of many components that influence the appearance, aroma, taste and mouthfeel. The main sources of these components are the grapes, the microorganisms present during fermentation and the wood (mainly oak) if the wine is aged in wooden barrels. The term flavor describes both effects of odor and taste. The aroma of wine is mainly associated with the volatile components perceived through the olfactory system while the bouquet is caused by more complex, non-volatile flavor compounds.[1] Grape-derived components in the must lead to varietal distinction and cause the basic wine structure typical for each grape variety, while the acids and tannins from the grape, together with ethanol and glycerol, contribute to the mouthfeel of the wine.

The usage of specific enzyme activities in winemaking has increased greatly in recent times. The treatment of grapes, musts and wines takes place to improve wine clarification and filtration, but also to improve juice yield, color and aroma.[2] An alternative to the use of enzyme preparations could be the inoculation with indigenous starter yeasts which produce these enzymes naturally during fermentation.[3]

The aroma components present in wine are either directly present in the grapes or emerge during the wine-making process. In order to better categorize them, they are divided into classes. The class of varietal aroma compounds is responsible for the primary aroma, which includes the odorless components that are converted into volatile aroma components during wine production. The class of prefermentation aromas are formed between harvest and fermentation by processes triggered, for example, by the destruction of the berries during transport (primary aroma). Fermentation aromas (secondary aroma), such as ethyl esters, are secondary products of microorganisms that are present during fermentation and contribute, for example, to the fruity impressions of wine. Postfermentation aromas (tertiary aroma) are formed during aging and contribute to the complexity of the wine.[4,5] In this context, the aroma compounds discussed among other aspects in this thesis are classified as varietal aroma compounds or primary aroma, since they result from the cleavage of odorless precursors already existing at the time when fermentation begins.

In order to meet the demands of consumers, the production of wines with defined characteristics is becoming increasingly important. To be able to modulate the great variety of aromas in wines accordingly, it is important to understand the synergies between different grape varieties and aroma-modifying yeast strains. The usage of this knowledge can result in tailored wines that appeal to specific customer groups[6] and corresponding studies may open

up opportunities for yeast starter strains that can significantly alter the aroma of wines[7] by releasing certain aroma compounds at specific concentrations.[8]

While some of the aroma compounds are derived from the metabolism of the microorganisms involved in the fermentation process, many grape-derived components are also modified by microorganisms. Thus, fermentation with yeasts not only causes the conversion of sugar to ethanol, but also releases a variety of sensory important volatile metabolites that cause the significant increase in flavor complexity between must and wine.[9] During these processes, 95 % of the initial sugar concentration of 22-24 % sugar is converted to ethanol while 1 % is converted to cellular material and the remaining 4 % to other end products during model fermentations.[1] This is the reason why wine in general has more aroma than the musts from which it is produced.

As described, yeasts are responsible for the conversion of sugars into alcohol and other by-products during wine production. Yeasts are unicellular microorganisms which belong to the fungi kingdom. Compared to bacteria, yeasts are larger and have an oval or elliptical cell shape. Yeasts are also traditionally used for many other processes in the food industry, such as baking for a long time.

It has also become increasingly clear that wine fermentation is not only dependent on yeast of the species *Saccharomyces cerevisiae*, but also on a variety of other wine yeasts that enter the fermentation process from both the grapes and the wine environment. Although grape musts contain all the necessary nutrients for cell growth, only specialized strains can establish during fermentation because of the high sugar content and low pH values. Nevertheless, a variety of different microorganisms can survive during spontaneous fermentation. Since they naturally occur in the described habitats, they are described as autochthonous microorganisms.

3.1 Autochthonous microorganisms in winemaking

Although *S. cerevisiae* is the predominant species in fermentations, the process of wine production is not sterile.[4] The yeasts that occur in spontaneous wine fermentations can be divided into two general groups. The *Saccharomyces* yeasts, which consist partly of *S. cerevisiae*, and the non-*Saccharomyces* yeasts, which include members of the genera *Candida, Pichia, Rhodotorula, Debaromyces, Metschnikowia, Hansenula*, and *Hanseniaspora*.[1] The microflora of grapes initially consists mainly of low alcohol tolerant strains, while *S. cerevisiae* is present only in small numbers.[1] For example, two *Saccharomyces* and 10 non-*Saccharomyces* strains were detected in spontaneous fermentations, with non-*Saccharomyces* yeasts accounting for 30 % of the identified isolates.[10]

While non-*Saccharomyces* yeasts dominate the early stages of fermentation, their growth is often limited to the first days of fermentation due to the increasing ethanol content. Subsequently, *S. cerevisiae* dominates growth until the end of fermentation.[11] The application of antioxidants and anaerobic conditions during fermentation leads to further selection of the wine microbiome.[9] Although the populations of non-*Saccharomyces* yeasts are no longer detectable at the end of vinification, the majority of their secreted enzymes is present until the end of this process.[12]

Although non-*Saccharomyces* yeasts were long considered a contaminant and fermentations were carried out using only *Saccharomyces* yeasts,[13] it has become increasingly apparent that these yeasts can also have many beneficial influences on the resulting wine[14] by increasing the complexity in mixed fermentations.[15,16]

For example, *Metschnikowia pulcherrima* was found to contribute to a decrease in final ethanol concentration,[17] while *Hanseniaspora vineae* led to an increase in fruity aromas.[18] In addition, after co-fermentation with *Torulaspora delbrueckii*, increased amounts of esters were observed,[19] while *Lachancea thermotolerans* led to an increase in acidity.[20] This increase in acid concentration, for example, is particularly interesting in terms of climate change, as the increasing temperatures lead to higher alcohol contents and lower acid concentrations. In general, it can be stated that non-*Saccharomyces* yeasts help to obtain "fresher" wines after fermentation.[21]

The positive influence of non-*Saccharomyces* yeasts is often due to hydrolytic extracellular enzymes,[22] which interact with must components and can thus have a major impact on the properties of the fermented wine.[23] Non-*Saccharomyces* yeasts can directly cause the release of aromatic substances typical of varietal must, such as aromatic glycosylated precursors and thiols conjugated to cysteine and glutathione, through the activity of these enzymes. In addition, many other extracellular enzyme activities with technological advantages, such as pectinases or enzymes with proteolytic activities, have recently become interesting for winegrowers. The corresponding enzyme activities have been found, for example, in the genera *Kloeckera, Candida, Debaryomyces, Rhodotorula, Pichia, Wickerhamomyces, Zygosaccharomyces, Hanseniaspora, Kluyveromyces* and *Metschnikowia*.[24]

Because non-*Saccharomyces* yeasts often have low fermentative power, sequential or mixed use with *S. cerevisiae* is usually necessary for complete fermentation.[21] It is believed that co-fermentation of non-*Saccharomyces* strains together with *S. cerevisiae* in these cases even partially results in yeast-yeast interactions that lead to further changes of the aroma profile[25] which can lead to masking or suppression of negative properties caused by non-*Saccharomyces* yeasts.[26]

However, when using non-*Saccharomyces* yeasts, these possible negative impairments such as the increase in volatile acidity or the increase of unintended sulfur components and fusel alcohol aromas[27] should be taken into account. For this reason, the microorganisms used have to be carefully selected.

However, the use of non-*Saccharomyces* yeasts is a useful extension of the methods for improving the production processes in wine making and for increasing the varietal aromas during fermentation. Since the described enzyme activities of oenological relevance (like *β*-glycosidases, *β*-lyases, pectinases and peptidases)[3] can vary greatly not only between different species but also between individual strains of a species,[12,28] it is necessary to screen high numbers of organisms to identify those with interesting properties. In order to find organisms that are also adapted to the harsh environmental conditions during fermentation, it makes sense to screen autochthonous microorganisms, since they have their natural habitat on grapes or in wine fermentations and may be added to the fermentation process without further labeling requirements. For scientific studies, the microorganisms are isolated, for example, from spontaneous fermentations or from the surface of the grapes. In contrast to filamentous fungi, yeasts with beneficial enzymatic endowment, could be used directly as starter cultures, obviating the application of enzyme preparations.[29]

The basis of the presented screening approaches is a library of the described autochthonous microorganisms. On one hand, these organisms were isolated from crushed grapes of the 2018 vintage as part of a related subproject at the Hochschule Geisenheim University (HGU). On the other hand, parts of the microorganisms originate from the strain collection of the HGU and were isolated from grape berries and from fermentations in previous projects. After exclusion of obvious isolates of the yeast-like fungus *Aureobasidium pullulans*, a total of 2112 isolates could be used in the screening for relevant enzyme activities. These enzyme activities are described in the following sections on the basis of their mechanism and significance for wine production.

3.2 Pectins

Pectins are polysaccharides and the main components of the middle lamella and primary cell wall of higher plants. They play a decisive role in the integrity of the cell wall.[23] As a central component of plant cells, pectins are found in many plant-based raw materials and influence their viscosity, the efficiency of extraction of liquid and raw material components and inhibit growth of desired microorganisms. For example, pectins lead to a reduction in the quality of paper, pulp and textile products.[30] During the pressing of fruits and therefore also in wine production, pectins pose a major challenge.

Pectins consist of long linear α-(1,4)-linked polymers of D-galacturonic acid, which can be methylated or actetylated (Figure 1).

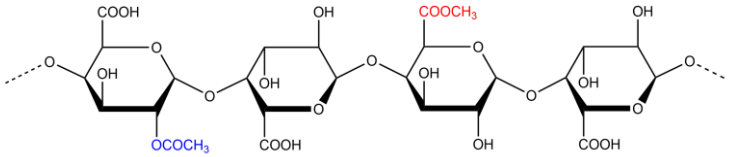

Figure 1: The basic chemical structure of pectins. Pectins are heterogeneous molecules consisting of "smooth" linear and "hairy" branched regions that are highly variable (not depicted). The linear regions consist of α-(1,4)-linked galacturonic acid residues that may be methylated (red) or acetylated (blue). Pectins show various degrees of branching and may contain various other carbohydrate residues.[31]

There are two types of pectins: Homogalacturonic pectins, consisting solely of D-galacturonic acid, and rhamnogalacturonic pectins, in which the galacturonic acid chains are interrupted by L-rhamnose residues joined together by an α-(1-2) bond, to which possible side chains consisting of sugars such as galactose and arabinose can be attached.[31–33] All side chains of neutral sugars are usually branched to rhamnose via 1,4-linkages and the D-galacturonic acid residues may be methylated.[34] Pectic substances have a high molecular weight and are negatively charged.[33]

3.2.1 Pectinases

Many enzyme activities are known that can degrade pectins. Pectinase is a generic name for this family of enzymes which is involved in the degradation of pectic substances.[35] Pectinases, also called pectolytic or pectic enzymes, belong to the family of polysaccharidases and degrade pectin by cleaving the linear and branched regions.

3.2.1.1 Pectinases in winemaking

The ability of pectinases to degrade the cell wall has been used for many years in the process of wine production and fruit juice pressing. Polygalacturonases, which catalyze the cleavage of the α-(1,4)-glycosidic bond between two non-methylated galacturonic acid residues are mainly used (Figure 2).[34]

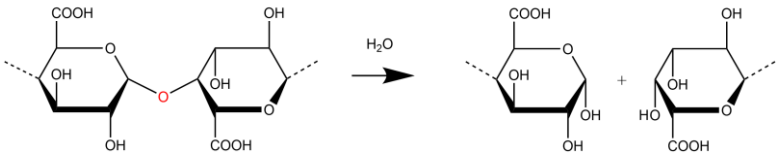

Figure 2: Mode of action of polygalacturonases. The cleavage of the α-(1,4)-glycosidic bond between two non-methylated galacturonic acid residues results in destruction of cell structures and reduces viscosity. Therefore, the juice yield and the extraction of aroma and flavor components is improved.

These enzymes thus help to improve the clarification and filterability processes and lead to higher release of color and flavor components.[36] The basic effect is the destruction of cell structures, as a result of which the substances can be better extracted from the pulp, the skin and from the peripheral zone of the grape skin. For example, the application of pectinases facilitates the diffusion of anthocyanins, tannins, and aroma molecules in the skins.[35] Commercial wineries also frequently apply pectinases to increase the yield of must. The commercial enzyme preparations also often have useful side activities such as glycosidases and petidases[35] and in most cases are derived from fungi such as *Aspergillus niger*.[37] However, fungal pectinases have several disadvantages. For example, impurities can occur in the form of undesired enzyme activities such as pectinesterases and enzymes derived from fungi are rarely active at low temperatures.[35,37]

3.2.1.2 Yeast pectinases

In addition to higher fungi, plants, and bacteria, pectinases are also synthesized by yeasts. These yeast enzymes are known to be active at a wide temperature range of 0-60 °C.[37] These "cold-active" enzymes allow fermentation at lower temperatures[35] reducing the growth of unwanted microorganisms (spoilage) and preserving sensory and nutritional properties.[30] In addition, yeasts often express only the desired type of pectinolytic enzymes, polygalacturonases,[38] and rarely exhibit unwanted side activities.

Yeasts synthesize pectolytic enzymes depending on their environment and genetic background.[37] These pectinolytic properties have been noted for example for the genera *Candida, Kluyveromyces, Rhodotorula*, and *Saccharomyces*.[39] Since it has been described that many *S. cerevisiae* strains have low pectinase activities,[40] high pectinase activities have only been detected for a few isolates.[41] For example, when 678 different species of yeast were examined, activity was detected in only a few,[42] while of 300 yeasts isolated from tropical fruits, only 7 % showed polygalacturonase activity.[32]

3.2.1.3 Genetic background of pectinases

Consequently, only a few genes coding for polygalacturonases have been characterized in yeasts. For example, *EPG1* and *EPG1-2* are known from *Kluyveromyces marxianus,*[43] while *S. cerevisiae* contains the gene *PGU1* (*PGL1*), which is also associated with galacturonase activity.[34] It has also been shown that polygalacturonase activity depends on the carbon source. Thus, the replacement of glucose with galactose, as well as the addition of pectins or their degradation products, resulted in higher enzyme activities.[44]

3.2.1.4 Further applications of pectinases

Pectins also lead to problems in the processing of plant raw materials other than grapes. For example, pectinases are also used during the extraction of vegetable oil,[45] for the removal of citrus fruit peels[33] and in paper production.[37] Because of this, about 25 % of the global market for food enzymes is related to microbial pectinases.[33] Thus, there is a great need for yeast strains that exhibit strong polygalacturonase activities.

3.3 Proteins

Typical protein concentrations in white wine are in the range of 10-500 mg L^{-1} [46,47] with proteins having molecular masses of 6 to 200 kDa (Figure 3 A).[48] Chitinases account for approximately 50 % of soluble proteins in ripe grapes,[49] while the exact protein composition depends on the type of grapevine and cultivation.[50] The proteins contained in wine play a major role in the haze formation of bottled wines (Figure 3 B) and are of great importance to the wine industry. Haze formation due to for example elevated temperatures after bottling[51] is caused by the precipitation of grape pathogenesis related proteins, which are mainly found in the grape pulp.[52] For this reason, pathological conditions during grapevine growth[53] and during grape transport and handling[54] have a great influence on the subsequent turbidity of the wine.

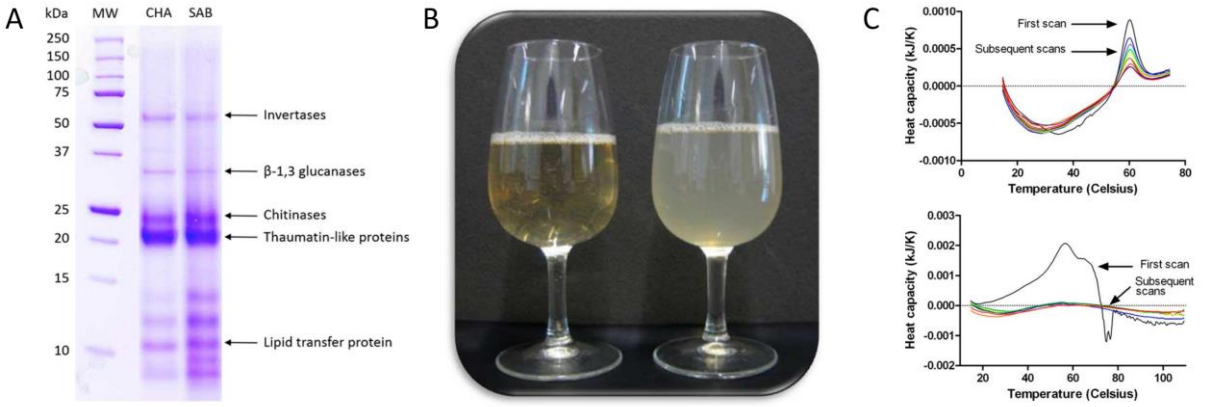

Figure 3: Wine proteins and haze formation during fermentation. A) Typical electrophoretic profiles of two unfined grape juices (CHA: Chardonnay, SAB: Sauvignon blanc) with protein band identities assigned by proteomic analysis, B) Clear white wine and turbid wine caused by protein aggregation, C) Repeated differential scanning calorimetry scans: Thaumatin-like protein C from Semillon juice showing a melting temperature of 61 °C and reversibility of thermal unfolding (upper side) and Chitinase F1 from Sauvignon blanc juice showing a melting temperature of 55 °C, no reversibility of thermal unfolding, and aggregation after unfolding (lower side). Reprinted with permission of [55] (Paragraph 7.5). Copyright 2023 American Chemical Society.

The proteins mainly involved in these processes are grape chitinases and thaumatin-like-proteins,[47] which are positively charged in wine. Due to a high number of disulphide bonds,[52]

these proteins are stable under wine conditions (despite the pH and processes like proteolysis) and remain in the wine after fermentation,[56] whereas the majority of other grape proteins precipitate or degrade during this process.[53] Chitinases and thaumatin-like proteins exhibit structural differences in the secondary structure,[57,58] in the mechanisms of denaturation and in aggregation. For example, the final step of chitinase aggregation is irreversible and denaturation occurs at comparatively low temperatures (Figure 3 C).[59] Since chitinases also exhibit significantly shorter half-lives at lower temperatures, this enzyme class is presumably mainly responsible for wine turbidity.[60]

This fact has already been demonstrated with the correlation between chitinase concentration and the severity of turbidity.[60] Although other proteins such as *β*-(1-3)-glucanases and the ripening-related protein Grip22p have also been identified as parts of protein turbidity,[61] their contribution to total turbidity is comparatively small.[62]

3.3.1 Wine turbidity

As described, proteins form insoluble aggregates over prolonged periods during the storage of white wines[63] that lead to wine turbidity.[60] Although this turbidity does not cause health risks[64] and does not significantly affect taste,[65] it is seen by consumers as a sign of poor quality[53] and is therefore negative for marketing. Protein instability in wine is thus one of the most widespread non-microbial defects of commercial wines[52] and causes major economic damage. In red wines, on the other hand, large parts of unstable proteins already react with the existing tannins during fermentation, which is why the problem of turbidity occurs rather rarely.[66]

The formation of turbidity by the different protein classes is also strongly influenced by many other wine components and conditions, such as pH value, the concentration of phenolic compounds and especially sulfate anions.[47,67] In this context, sulfates may be involved in the conversion of soluble aggregates into larger turbidity particles.[64] For this reason, the protein content and type of wine cannot necessarily be used to infer the risk of turbidity.[46]

3.3.1.1 Prevention of wine turbidity

To prevent haze formation, clarification of the wine with bentonite is often carried out before bottling to remove the proteins before storage. Although bentonite clarification is based on the electrical charge of the protein classes described, it is not specific to proteins and charged molecules. Therefore, important uncharged aroma components are also partly extracted at the same time.[53] In addition, further costs are arising, which is why more sustainable and gentle methods for preventing turbidity in wine are being sought.

Thus, other adsorbents for wine proteins have been investigated in the past. ZrO_2, for example, is able to bind unstable wine proteins[68] without a major impact on the sensory properties and can be easily regenerated.[69] The addition of natural zeolites, on the other hand, leads to

complete heat stability of the treated wine within three hours without significant influence on the aroma and the zeolites can be recycled in agriculture.[70]

Another way to minimize the general input of proteins into the fermentation process is to apply certain winemaking practices, such as preventing the grapes from extensive ripening in order to prevent high levels of proteins. In addition, the use of pectolytic enzymes with proteolytic side activities, the avoidance of maceration before fermentation, or the minimization of SO_2 levels can contribute to the reduction of turbidity in the finished wines.[71]

Another way of preventing visible haze in wines is stabilization by mannoproteins, which lead to less visible haze by reducing particle size.[63] Although the reduction of haze formation by certain mannoproteins from yeasts has already been described, the amounts secreted by yeasts during fermentation and storage are too small to make a significant difference.[72] However, the treatment of wine with mannoproteins from yeasts is approved by the Organization of Vine and Wine.[73]

Moreover, since the proteins responsible for turbidity are also responsible for protecting the plant from pathogens, the development of more resistant grape varieties poses a challenge by increasing the number of proteins potentially responsible for turbidity in wine.[53]

For this reason, additional possibilities to reduce the haze of the wines were investigated. One approach is based on the fact that the addition of polysaccharides such as chitin has been shown to strongly reduce haze,[74] as they bind to the chitinases, which are significantly involved in the processes responsible for haze. It has also been shown that the amounts of chitin in the cell walls of the organisms used and the reduction of turbidity correlated. It is likely that binding of the chitinases to the cell membrane occurs, thus contributing to the reduction of turbidity.[75]

All other methods of reducing proteins in wine, such as ultrafiltration, binding to flavonoids, and flash pasteurization, have adverse effects such as the loss of important organoleptic components, or are expensive and cumbersome to apply.[49,58]

3.3.1.2 Yeasts with high peptidase activity

In addition to the previously mentioned methods for stabilizing proteins in wine, enzymatic degradation of wine proteins has been discussed as a useful alternative for clarification. The use of peptidases can take place without the reduction in volume that occurs when bentonite or other adsorbents are used, and the aroma composition of the treated wines is rarely negatively affected.

Peptidases are divided into the four classes of serine endopeptidases, cysteine endopeptidases, aspartic endopeptidases and metalloendopeptidases on the basis of their catalytic mechanism. Each of these classes catalyzes the hydrolysis of specific peptide bonds

and has a characteristic composition of amino acids in the catalytic center.[76] The aspartic peptidases secreted by non-*Saccharomyces* yeasts consist of two symmetrical regions in the tertiary structure, which form the catalytic center with the aid of aspartic acid residues. Similar to other classes of peptidases, the enzyme activity of this class is pH dependent.[77] The most widely accepted mechanism for aspartic peptidases is illustrated in Figure 4.

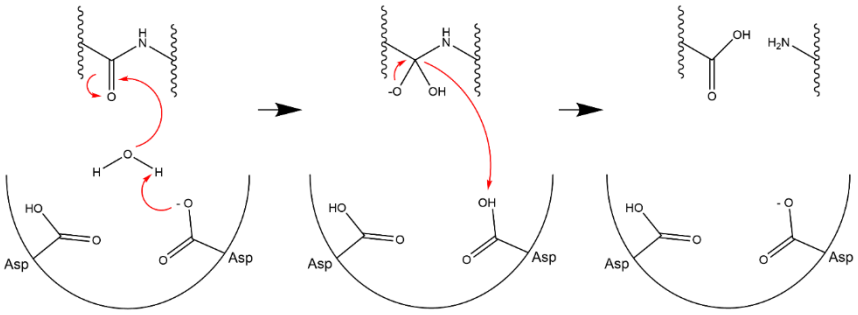

Figure 4: The most widely accepted mechanism for aspartic peptidases is an acid-base mechanism involving the coordination of a water molecule between two aspartate residues. Activation of the water molecule by abstraction of a proton by an aspartate residue enables the water to perform a nucleophilic attack. A tetrahedral oxyanion is generated, which is stabilized by hydrogen-bonding with the second aspartic acid. Hydrolysis of the peptide is caused by rearrangements of this intermediate.[78] (Illustration adapted[79])

Although it has been confirmed that peptidase A, an intracellular enzyme for the degradation of polypeptides and proteins, is released during autolysis of *S. cerevisiae,*[80] the influences of this peptidase are minor in the overall context. Sequential fermentation of yeasts with proteolytic properties eliminates the possible legal restrictions and purification prior to the addition of enzyme preparations, and a large effect can be achieved by initially using small amounts of cells.[81] Although the proteins responsible for cloudiness in wine are largely stable to yeast peptidases,[53] it may be possible to identify individual strains that enable the degradation of these proteins based on the variety of microorganisms that occur autochthonously on the surface of wine grapes. For example, *Hanseniaspora* strains have already been identified that could strongly influence protein levels in the final product.[82]

In addition of preventing turbidity in wine, the use of peptidases can have a further advantage in terms of the available nitrogen content in the must, thus preventing fermentation from stopping due to low nitrogen content.[83] The degradation of amino acids by yeasts also leads to esters, higher alcohols and volatile fatty acids, which play a major role in the aroma of the wine.[9]

Peptidases from *Aspergillus niger* and *Botrytis cinerea* have also been successfully used to reduce wine turbidity.[84,85] In addition, plant enzymes such as bromelain, in free and immobilized form, have been used to reduce wine haze potential by up to 70 %.[86]

3.4 Aroma glycosides

The presence of aroma glycosides is confirmed for many industrially processed fruits like apricot, peach, yellow plum, quince, sour cherry, passion fruit, kiwi, papaya, pineapple, mango, lulo, raspberry and strawberry[87] in concentrations from 2-8 fold[88,89] to their volatile counterparts. These glycosides are not directly accessible to the human aroma perception due to the high polarity (and thus low volatility) of the sugar residues and do not contribute to the aroma profile.[90] More than 200 compounds bound to glucose have also been identified in *Vitis vinifera*.[91] Studies with grape juices or vine grapes showed that aroma glycoside concentrations are two to ten times higher than the concentrations of the free aromatic molecules.[87,92] While in Riesling the bound aroma molecules were 3-5 times higher than the free aroma molecules,[88] 90 % of the monoterpenes, which dominate as aroma molecules, were found to be bound to glycosides in Muscat.[93,94] Thus, the largest proportion of odor-active compounds at the time of full ripeness of grapes is glycosidically bound,[95] with glycoside precursors occurring in absolute concentrations between 6.5 and 28 mg L^{-1} in grape juice.[96]

For example, alcohols, terpenes, C_{13}-norisoprenoids, volatile phenols, benzene derivatives, aromatic alcohols and acids are bound to glycosides in grapes.[97–99] Of these substances, terpene glycosides are among the most important for the aroma of wine and are described, for example, in Muscat, Gewürztraminer, Riesling, or Sauvignon Blanc.[100] Precursors of linalool, nerol, and geraniol are found primarily in these grape varieties.[101,102] Conversions of glycoside precursors and the release of terpenes result in wines that exhibit floral, spicy, and sweet characteristics.[96]

3.4.1 Monoterpenes

The above-mentioned terpenes essentially consist of two isoprene units, whose synthesis takes place via the mevalonate pathway or the 1-deoxy-D-xylulose-5-phosphate pathway. According to current knowledge, the synthesis of terpenes in the plastids of grapes takes place via the 1-deoxy-D-xylulose-5-phosphate pathway.[103] Starting from geranyl diphosphate, various terpenes are subsequently formed via different mechanisms. Due to the reactivity of the terpenes caused by their hydroxy-groups and double bonds, further reactions and isomerizations often occur.[104]

Terpenoid compounds play a central role in wine. At least 70 different monoterpene components are known, while linalool, geraniol, nerol, α-terpineol and citronellol dominate.[105] Those structures show perception thresholds between 100 and 400 µg L^{-1} in wine.[105] However, some terpenes also have significantly lower odor thresholds, such as citronellol with 15 µg L^{-1}.[97] Terpenes also frequently occur as monoterpene ethyl esters and acetates.

The composition of the monoterpene compounds of wines is very characteristic. For this reason, wine varities have been classified on the basis of gas chromatographic analysis of so called "fingerprint patterns".[106] The amounts of free terpenes used for this purpose are also reflected in the concentrations of the glycosylated precursors.[97]

3.4.2 Glycosidically bound aroma compounds

As described, large parts of the aroma components present in wine, such as the terpenes, are covalently bound to *β*-D-glucopyranose. Depending on the grape variety, two sugar molecules may also be bound to the substances and diglycosides such as arabinofuranosyl glycosides, rutinosides, or apiofuranosyl glycosides may be present.[97] In the distribution of glycoside residues of the most aromatic aglycones, apiosyl glycosides are the most represented with 50 %, followed by rutinosides (6-13 %) and glucosides (4-9 %).[87] Thus, disaccharides represent the major part of the bound terpenes, while monoterpene *β*-D-glucosides occur only in relatively small amounts. Trisaccharides also occur rarely in wines.[107]

Studies of glycosidically bound aroma precursors in ripe grapes described the localization of large amounts of the precursors for Muscat, Cabernet Sauvignon and Tempranillo in the berry skin,[88] whereas they are evenly distributed in Riesling and Gewürztraminer.[108] The authors suggested that berry size is causal for this shift in the ratio towards the pulp. The site of synthesis of these substances has not been definitely determined.

The formation of glycosylated precursors can be influenced during grape ripening by environmental factors, microbial infestation,[88] and viticultural methods.[109] The transfer of glycosides into the must can also be significantly influenced by the mashing time.[108,110]

3.4.3 Cellular reasons for glycoside formation

Molecules like monoterpenes, which are increasingly formed during ripening, have to be accumulated by the plant. Due to their lipophilic character, however, these substances are toxic to the cells in higher concentrations, as they can destroy cell components of the plant, such as membrane structures. Due to the binding to sugars, the substances are easier to store and transport into the vacuole.[111] Thus, the formation of glycosides primarily serves to improve chemical solubility, stabilization, transport, storage, and also contributes to detoxification mechanisms.[91,112–116] The binding of the respective aglycones to the corresponding sugar residue via the anomeric C-atom of the *β*-D-glucose residue and the hydroxyl group of the respective monoterpene alcohol is mainly catalyzed by glycosyltransferases.[114]

As described, terpene-glycosides represent a great opportunity to enhance the aroma intensity of the products during the industrial processing of fruits. The hydrolysis of these molecules is either a result of acidic hydrolysis or an enzymatic process mainly catalyzed by *β*-glycosidases.

3.4.4 Acid catalyzed hydrolysis

Acid catalysis results in the release of the aglycones without catalysis by an enzyme at low pH values. Acid hydrolysis is strongly dependent on the pH value, temperature and structure of the aglycone.[113]

Moreover, due to the acid catalytic cleavage of aroma glycosides, which in some cases takes place slowly, the aroma profile of wines can change significantly during storage.[117] It has been shown that, in particular, tertiary alcohols such as linalool as well as linalool oxides and α-terpineol are more frequently cleaved from the sugar residue by acid hydrolysis compared to primary alcohols such as geraniol and nerol.[88,118]

A comparison of acid hydrolysis at pH 2.5 to enzymatic hydrolysis with the enzyme preparation AR2000 of synthetic glucosides showed in both cases an almost complete cleavage of the compounds of 85-91 %. However, acid hydrolysis results in strong rearrangements of the molecules,[97,107] whereas enzymatic hydrolysis preserves the native structure of the compounds.[107]

3.4.5 *β*-Glycosidases

As an alternative to acid-catalytic cleavage, the hydrolysis of glycosides can be enzymatically catalyzed by glycosidases. Glycosidases belong to the hydrolases and hydrolyze carbohydrates with aryl, amino or alkyl-*β*-D-glycoside residues, as well as oligosaccharides and disaccharides.[28,101] In the field of glycosidases, *β*-glycosidases have been studied particularly intensive. *β*-Glycosidases hydrolyze glycosidic linkages for example of terminal non-reducing glucosides.[119] *β*-Glycosidases occur ubiquitously and catalyze the hydrolysis of *β*-1,4-bonds[119] in many biological processes, host-parasite interactions, cell wall degradation and in biotechnological applications such as flavor intensification of beverages.[99,113] *β*-Glycosidases are often classified according to their substrate specificity as aryl-*β*-glycosidases, cellobiases which hydrolyze disaccharides like cellobiose and broad substrate specificity enzymes, with most characterized *β*-glycosidases belonging to the latter category.[101] There are two mechanisms of glycoside hydrolysis, one occurring while maintaining the stereochemistry at the anomeric carbon atom and the other leading to an inversion.[120]

The enzymatic hydrolysis of diglycosidic structures takes place in two steps (Figure 5). First, the inter-sugar bond is cleaved by exoglycosidases such as α-rhamnosidases or α-arabinofuranosidases. The resulting *β*-D-glycoside is subsequently hydrolyzed by a *β*-glycosidase.[121]

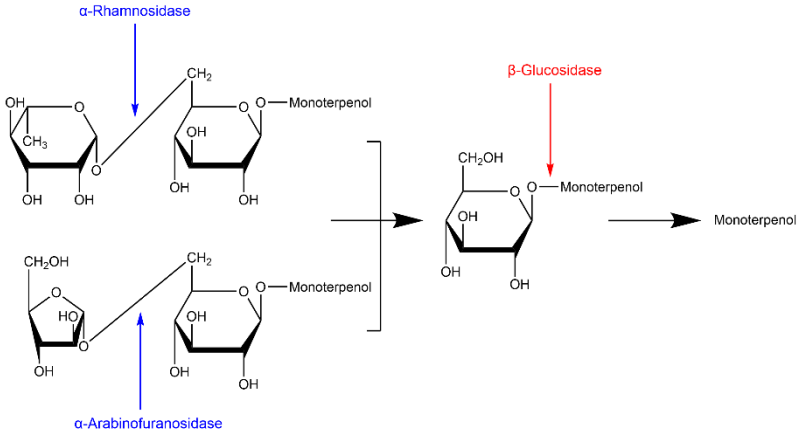

Figure 5: Exemplary enzymatic hydrolysis of terpenol-diglycosides. After cleavage of the inter-sugar bond by exoglycosidases (blue), the resulting *β*-D-glycoside is hydrolyzed by *β*-glycosidases. (Illustration adapted[121])

Although *β*-glycosidases are also present in plants such as grapevine, these enzymes are not stable at the pH values present during fermentation[122] and are therefore not relevant for the winemaking process.[119] The enzyme preparations currently used commercially for wine aroma improvement are therefore often originating from fungi.[123] Treatment of wines with *β*-glycosidase preparations from fungi can lead to an increase in free volatile compounds of 265-2,000 %.[96] However, the application of these preparations is only successful in dry wines, as the enzymes are otherwise inhibited by sugar. For this reason, their use is more effective towards the end of fermentation, preventing the aromatic substances from further reactions which contribute to positive aging effects.[99] The enzymes are thus limited in their enzymatic capacity due to the harsh fermentation parameters,[124] also including low pH values and, in the course of the fermentation process, the increasing amounts of ethanol. Moreover, fungal *β*-glycosidases can also mediate hydrolysis of unstable pigments like anthocyans and the release of unpleasant flavors like vinyl-phenols.[87,125]

Because of this, other exogenous enzymes are often used to compensate for insufficient enzyme activities in grapes in viticulture. Yeasts and lactic bacteria can be a good source of these enzymes[119] by adding strains with known *β*-glycosidase activities to the fermentations.[126] For this purpose, the strains are used in co-inoculations[127] or sequential fermentations[128] together with *S. cerevisiae*.

3.4.5.1 Inhibition of β-glycosidases

As described, *β*-glycosidases are inhibited by various factors such as glucose and ethanol concentration, pH value, temperature, and SO_2 content during fermentation.[129] It should be noted that the individual factors can also have combined influences on the activity of *β*-glycosidases. In addition, other components of must can negatively affect enzyme activity.[119] The optima of glycosidases from different non-*Saccharomyces* yeasts vary greatly and cannot be generalized.[97]

In addition, *β*-glycosidases can be influenced by increasing glucose concentration due to its hydrolysis activity.[130,131] The fact that *β*-glycosidase from *Wickerhamomyces anomalus* strain AL112 still exhibited 50 % of its maximum enzyme activity at 20 % glucose (w/v),[132] but the activity of *β*-glycosidase from *Wickerhamomyces anomalus* strain MDD24 was significantly reduced at a glucose concentration of 5 %[133] illustrates, that the sugar tolerance of the respective *β*-glycosidase is strain dependent. The *β*-glycosidases secreted by eukaryotes belong to the GH3 family. This family has a shallow binding site that is easily occupied by glucose due to the specific conserved domains which leads to the loss of activity.[134] *β*-Glycosidases are also inhibited by substrate-analogous glycosides, by sugar analogs in the transition state, by free aglycones, and by substrates that are only slowly hydrolyzed.[135]

High ethanol concentrations can also lead to the inhibition of *β*-glycosidase activities.[136] However, many *β*-glycosidases have been found to be tolerant to high ethanol concentrations. For example, *β*-glycosidases from non-*Saccharomyces* yeasts were described that still showed 60-80 % of their initial activity at 20 % ethanol.[129,133,137,138] Furthermore, a *β*-glycosidase from *Pichia anomala* was characterized that even showed increased activity (150 %) in the presence of 4-20 % ethanol and stability at low pH values.[133]

Low pH values in fermentations also play an important role in the inhibition of *β*-glycosidases. The pH optimum of most *β*-glycosidases is between 4 and 7.5, with enzyme stability between pH values of 4 and 9.[135] In various screenings, however, extracellular *β*-glycosidases have already been identified that showed activity at the typical wine pH values between 3 and 4. In particular, *β*-glycosidases secreted from *Hanseniaspora* and *Debaryomyces*, as well as from *Rhodotorula* strains should be mentioned, which are stable even at low pH values and still exhibited 40-60 % of their initial activity at pH values of 3.[125,139] A strain dependency of *β*-glycosidase pH tolerance has also been described.[119]

3.4.5.2 Induction of β glycosidases

Although inducible *β*-glycosidase activities have been described for *Hansenula* yeasts, these activities are inhibited by low glucose concentrations and are therefore not suitable for the application during the fermentation process.[130] In other studies, the presence of substrates in

culture media was described to contribute to enzyme production[140] and for *Aureobasidium pullulans*, *Rhodotorula glutinis*, and *Debaryomyces hanseni*, for example, increased *β*-glycosidase activities were found after cultivation in medium containing cellobiose.[141–143]

3.4.5.3 Specificity of β glycosidases

The substrate spectrum of potentially glycosidase-active enzymes is highly dependent on their biological origin.[97] For example, the structure of the aglycone influences the activity of plant *β*-glycosidases. Thus, glycosides of primary and secondary alcohols are good substrates for plant glycosidases, whereas *β*-glycosidases of higher fungi primarily hydrolyze glycosides of tertiary alcohols.[87,113]

In contrast, most of the described microbial *β*-glycosidases show a broad substrate specificity.[120] The specificity of these enzymes rarely relates to the aglycone but mainly to the glycosidic portion of the precursor molecule. Because of this, aryl-*β*-glycosidases are distinguished from cellobiases and nonspecific glycosidases.[101] Most *β*-glycosidases that have been characterized up to now belong to the category of non-specific glycosidases.

The cleavage of the outer sugar residue in the presence of disaccharides is also independent of the aglycon.[113] This is due to the fact that the orientation of the terminal sugar molecule remains the same regardless of the aglycone. For example, the *β*-glycosidases of non-*Saccharomyces* yeasts such as *Candida molischiana* and *Candida wickerhamii* cleaved many diglycosides, with the structure of the aglycone causing only low-level effects.[144]

Thus, the *β*-glycosidases expressed by yeasts are not very specific[145] and release a high variety of glycosidically bound substances from the must.

3.4.5.4 Localization of β-glycosidases

β-Glycosidases produced from yeasts are from the GH3 class, which are found in various locations such as the cytosol, cell membrane, and cell wall, but rarely reach high concentrations intracellularly.[120,146] For this reason, the usage of yeasts with intracellular *β*-glycosidases is currently of small importance for industrial application. Research in recent years has focused on extracellular activities in the supernatant.[16] To determine extracellular *β*-glycosidase activity, activity in the supernatant and in the cell pellet was evaluated[147] and compared. Currently, however, only a few methods for determining *β*-glycosidase localization, such as using cellobiose as a substrate and measuring the released glucose in different cell fractions,[146] have been described. For some strains, such as *Brettanomyces bruxellensis*,[148,149] *Hanseniaspora uvarum, Hanseniaspora osmophila* and *Metschnikowia pulcherrima*,[146]

intracellular *β*-glycosidase activity has been reported, but the application possibilities of these yeasts have not been studied in detail.

These extracellular enzymes are easy to find and characterize, but intracellular enzymes with interesting properties might have been missed.

3.4.5.5 Alternative applications of β-glycosidases

Moreover, *β*-glycosidases are not only interesting with regard to the release of aroma-active substances, but also play an important role in several other industrial applications like the degradation of lignocellulosic biomass through the enzymatic route,[150,151] processing of laundry and detergents, paper and pulp industry, biofuel production and textile industry.[120,152]

β-Glycosidases are also involved in the hydrolysis of other bioactive compounds.[152] For example, autochthonous yeasts with *β*-glycosidase activity have been found to increase the concentration of phenolic components such as resveratrol by hydrolyzing the glycosidic precursors in red wine.[153] Resveratrol is known for health benefits by reducing coronary events in humans.

β-Glycosidases can also be used in reverse hydrolysis reactions in which monosaccharides are used as glycosyl donors. This reaction can be thermodynamically shifted toward the synthesis of glycosides by removing them from the system or adding glucose and alcohol substrates in excess.[152]

It has also been described, that volatile phenols that come into contact with grapevines through the air after bushfires, are glycosylated by glycosyltransferases. Application of glycosidases then results in undesirable aroma from smoke as the captured phenols are released again.[154,155] In this way, glycosidases can also have a negative impact on the taste of wines at specific conditions.

3.4.6 *β*-Glycosidase screening

Because of the immense industrial relevance, several surrogate substrates for *β*-glycosidase screening are described. Since the first description of 4-nitrophenyl-*β*-D-glucopyranoside (pNPG) for the assessment of *β*-glycosidase activities,[156] this substrate has been widely used for the kinetic characterization of enzymes. Arbutin (hydroquinone-*β*-D-glucopyranoside) was used previously as a surrogate substrate for the screening of *β*-glycosidase activities in yeasts of oenological origin.[148] 6-*O*-(-D-Glucosyl)aesculetin (esculin) has traditionally been used to identify bacteria,[157] and has recently been used in an esculin-glycerol solid medium for rapid screening of larger collections of native wine yeast strains.[158] Beside the frequent use of 4-methylumbelliferyl-*β*-D-glucopyranoside (4-MUG) in the context of human *β*-glycosidase

research,[159,160] the use of agar plates containing this surrogate substrate for microbiological screening purposes was described.[161] In 2005, a modified fast 4-MUG-based assay method in microplates with the possibility of *β*-glycosidase activity quantification was developed.[162]

The structures of the aforementioned compounds are very similar (Figure 6). Hydrolysis of the *β*-glycosidic bond can be photometrically detected due to the absorbance or fluorescence properties of either the glycoside or the aglycon forms.

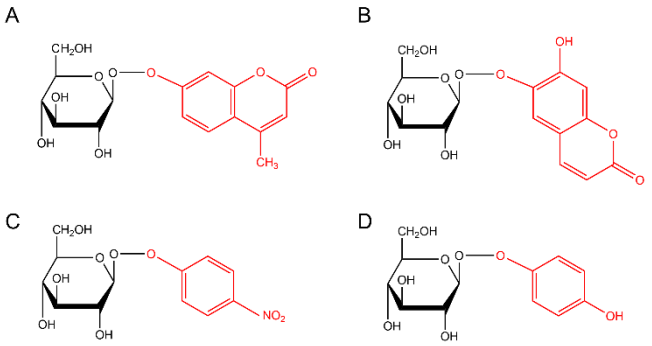

Figure 6: Most common surrogate substrates for the detection of *β*-glycosidase activities. A) 4-MUG, B) Esculin, C) pNPG, D) Arbutin. The parts of the molecules that can be photometrically determined after hydrolysis are illustrated in red.

However, these surrogate substrates differ in their spectroscopic properties and in their application possibilities for *β*-glycosidase screening.

3.4.7 Organisms exhibiting *β*-glycosidases

The search for yeasts with *β*-glycosidase activity has been intensively pursued in the past using the formerly described surrogate substrates. Especially non-*Saccharomyces* yeasts are attractive due to their generally higher *β*-glycosidase activity and the resulting influence on primary and secondary aroma.[4] *β*-Glycosidase activity is dependent on the yeast species and strain, with some strains not producing these enzymes at all.[163] Most often, *β*-glycosidases are produced during the exponential growth phase of the organisms.[162,164] However, the observation and determination of the effects of the release catalyzed by *β*-glycosidases is difficult, because the microorganisms also release aromatic substances through other ways, partly synthesize them and further modify the molecules produced. For example, *S. cerevisiae* is able to convert geraniol and nerol to citronellol[147] and synthesizes terpenes *de novo.*[163] This ability has also been described for many other non-*Saccharomyces* yeasts. For example, the synthesis of α-terpineol and linalool has been demonstrated in relevant amounts.[97]

The importance of *S. cerevisiae* for the hydrolysis of glycosylated aromatic compounds is controversially discussed.[97,108,165–171] Overall, high *β*-glycosidase activity is rare in indigenous *S. cerevisiae* strains with generally lower activity than non-*Saccharomyces* yeasts.[119]

Thus, *β*-glycosidase activity has been described for *S. cerevisiae* only in exceptional cases. For example, in a study of 153 strains of this species, glycosidase activity was detected in only one strain[148] and the observed release is most likely caused by side activities of the exo-*β*-glucanase Exg1p.[172,173]

β-Glycosidase activities of non-*Saccharomyces* yeasts, on the other hand, have been described in varying degrees for many genera such as *Candida, Brettanomyces, Debaryomyces, Hanseniaspora, Lachancea, Metschnikowia, Pichia, Rhodotorula, Trichosporon, Torulaspora, Wickerhamomyces,* and *Zygosaccharomyces*.[119] Particularly promising activities have been found for *Hanseniaspora uvarum* and *Wickerhamomyces anomalus* strains,[146,149] as well as for *Aureobasidium pullulans*[141,174,175] and *Issatchenkia terricola*.[176]

In addition to the *β*-glycosidase activities addressed, many non-*Saccharomyces* yeasts, such as *Hanseniaspora uvarum, Wickerhamomyces anomalus, Torulspora delbrueckii*, and *Issatchenkia tericola*, also exhibit the enzyme activities necessary for the cleavage of diglycosides.[119] It is equally suggested that the cleavage of small amounts of diglycosidic bonds is also catalyzed by side activities of the *β*-glycosidase activity studied.[133]

3.4.8 *β*-Glycosidase activities during malolactic fermentation

After the completion of yeast fermentation, malolactic fermentation of the must often follows, especially in red wines.[177] During this process, certain species of lactic acid bacteria, mainly *Oenococcus* strains, grow. This second fermentation is used for deacidification of the wine, but can also influence the organoleptic quality. *Oenococcus oeni* is the main species responsible for this fermentation[178] and is also able to release high amounts of *β*-glycosidase.[126]

3.4.9 Further methods for the application of *β*-glycosidases in fermentations

β-Glycosidases have also been immobilized and used for repeated use in musts.[179] Immobilized *β*-glycosidases are more stable.[100,164] The use of immobilized *β*-glycosidases is still at the experimental stage and only free enzyme forms are currently used commercially.

Genetically modified *S. cerevisiae* cells expressing an *Aspergillus niger β*-glycosidase on their cell wall released comparatively higher amounts of terpenols during the fermentation of synthetic medium supplemented with precursor extract than the commercial *β*-glycosidase preparation AR2000. The authors hypothesized that glucose in the direct surrounding of the enzymes is consumed by the cells and the formation of a "low glucose zone" attenuates the

inhibitory effect of glucose.[134] Such a system could also be a new solution for aroma improvement if genetically modified organisms were approved and accepted by customers.

3.5 Volatile thiols

Another good example for tailored processes in wine production are Sauvignon Blanc wines, one of the world's most commercially important grape varieties, grown second most often in France and most often in California and Australia.[180] The aroma of this grape variety can vary greatly depending on origin and aging. Sauvignon Blanc wines are often divided into two classes, "green" and "tropical". The green aromas are mainly caused by methoxypyrazines,[181,182] while the tropical aromas are caused by esters, higher alcohols, fatty acids, monoterpenes and volatile thiols.[183]

These volatile thiols belong to the group of volatile sulphur compounds, which, in addition to the positive effects described, can also result in negative aromas. For example, the formation of H_2S leads to odors of rotten eggs, while the reductive sulfurous off-odors such as thioacetic esters and mercaptans lead to imprints of cooked vegetables, which are held responsible for up to 30 % of defective wines.[184]

As described, volatile thiols can also cause strong impressions of guava, tropical fruits and passion fruit on the other hand and improve wine aroma.[185] The properties of the most important volatile thiols responsible for the described odor impressions of for example Sauvignon Blanc wine are shown in Table 1. 4-Mercapto-4-methylpentan-2-one (4MMP) has a characteristic odor of passion fruit and boxtree, while 3-mercaptohexan-1-ol (3MH) and its acetylated form 3-mercaptohexyl acetate (3MHA) lead to the impression of grapefruit and citrus.[183]

Table 1: The most important volatile thiols contributing to Sauvignon blanc aroma. Structures of the molecules are given in the following sections. (Modified from [183])

Compound	Olfactory description	Range in wines [ng L^{-1}]	Perception threshold [ng L^{-1}]
4MMP	Box tree, passion fruit, black currant	4-40	0.8
3MH	Passion fruit, grapefruit, guava	26-18,000	60
3MHA	Passion fruit, grapefruit, box tree, guava	0-2,500	4.2

As for many aroma molecules, stereochemistry also plays a role in the human perception of thiols. The different enantiomers of 3MH and 3MHA differ in occurrence, odor thresholds, and perception, and occur in different proportions in wines of different regions.[5,186]

For example, (*R*)-3MHA smells like passion fruit, while (*S*)-3MHA is more commonly perceived as boxwood.[187]

In addition to the described volatile thiols, which are responsible for tropical odor impressions, storage in oak barrels leads to the formation of other aroma-relevant thiols such as the furanthiol derivatives 2-furanmethenethiol and 2-methyl-3-furanthiol, which contribute to the empyreumatic aroma of wines.[188] In addition, the characteristics of the wines can still change in the bottle after bottling, as 3MH and 3MHA degrade during storage. The formation of 3MH from 3MHA during storage has also been observed.[189]

Although volatile thiols are often only present in trace amounts in the wines, their concentrations are mostly above the odor thresholds and thus these molecules may have a major influence on the aroma perception of these wines. However, since volatile thiols in higher concentrations lead to negative odor impressions such as cat urine,[6] the concentrations must lie within certain concentration ranges for a pleasant perception.

Volatile thiols are also part of the aroma impression of the resulting wines from other white grape varieties such as Gewürztraminer, Riesling and Colombard, Petit Manseng and Semillon[190] and also influence the taste of red wines such as Merlot and Cabernet Sauvignon.[191] In general, the volatile thiols 3MH and 3MHA are more prevalent than 4MMP.[5] However, 4MMP is found in high concentrations in the Scheurebe grape variety, for example, where it has a considerable influence on the aroma.[192]

3.5.1 Formation of thiols in wines

Unlike other aroma components, the volatile thiols described above are rarely present in the grape juice, but are formed during fermentation with the help of yeasts and released from precursors through various pathways. Although most of the research was performed with focus on the release mechanisms of 3MH, it is presumed, that these results can be transferred to the release of 4MMP.

3.5.1.1 Formation of 3MHA

The formation of 3MHA occurs through the esterification of acetic acid and 3MH by the yeast alcohol acetyltransferase Atf1p (Figure 7).[193] While the final concentration of 3MHA can be up to 10 % of the amount of 3MH,[194] there are significant differences between yeast strains in their ability to catalyze this reaction.[9]

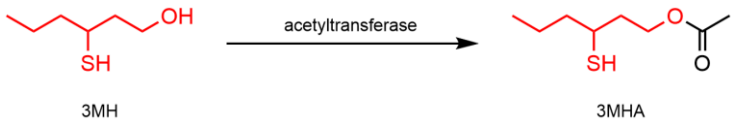

Figure 7: 3MHA is originating from 3MH through an esterification with acetic acid. This reaction is mainly catalyzed by the yeast acetyltransferase Atf1p.

In addition to the acetyltransferase Atf1p described above, *S. cerevisiae* expresses other acetyltransferases such as Atf2p and Eht1p, which catalyze the formation of major aroma components such as ethyl acetate and isoamyl acetate.[195] Involvement of these enzymes in the formation of 3MHA is likely, but occurs at a comparatively lower level.[196]

3.5.2 Cysteine conjugates

One of the described pathways for thiol release is the formation from cysteinylated and glutathionylated precursors. In addition to their occurrence in wine grapes, aroma compounds bound to cysteine residues have also been found, for example, in onions and garlic[197] and could be a good source of aroma compounds for the aroma industry in the future.[198]

Although these precursors in berries are present in the pulp of the berries as well, higher concentrations are often found in the skin.[192] The formation of precursors occurs mainly in the last days before the harvest at the ripe stage of the grapes,[199] as the decay of the grapes favors the processes of their formation.[200]

The concentration of the precursors of volatile thiols in the final wine is influenced by many factors during vine growth and winemaking. For example, ripening or growth conditions such as low nitrogen availability, location, or infection with pathogens such as *Botrytis cinerea*, as well as certain conditions during winemaking can alter the concentrations of precursors.[183,201] These include, for example, methods with longer contact of the must to the grape skin, higher temperatures during pressing and the application of higher pressure, which result in increased Cys-3MH concentrations.[202]

It was also found that large portions of the cysteine-conjugated precursors are already present in the berries, whereas the glutathione-bound precursors are mostly formed after harvesting.[199]

The release of thiols from the cysteinylated precursors already present in berries with the help of specific *β*-lyase activities was first demonstrated using extracts of *Eubacterium limosum* and purified tryptophanase from *Escherichia coli*.[203] Since then, it has been assumed that these *β*-lyase reactions also lead to the release of thiols during fermentation. This is supported by further studies showing that the concentration of Cys-3MH in model fermentations decreases at the same rate as the concentration of 3MH increases. Although (*S*)-Cys-3MH is most

abundant, the distribution of isomers can differ greatly, whereas stereoisomerism is unlikely to affect the cleavage rates of *β*-lyases.[204]

Cysteine-S-conjugate lyases are part of the large enzyme family of carbon-sulfur lyases. These enzymes catalyze the cleavage of a carbon-sulfur compound in an α,β-elimination reaction. This reaction leads to the formation of the thiol molecule and an intermediate that spontaneously decomposes into pyruvate and ammonia (Figure 8).[7]

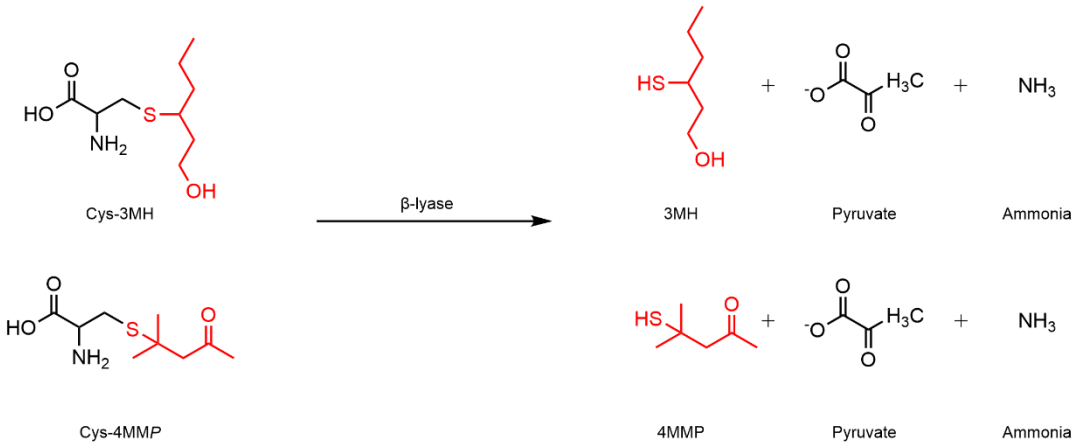

Figure 8: The potent volatile thiols 3MH and 4MMP are released from cysteinylated precursors through carbon-sulfur lyases. Several enzymes like Bna3p, Cys3p, Glo1p and Irc7p are assumed to catalyze this reaction in yeasts.

Some studies suggest the involvement of the genes *BNA3, CYS3, GLO1* and *IRC7* in the release of 4MMP,[7] while others postulate that only Irc7p can release 3MH and 4MMP from cysteinylated precursors.[205] The expression of IRC7 is also thought to be controlled by nitrogen catabolite repression through the transcriptional regulation of Ure2p/Gln3p proteins.[205] It is also known that a large number of wine yeasts used for fermentation contain a 38 bp deletion, resulting in a truncated version of Irc7p that lacks cysteine-S-conjugate *β*-lyase activity.[206] However, it has also been shown that the ability of a yeast to release thiols is not solely dependent on the *IRC7* allele length, as many yeasts contain single nucleotide polymorphisms that can significantly reduce *β*-lyase activity, yet are still able to release thiols.[206] Presumably, therefore, the cleavage of cysteine precursors cannot be attributed to a single gene.[7]

With the protein Str3p, an additional pyridoxal-5-phosphate-dependent cystathionine *β*-lyase was identified in *S. cerevisiae,* that is capable of cleaving cysteinylated precursors of 3MH and 4MMP with low side activities and the release of the corresponding thiols.[207]

However, it was found that although Cys-3MH was cleaved more effectively by yeast cells in synthetic musts,[208] it quantitatively may not be the major precursor, since the concentration of the corresponding glutathionylated precursor Glut-3MH is up to 35 times higher in the musts.[209] For this reason, the release of thiols from glutathione conjugates was also studied.

3.5.3 Glutathione conjugates

The formation of glutathione conjugates has already been characterized for 3MH and 4MMP[8] and occurs through the chemical or enzymatic synthesis from glutathione and mesityl oxide or *(E)*-2-hexenal (Figure 9).[209,210] The enzymatic catalysis is part of detoxification mechanisms known in many organisms. For the genesis of Glut-3MH, the intermediate formation of an aldehyde molecule (Glut-3MHAl) is described, which is subsequently modified by reductive enzymes to Glut-3MH.[199]

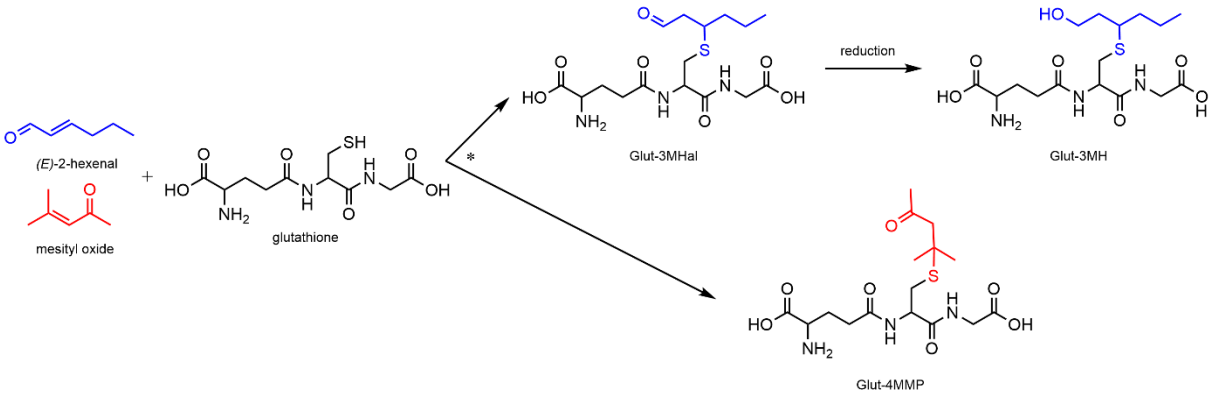

Figure 9: Genesis of glutathione-conjugated volatile thiol precursors. Asterisk: Conjugation with glutathione occurs either through chemical reactions or through catalysis by glutathione-*S*-transferases. The formation of an aldehyde intermediate is described for the conjugation of *(E)*-2-hexenal.

The role of Glut-3MH as a precursor molecule for the generation of 3MH was confirmed by the finding that lower levels of 3MH were observed after deletion of the *OPT1* gene encoding the main glutathione transporter.[211] In general, uptake of glutathione precursors by amino acid transporters is likely due to structural similarity.[205]

3.5.3.1 Conversion of glutathione precursors to cysteine precursors

It is assumed that the Glut-3MH molecule acts as a pro-precursor and in later reactions is converted by enzymes to Cys-3MH (Figure 10),[183,211,212] which is subsequently cleaved by a *β*-lyase. For this purpose, after the transfer of glutathione to a volatile thiol compound by a glutathione transferase, glutamic acid is cleaved by a γ-glutamyl transpeptidase and glycine is removed by a carboxypeptidase.[198] Glutamyltranspeptidases that may catalyze this reaction are Ecm38p and Cis2p,[213,214] whereas the carboxypeptidase that catalyzes the final formation of Cys-3MH has not yet been identified. The conversion of Glut-4MMP to 4MMP has also not yet been validly demonstrated.[206] Degradation of conjugated glutathione molecules could also be accomplished in parallel by alternative pathways of glutathione degradation.[215]

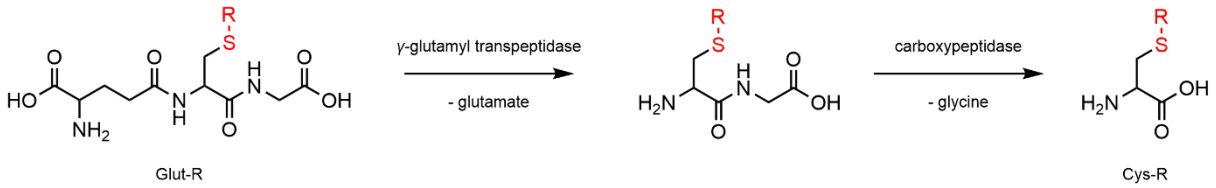

Figure 10: Transformation of glutathione-conjugated precursor structures to cysteinylated precursors is catalyzed by several enzymatic reactions. Volatile thiols are subsequently released from the synthesized cysteine conjugates by *β*-lyases. R) 3MH or 4MMP residues.

The assumption that precursors bound to glutathione are first degraded to cysteinylated precursors is supported by experiments in which Sauvignon Blanc must was passed through a column containing immobilized *γ*-glutamyltranspeptidase and the subsequent measurement of elevated 3MH-cysteine levels.[216] The use of labeled Glut-3MH in Sauvignon Blanc must and the subsequent detection of labeled 3MH further confirmed the role of Glut-3MH as a precursor for the formation of free thiols. Regardless of the amount of Glut-3MH used, the conversion rate in these experiments was 4.5 %. Similar experiments with Glut-4MMP also confirmed the release of labeled 4MMP at a rate of 0.3 %, which was accounting for 20 % of the total 4MMP release.[217]

However, it was found that there was no direct correlation between the concentration of the previously described precursors present in the must and the final thiol concentrations.[5,209] Another formation pathway of volatile thiols that could fill this gap is the reaction of mesityl oxide and *(E)*-2-hexenal with sulfur donors.[210]

3.5.4 Hexenal pathway

(E)-2-hexenal is a known component in grape must which is present in large amounts before the fermentation. It is formed in the must from unsaturated lipids in amounts ranging from a few to hundreds of micrograms per L, depending on the grape variety and the treatment of the must, and could therefore have very large effects on the amounts of volatile thiols. Other similar components such as *(E)*-2-hexen-1-ol and *(Z)*-2-hexen-1-ol could similarly contribute to the formation of thiols.[218] These assumptions are confirmed by experiments in which musts spiked with H_2S showed significantly increased 3MH amounts and the fact that the molecules *(E)*-2-hexenal and *(E)*-2-hexen-1-ol were identified as precursors in this reaction.[219]

Furthermore, the transformation of *(E)*-2-hexenal and mesityl oxide into the structurally similar thiols 3MH and 4MMP during fermentation was demonstrated using deuterated analogues.[210]

Thus, a possible pathway of Glut-3MH synthesis could take place during the prefermentation operations, during which *(E)*-2-hexenal reacts with glutathione in the oxidative environmental conditions.[220] It has also been shown that the content of glutathione and *(E)*-2-hexenal in

grapes increases at the time before harvest.[221] An increase in reactant concentrations could be a reason for the formation of these precursors at this time.

According to the current opinion, the amounts of the three precursors described and the conversion rates observed cannot account for the amounts of volatile thiols released. In studies in Melon B. most, for example, only 10 % of the total 3MH could be attributed to labeled *(E)*-2-hexenal.[210] For this reason, there are most likely other, currently unknown pathways that contribute to the formation of volatile thiols. A possible additional source could be derivatives of the described molecules, like aldehydes[222] or cyclic forms,[5] or dipeptide conjugates of 3MH (cysteinyl glycinhexan-1-ol and *S*-3-γ-glutamyl cysteinylhexan-1-ol).[213,223]

3.5.5 Release during fermentation

During fermentation, volatile thiols are released from their precursors, contributing to the aroma of the resulting wines. It has been found that this release can be influenced during fermentation. Thus, higher temperatures can lead to higher amounts of volatile thiols released, while rather low temperatures promote the formation of esters and acetates.[185] During fermentation, the number of volatile thiols released is also influenced by the addition of certain agents such as glutathione or SO_2.[183] But in most cases, the choice of the fermenting yeast strains has the greatest influence on the detected amounts of volatile thiols.

The *β*-lyase expression of yeasts appears to limit the production of varietal thiols in wines.[193] Thus, an up to 10-fold difference in the ability to release thiols between different *S. cerevisiae* strains was observed.[205] The different ability of various wine yeasts of other species to release volatile thiols from the precursors during fermentation was also investigated and demonstrated.[191] In fermentations, it was also found that co-fermentation of *S. cerevisiae* and *Torulaspora delbrueckii* resulted in a synergistic effect, thanks to which higher concentrations of 3MH and 3MHA were measured than after the fermentation with *T. delbrueckii* alone.[224]

Another essential aspect is the transport of precursor molecules into the cells (Figure 11). For 3MH, the mechanisms of uptake have already been studied in more detail. Thus, the transport of the glutathione conjugated form of the precursor is carried out by the glutathione transporter Opt1p,[211] while in synthetic medium the amino acid transporter Gap1p was found to be one of the transporters of Cys-3MH.[218] Since Gap1p is at least partially dependent on nitrogen catabolite repression, this could be a cause for the increase in volatile thiol components after nitrogen feeds.[225] It has also been found that nitrogen availability is responsible for 35 % of the observed variation in thiol release.[205]

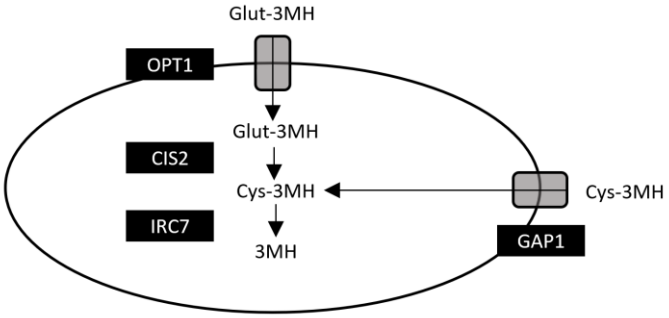

Figure 11: Exemplary presentation of the release of 3MH from cysteine- and glutathione-conjugated precursors by yeasts. After import of Glut-3MH, conversion to Cys-3MH occurs. However, Cys-3MH can also be imported directly into the cell. Subsequently, 3MH is released from the cysteinylated precursor by a *β-lyase*. (Modified from [214])

In general, only a small fraction of the present precursors appears to be converted during fermentation. While Cys-3MH is converted up to 12 %, the conversion rates of Glut-3MH are significantly lower with only up to 5 %.[191,194,208,212] For this reason, large aroma potentials of musts are currently not exploited. The identification of new yeast strains with high *β*-lyase activity and the improvement of existing strains could thus help to better exploit the existing potential of wines.

3.5.6 Oxidation

During the production of wines, the must components may come into contact with high amounts of O_2. This can lead to oxidation of various components, including the thiols. Since the thiol precursors have a relatively stable thioether bond, they are less susceptible to these oxidation reactions[5] and the oxidation of thioethers to sulfones and sulfoxides during wine processing has not yet been described. The volatile thiols, on the other hand, are reactive components that can easily oxidize and whose aroma potential is lost as a result.[188] This oxidation can not only occur during production but also, especially for 3MH, during aging due to dissolved oxygen or reaction with other reactive species such as polyphenols.[220] This oxidation can be prevented by the addition of SO_2.[188] Another reason for the decrease in the concentrations of volatile thiols during storage could be the specific adsorption of the aroma components 3MH and 3MHA by the cork.[226]

3.5.7 Analytics and synthesis

Since volatile thiols are only present in very low concentrations and wine or grape musts are highly complex matrices, purification, concentration and sample preparation are often necessary prior to measurement. This makes the quantification of volatile thiols complex. For the determination of volatile thiols by gas chromatography–mass spectrometry measurements,

derivatizations with the aid of ethyl propiolate,[227] 2,3,4,5,6-pentafluorobenzyl bromide[228] or extraction with metal ions such as mercury or silver[229] are therefore often necessary.

In contrast, the precursors, which also occur in very low concentrations, can be quantified directly with liquid chromatography–mass spectrometry measurements (LC-MS) without derivatization.[209,216,230] Another approach, but less accurate, involves indirect measurement of precursors after the cleavage or derivatization of these molecules. For example, the first quantification method for thiol precursors was realized by measuring the free thiols after passing through a column containing immobilized tryptophanase enzyme.[231]

The simplest way to synthesize thiols is a Michael addition of a sulfur donor to α,β-unsaturated ketones, aldehydes or esters. Through this way, deuterated analogues can be prepared for more detailed studies and as standards. The same route of synthesis is also possible for synthesis of the cysteinylated and glutathionylated precursors. Moreover, the introduction of labeling into the aglykon region of these molecules allows studies on the release from such molecules.[5]

3.6 Production of specific volatile thiols

As described earlier, volatile thiols have great importance for the wine sector as well as for many other parts of the food industry due to their low odor thresholds. The chemical synthesis for many of these molecules is already known. For example, volatile thiols are formed by nucleophilic substitution of halide ions by the nucleophilic sulfhydryl ion either spontaneously or with the use of catalysts.[232] Furfural and H_2S, for example, react in a Maillard reaction to give furfurylthiol,[233,234] while the synthesis of *p*-1-Menthen-8-thiol (terpineolthiol) by H_2S addition to α-terpineol, limonene and β-pinene is described.[235,236] *p*-1-Menthen-8-thiol is described as the substance with the lowest known odor threshold and is the key aroma of grapefruits.[236] The reaction of pulegone with H_2S in alkaline medium results in 8-mercapto-*p*-menthan-3-one formation, a compound that is known for its black currant and tropical flavours.[235,236]

However, due to possible negative environmental impacts, lack of matrix selectivity and customer perceived value, alternative approaches for the production of certain volatile thiols known from the food sector are increasingly established.[237] A promising attempt to enable the release of certain volatile thiols is to realize the catalysis with the help of microorganisms.

However, until now, the synthesis of specific compounds has been only described via the addition or prior chemical synthesis of glutathione and cysteine conjugates. A patent from 1987,[238] for example, involves the production of 8-mercapto-*p*-menthan-3-one starting from pulegone-cysteine conjugates, while the synthesis of 2-furfurylthiol from furfural after the

synthesis of this conjugate has also been described.[239,240] Moreover, the synthesis of 5-methyl-2-furfurylthiol, benzylthiol, 2-thiophenemethanethiol, 3-methyl-2-thiophene-methanethiol and 2-pyrrolemethanethiol was obtained by *S. cerevisiae* from cysteine-aldehyde precursors. In addition, the production of 8-mercapto-*p*-menthan-3-one from a pulegone-cysteine conjugate using *Eubacterium liosum* was already mentioned in a patent in 1987.[238]

Another aim of the presented work was to establish the one-step synthesis of volatile thiols from alcohol- and aldehyde structures with an optimized yeast laboratory strain and to enable the synthesis of previously undescribed volatile thiol compounds from the respective substrates via the optimized whole cell catalyst (Figure 12). This could be highly useful for aroma compound studies and the engineered strains are furthermore ideal models for the described natural volatile thiol biosynthesis, which are well equipped to perform comparative studies with regard to for example substrate acceptance of specific plant or yeast enzymes.

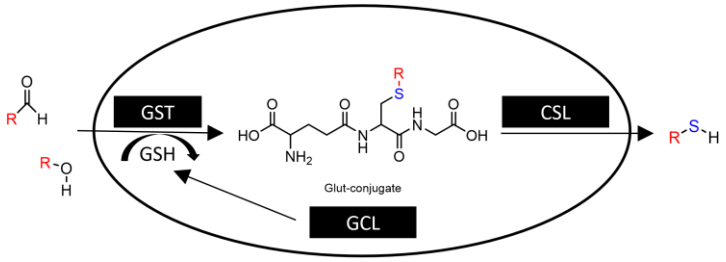

Figure 12: Pathway for the production of thiol structures from aldehydes and alcohols with genetically modified yeasts. After conjugation of the substrate with glutathione by a glutathione-*S*-transferase (GST), the glutathione residue is converted to cysteine (described in Figure 10, not illustrated). The cysteine-conjugate is subsequently cleaved by a carbon-sulfur lyase (CSL) and the volatile thiol is released. Increase of the glutathione concentration through overexpression of a glutamylcysteine synthetase (GCL) might be beneficial for the achieved product amounts.

To enable the synthesis of volatile thiols, the pathway described in the previous chapters for the synthesis of precursors and subsequent cleavage needs to be established and overexpressed in yeast cells. The first step of the targeted reaction is the transfer of the applied substrates to glutathione and the formation of a glutathione-substrate conjugate, which could be facilitated by glutathione-*S*-transferases (GSTs).

3.6.1 GSTs

The enzymes belonging to the superfamily of GSTs are multifunctional proteins that occur naturally in eukaryotes and prokaryotes. In order to fulfill their multiple functions, which include protection against toxic substances and oxidative stress, many different hydrophobic and electrophilic substances are transferred to GSH by these enzymes and the conjugates are subsequently transported out of the cell. GSTs additionally have functions in many other

catalytic reactions such as glutathione peroxidase activities and organic hydroperoxide reduction and can modulate signal transduction pathways.[241] In the targeted pathway, these enzymes are used to increase the formation of glutathione-conjugated precursors of the molecules used as substrates. For this purpose, the two central GSTs GTT1 and GTT2 from *S. cerevisiae*, and VvGST4, a GST with strong activity from *Vitis vinifera*,[242] were selected.

3.6.2 GSH1

To further push the production of glutathione conjugates, it is an obvious target to increase the intracellular concentration of GSH. For this purpose, the overexpression of GSH1 was selected. GSH1 is a glutamate-cysteine ligase (formerly also named γ-glutamylcysteine synthetase) that catalyzes the rate-limiting step in yeast glutathione synthesis.[243] This reaction is the first step in the synthesis of GSH and represents the condensation of cysteine and glutamate with the help of ATP to form dipeptide γ-glutamylcysteines.[244] The resulting γ-peptide bond is unique in its form[245] and cannot be degraded by cellular peptidases, but can only be cleaved by the special enzyme γ-glutamyl transpeptidase.[246] The activity of GSH1 is critical for cell survival and its expression is normally tightly regulated in yeast, including the transcriptional regulation of YAP-1.[243]

3.6.3 *tnaA*

To accelerate the cleavage of the resulting conjugates, carbon-sulfur lyases are particularly useful because of their role during the release of thiols from cysteinylated precursors. These enzymes are normally involved in the transfer of sulfur-containing molecules in amino acid metabolism, for example by catalyzing the hydrolysis of cystathionine from which homoserine and pyruvate are formed.[247] Pyridoxal-5-phosphate is required as a cofactor for this reaction.

An extraordinarily high *β*-lyase activity has been found for the tryptophanase enzyme t*naA* of *E. coli*, whose physiological function is tryptophan cleavage towards indole, a carbon-carbon lyase reaction.[248] Expression of *E. coli tnaA* in yeast has been demonstrated to result in a 25-fold increase of released thiol levels from cysteine- or glutathione-bound precursors during must fermentation.[193] For this reason, *tnaA* was selected for the attempt to increase the *β*-lyase activity within the cells.

3.7 Yeast improvement with evolutionary experiments

Since genetic modification of yeasts for wine production is not allowed in nearly all parts of the world and is not accepted by consumers, the improvement of yeast properties useful for the winemaking process by adaptive evolution is a promising method.

For example, an adaptive laboratory evolution of *S. cerevisieae* was carried out under hyperosmotic stress, resulting in increased production of glycerol and lower ethanol concentration[249] and with the addition of sulfite at alkaline pH as a selective agent, it was possible to isolate a mutant that produced 41 % more glycerol than the parental strain after the adaptive evolution experiments.[250] In addition, the application of ethanol stress enabled the development of strains that showed increased tolerance to ethanol.[251] Moreover, scientists were able to identify mutants that showed altered production of succinic acid and acetic acid and were able to metabolize sugar more rapidly.[252] It was also possible to identify yeast cells that exhibited higher fermentation rates, increased production of aroma components[253] and showed higher GSH-contents which resulted in higher oxidative resistance.[254] Finally, multiple-stress resistant cells were observed, which survival after freezing-thawing was improved among other desired properties.[255]

The aforementioned examples impressively demonstrate how evolutionary approaches can be used as a powerful tool for the improvement of targeted wine yeast properties. Another part of the presented work is an attempt to improve the ability of volatile thiol release from cysteine- and glutathione-precursors by means of an evolutionary approach using the substrate SMC (Figure 13 A).

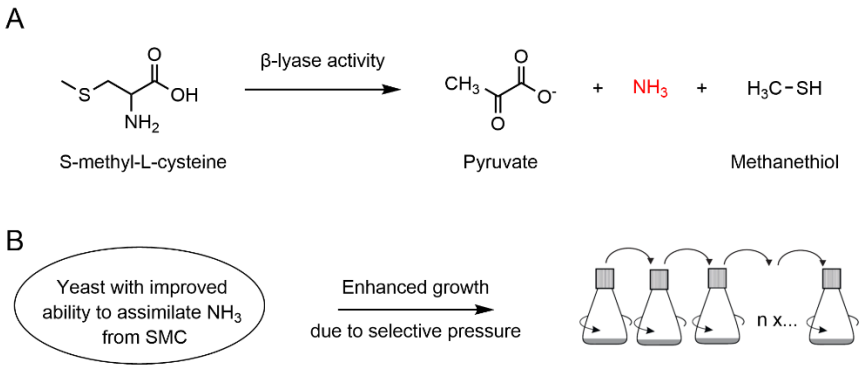

Figure 13: Principle of the applied method for the generation of yeasts with improved nitrogen utilization from SMC. A) Import and export mechanisms, as well as *β*-lyase activity, are required to metabolize SMC and make the incorporated nitrogen available for the microorganisms. B) Cells with improved nitrogen utilization accumulate in the culture after repeated over-inoculation. (Illustration partly adapted[254])

In these experiments, a selective pressure is applied to the cultures, resulting in cells that have randomly undergone advantageous mutations under the selected conditions. These cells have a growth advantage and therefore accumulate in the culture (Figure 13 B). The application of the described adaptive laboratory engineering approach for the purpose of improving thiol release from natural precursors in non-*Saccharomyces* yeasts and commercial wine yeast strains could lead to the discovery of mutant yeasts with significantly improved properties without the use of genetic engineering methods.

4 Materials and Methods

4.1 General

4.1.1 Chemicals

Unless otherwise stated, all chemicals were purchased from Sigma Aldrich (Merck KGaA, Taufkirchen, Germany).

4.1.2 Water

Double distilled water (ddH_2O) derived from a PureLab Ultra Model ULXXXGEM2 water purification system (ELGA LabWater, Paris, France) was used for the experiments.

4.1.3 Media

4.1.3.1 YPD-Medium

YPD-medium was prepared by autoclaving a solution of 20 g L^{-1} bacto peptone and 10 g L^{-1} of yeast extract in water. Subsequently, the solution was supplemented with 50 mL L^{-1} of a 400 g L^{-1} glucose solution and 34 µg mL^{-1} of chloramphenicol. For YPD-Plates, 24 g L^{-1} bacto agar were added before the autoclaving step and the mixture was poured into Petri dishes.

4.1.3.2 SMC-Medium

SMC-Medium was prepared according to Belda et al.[256] The pH of a 10 × stock solution containing 0.01 g L^{-1} SMC, 0.001 g L^{-1} pyridoxal-5-phosphate and 0.12 g L^{-1} BD DIFCO Yeast Carbon Base (Becton Dickinson, New Jersey, USA) was adjusted to a pH value of 3.5 with HCl. All components were sterile filtered through 0.22 µm filters and the medium was stored at 4 °C until use.

4.1.3.3 SC-Medium

The components of 100 mL SC-Medium (10 × stock solution) are shown in Table 2. The solution was filtrated through a 0.22 µm filter before use and stored at 4°C. 24 g L^{-1} agar were added for pouring of agar plates.

Table 2: Composition of the SC-Medium stock solution. Amino acids were added according to the transformed plasmid. Yeast Nitrogen Base was purchased from Carl Roth GmbH & Co. KG (Karlsruhe, Germany), yeast synthetic drop-out medium and supplements were purchased from Sigma Aldrich (Taufkirchen, Germany).

Compound	Amount [g]
Yeats Nitrogen Base w/o amino acids w NH_4SO_2	6.7
Glucose	5

Compound	Amount [g]
Yeast synthetic drop-out medium supplements without histidine, leucine, tryptophane and uracil	1.4
Histidine	0.076
Leucine	0,38
Uracil	0.076
Tryptophane	0.076

4.1.4 Yeast transformation

4.1.4.1 Yeast strains

CEN.PK2-1C cells were obtained from EUROSCARF (SRD GmbH, Oberursel, Germany). AWRI1631 cells were obtained from the Australian Wine Research Institute.

4.1.4.2 Plasmids

4.1.4.2.1 pBKD_*tnaA*

The pBKD_*tnaA* plasmid was obtained from the Macquarie University in Sydney, Australia. The expression construct including a KanMX resistance marker cassette is flanked by delta sequences from the Ty retrotransposon of *S. cerevisiae,* which can be integrated into the genome of *S. cerevisiae* after plasmid digestion with *XhoI.*[257] The full plasmid map is depicted in Figure S 1. Figure 14 illustrates the relevant features of the plasmid.

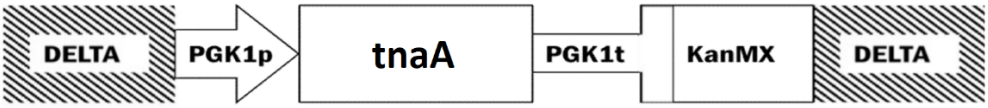

Figure 14: Relevant features of the pBKD-derived plasmid used in this study. Plasmids were linearized with *XhoI* endonuclease. (Adapted from [196])

pBKD_*tnaA* plasmid digestion was performed for 2 h at 37 °C with 35 µL plasmid solution (600 ng μL^{-1}), 4 µL NEB CutSmart Buffer and 1 µL *XhoI* (NEB).

4.1.4.2.2 pPK245/pPK448

Empty vectors pPK245 and pPK448 were obtained from EUROSCARF (SRD GmbH, Oberursel, Germany). The used DNA constructs were synthesized by BioCat GmbH (Heidelberg, Germany) and cloned into the pPK plasmids. Table 3 provides an overview of the constructed plasmids. The gene sequences used are shown in Table S 2. The full plasmid maps are depicted in Figure S 2 – Figure S 5.

Table 3: Overview of the genes used for plasmid construction. The genes were overexpressed with the plasmids pPK245 or pPK448. The *V. vinifera* VvGST4 DNA sequence was codon-optimized for expression in *S. cerevisiae*. An overview of the DNA sequences is given in Table S 2.

Plasmid name	Backbone	Origin of protein encoding gene	GenBank accession number
GSH1	pPK245	*S. cerevisiae*	NM_001181534.1
GTT1	pPK448	*S. cerevisiae*	NM_001179560.1
GTT2	pPK448	*S. cerevisiae*	NM_001181880.1
VvGST4	pPK448	*V. vinifera*	AY971515.1

4.1.4.3 Trans*formation procedure*

Transformation took place according to a published method for quick and easy yeast transformation using the LiAc/SS carrier DNA/PEG method.[258]

4.1.5 Strain identification

Sequencing of internal transcribed spacer 1 and 2 regions was used to conduct a taxonomic classification after BLAST analysis using the NCBI nucleotide database. DNA isolation and sequencing were performed by GENEWIZ GmbH (Germany, Leipzig) according to their standard procedure.

4.1.6 Photometric measurements

A multimode microplate reader (Tecan Spark, Tecan AG, Männedorf, Switzerland) was used for all photometric measurements in microtiter plates.

4.1.7 Cultivation in microtiter plates

Yeast cells were cultivated in microplates at 30 °C, 600 rpm and 80 % humidity in an Infors HT microtron incubator (Infors AG, Bottmingen, Switzerland).

4.1.8 Centrifugation

If not other stated, centrifugation steps took place at 1190 × g for 10 minutes at 20 °C in an Eppendorf 5810R centrifuge. Suitable inlets were used for centrifugation of microtiter plates.

4.1.9 GC-MS-Instrument

Desorption of PDMS twisters with 10 mm length and 1 mm film thickness (Gerstel GmbH & Co.KG, Mühlheim an der Ruhr, Germany) took place in a Shimadzu TD30 thermo-desorption-unit. A VB5 column with 30 m length, 0.25 µm film thickness und 0.25 mm diameter (VICI AG International, Schenkon, Switzerland) was used in a Shimadzu GC-2010 device with a Shimadzu QP2020 Mass Spectrometer (Shimadzu Europa GmbH, Duisburg, Germany). For direct injection of gas phases, a Shimdazu AOC600 autosampler was used.

4.1.10 Determination of *β*-lyase activity

The assays were conducted in a microtiter plate format. Figure 15 represents the principle of the performed assay. Cells which exhibit *β*-lyase activity are able to release methanethiol from SMC. The resulting methanethiol subsequently reacts with DTNB to form TNB^{2-}, whose yellow coloration can be quantified using a photometer.

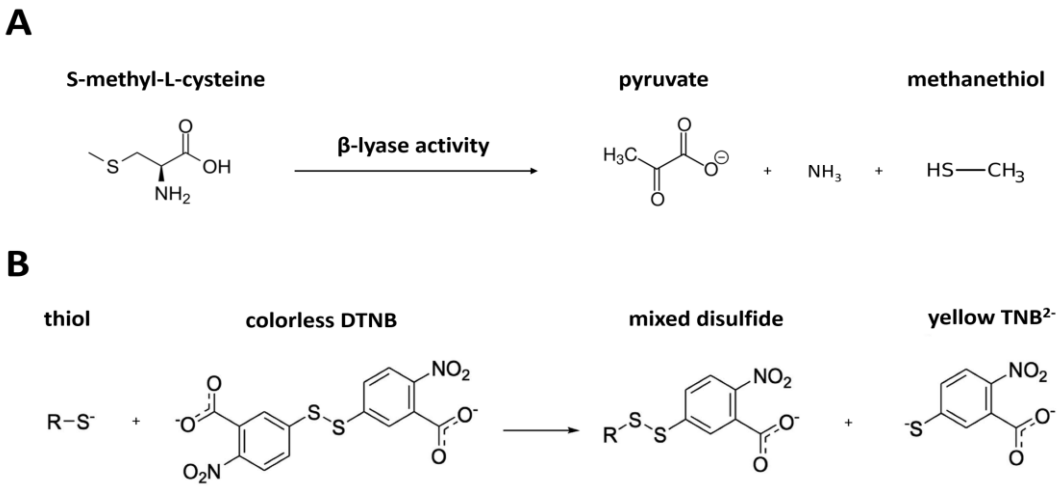

Figure 15: Principle of operation of the DTNB assay for the indirect quantification of *β*-lyase activity at pH 7. A) Methanethiol is released from SMC by *β*-lyase activity. B) TNB^{2-} is generated by the reaction of methanethiol with DTNB.[259]

After growing the yeasts for 24 h in 600 µL YPD-medium, the cells were centrifuged and resuspended in 100 mmol L^{-1} citrate-phosphate buffer pH 7. The cell suspensions were subsequently diluted to an optical density of 2 at 600nm.

150 µL of each cell suspension was transferred to two different microtiter plates. One sample was mixed with 150 µL of a 100 mmol L^{-1} citrate-phosphate buffer pH 7 containing 400 µmol L^{-1} DTNB and 40 µmol L^{-1} pyridoxal-5-phosphate, the other sample with the same buffer additionally containing 4 mmol L^{-1} SMC.

Subsequently, all samples were incubated for 24 h at 25 °C and 350 rpm. After incubation, the samples were centrifuged and 100 µL of the supernatant was transferred to a new microtiter plate to perform the absorbance measurements at 412 nm. To minimize background signals due to sulfur-containing metabolites of the cells, the measured values of the assays without SMC addition were subtracted from the measured values of the assays which contained SMC. The calculated difference was used to quantify the relative amount of liberated methanethiol.

4.1.10.1 Detailed comparison of β-lyase activities

For a detailed comparison of *β*-lyase activities at different pH values, the DTNB assays were prepared in 10 mL headspace vials in this experiment. The previously described basic methodology was used with modifications. The cultures were grown in 50 mL YPD-medium in

250 mL Erlenmeyer flasks. 25 mL of this culture was centrifuged, resuspended in 100 mmol L^{-1} citrate-phosphate buffer pH 7, and diluted with the same buffer to an OD_{600nm} value of 2. 4 mL of this cell suspension was mixed with 4 mL of 100 mmol L^{-1} citrate-phosphate buffer pH 7 containing the assay components with or without SMC. The values shown represent the difference of the measured absorbance values of the two assays with or without SMC, respectively. To analyze thiol release activity at pH 3 via detection of the released thiols, the remaining 25 mL of the yeast cultures were centrifuged. The cells were resuspended in 100 mmol L^{-1} citrate-phosphate buffer pH 3 and diluted with the same buffer to an OD_{600nm} value of 2. 4 mL of the cell suspension was mixed with 4 mL 100 mmol L^{-1} citrate-phosphate buffer pH 3 with the assay components with SMC or without DTNB.

Headspace detection of the *β*-lyase-mediated release of thiols from SMC took place with a direct injection of 200 µL of headspace gas into the GC-MS instrument. The GC program started with a hold time of two minutes at 30 °C, then the temperature was increased to 40 °C at a rate of 2 °C min^{-1}. Afterwards, the temperature was further raised to 300 °C at a rate of 25 °C min^{-1}. The peaks of interest eluted after 1.85 minutes (methanethiol) and 5.45 minutes (dimethyl disulfide) with the described method. Peak areas were determined with a SIM method using the three most abundant ions for methanethiol (*m/z* 45, *m/z* 47, and *m/z* 48) and dimethyl disulfide (*m/z* 94, *m/z* 79, and *m/z* 45).

As methanethiol partly dimerizes to dimethyl disulfide under the given conditions, the proposed methodology of Belda *et al*. for the calculation of relative *β*-lyase activity was used.[256]

4.2 Peptidase activities

4.2.1 Screening with skim milk agar plates at pH 3

For initial screening, skim milk agar plates were used, on which peptidase activity could be identified by clear halos around the cultures. For the preparation of these plates, 5 g L^{-1} casein and 28 g L^{-1} skim milk powder were dissolved in ddH_2O, the pH was adjusted to a value of 3 with HCl and the solution was boiled several times in the microwave for a period of 15 minutes. The solution was then stored for one hour at 80 °C in a drying oven and incubated overnight at room temperature. On the next day, the solution was again boiled several times in the microwave for 15 minutes and stored in the drying oven at 80 °C for one hour.

After cooling to approximately 70 °C, the solution was combined with 700 mL of an autoclaved solution of 2.5 g L^{-1} yeast extract, 1 g L^{-1} glucose, and 15 g L^{-1} agar in ddH_2O. 34 µg mL^{-1} chloramphenicol was added and plates were poured.

10 µL of yeast cultures grown overnight in microplates in YPD-medium were transferred to the plates and the plates were incubated at 30 °C for 48 h. Subsequently, the formation of clear halos was examined.

4.2.2 Assessment of peptidase activity in must

The must peptidase assays were performed using a Pierce BCA protein assay kit from ThermoFisher scientific (Massachusetts, USA) in a microtiter plate format. Prior to the experiments, the strains were cultured in YPD-medium. Subsequently, the cultures were centrifuged and resuspended in ddH_2O. The optical density of the suspensions was measured at 600 nm and diluted to a value of 0.1. 600 µL of the respective must were inoculated with 10 µL of the cell suspension and incubated for the indicated period of time.

Subsequently, the cultures were centrifuged again and 25 µL of a 1:100 dilution of the supernatant was added to the BCA assays. The BCA assay was performed according to the protocol for use in microtiter plates.

The illustrated results represent the relative reduction of the measured signal in relation to the signals of the corresponding must without yeast inoculation.

4.3 Pectinase activities

4.3.1 Initial screening on pectin agar plates

Since an antimicrobial effect of pectin has been described,[260] an initial screening was first performed to check whether the yeast strains are able to grow well in the presence of pectin. For this purpose, 5 g pectin from citrus peel in 300 mL ddH_2O and 7.5 g agar in 150 mL ddH_2O were separately autoclaved. After cooling to 70 °C, the two solutions were combined with 50 mL of a sterile-filtered (0.22 µm) 10 × stock solution of yeast nitrogen base with sugar (67 g L^{-1} Yeast Nitrogen Base, 50 g L^{-1} glucose). Subsequently, 10 µL of a culture grown over 48 h in YPD-medium from each isolate of the library of autochthonous microorganisms was dropped onto the agar plates. After 48 h of incubation at 30 °C, the growth of the cultures was observed. The cultures that stood out by forming large colonies were selected for the screening on polygalacturonic acid plates.

4.3.2 Screening on polygalacturonic acid plates

For galacturonase screening, the same recipe as for the pectin plates was used in which pectin was replaced with 2.5 g polygalacturonic acid. After 48 h of incubation at 30 °C, the agar plate was flooded with 5 mol L^{-1} HCl and incubated at room temperature for one hour. Subsequently, the appearance of clear halos due to polygalacturonic acid degradation was evaluated. The enzyme preparations for positive controls were purchased from https://schnapsbrenner.eu/.

4.4 *β*-Glycosidase activities

4.4.1 Comparative investigations on different *β*-glycosidase surrogate substrates

4.4.1.1 Agar plate assays

For esculin agar plates a solution of 0.3 g ferric chloride, 1 g casein hydrolysate, 25 g yeast extract, 8 mL glycerol, 20 g agar and 1 g esculin in 1 L ddH_2O was autoclaved and poured into Petri dishes.[158] For arbutin plates, an equal amount of arbutin instead of esculin was used (respective data is not shown). For liquid assays with arbutin or esculin, the medium was prepared without agar. After incubation of the commercially available yeasts for 48 h, the formation of brown color was examined.

4.4.1.2 Photometric measurements

The below mentioned wavelengths for the measurements were previously identified for each surrogate substrate by performing excitation and emission scans between 300 and 600 nm of 100 µL samples with 5 mmol L^{-1} surrogate concentration in 100 mmol L^{-1} citrate-phosphate buffer pH 7. The absorbance of p-nitrophenol (pNP) was measured at 400 nm. Fluorescence emission of 4-methylumbelliferone (4-MU) was measured at 450 nm after excitation at 330 nm, whereas fluorescence emission of esculin was measured at 454 nm after excitation at 367 nm. Fluorescence emission measurements of arbutin were performed at 325 nm after excitation at 260 nm. For the assay with pNP, transparent microplates were used. Arbutin, esculin and 4-MU were analyzed in black microplates. The amplification of the fluorescence signal after the transformation from light into electricity (Gain) was set to 60 AU for all fluorescence measurements.

4.4.1.3 β-Glycosidase substrate hydrolysis in solution

Enzyme kinetics were measured in 100 mmol L^{-1} citrate-phosphate buffer pH 7 at room temperature after the addition of 10 µL of a 2.5 U mL^{-1} solution of *β*-glycosidase from almonds to the samples. Arbutin, esculin or 4-MUG were added using 100 µL of a 5 mmol L^{-1} solution. Fluorescence spectra were measured in the same samples following the kinetic measurements. Accordingly, 50 µL of a 10 mmol L^{-1} solution of pNPG were used for the experiments. Before measurement, 50 µL of 0.1 mol L^{-1} Na_2CO_3 was added to the sample. The absorbance spectra of pNP were determined 20 min after enzyme addition. The total assay volume was 110 µL.

4.4.1.4 Comparison of assay sensitivity and linearity

50 µL of a 10 mmol L^{-1} 4-MUG or pNPG solution in 100 mmol L^{-1} citrate-phosphate buffer pH 7 were used and the assay was started by the addition of 10 µL of different almond *β*-glycosidase sample dilutions. Afterwards, the increase in absorbance or fluorescence was measured for five minutes. Samples of pNPG were mixed with 40 µL of a 0.1 mol L^{-1} Na_2CO_3 solution, samples of 4-MUG with 40 µL H_2O before measurement. The signal emission slope per minute was calculated based on the measured values. For the pNPG assays, enzyme amounts which resulted in constant slopes over an assay time of five minutes were used.

4.4.1.5 Determination of pH robustness of 4-MU quantification

Fluorescence spectra were measured in 50 µL of a 10 mmol L^{-1} 4-MU solution which was combined with 50 µL of a 100 mmol L^{-1} citrate-phosphate buffer of the mentioned pH value. For the estimation of glucose and ethanol influences, the applied buffer was supplemented with the respective component. The total volume of the reaction mixture was 100 µL.

4.4.1.6 Fluorescence microscopy

The investigated cultures were grown for 48 h in deepwell plates containing 600 µL YPD-Medium. After 10 min incubation at room temperature, images were acquired with an Axio Imager Z1 m fluorescence microscope (Carl Zeiss AG, Oberkochen, Germany) using a DAPI filter. The exposure time was set to 15 seconds.Prior to imaging, 50 µL of cultures of *Aureobasidium pullulans* (CBS 100280) and *Issatchenkia terricola* (obtained from the strain collection of the HGU) were combined with 50 µL of a 0.76 mmol L^{-1} 4-MUG solution[162] in 100 mmol L^{-1} citrate-phosphate buffer pH 5.6.

4.4.2 Investigation of non-*Saccharomyces* yeasts with intracellular *β*-glycosidase activity for wine aroma modification

4.4.2.1 Screening

A library of 2112 strains, originating from the strain collection of the HGU, was cultivated in YPD-medium for 48 h. Activity in the supernatant was measured after a centrifugation step. For the activity assessment of the cell lysates, the cells were resuspended in an equivalent amount of 100 mmol L^{-1} citrate-phosphate buffer pH 7 after the centrifugation and mixed with 0.1 g glass beads. Cell disruption was performed by mixing for 20 minutes at 2000 rpm on a BioShake iQ shaker (QInstruments, Jena, Germany). The cell lysate was centrifuged again followed by careful separation of the supernatant.

β-Glycosidase activity was measured using the surrogate substrate 4-methylumbelliferyl-*β*-D-glucopyranoside (4-MUG) in a microtiter plate assay.[162] 10 µL of culture, supernatant or cell lysate were combined with 50 µL of 100 mmol L^{-1} citrate-phosphate

buffer of the respective pH value. 50 mmol L^{-1} 4-MUG stock solution in DMSO was diluted with the appropriate buffer to a concentration of 0.76 mmol L^{-1}. After starting the reaction by mixing the 4-MUG solution with the buffer and the sample, the fluorescence signal was measured every 30 seconds for 15 minutes. Respective graphs show the calculated increase of the fluorescence signal per minute in arbitrary units (AU).

4.4.2.2 Cultivation in the presence of putative β-glycosidase inducers

In preliminary studies, the exponential growth phase of the investigated strains was observed after 48 h of cultivation under the applied conditions. Therefore, this cultivation time was selected for conducting the experiments. The strains were cultivated for 48 h either in YPD-medium (50 g L^{-1} glucose), or in YPD-medium with reduced glucose content (5 g L^{-1}) and the addition of 15 g L^{-1} naringin, hesperidin or cellulose. In all cases, *β*-glycosidase activity was determined with the aforementioned assay in 100 mmol L^{-1} citrate-phosphate buffer at pH 3.

4.4.2.3 Investigation of pH-tolerance of whole cells and cell lysates

For the examination of whole cells, the cells were centrifuged and resuspended in the respective buffer. Cell lysates were obtained following the procedure described above, using 100 mmol L^{-1} citrate-phosphate buffer of the pH value mentioned. The 4-MUG assay[162] was performed after 2 h of incubation at room temperature. Subsequently, the differences in fluorescence signal strength caused by the released 4-MU were determined.

4.4.2.4 Confocal laser scanning microscopy

A Leica TCS SP8 microscope with an HC PL AP0 CS2 63x/1.20 objective was used for the images shown. The laser intensity was set to 12 % with a 405 nm diode, a PMT detector (415 nm - 600 nm) was operated with a scanning speed of 400 Hz.

4.4.2.5 Aroma compound release from glucoside extracts

The used glucoside extracts were obtained following a modified method for solid phase microextraction[261] from Muscaris must derived from grapes harvested in 2018. 200 mg Lichrolut EN tubes were equilibrated with 4 mL dichloromethane and 4 mL methanol, then 20 mL must was passed through the column. Afterwards, the column was rinsed with 10 mL distilled water and free terpenes were separated with 2 mL dichloromethane. The terpene-glycosides were eluted with 2 mL methanol, concentrated to dryness and dissolved in 2 mL 100 mmol L^{-1} citrate-phosphate buffer pH 5.6. For the negative control, the glycoside extract was incubated under the same conditions without addition of culture or cell lysate.

200 µL of the glycoside extract was added to 100 µL of the cell suspensions or extracts and incubated in 2 mL glass vials at room temperature. A Gerstel PDMS twister (Gerstel GmbH & Co. KG, Mülheim an der Ruhr, Germany) was attached to the headspace of the vial with a magnet.

After 24 h of incubation, the substances bound to the twister were measured by GC-MS. The GC program started with a hold time of 1.5 minutes at 40 °C, then the temperature was increased to 100 °C at a rate of 10 °C min^{-1}. Afterwards, the temperature was elevated to 165 °C at a rate of 4 °C min^{-1}. The column was then heated to 250 °C at a rate of 10 C° min^{-1} and finally reached 300 °C at 13 °C min^{-1}. The components were tentatively identified using the NIST Mass Spectral Library.

4.4.2.6 Determination of ethanol, glucose and must effects on β-glycosidase activity

To determine the influence of glucose and ethanol, assays were performed according to the screening procedure. The cells were centrifuged after cultivation and resuspended in 100 mmol L^{-1} citrate-phosphate buffer pH 3. The buffer was mixed with 2.2 times the indicated concentration of glucose or ethanol. For the investigation of the activity in must, the whole assay was performed directly in must or the indicated dilutions.

4.5 *β*-Lyase activities

4.5.1 Engineering yeast strains for high thiol release activity by a directed evolution approach using SMC

4.5.1.1 Screening in medium with SMC as sole nitrogen source

For growth-based screening for strains with high *β*-lyase activity, a SMC-medium[256] was used as described previously. For further investigations, a synthetic medium according to the same recipe but without the addition of SMC was prepared and supplemented with nitrogen sources as described in the figure legends. Cells were first grown in 600 µL YPD-medium for 48 h. From these cultures, 20 µL were transferred into 180 µL of SMC medium and cultured under identical conditions for additional 48 h. Subsequently, the cell density of the cultures (OD_{600nm}) was determined using a microtiter plate reader and adjusted to a value of 1.0 by addition of SMC medium. 180 µL SMC medium was inoculated with 20 µL of these cell suspensions and incubated for 48 h before the cell density (OD_{600nm}) was determined using a microtiter plate reader.

4.5.1.2 **Trans***formation procedure*

After transformation with pBK_*tnaA*, the cells were plated on YPD-agar containing 0.2 mg mL^{-1} G418.[196] A strain linked to the highest *β*-lyase activity in previous experiments (data not shown) was used for the described experiments.

4.5.1.3 Adaptive laboratory engineering approach with SMC medium

The directed evolution approaches were performed in 10 mL SMC medium in 100 mL Erlenmeyer flasks. The cultures were grown for 48 h at 180 rpm and 30 °C. Subsequently,

10 µL of the culture was transferred to another flask containing new SMC medium, followed by further cultivation. In total, the over-inoculation procedure was performed 25 times before the growth of the populations was characterized.

To determine the growth characteristics of the different strains in SMC medium, cells were precultured in microtiter plates for 24 h. Afterwards, the cell density (OD_{600nm}) was determined, and the cultures were diluted with SMC medium to achieve an OD_{600nm} value of 1.0. 180 µL of SMC medium in microtiter plates was inoculated with 20 µL of this cell suspension and incubated at 30 °C. Every 30 minutes, shaking was performed for 10 seconds at 240 rpm with an amplitude of 2 mm, and the optical density was determined at 600 nm with a microtiter plate reader.

4.6 Engineering volatile thiol formation in yeast

4.6.1 Post-transformation procedure

Post-transformation methods differed depending on the transformed plasmid. After transformation with the *tnaA* expression construct, the cells were plated on YPD-agar containing 0.2 mg mL^{-1} G418.[196] Twelve transformants were randomly selected from the transformation plate and used in the DTNB assays. After transformation with the pPK plasmids, the yeast cells were plated on synthetic complete dextrose (SCD) medium (6.7 g L^{-1} yeast nitrogen base without amino acids and with ammonium sulfate, appropriate yeast synthetic drop-out medium supplements and 20 g L^{-1} glucose) plates. SCD medium pH was adjusted to 6.3 with potassium hydroxide. SCD medium agar plates lacked uracil or L-tryptophan or both, depending on the used plasmid or plasmids.

4.6.2 Whole cell bioconversions

For the assessment of thiol production, cells were cultivated for 48 h at 30 °C and 180 rpm in 50 mL SCD medium in 250 mL Erlenmeyer flasks. Since the integration of *tnaA* into the genome is stable, G418 was not added to the media after the initial selection. *S. cerevisiae* strains were cultivated in YPD-medium or SCD medium. If needed for selection or plasmid maintenance, medium without uracil and L-tryptophan was used.

After 48 h of growth, the cultures were transferred to 50 mL falcon tubes and centrifuged. Subsequently, the cells were resuspended in 5 mL 100 mmol L^{-1} citrate-phosphate buffer pH 7 and the cell density was determined by measuring the OD_{600} value with a photometer. For the assay, 100 µL of 1 mg L^{-1} substrate stock in H_2O were combined with the amount of cell suspension corresponding to the indicated optical density in the final volume. Afterwards, 100 mmol L^{-1} citrate-phosphate buffer pH 7 was added until the final volume of 1 mL was reached. The assays were performed in 10 mL screwcap-vials and a twister was

attached to the headspace of the vial with a magnet. Thereafter, the assays were incubated for 24 h at 25 °C and 350 rpm on a BioShake iQ shaker (QInstruments, Jena, Germany).

2 h before the end of the incubation period, the magnet was removed, the twister was transferred to the liquid and subsequently stirred with a magnetic stirrer at 80 rpm. Afterwards, the twister was removed from the vial, rinsed with ddH_2O, dried and transferred to sample tubes for thermodesorption.

For the pH value optimization, 100 mmol L^{-1} citrate-phosphate buffer of the specified pH value was used for all steps. Pyridoxal-5-phosphate, glutathione and cysteine were added to the assays via 10 mmol L^{-1} stock solutions. Furthermore, different buffers and media were used instead of 100 mmol L^{-1} citrate-phosphate buffer for the reactions to test resulting effects.

4.6.3 GC-MS analysis

The GC program started with a hold time of 1.5 min at 40 °C, then the temperature was increased to 100 °C at a rate of 10 °C min^{-1}. Afterwards, the temperature was elevated to 115 °C at a rate of 4 °C min^{-1}. The column was heated to 300 °C at a rate of 13 °C min^{-1}. The thiol compound measurements were performed in scan mode between *m/z* 45 and *m/z* 400. After a twister was incubated for 2 h in 1 mL solution of water containing 100 µg L^{-1} of each substrate, a preliminary measurement was taken with a split setting of 20 to determine the elution time of the substrate peak. The split ratio was adjusted according to higher product volumes to prevent overloading of the column and the detector. For the same reason, the detector was switched off 0.1 s before and after the substrate peak. In the comparative analysis of the product peaks using aldehydes and alkenols as substrates, the samples of the C_5-compounds were measured with a split setting of 20 while the samples of the C_6- and C_7-compounds were measured with a split setting of 60.

The 3MH reference compound eluted after 10.84 min with the described method. For the detection of 3MH, a SIM method based on the three most abundant fragments *m/z* 55, *m/z* 57, and *m/z* 100 and measurements between 10 and 12 min was used.

To quantify the measured 3MH amounts, calibrations were performed at pH 7 with different cell densities and split settings. For this purpose, assays were prepared without the addition of substrate and incubated with twisters in the headspace for 21 h. The reactions were then supplemented with 3MH concentrations between 0.5 µg L^{-1} and 25 µg L^{-1} and incubated for 1 h. Afterwards, the twisters were transferred to the liquid and measured after an additional incubation time of 2 h. Since the slope of the calculated calibration lines differed considerably between large and small 3MH concentrations, two independent calibrations were prepared.

5 Results

5.1 Peptidase activities

5.1.1 Initial screening on milk-agar plates

The procedure of the prescreening is visualized in Figure 16. After the initial screening of 2112 examined yeasts, 179 isolates (8.5 %) were found to produce noticeable clear halos around the colonies. These 179 strains were reapplied to milk agar plates and the size of the halos was examined. Subsequently, 45 isolates were selected for which the largest halos around the colonies were observed.

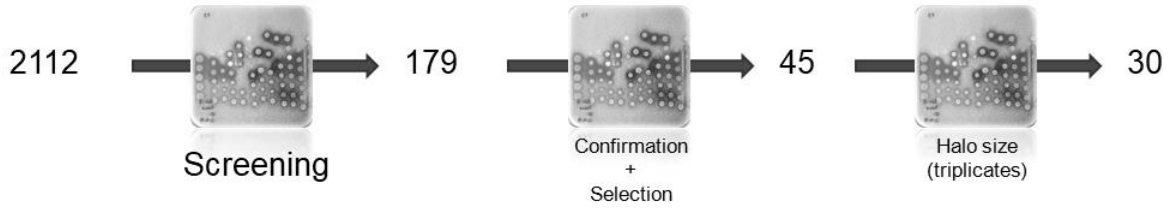

Figure 16: Screening procedure using skim-milk-agar plates. Strains with reproducible peptidase activity were identified by clear halos around their colonies due to protein degradation.

These selected 45 isolates were re-examined in triplicates. The 30 isolates with reproducible large halos were used in the subsequent experiments.

5.1.2 Activitiy confirmation with BCA-Protein assays

The 30 identified isolates from the previously described screening procedure were cultivated for 96 h in grape must. Afterwards, the reduction of BCA signal corresponding to the protein amount was examined in comparison to must samples without inoculation (Figure 17).

In general, the BCA signal reduction was lowest in Müller-Thurgau must. After incubation, the values decreased up to 39 %. The samples of the grape varieties Gewürztraminer and Muscaris revealed even greater reductions of the measured values. The strains 1-8 showed the steepest decrease in signal strength in Gewürztraminer must, while strain 7 led to the highest decrease with 76 % reduction. In Muscaris must, the strains 1-8 led to a BCA signal decrease of over 60 %, while strain 7 again led to the lowest values which were reduced about 74 %.

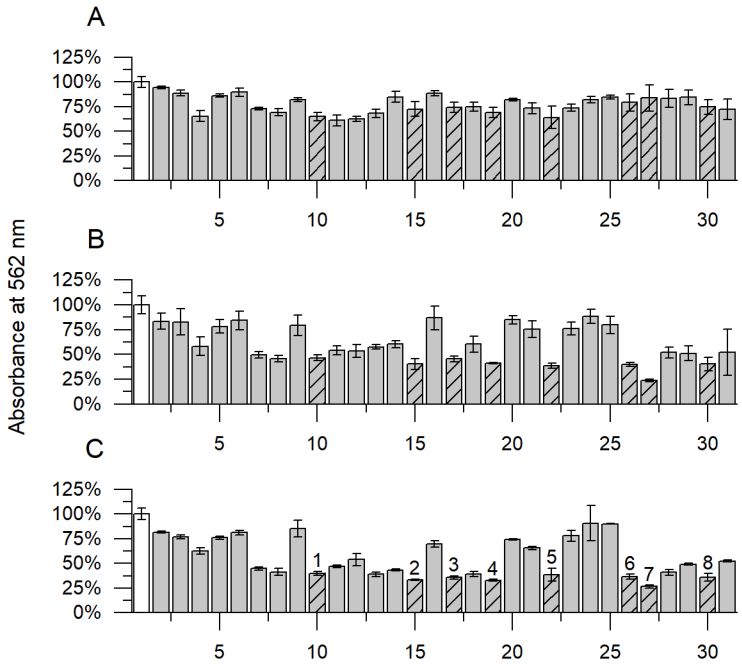

Figure 17: BCA signal reduction after 96 h cultivation of the identified strains in various musts. Some of the selected strains led to strong reduction of the protein signal at 562 nm. The measured absorbance values for the non-inoculated negative controls of A) Müller-Thurgau must: 0.41 AU, B) Gewürztraminer must: 0.46 AU, C) Muscaris must: 0.56 AU were set to 100 % (white bars).

The 8 strains with the greatest reduction of the BCA signal after the cultivation in Gewürztraminer and Muscaris must (dashed bars) were identified by sequencing of their ITS regions. While all strains belonged to the *Metschnikowia* genus, two strains were identified as *Metschnikowia chrysoperlae* (Table 4).

Table 4: Classification of the selected strains which resulted in strong decreased values in the protein quantification assays. Strains with the most pronounced reduction in protein signals were identified using ITS sequencing. All identified isolates were assigned to the genus *Metschnikowia*.

ID	Identification
1	*Metschnikowia pulcherrima*
2	*Metschnikowia pulcherrima*
3	*Metschnikowia chrysoperlae*
4	*Metschnikowia chrysoperlae*
5	*Metschnikowia pulcherrima*
6	*Metschnikowia pulcherrima*
7	*Metschnikowia pulcherrima*
8	*Metschnikowia pulcherrima*

The identified isolates of Table 4 were subsequently inoculated into Muscaris must of a different vintage (2020) and the decrease of BCA signal was additionally examined after a longer period of time (168 h). To better assess the peptidase activity of the identified isolates, a commercially available *Metschnikowia pulcherrima* preparation (Lallemand Flavia MP346) was also included in these experiments.

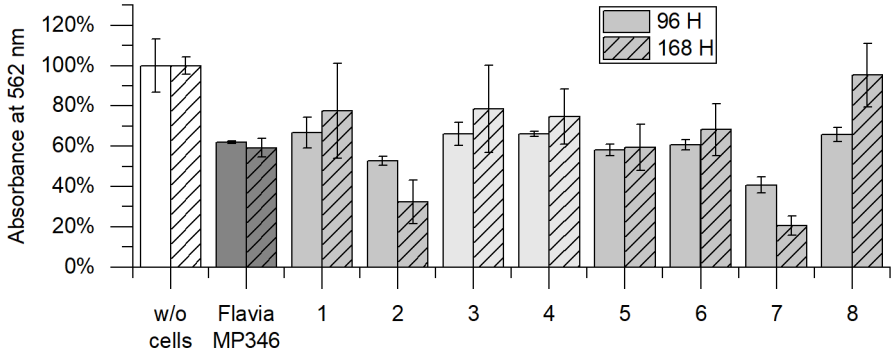

Figure 18: BCA signal reduction after 96 h and 168 h cultivation of the identified strains in Muscaris must derived from grapes harvested in the year 2020. The absorbance values of the negative controls without yeast addition after 96 h (0.56 AU) and 168 h (0.54 AU) were set to 100 % (white Bars). *Metschnikowia chrysoperlae* strains are illustrated in light grey.

As shown in Figure 18, some of the previously identified isolates led to significantly reduced values in the BCA assay with Muscaris must of the 2020 vintage. The commercial *Metschnikowia pulcherrima* preparation Flavia MP346 led to a reduction of the protein signal by 38 % after 96 h. No further decrease in signal was detected after 168 h. Isolates 1 and 3-6 showed similar patterns to the commercial preparation. Values of isolate 8, after an initial 40 % reduction at 96 h, again increased to levels comparable to the non-inoculated must at 168 h.

Strains 2 and 7, however, showed even more significant changes in the protein concentrations. In strain 2, the signal was reduced by 48 % after 96 h and by 68 % after 168 h. Strain 7 resulted in a reduction of 60 % after 96 h and 80 % after 168 h.

The strains associated above with the highest peptidase activities were subsequently used in fermentation experiments with the assessment of the liberated aroma compounds at the HGU.

5.2 Pectinase activities

Out of the 2112 screened isolates, only 161 isolates (7.6 %) were able to grow well on the pectin medium. An additional screening on YNB plates with polygalacturonic acid was performed with the 161 strains exhibiting strong growth on pectin media.

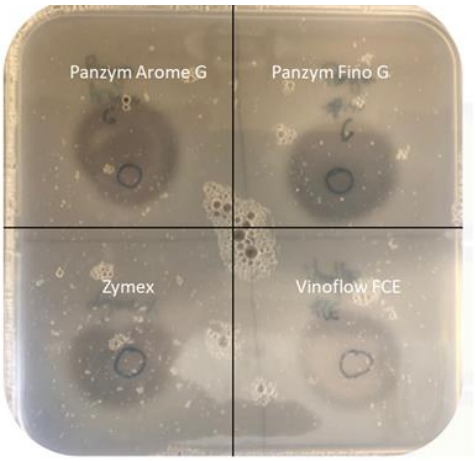

Figure 19: Positive control of the polygalacturonic acid agar plate assay with commercial preparations advertised with pectinase activity. 50 µL of a 100 mg mL^{-1} enzyme solution was applied and the plate was incubated overnight at 37 °C. Subsequently, the plate was flooded with 5 M HCl and incubated for one hour at room temperature.

Unfortunately, no clear halo formation could be detected for any isolate during the screening performed. Figure 19 illustrates a positive control with commercial pectinase preparations, the application of which resulted in the formation of the sought-after clear halos.

5.3 *β*-Glycosidase activities

5.3.1 Comparative investigations on different *β*-glycosidase surrogate substrates

5.3.1.1 3.1. Necessity of photometric assays for reliable β-glycosidase activity determination

In published *β*-glycosidase activity screenings, arbutin and esculin are often used in the context of agar plates to which iron compounds like ferric ammonium citrate[14] or ferric chloride[158] are simultaneously added. The complexation of iron by the released aglycons leads to the visible formation of a dark brown precipitate which indicates *β*-glycosidase activity. Initial tests with both compounds confirmed their suitability for the respective assays in liquid culture. However, the outcome of the respective tests with yeast suspension cultures of several commercially available wine yeasts was different from the corresponding agar plate assay result in many

cases (Figure 20). Only two of the commercial wine yeast strains caused a dark staining in the agar plate assay and in the liquid culture assay with esculin. According to the supplier specifications, Kitzinger Aromatic is able to improve flavor diversity during fermentation, while Bioferm Malic improves the degradation of malic acid. One strain (Bioferm Rouge) caused no staining in both assays, but the other eight strains led to contrary results. Whereas the Kitzinger strains Champagner, Portwein, Universal, Bordeaux and Steinberg showed positive signals only in the liquid assays, the Bioferm strains Blanc, Doux and Killer caused iron complexation only in the agar plate assays.

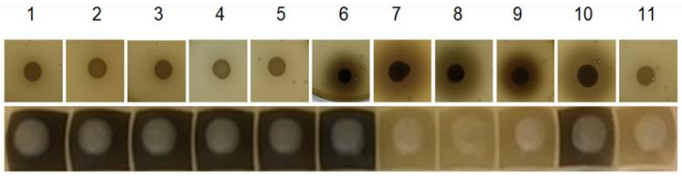

Figure 20: Comparison of esculin-based *β*-glycosidase activity detection on agar plates and in liquid culture. The *β*-glycosidic activity of commercial wine yeasts was detected by the occurrence of dark staining after cultivation on esculin-agar plates (top row) and in liquid esculin-containing media (bottom row). Details are described in the material and methods section. 1) Kitzinger Champagner, 2) Kitzinger Portwein, 3) Kitzinger Universal, 4) Kitzinger Bordeaux, 5) Kitzinger Steinberg, 6) Kitzinger Aromatic, 7) Bioferm Blanc, 8) Bioferm Doux, 9) Bioferm Killer, 10) Bioferm Malic, 11) Bioferm Rouge.

Because previous experiments revealed the possibility of direct fluorescence measurement of arbutin and esculin (data not shown), these compounds were measured in the following experiments without the addition of iron to estimate their suitability for photometric assays.

5.3.1.2 Comparison of the surrogate substrates for photometric assays

After investigation of the absorbance or fluorescence properties of all compounds in form of the glycoside or the aglycon in scanning experiments (Figure S 6), their hydrolysis was followed photometrically in experiments with 100 µL of a 5 mmol L^{-1} glycoside solution to which almond *β*-glycosidase was added to a final concentration of 0.23 U mL^{-1} (Figure 21). The corresponding fluorescence emission and absorbance spectra are presented in Figure S 6.

Investigation of the arbutin solution showed fluorescence signals with an emission maximum at 325 nm under the selected conditions (Figure 21 A). After the addition of almond *β*-glycosidase, the signal intensity slowly decreased within 12 h of measurement. Esculin showed higher fluorescence signals with an emission maximum at 455 nm, which rapidly decreased over 5 min after the addition of *β*-glycosidase (Figure 21 B).

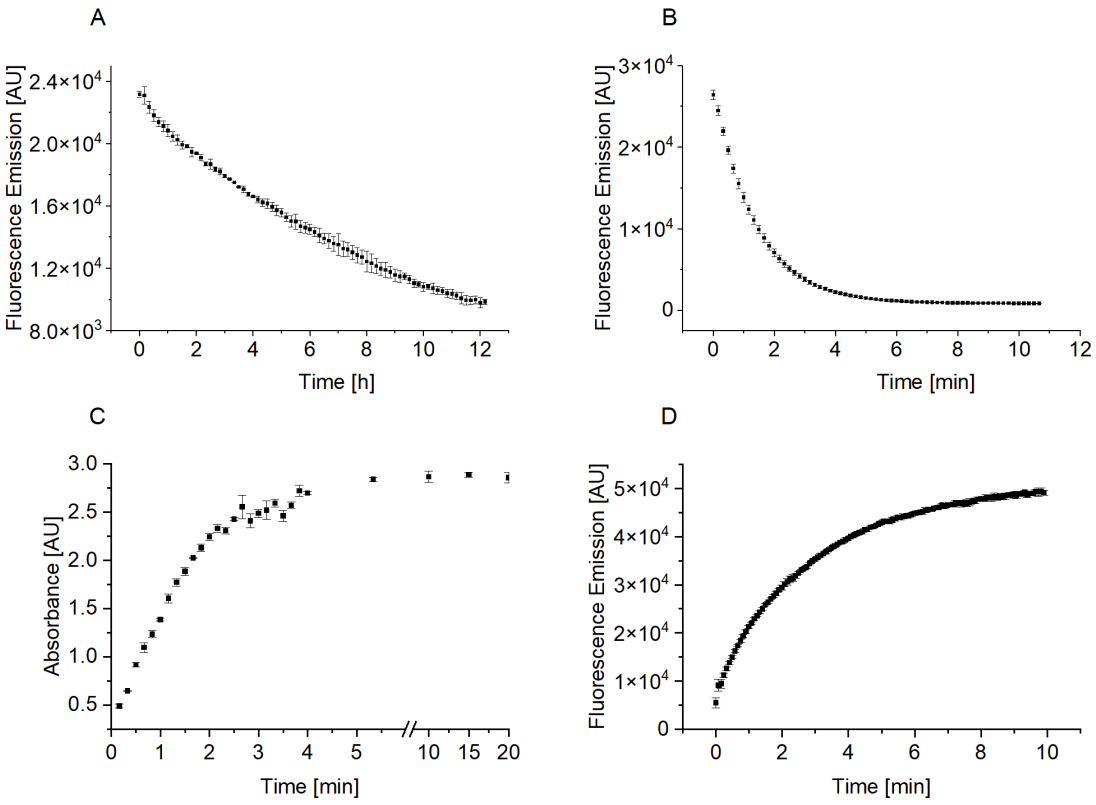

Figure 21: Photometric detection of *β*-glycosidase surrogate substrate hydrolysis in liquid assays. Shown are the resulting changes of signal intensity after the addition of almond *β*-glycosidase to a final concentration of 0.23 U mL^{-1} to 100 µL of a 5 mmol L^{-1} solution of A) Arbutin, B) Esculin, C) pNPG, D) 4-MUG. Used wavelengths are given in the material and methods section. Experiments were conducted in triplicates. The values represent the mean values of three experiments and respective standard deviations.

In comparison, *β*-glycosidase-catalyzed pNPG hydrolysis led to increasing absorbance values with a maximum at 400 nm (Figure 21 C). 4-MUG hydrolysis led to increasing fluorescence signals at 450 nm up to 50,000 units within 10 min after addition of the enzyme (Figure 21 D).

Hydrolysis of arbutin, esculin, pNPG or 4-MUG by almond *β*-glycosidase clearly resulted in changes of the detectable photometric signals.

5.3.1.3 Assessment of assay limitations and linearity

Based on the previously performed experiments, 4-MUG and pNPG were identified as the most promising surrogate substrates. However, for the detailed characterization of *β*-glycosidases, a reliable quantification of the activity is of high importance. Due to the different measurement methods of the two surrogate substrates, differences in the quantification limits are very likely. To further investigate these differences, varying amounts of almond *β*-glycosidase were added to the surrogate substrates and the resulting signal increase was compared (Figure 22).

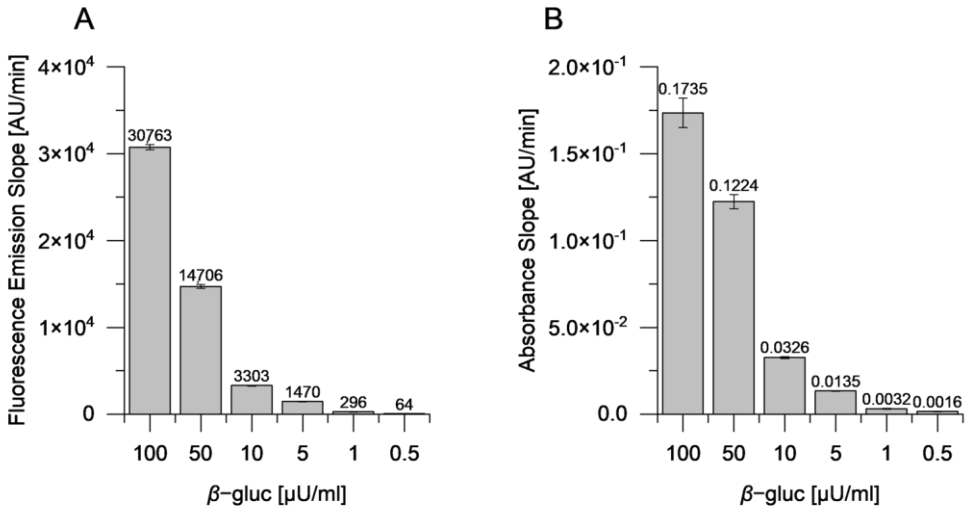

Figure 22: Comparison of enzyme activity quantification using 4-MUG or pNPG as surrogate substrates. The intensity increases of A) 4-MU and B) pNP signals after the addition of almond *β*-glycosidase to a final concentration of 100 µU mL^{-1}, 50 µU mL^{-1}, 10 µU mL^{-1}, 5 µU mL^{-1}, 1 µU mL^{-1} and 0.5 µU mL^{-1} are illustrated. The signal emission slopes were calculated from measurements for 5 min after the addition of almond *β*-glycosidase. Experiments were conducted in triplicates. The values represent the mean values of three experiments and respective standard deviations. The values for fluorescence and absorbance increase per minute are given in arbitrary units and were calculated as described in paragraph 4.4.1.4.

While a fluorescence signal intensity increase of 30763 AU per minute could be detected with 100 µU mL^{-1} of the enzyme in the reaction with 4-MUG as substrate, the signal strength was reduced from 14706 AU per minute (50 µU mL^{-1} *β*-glycosidase), over 1470 AU (5 µU mL^{-1} *β*-glycosidase) to 64 AU (0.5 µU mL^{-1} *β*-glycosidase). In comparison, the absorbance increase resulting from pNP formation by equal amounts of almond *β*-glycosidase declined unequally especially with high enzyme concentrations. The absorbance signal increase of 0.1735 AU per minute determined with 100 µU mL^{-1} of enzyme dropped to an absorbance increase of 0.0016 AU after the addition of 5 µU ml^{-1} of almond *β*-glycosidase.

The fluorescence signal increase of 4-MU is proportional to concentrations of almond *β*-glycosidase from 100 µU mL^{-1} to 1 µU mL^{-1}. Only the lowest tested enzyme amount

(0.5 µU mL^{-1}) was outside of the linear range. The observed changes in the absorbance signal of pNP, in contrast, did only show a linear correlation for enzyme concentrations up to 10 µU mL^{-1}.

5.3.1.4 Investigation of the pH robustness of 4-MUG assays

Due to the strong pH-dependence of pNP absorbance,[262] the samples have to be mixed with a Na_2CO_3 solution before the measurement. This procedure is time consuming, increases measurement inaccuracies and complicates kinetic measurements. To identify potential changes in the spectral properties of 4-MU, its emission spectra were analyzed at different pH levels (Figure 23 A). Furthermore, the influence of different concentrations of glucose (Figure 23 B) or ethanol (Figure 23 C) was investigated.

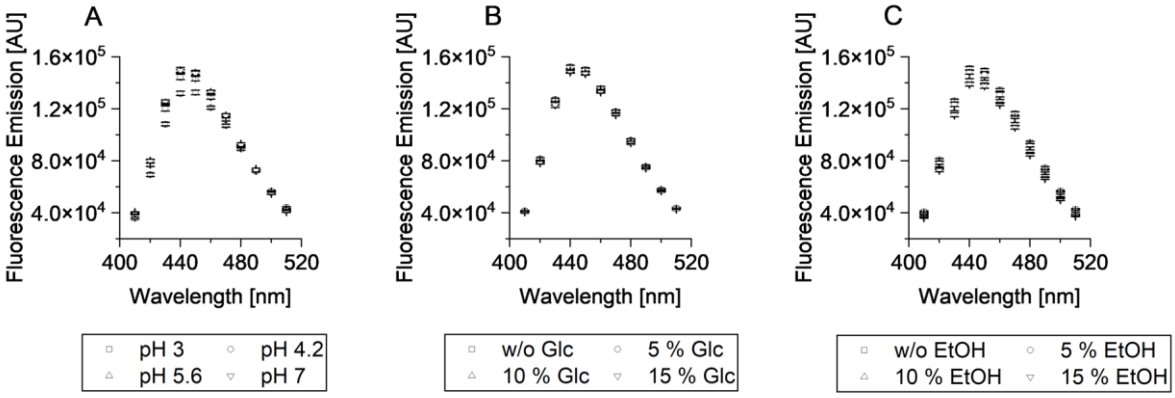

Figure 23: Investigation of 4-MU fluorescence variation due to changes of pH and ethanol or glucose addition. The absorbance spectra illustrate the 4-MU emission spectra at A) different pH values, B) different concentrations of glucose or C) different concentrations of ethanol. The excitation wavelength was 330 nm. Experiments were conducted in triplicates. The values represent the mean values of three experiments and respective standard deviations.

Whereas the addition of glucose did not affect the fluorescence emission, changes in the pH value or ethanol concentration resulted in slight changes of the signal intensity. With decreasing pH values, the fluorescence signal of 4-MUG was reduced from 150, 000 units (pH 7) to 130,000 units (pH 3). Moreover, the signal decreased from 150,000 units without the addition of ethanol to about 135,000 units at 15 % v/v ethanol.

5.3.1.5 Microscopic investigation of 4-MU localization in cultures with β-glycosidase activity

In order to evaluate, if 4-MUG can be used to investigate the localization of *β*-glycosidase enzymes in different strains, fluorescence microscopy analyses of cell cultures before and after the addition of 4-MUG (Figure 24) were performed.

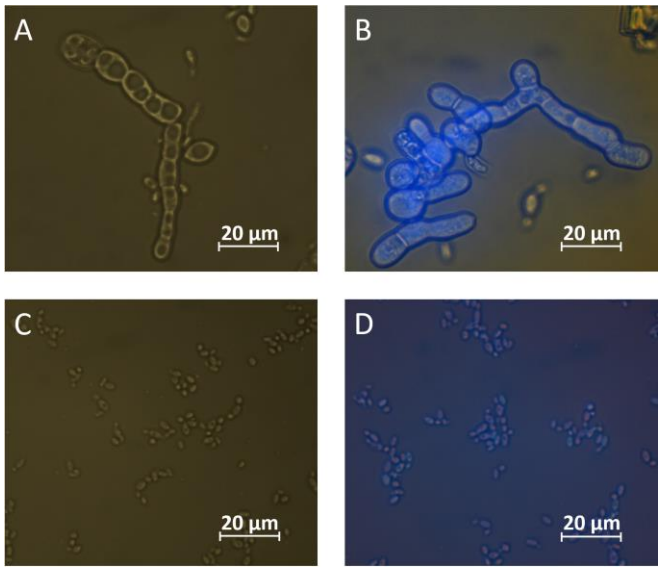

Figure 24: Visualization of 4-MU localization before (left) and after (right) the incubation of yeast cultures with 4-MUG. *A. pullulans* (A, B) and *I. terricola* (C, D) cultures were incubated with 4-MUG and analyzed via fluorescence microscopy as described in the material and methods section. The exposure time was identical for all pictures.

After addition of the surrogate substrate, *A. pullulans* cells exhibited 4-MU fluorescence signals in the cytoplasmic area (Figure 24 B). In the case of *I. terricola*, 4-MU fluorescence could be detected in the cells and in the culture medium (Figure 24 D).

5.3.2 Investigation of non-*Saccharomyces* yeasts with intracellular *β*-glycosidase activity for wine aroma modification

5.3.2.1 Screening approach to identify yeasts with cell-associated β-glycosidase activity

To identify yeast strains with cell-associated *β*-glycosidase activity, the strain collection was screened under different conditions. Besides sampling of culture supernatants, untreated culture samples including the cells and cell lysates were tested. A high diversity of *β*-glycosidase properties in the investigated yeast cultures was observed. Figure 25 shows exemplary data of the respective 50 strains with the steepest increase of the fluorescence signal resulting from hydrolysis of 4-MUG for each condition. Nearly all strains, whose cell cultures showed very high activity values at pH 7 (Figure 25 A), showed lower activity levels at pH 3. After glass beads treatment, the values decreased in comparison to the untreated cell culture values at pH 7 in all cases.

Figure 25 B shows the top 50 strains with regard to high activity of the culture samples at pH 3. Several cultures showed higher activity at pH 3 than at pH 7. Most of the presented strains showed almost no activity in the supernatant.

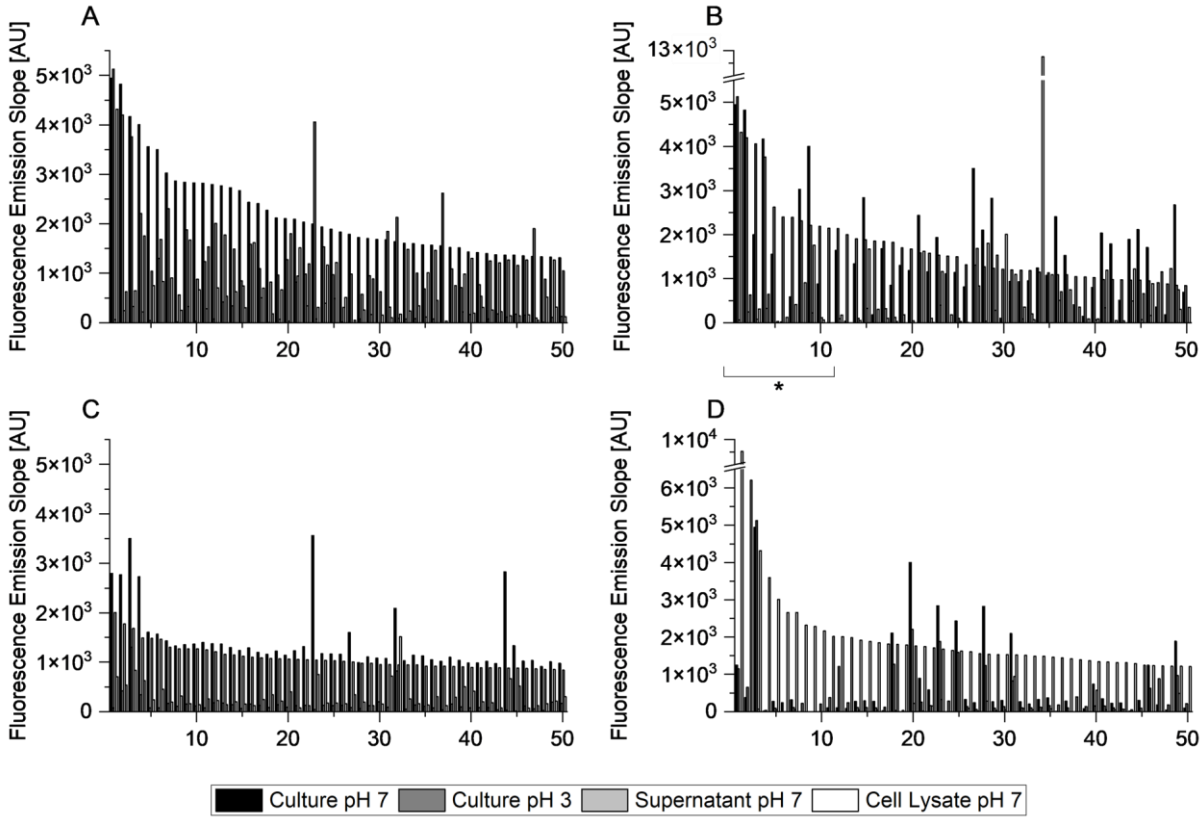

Figure 25: Comparative investigation of the top 50 strains obtained in the four different screenings. Each of the four graphs shows the data for one of the selected strain sets, which were analyzed again for *β*-glycosidase activities in the culture at pH 7 or pH 3, in the supernatant at pH 7 or in the cell lysate at pH 7. A) Strain set obtained in screening for high activity in whole culture samples measured at pH 7, B) Strain set obtained in screening for high activity in whole culture samples measured at pH 3, C) Strain set obtained in screening for high activity in culture supernatant samples measured at pH 7, D) Strain set obtained in screening for high activity in cell lysate samples measured at pH 7. The asterisk indicates the strains used in further experiments. The values for fluorescence increase per minute are given in arbitrary units and were calculated as described in paragraph 4.4.2.1. The calculated values are listed in Table S 1.

Although the focus of the approach was on the identification of strains with cell-associated *β*-glycosidase activity, the top 50 organisms with the highest values in supernatant samples measured at pH 7 (Figure 25 C) are also illustrated. In most cases, *β*-glycosidase activity of comparable extent could be detected at pH 7 in the untreated culture samples. It is however noticeable, that strains with high activity in the supernatant revealed only low activity in cell culture samples measured at pH 3. In general, a high number of organisms showed highly similar activity patterns.

In order to investigate the 96 strains with the highest activity in the culture supernatants for so far undiscovered organisms with suitable properties, a more detailed investigation was performed (Figure S 7). To simulate the particular conditions prevailing during must

fermentation, the activities of individual strains were additionally measured after addition of glucose and ethanol. Only a few strains showed *β*-glycosidic activity at low pH values, while one strain was capable of 4-MUG hydrolysis at pH 3 and at pH 5.6 after the addition of glucose and ethanol. Further experiments (Figure S 7 B) confirmed the properties of this strain identified as *Rhodotorula mucolaginosa*.

Most of the strains with the highest activities after cell disruption (Figure 25 D) showed only marginal activity in the culture samples measured at pH 7 or pH 3. As shown in Figure S 8, further investigations about the activity in cell lysates revealed, that there was no substantial *β*-glycosidase activity detectable at pH 3 and pH 5.6 with the addition of glucose and ethanol, while some strains showed activity at pH 5.6 after the addition of glucose. As mentioned before, the investigations were focused on the whole-cell biocatalyst approach using the top twelve candidates from Figure 25 B due to the promising activity levels at pH 3. The results of the sequencing of the ITS regions are illustrated in Table 5.

Table 5: Identity and quantity of the further investigated strains associated with promising *β*-glycosidase activity of whole cells at pH 3.

Strain identification	Number of identified strains
Wickerhamomyces spec.	4
Issatchenkia terricola	1
Aureobasidium pullulans	2
Nakazawaea ishiwadae	2
Hanseniaspora occidentalis	1
Candida railenensis	1
Bulleromyces albus	1

As the *β*-glycosidic properties of the yeast strains *H. occidentalis*, *C. railenensis* and *B. albus* have not been studied so far, these strains and the *N. ishiwadae* strain with higher activity at pH 3 were selected as potential whole cell biocatalysts for the following investigations.

5.3.2.2 Investigation of influences of possible β-glycosidase inducers

It has been reported that the addition of potential substrates to the culture medium can increase the production of hydrolytic enzymes.[263] For this reason, the selected strains were cultivated in media containing the natural glycosylated flavonoids hesperidin or naringin, or the disaccharide cellobiose. Figure 26 illustrates the measured activities of whole cultures of the selected strains at pH 3.

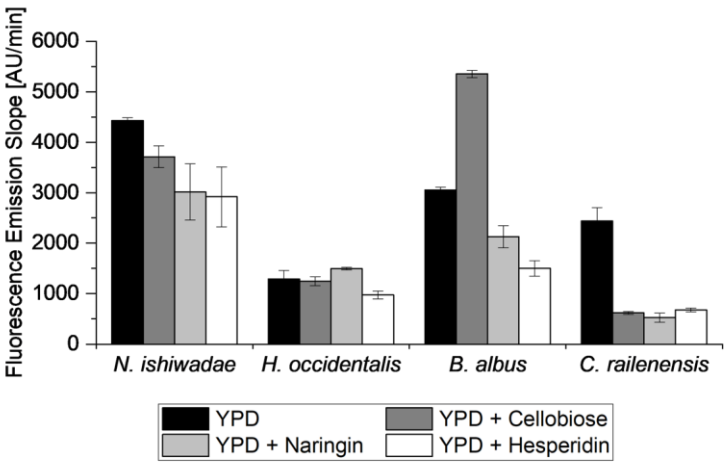

Figure 26: Influence of cellobiose, naringin or hesperidin addition on *β*-glycosidic activity. Measurements were performed with whole cultures at pH 3 after cultivation of the strains for two days in YPD-medium containing 5 % glucose or 0.5 % glucose and 1.5 % of the respective compound added. The values for fluorescence increase per minute are given in arbitrary units and were calculated as described in paragraph 4.4.2.1.

N. ishiwadae demonstrated the highest *β*-glycosidase activity (4427 AU min^{-1}) after cultivation on YPD, while other media led to a slight decrease in activity. In case of *H. occidentalis*, the compounds showed no clear effect on the 4-MUG conversion rate. *B. albus* showed clearly higher conversion rates after cultivation in the presence of cellobiose (5350 AU min^{-1}), while cultivation with naringin or hesperidin led to a decrease in activity. The activity of *C. railenensis* in media with cellobiose, naringin or hesperidin was much lower compared to the culture cultivated in YPD-medium (2440 AU min^{-1}).

5.3.2.3 Further investigation of β-glycosidase localization

The cultures of *N. ishiwadae*, *H. occidentalis*, *C. railenensis* and *B. albus* showed high *β*-glycosidase activity at pH 3 in untreated cell cultures, which suggests the involvement of cell-associated enzymes. However, it cannot be excluded that cells were partially lyzed before or during the assays and therefore 4-MUG hydrolysis did not necessarily involve import of the substrate. To investigate this issue in detail, the fluorescence of intact cells incubated with 4-MUG was examined under a confocal laser scanning microscope (Figure 27).

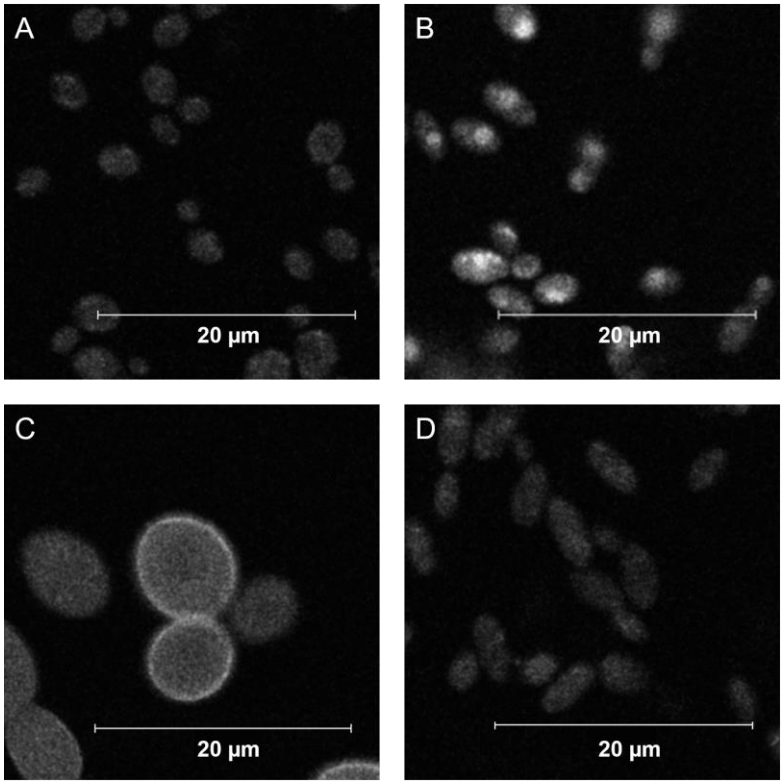

Figure 27: Investigation of the subcellular localization of the 4-MU fluorescence signal in cells of A) *N. ishiwadae*, B) *H. occidentalis*, C) *C. railenensis* and D) *B. albus*. Cells were incubated with 4-MUG and analyzed with a confocal laser scanning microscope as described in the material and methods section.

After addition of the surrogate substrate, cells of *N. ishiwadae* and *C. railenensis* showed predominantly homogeneous distribution of fluorescence all over the cytoplasma (Figure 27 A, D). For *B. albus*, an intensification of the signal at the periphery of many cells could be observed (Figure 27 C). *H. occidentalis* showed an accumulation of 4-MU-derived fluorescence signals in specific compartments of the cells (Figure 27 B).

5.3.2.4 Impact of whole cells on the pH stability of intracellular β-glycosidases

In order to investigate the proposed preservation of intracellular *β*-glycosidase activity by the cells, comparative measurements of enzyme activities of whole cells and cell lysates at different pH values were performed. Figure 28 illustrates the *β*-glycosidic activity of cells compared to disrupted cells at different pH values.

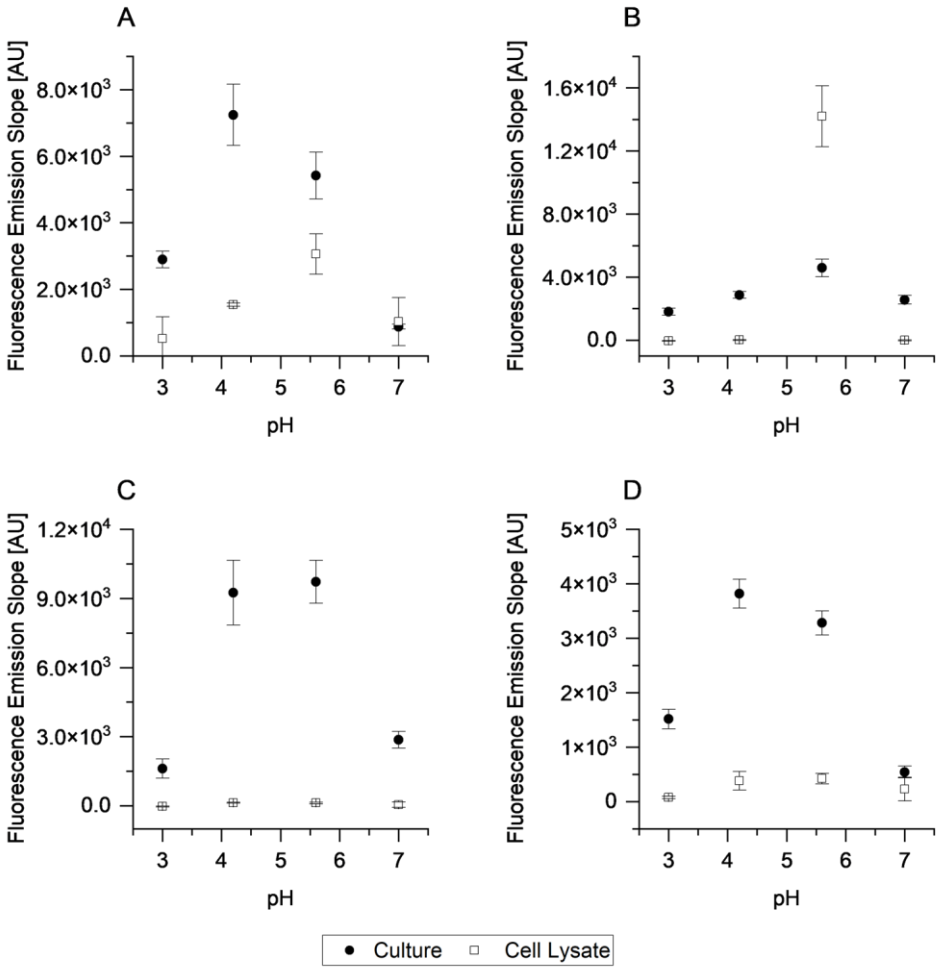

Figure 28: Comparison of pH profiles of *β*-glycosidase activity of cell cultures and cell lysates. Equal amounts of cells were used as biocatalysts in the form of cells or cell lysates. 4-MUG hydrolysis rates were determined as described in the material and methods section for A) *N. ishiwadae*, B) *H. occidentalis*, C) *B. albus*, and D) *C. railenensis*. The values for fluorescence increase per minute are given in arbitrary units and were calculated as described in paragraph 4.4.2.1.

In the cell lysate samples of *B. albus,* no significant activity was found. The highest values of the cell lysates *of N. ishiwadae*, *H. occidentalis* and *C. railenensis* were found at pH 5.6. The intact cells showed different results. For *N. ishiwadae* and *C. railenensis*, the highest activity was found at pH 4.2 and enzyme activity was still detectable at pH 3. For the selected strains, only whole cells showed *β*-glycosidic activity at low pH values.

5.3.2.5 Aroma liberation potential of whole cells and cell lysates

To investigate possible selectivity effects of whole cells on the release of terpenes as prominent example of aglycons in comparison to the free enzymes in cell lysates, the biocatalyst samples were combined with a glycoside extract prepared from Muscaris must (Figure 29). Since the highest activity levels after disruption were found at pH 5.6, this pH value was selected for the following experiments.

After 24 h, the samples of *C. railenensis* did not release any measurable amounts of aroma-active compounds derived from the hydrolysis of a *β*-glycosidic bond (data not shown). The other strains were able to release distinct amounts of different terpenes from the glycoside extract. Intact cells of *B. albus* and *H. occidentalis* released comparable amounts of (*Z*)-geraniol, α-terpineol and linalool. In addition, (*E)*-geraniol could be measured only after incubation with the cell lysates. The cell lysate of *H. occidentalis* furthermore released hotrienol. For *N. ishiwadae*, differences in the terpene profile released from the glycoside extract by whole cells and cell lysates were more pronounced. Whereas the amounts of (*E*)-geraniol, α-terpineol and linalool were higher with whole cells, the cell lysate released higher amounts of (*Z*)-geraniol. Hotrienol and terpinen-4-ol were only released from the glycoside extract by intact cells.

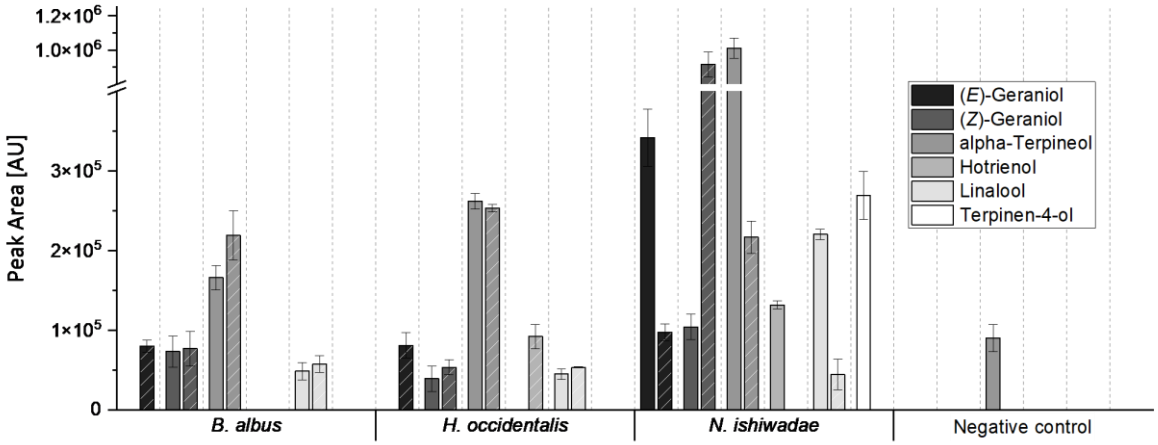

Figure 29: Comparative analysis of terpene release from Muscaris must glycoside extract by cell culture or cell lysate samples. After a 24 h incubation of glycoside extract with 100 µL of culture sample or cell lysate prepared from 100 µL cell culture at room temperature, the amounts of released terpenes were determined by trapping with a twister in the gas phase and subsequent GC-MS analysis. Solid bars show the peak areas determined in experiments with cell culture samples, dashed bars show the peak areas determined in experiments with cell lysates.

To further investigate the oenological potential of the described strains, the effect of glucose, ethanol or must on the 4-MUG hydrolysis rate of the cells was measured (Figure 30). A strong decrease of the *β*-glycosidic activities measured at pH 3 after the addition of glucose and ethanol was observed.

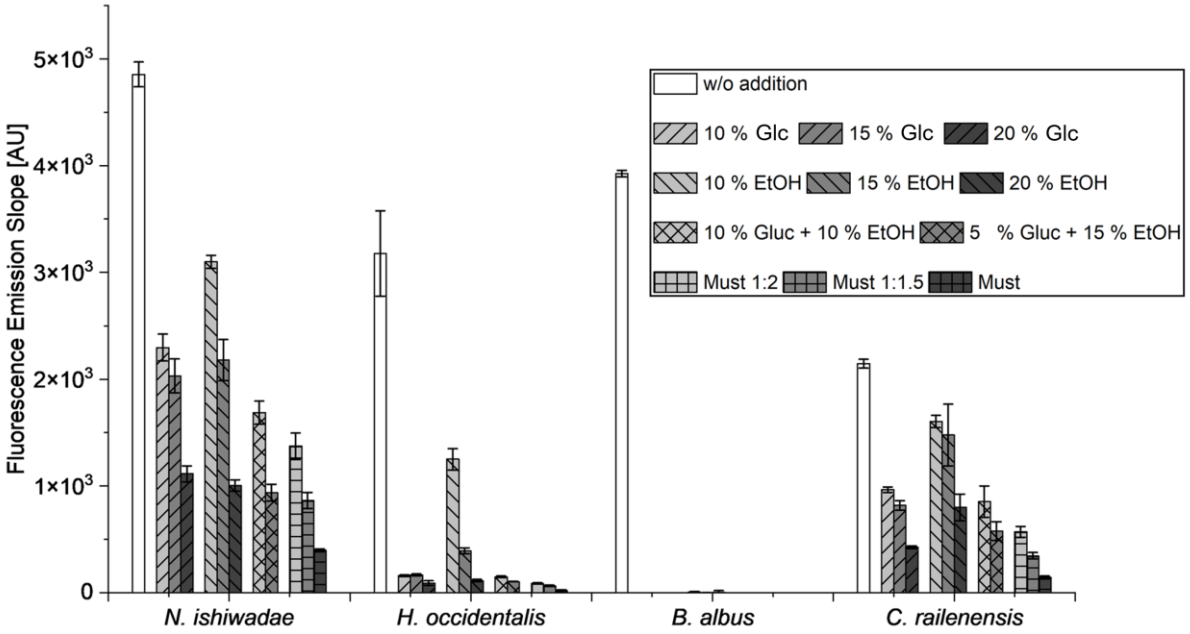

Figure 30: Impact of glucose, ethanol and Muscaris must on the *β*-glycosidase activity of whole cells. 4-MUG hydrolysis was measured for the different cell culture samples in buffers containing different amounts of glucose, ethanol or Muscaris must harvested in the year 2020. The values for fluorescence increase per minute are given in arbitrary units and were calculated as described in paragraph 4.4.2.1.

The high *β*-glycosidic activity of *B. albus* disappeared completely after the addition of glucose and ethanol. *H. occidentalis* showed only very low residual activity after the addition of glucose. For *N. ishiwadae* and *C. railenensis*, *β*-glycosidase activity was still measurable.

5.4 *β*-Lyase activities

5.4.1 Engineering yeast strains for high thiol release activity by a directed evolution approach using SMC

5.4.1.1 Identification of yeast strains with high β-lyase activity via growth-based screening in SMC medium

To test, if growth-based screenings in medium with SMC as sole nitrogen source can be used to isolate yeast strains with high *β*-lyase activity, a previously described agar plate-based screening procedure was transferred to liquid medium and applied to 2112 yeast strains. This modification, in combination with the use of 96-well plates, offers the advantage of a simple cell growth screening via quantification with a microplate reader. Figure 31 A illustrates an overview of the cell densities determined for the 2112 investigated yeasts after 48 h of growth in SMC medium. The isolates were sorted from high (left) to low (right) OD_{600nm} values.

A minimal OD_{600nm} value of 0.34 AU was observed for all yeasts examined. For 168 of the yeasts screened, the measured OD_{600nm} value after 48 h of incubation was between 0.34 AU and 0.35 AU. 314 yeasts reached higher optical densities which remained below 0.43 AU. For 1168 yeasts, even higher OD_{600nm} values up to 0.88 AU were measurable. Furthermore, 366 of the investigated yeasts achieved OD_{600nm} values of up to 1.23 AU, whereas for the 96 yeast strains with the highest cell densities, OD_{600nm} values of up to 3.09 AU were measured.

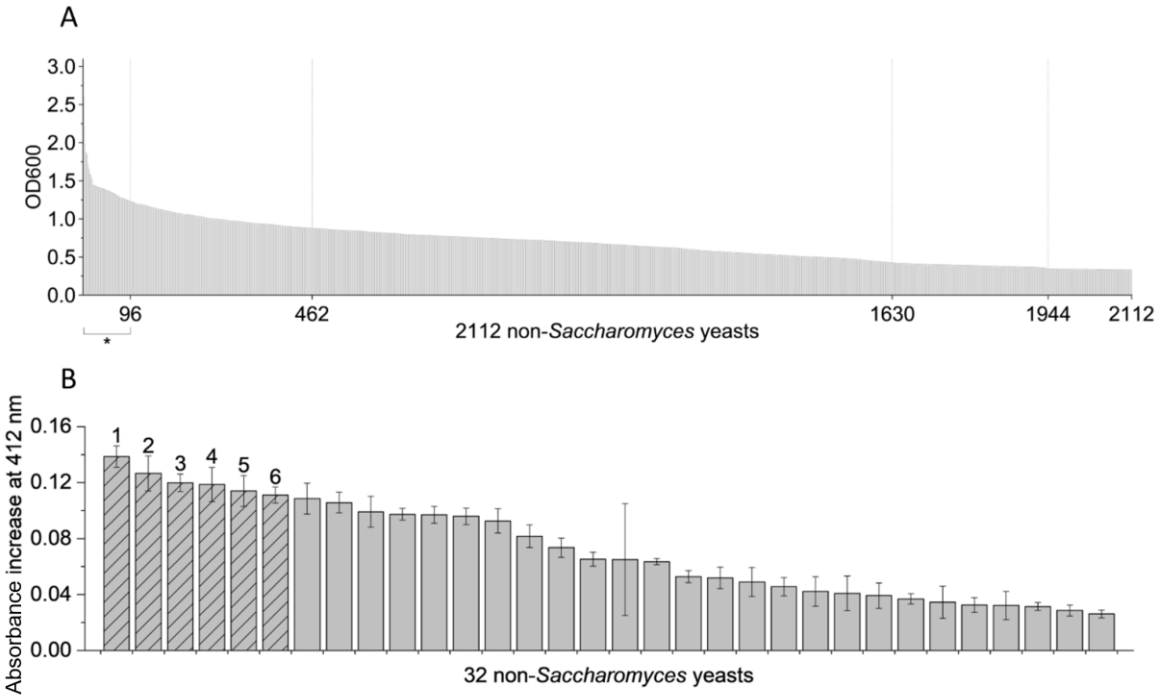

Figure 31: A) Observed cell densities of the 2112 non-*Saccharomyces* yeast strains after 48 h of cultivation in SMC medium. The experimental procedure is described in the material and methods section in 4.5.1.1. B) Comparative analysis of yeast strains for thiol release activity during incubation in 100 mmol L^{-1} citrate-phosphate buffer. The 32 strains with highest values identified in a preliminary experiment (Figure S 9) were analyzed again in triplicates. Shown are the absorbance increase values measured in the DTNB assays. For the six strains with the highest values (dashed bars) taxonomic investigation was performed. All experimental details are described in the material and methods section.

The 96 yeasts with the highest measured optical densities in the previous screening were afterwards characterized for their thiol release capability during incubation in 100 mmol L^{-1} citrate-phosphate buffer at pH 7. Figure S 9 illustrates the determined values sorted by the calculated absorbance differences of the performed assays, in which the reaction of thiols with DTNB leads to an absorbance increase at a wavelength of 412 nm.

The 32 isolates with the highest differences between the assays with and without the addition of SMC were subsequently investigated with identical measurements in triplicates (Figure 31 B). As shown, clear differences in the amount of released methanethiol were observed.

The six strains with the highest values in these experiments (ID 1-6) were taxonomically classified by sequencing of their ITS regions.

Table 6: Identity and strain ID of the investigated strains associated with high signals in the *β*-lyase screening experiments.

Strain ID	Identification
1	*Pichia kudriavzevii*
2	*Pichia kudriavzevii*
3	*Wickerhamomyces anomalus*
4	*Wickerhamomyces anomalus*
5	*Pichia kudriavzevii*
6	*Pichia kudriavzevii*

The *P. kudriavzevii* strain with ID 1 and the *W. anomalus* strain with the ID 3 were selected for the following experiments.

As already described, an alternative way for the determination of *β*-lyase activity relies on the detection of methanethiol and dimethyl disulfide, which are products resulting from the cleavage of SMC, via GC-MS headspace measurements.[256] In order to compare the results of the DTNB assay performed at pH 7 with headspace thiol measurements in reactions performed at pH 3, the following experiments were carried out on a 5 mL scale, in which the outcome of the DTNB assay and the relative *β*-lyase activity were comparatively analyzed. Figure 32 illustrates the results of the headspace measurement from reactions performed at pH 3 in comparison to the absorbance difference values of the DTNB assay at pH 7. To be able to classify the results obtained with the two most promising strains from the screening, the wine yeast strains Anchor VIN13 and Oenoferm X-thiol were included, hereafter named VIN13 and X-thiol. Whereas a low thiol release activity was observed for VIN13,[264] X-thiol was developed to enable the release of high thiol amounts.

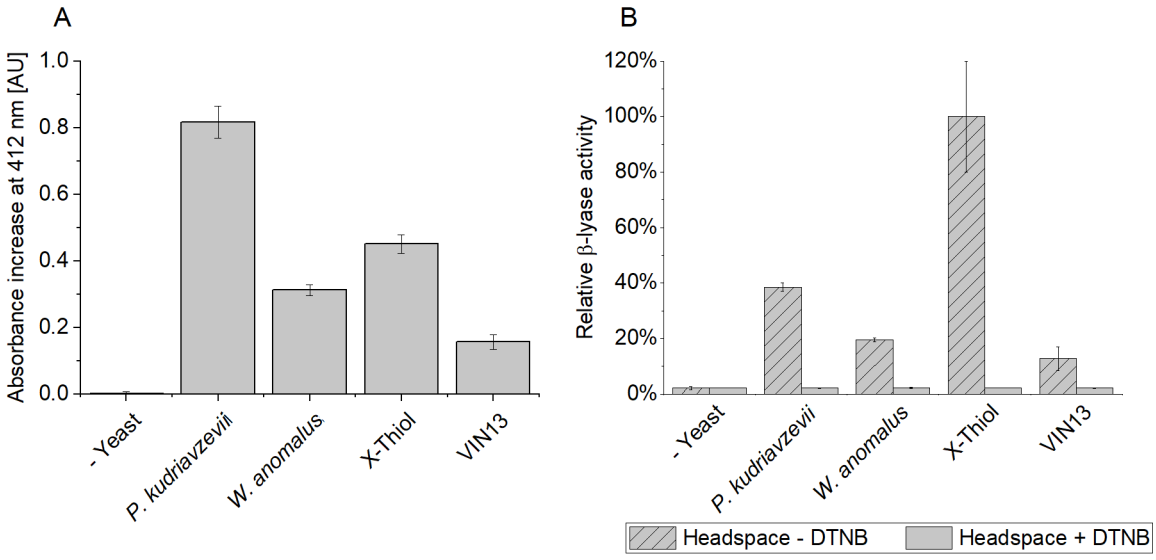

Figure 32: Comparison of *β*-lyase activities of different strains measured via two different assays at different pH values. DTNB-assays at A) pH 7 indicated high activities for the identified strains from the screening, whereas headspace measurements of the reaction B) revealed a strong decrease of the respective enzyme activities at pH 3. The value given corresponds to the relative *β*-lyase activity value described by Belda et al.[256]

The measured absorbance differences of the DTNB assays were highest for *P. kudriavzevii* (0.82 AU) and significantly higher than the values of X-thiol (0.45 AU). The DTNB assay with *W. anomalus*, on the other hand, resulted in lower values (0.31 AU), which were still significantly higher than the values of VIN13 (0.16 AU). The negative control without the addition of yeast cells showed only very small absorbance differences. Within the experiment aiming at quantification of the SMC-derived thiols in the headspace, incubation of X-thiol cells resulted in the highest peak areas which were set to 100 %. The peak areas after incubation of the *P. kudriavzevii* strain (38.6 %) and the *W. anomalus* strain (19.5 %) identified in the screening were lower. Incubation with VIN13, on the other hand, resulted in the lowest peak area corresponding to 12.8 % of the X-thiol value. For the negative control without addition of cells, a negligible amount of methanethiol and dimethyl disulfide was found.

5.4.1.2 Improvement of SMC usage by adaptive laboratory engineering

Although the screening approach using SMC led to the identification of two yeast strains with reasonable thiol release capabilities, a comparison with the respective activity of wine yeast strain X-thiol demonstrated their inability to compete or even outperform established and commercially available products. However, due to the principal functionality of linking thiol release activity to growth via the provision of SMC as sole nitrogen source, an attempt was made to further optimize this trait by means of a directed evolution approach.

To check whether the intended evolutionary approach using SMC medium is promising, the growth of *P. kudriavzevii*, *W. anomalus*, VIN13 and X-thiol was investigated in synthetic medium with different $(NH_4)_2SO_4$ concentrations and in SMC medium (Figure S 10). Without the addition of a nitrogen source in the medium, no growth was detectable for any of the selected strains. In contrast, addition of $(NH_4)_2SO_4$ as nitrogen source in different amounts enabled growth for all strains tested with a correlation between $(NH_4)_2SO_4$ concentration and maximal cell density. If SMC was used as sole nitrogen source, long lag phases were observed for all strains. For *P. kudriavzevii*, *W. anomalus* and VIN13, exponential growth started after 20 h. Exponential growth of the X-thiol cells was only observable after 30 h.

A comparison of the growth of the selected cells with different nitrogen sources (Figure S 11) showed slight inhibitory effects of SMC in media, which contained $(NH_4)_2SO_4$ and SMC. However, these effects are only minor. Therefore, the observed slowed growth in SMC medium is most probably due to limited nitrogen uptake from SMC and the intended evolutionary approach was found to be a straightforward approach.

To further investigate the proposed correlation between *β*-lyase activity and cell growth in SMC medium, a wine yeast AWRI1631 strain expressing a highly active *β*-lyase was investigated with respect to growth behavior in SMC medium (Figure S 12). In comparison to the wild type, the AWRI1631 *tnaA* cells grew faster, although the difference was not very pronounced.

These preliminary tests indicated that the use of SMC as nitrogen source and thereby its uptake and/or cleavage limits cell growth in the investigated strains and that an increase of *β*-lyase activity can at least partially improve the use of SMC as nitrogen source and growth. Therefore, a directed evolution approach with the selected strains *P. kudriavzevii*, *W. anomalus*, VIN13 and X-thiol towards better growth in SMC medium via a very simple serial transfer procedure was performed. After 25 over-inoculations, the populations were streaked out to isolate single clones for detailed characterization. For each yeast, three clones were examined (Figure S 13), which in some cases exhibited slightly different growth behavior. The respective clones with the greatest differences to the starting strain were chosen for further characterization. Figure 33 demonstrates the growth curves for the selected strains in SMC medium in comparison to the growth curve of the corresponding starting strain.

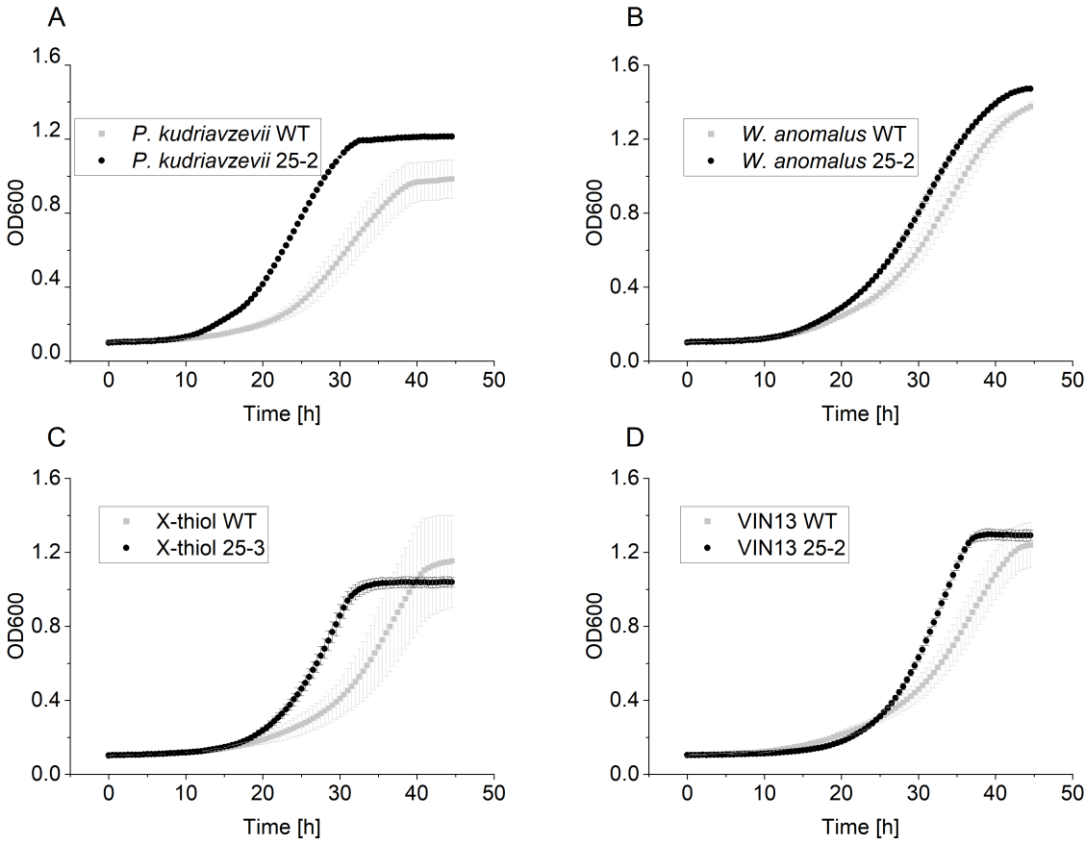

Figure 33: Comparison of the growth curves of evolved strains and corresponding parental strains (WT) in SMC medium. Precultures were grown in 600 µL synthetic medium with 0.1 mmol L^{-1} $(NH_4)_2SO_4$ for 24 h at 30 °C, 600 rpm and 80 % humidity.

For all four yeasts, an evolved mutant strain has been isolated, that shows clear growth improvement in SMC medium. All mutants obviously have an improved growth rate in comparison to the starting strain. In case of *P. kudriavzevii*, the 25-2 strain reached furthermore higher cell densities, which cannot be found for at least the X-thiol and VIN13 mutants. Compared to the other organisms, the growth improvement for the evolved *W. anomalus* strain is least pronounced. Interestingly, the VIN13 25-2 strain shows an elongated lag phase, but nevertheless an increased growth rate in comparison to the wild type.

To rule out the possibility that the mutants acquired a general growth improvement irrespective of the SMC metabolization, their growth behavior in medium with $(NH_4)_2SO_4$ as sole nitrogen source was also investigated. However, the growth curves revealed only minor differences between the nevolved strains and wild type strains (Figure S 14). For *W. anomalus* and VIN13, the evolved mutants even showed a slight growth disadvantage.

5.5 Engineering volatile thiol formation in yeast

5.5.1 Conversion of *(E)*-2-hexenal into 3MH by *tnaA*-expressing yeast strains

The synthesis of 3MH from *(E)*-2-hexenal was used as a model reaction to demonstrate the possibility of production of volatile thiols by genetically modified yeasts. The initial focus for optimizing thiol synthesis was on increasing the *β*-lyase activity, as the endogenous enzyme activity of yeast cells was found to be relatively low in contrast to cells expressing the tryptophanase-encoding *E. coli* gene *tnaA*.[7] To increase the *β* lyase activity of the cells, the *E. coli* gene *tnaA* was integrated into the delta sequences of the genome of the two yeast strains AWRI1631 and CEN.PK2-1C. Figure 34 illustrates the indirect measurement of *β*-lyase activity of both yeast strains with and without expression of the *tnaA* gene. The absorbance values at 412 nm after incubation of cells with SMC and DNTB are shown. The *β*-lyase reaction releases methanethiol from SMC and after the reaction of methanethiol and DNTB, the TNB^{2-} anion is formed which shows absorbance at 412 nm.[265]

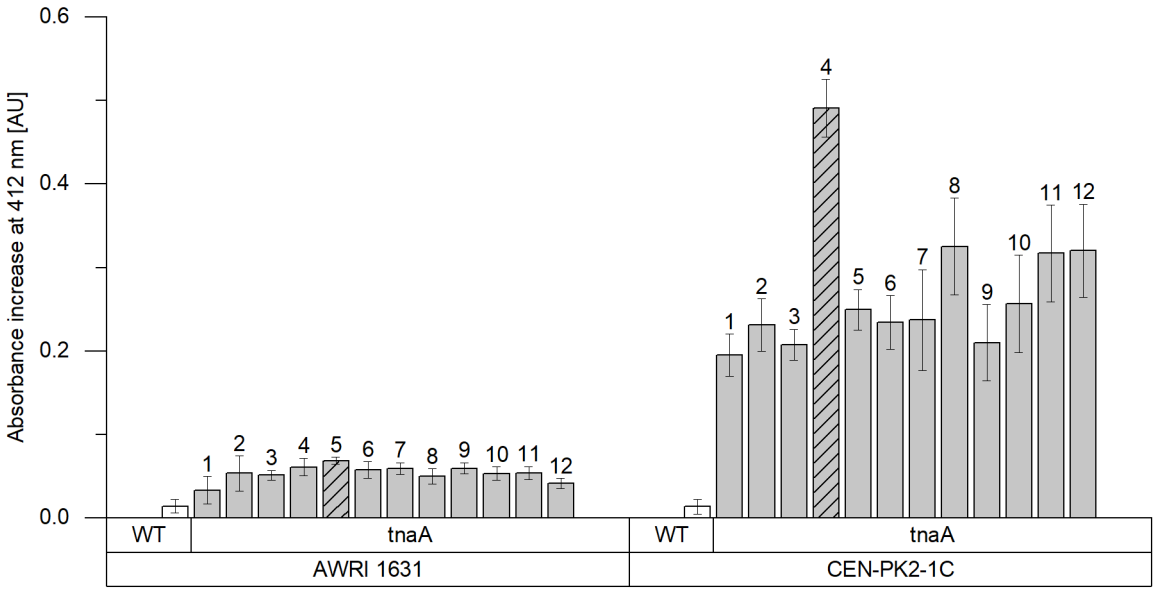

Figure 34: Indirect measurement of *β*-lyase activity increase of yeast cells after transformation with the *E. coli tnaA* expression construct by quantifying the amount of free thiol-groups with an assay based on DTNB. White bars: Wild type strains, Grey Bars: Transformants tested, Dashed Bars: Strains with highest values selected for further experiments. Assay details are described in the material and methods section. The data points and error bars represent the mean values and standard deviations for three biological replicates. A significant difference with a 95 % level of significance ($p<0.05$) for the values of the *tnaA*-transformed strains in comparison to the untransformed strains was found via a two-sample t-test assuming equal variance for all strains except AWRI 1631 + *tnaA* transformant 1.

After genome integration of *tnaA*, the AWRI1631 transformants 2-12 showed a significantly increased difference in the measured absorbance at 412 nm. As the values obtained with the

different transformants were comparable, transformant 5 was randomly selected for further experiments. Untransformed CEN.PK2-1C cells led to an absorbance difference of 0.014, but most *tnaA* gene transformants showed values between 0.2 and 0.3. Transformant 4 however showed an exceptionally high value of 0.49 and was therefore selected for the following experiments, in which the peak area of synthesized 3MH was quantified after the addition of *(E)*-2-hexenal on a 10 mL scale (Figure 35).

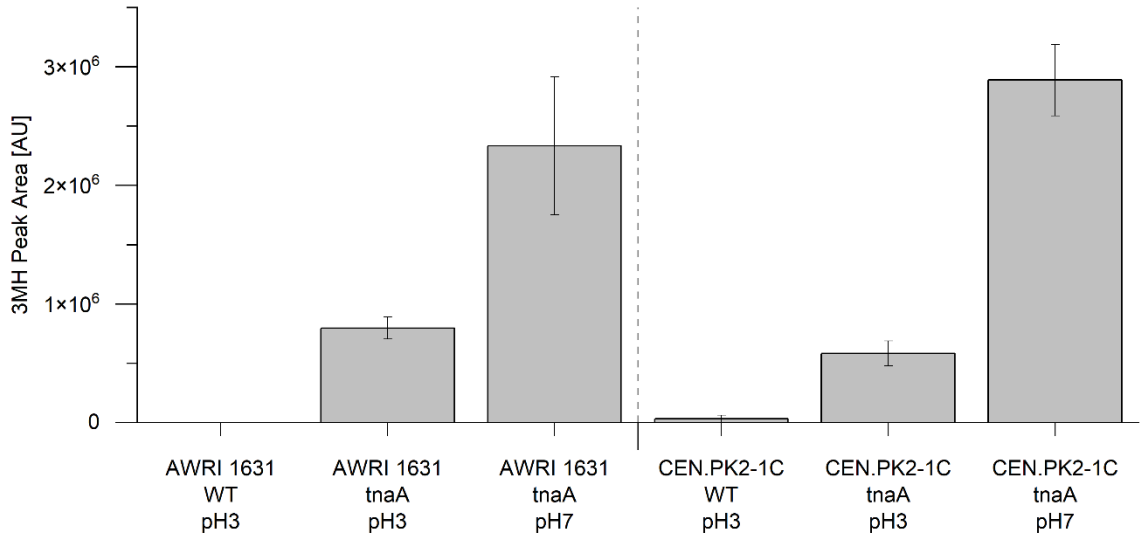

Figure 35: Comparison of the 3MH production capability of the yeast strains AWRI1631 and CEN.PK2-1C with or without *tnaA* expression construct in the genome at a pH value of 3 and of yeast strains with *tnaA* expression construct at a pH value of 7. The 3MH peak areas were determined after incubation of cells (OD_{600nm} of 15) in 100 mmol L^{-1} citrate-phosphate buffer with 100 µg L^{-1} *(E)*-2-hexenal for 48 h. The data points and error bars represent the mean values and standard deviations for three biological replicates.

Since formation of Cys-3MH from *(E)*-2-hexenal and cysteine was described to occur spontaneously at low pH,[266] pH 3 was also examined in addition to a neutral pH value. From the peak areas of the product 3MH detected for the AWRI1631-based strain, it is apparent that the reactions with the wild type cells did not result in detectable amounts of the product (lower than 0.5 µg L^{-1}), whereas the *tnaA*-transformed cells were able to produce higher amounts of 3MH at pH 3 and pH 7. The wild type strain of CEN.PK2-1C was able to produce small amounts of 3MH and increased 3MH amounts after genomic integration of *tnaA*. The measured peak areas of the product were larger at pH 7 than at pH 3 for both investigated strains.

Since biotransformations with CEN.PK2-1C-based cells resulted in slightly higher 3MH values and plasmid transformations are easy to perform due to the strain´s auxotrophies, the *tnaA*-expressing CEN.PK2-1C strain was used for the following experiments.

5.5.2 Optimization of bioconversion reaction parameters

The experiments of the previous section suggested that the pH value has major influence on the produced 3MH amount. For this reason, different pH values were investigated for optimization of the reaction conditions (Figure S 15 A). These results confirmed the observed trends from Figure 35. Whereas only a small peak area was observed after incubation at pH 3, the highest product concentration could be determined in the bioconversion reaction performed at pH 5.6. A further increase of the pH value did not lead to higher product amounts. Another important aspect is the incubation time of the reaction. Figure S 15 B illustrates that high product concentrations could already be observed after a bioconversion time of 24 h.

Based on the described findings, the basic reaction parameters were set to pH 7 and an incubation time of 24 h. Figure S 16 represents further optimizations of the assay conditions, in which different concentrations of *(E)*-2-hexenal or the corresponding alkenol *(E)*-2-hexen-1-ol were used. In case of *(E)*-2-hexenal, 100 µg L^{-1} resulted in the highest product concentration. When *(E)*-2-hexen-1-ol was used as substrate, higher amounts of 3MH were detected if compared to the *(E)*-2-hexenal conversion reactions. Here again, a substrate concentration of 100 µg L^{-1} yielded the highest product concentration. Based on these results, *(E)*-2-hexen-1-ol at a concentration of 100 µg L^{-1} was used in the following experiments.

In the next step, the influence of the reaction volume and cell growth time was investigated (Figure S 17). In both cases, the tested variation resulted in strong decrease of the observed 3MH product concentrations. Moreover, supplementation of the reaction with different amounts of pyridoxal-5-phosphate, an important cofactor for *β*-lyases, did not influence the amounts of 3MH (Figure S 18 A). The same applies for the reaction supplementation with glutathione or cysteine (Figure S 18 B).

However, variations of cell density and reaction medium, as well as supplementation with glucose, H_2O_2, and $ZnCl_2$ showed strong effects on the detectable 3MH amounts (Figure S 19). The peak area increased in proportion to the cell density used in 100 mmol L^{-1} citrate-phosphate buffer between an optical density of 5 to an optical density of 12.5. Further increase in cell density did not further increase the amount of product. Supplementation of the reaction buffer with glucose led to inconsistent results with partly strong decreases of the product concentration and addition of H_2O_2 and $ZnCl_2$ led to even stronger decreases of the product concentration. Use of YPD- or SCD-medium as bioconversion reaction media led to relatively low product concentrations. For the following experiments, a cell density of 15 (OD_{600nm}) and 100 mmol L^{-1} citrate-phosphate pH 7 were used.

To quantify the produced 3MH amounts, calibrations were performed using spiked cell suspensions in 100 mmol L^{-1} citrate-phosphate buffer pH 7 (Figure S 20) with which the concentrations of 3MH could be estimated. Figure 36 summarizes the results of the previously performed optimizations. CEN.PK2-1C wild-type cells without genetic modifications produced only very low 3MH amounts (9.9 ng L^{-1}). After genomic integration of *tnaA* and the selection of the best-performing clone, this strain with the highest *β*-lyase activity was found to produce 220 ng L^{-1} 3MH. Using *(E)*-2-hexen-1-ol as alternative substrate, the product amount was further increased to 450 ng L^{-1}. After the optimizations described in the previous part, the product amount could be finally increased to 730 ng L^{-1}.

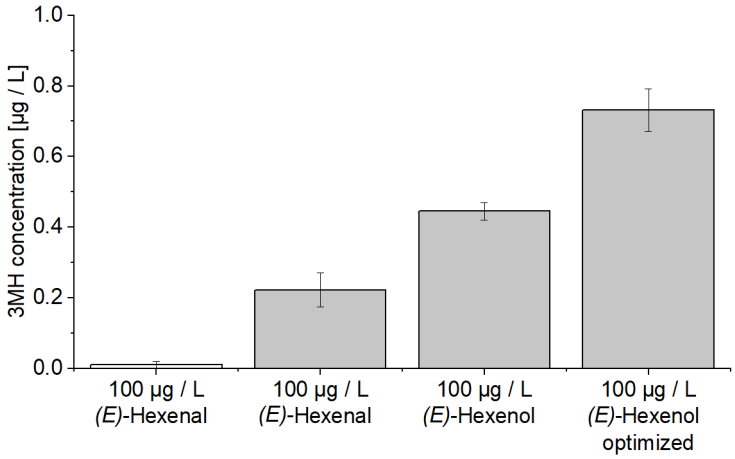

Figure 36: Quantitative comparison of bioconversion results before and after strain and reaction condition optimizations. All assays were performed in 100 mM citrate-phosphate buffer pH 7. The growth and bioconversion time was 24 h each. Under optimized conditions, a cell density (OD_{600nm}) of 15 instead of 7.5 was used. White bar: CEN.PK2-1C wild type cells without *tnaA* expression construct. The data points and error bars represent the mean values and standard deviations for three biological replicates.

5.5.3 Improving Glut-3MH formation by increased glutathione production and GST activity

Aim of the further strain engineering approaches was the increase of product formation by elevating the glutathione content and the GST activity. As the external addition of glutathione did not result in the synthesis of higher 3MH concentrations (Figure S 18 B), the *γ*-glutamylcysteine synthetase-encoding gene *GSH1* was overexpressed to increase the intracellular glutathione concentration. The corresponding enzyme catalyzes the first step in glutathione biosynthesis in *S. cerevisiae* and gene overexpression was found to result in 42 % increased intracellular glutathione levels compared to the wild type.[267] Furthermore, attempts were made to enhance the synthesis of 3MH by overexpressing different GST's, which are known to transfer glutathione to electrophiles.

The yeast genes *GTT1* and *GTT2* as well as the gene *VvGST4* from wine were used for episomal overexpression experiments (see also Table 3). Figure 37 represents the estimated 3MH concentrations in bioconversion reactions with different transformants.

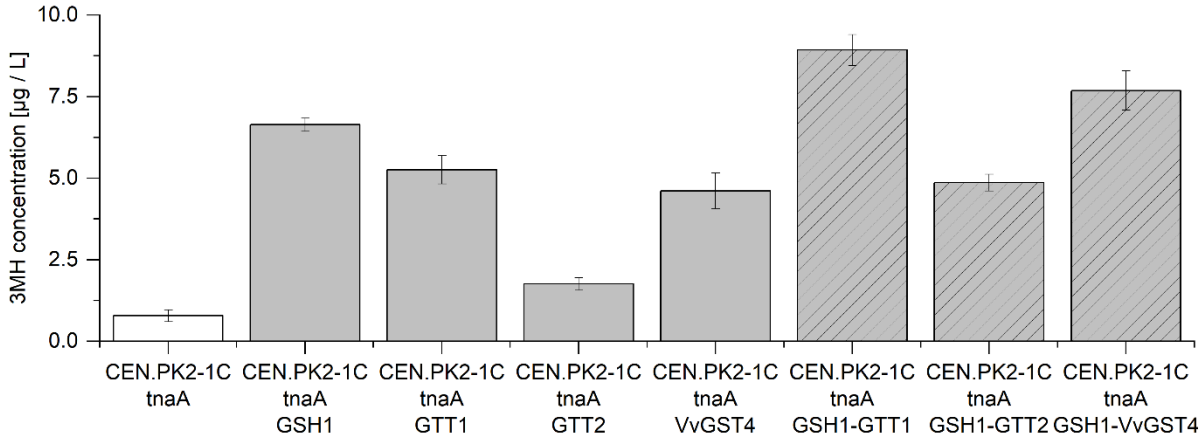

Figure 37: Comparison of the produced 3MH amounts under the optimized conditions after further genetic modification of CEN.PK2-1C *tnaA*. The reference strain CEN.PK2 1C *tnaA* contained no plasmids. All other strains contained expression constructs for the γ-glutamylcysteine synthetase-encoding gene *GSH1* and/or one of the GST-encoding genes *GTT1, GTT2* or *VvGST4* on one or two plasmids, respectively. 100 µg L^{-1} (E)-2-hexen-1-ol was used as substrate. The data points and error bars represent the mean values and standard deviations for three biological replicates.

As previously described, the CEN.PK2-1C cells transformed with *tnaA* produced nearly 0.8 µg L^{-1} 3MH within an incubation time of 24 h. Cells, which harbored the *GSH1* overexpression plasmid in addition, synthesized higher amounts of 6.6 µg L^{-1} 3MH in the same time. Cells transformed with the three different GST gene overexpression plasmids also produced higher amounts compared to CEN.PK2-1C *tnaA*. Cells transformed with the plasmid for overexpression of *GTT1* produced higher amounts (5.3 µg L^{-1}) of 3MH than cells transformed with the *GTT2* gene (1.85 µg L^{-1}). Overexpression of the codon-optimized *V. vinifera*-derived gene VvGST4 resulted in 4.6 µg L^{-1} of 3MH.

Strains, which were overexpressing one of the GST genes in addition to *tnaA* and *GSH1*, partly showed even higher 3MH concentrations. Strains overexpressing *GSH1* and *GTT1* reached the highest product concentrations observed in this set of experiments (8.9 µg L^{-1}).

5.5.4 Product spectrum expansion of engineered thiol-synthesizing yeast strains

An attempt was made to expand the described conversion of *(E)*-2-hexen-1-ol via the use of other substrates. For this purpose, a number of different compounds was used as substrates in reactions with the established conditions. The results of these experiments are described subsequently and summarized in Table 7. The corresponding chromatograms and mass spectra are presented in the supplementary section (Figure S 21 to Figure S 32).

Table 7: Used substrates and the expected products in bioconversion reactions with engineered yeast strains. Products were identified by comparison of the chromatograms of CEN.PK2-1C *tnaA* cells containing plasmids for overexpression of the *GSH1* gene and one of the described GST genes to a reference strain of CEN.PK2-1C cells with empty plasmids. Peaks which only occurred in reactions with engineered strains were indicative for bioconversion and were tentatively identified. Some products showed similarity in their mass spectra to the spectra of the assumed products deposited in the NIST database. Two peaks were tentatively identified after the incubation with (R)-(+)-pulegone, three peaks were tentatively identified after the incubation with 3-penten-2-one.

Substrate(s)	Expected product(s)	Exact Mass of products(s) [u]	Specific peak identified (occurred only in reactions with engineered strains)	Similarity (value given by GC-MS software)
(Z)-3-Hexenylacetate	3-Mercaptohexyl acetate, 4-Mercaptohexyl acetate	176.09	✗	✗
Furfural	Fufurylthiol	114.01	✗	✗
(Z)-6-Nonenal	6-Mercaptononan-1-ol, 7-Mercaptononan-1-ol	176.12	✗	✗
β-Pinene	2,6,6-Trimethylbicyclo[3.1.1]heptane-2-thiol	170.11	✗	✗
Citronellol	6-Mercapto-3,7-dimethyloctan-1-ol, 7-Mercapto-3,7-dimethyloctan-1-ol	190.14	✗	✗
Limonene	1-Methyl-4-(prop-1-en-2-yl)cyclohexane-1-thiol, 2-Methyl-5-(prop-1-en-2-yl)cyclohexane-1-thiol, 2-(4-Methylcyclohex-3-en-1-yl)propane-2-thiol	170.11	✗	✗
α-Terpineol	2-(4-Mercapto-4-methylcyclohexyl)propan-2-ol, 2-(3-Mercapto-4-methylcyclohexyl)propan-2-ol	188.12	✗	✗
3-Methyl-2-buten-1-ol	3-Mercapto-3-methylbutan-1-ol 2-Mercapto-3-methylbutan-1-ol	120.06	✓	86 %

Substrate(s)	**Expected product(s)**	**Exact Mass of products(s) [u]**	**Specific peak identified (occurred only in reactions with engineered strains)**	**Similarity (value given by GC-MS software)**
3-Buten-2-one	4-Mercaptobutan-2-one, 3-Mercaptobutan-2-one	104.03	✓	90 %
(R)-(+)-Pulegone	8-Mercapto-*p*-menthan-3-one derivate	186.11	✓ (2 peaks)	90 % / 92 %
(Z)-2-Hexen-1-ol	2-Mercaptohexan-1-ol, 3-Mercaptohexan-1-ol	134.08	✓	89 %
(E)-3-Hexen-1-ol	3-Mercaptohexan-1-ol, 4-Mercaptohexan-1-ol	134.07	✓	✗
(E)-2-Pentenal, *(E)*-2-Penten-1-ol	3-Mercaptopentan-1-ol, 2-Mercaptopentan-1-ol	120.06	✓	✗
(E)-2-Heptenal, *(E)*-2-Hepten-1-nol	3-Mercaptoheptan-1-nol, 2-Mercaptoheptan-1-ol	148.09	✓	✗
(E)-2-Nonenal	3-Mercaptononan-1-ol, 2-Mercaptononan-1-ol	176.12	✓	✗
1-Octen-3-ol	1-Mercaptooctan-3-ol, 2-Mercaptooctan-3-ol	162.11	✓	✗
3-Pentene-2-one	4-Mercaptopentan-2-one 3-Mercaptopentan-2-one	118.05	✓ (3 peaks)	✗

As not all of the expected thiol products were commercially available, tentative product identification was performed via the comparison of potential product peak mass spectra with NIST database entries or via the search for compound peaks with the expected molecular ion masses and the comparison of the calculated estimated mass intensity ratios based on the natural occurring isotope distribution to the measured values in order to identify potential products containing thiol groups (an overview is given in Table S 3). After incubation with some of the selected substrates, no peaks could be identified that corresponded to the expected products. In addition, no potential product peaks could be detected by searching for the calculated masses of these molecules. For some other substrates, however, peaks could be identified that were clearly detectable for all transformed cells, while they were not or only to a small extent visible in the control reaction with a CEN.PK2-1C wild type strain transformed with empty plasmids. A comparison led to similarities of the measured spectra with the spectra deposited in the NIST database as further described.

Compared to the reference spectrum deposited in the NIST library for the estimated product 3MH, the mass spectra after incubation with *(Z)*-2-hexen-1-ol comprised similarities concerning the fragments with *m/z* 100, *m/z* 82, *m/z* 67, *m/z* 61, *m/z* 57, and *m/z* 55. These commonalities result in a similarity value of 88 % given from the GC-MS software. Although the described peak had a similar retention time to reference measurements with a 3MH standard (10.75 min), the masses calculated based on the natural isotope distribution could not be confirmed in the respective mass spectrum.

When comparing the mass spectra of the identified peak after bioconversion of 3-methyl-2-buten-1-ol and the tentative product 3-mercapto-3methylbutan-1-ol, analogies in the intensities of the fragments with *m/z* 87, *m/z* 86, *m/z* 71, *m/z* 69, *m/z* 59, *m/z* 57, *m/z* 55, and *m/z* 53 are noticeable, resulting in a similarity value of 86 %. However, the calculated mass intensities for identifying the expected products containing a thiol group showed very large standard deviations between the three yeast strains.

For the substrate 3-buten-2-one, the observed peak in the bioconversion attempt with the GSH1-GTT1 transformant showed an ion with the expected molecular mass in the mass spectrum, but it could not be assigned to a specific compound by comparison of the mass spectrum with the NIST database. However, a similar ratio of the measured mass intensity of the fragments as in the theoretically calculated values based on the isotope distribution was identified in the recorded data.

In the bioconversion reaction with (R)-(+)-pulegone as substrate, two peaks could be detected in the chromatogram, whose mass spectra both strongly resembled the mass spectrum of the sought product 8-mercapto-*p*-menthan-3-one containing the most prominent fragments *m/z* 186, *m/z* 153, *m/z* 135, *m/z* 123, *m/z* 109, *m/z* 81, *m/z* 69 and *m/z* 55. These two spectra also showed strong similarities to each other. For both mass spectra, reasonable ratios of mass intensities based on the estimated values for products containing a thiol group were identified. Moreover, the calculated molecular mass of the product was observable in both spectra.

In comparison to *(E)*-2-hexen-1-ol, *(E)*-3-hexen-1-ol only differs in the position of the double bond. However, the mass spectrum of the tentative product did not correspond to the spectrum of the product 3MH and did not contain a signal for the expected molecular ion (*m/z* 134). The biggest ion detected was *m/z* 124*.* Furthermore, the observed ratios of the masses expected due to the natural occurring isotope distribution did not allow any conclusions about the presence of a sulfur group in the tentative product.

In case of *(E)*-2-pentenal and *(E)*-2-pentenol, the retention times and the mass spectra of the products were identical for both substrates. Identical products were furthermore observed for the C_7-compounds *(E)*-2-heptenal and *(E)*-2-hepten-1-ol. In all these mass spectra, signals for the expected molecular ions could be detected and the observed distribution of mass intensities in the spectra are matching the calculated values based on the estimated products containing a thiol group.

After the bioconversion reaction with *(E)*-2-nonenal, a peak was identified whose fragments had the expected molecular mass of *m/z* 176 and the observed distribution of mass intensities was similar to the calculated values for the expected sulfur containing molecules.

For *(E)*-2-heptenal, *(E)*-2-hepten-1-ol and *(E)*-2-nonenal-derived products very high peak areas were observed. Incubation with 1-octen-3-ol, on the other hand, led to a potential product with lower peak area whose mass spectrum did neither contain a signal for the expected molecular mass of *m/z* 162 nor the expected mass distribution for the expected molecules.

After the conversion of 3-penten-2-one, three peaks were identified that occurred only in the reactions with the engineered strain, but not in the reaction with the CEN.PK2-1C wild type strain. The corresponding mass spectra of the peak at 6.6 min and the peaks at 16.25 min and 16.4 min are shown in Figure S 32. The spectra of the peaks at the later retention times were virtually identical, but the spectrum of the peak at 6.6 min showed clear differences. While all three mass spectra contained the expected molecular ion with a mass of *m/z* 118, only the mass intensity ratio of the peak at 6.6 min was matching the calculated values based on the naturally occurring isotope distribution.

5.5.5 Influence of the functional group on the product amount

As described in the previous section, peaks with identical retention times and mass spectra were observed for the products of each pair of C_5-, C_6- and C_7- aldehydes and the corresponding alkenols. In addition, it was already observed for *(E)*-2-hexenal and *(E)*-2-hexen-1-ol, that the alkenol led to higher product concentrations in direct comparison (Figure S 16). In order to investigate this issue in more detail, respective experiments were carried out again in triplicates to compare the product amounts produced from the aldehyde and the alkenol, respectively (Figure 38).

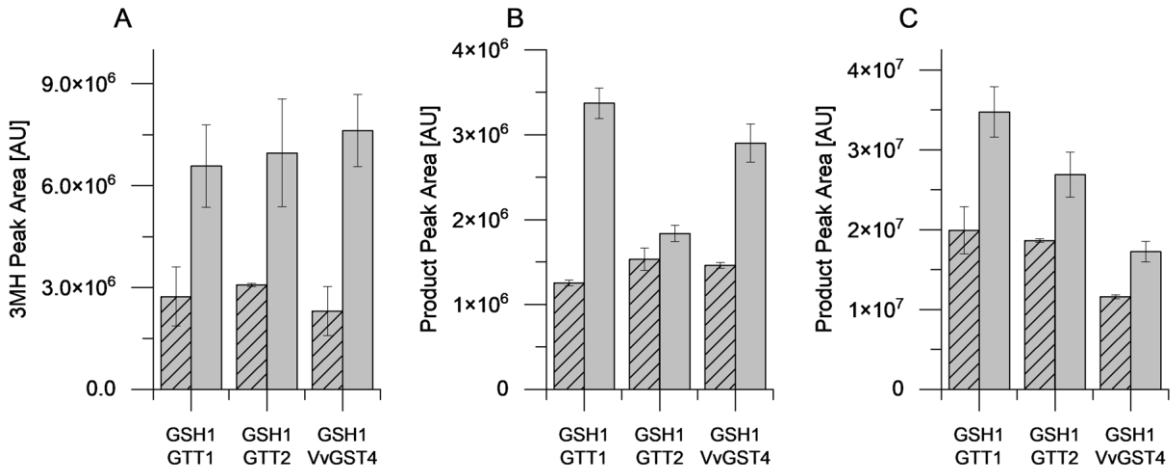

Figure 38: Comparison of thiol formation from pairs of aldehyde and alkenol by CEN.PK2-1C *tnaA* strains additionally overexpressing *GSH1* and one GST gene (*GTT1, GTT2* or *VvGST4*). Dashed bars represent the values for the aldehyde compounds. A) C_5-compounds *(E)*-2-pentenal / *(E)*-2-penten-1-ol, B) C_6-compounds *(E)*-2-hexenal / *(E)*-2-hexen-1-ol, C) C_7-compounds *(E)*-2-heptenal / *(E)*-2-hepten-1-ol. It should be noted that the peak areas are not comparable between the graphs A), B) and C) because different split settings were used as stated in the material and methods section. The used substrate concentration was 100 µg L^{-1}. The data points and error bars represent the mean values and standard deviations for three biological replicates.

When comparing the product amounts after incubation with the C_5-molecules, it is noticeable that the relative product concentrations of all three strains overexpressing different GST´s were comparable in each case. However, the product peak areas were twice as large if *(E)*-5-penten-1-ol was used as substrate in comparison with the substrate *(E)*-2-pentenal (Figure 38 A).

After incubation with the C_6 molecules, similar product peak areas were obtained with *(E)*-2-hexenal for the three different strains. In contrast, with the use of *(E)*-2-hexen-1-ol, there were pronounced differences. For the strain expressing *GSH1* and *GTT2*, the peak area only reached 1.84×10^6 AU, whereas a peak area of 3.05×10^6 AU was determined for the strain expressing *GSH1* and *VvGST4* and a peak area of 3.37×10^6 AU was found for the strain expressing *GSH1* and *GTT1* (Figure 38 B).

The results of the C_7-molecule bioconversions revealed different patterns. With *(E)*-2-heptenal as substrate, a peak area of 2.0×10^7 AU was obtained for the strains expressing *GSH1* and *GTT1* or *GSH1* and *GTT2*, whereas only 1.16×10^7 AU were detected with the strain expressing *GSH1* and *VvGST4*. When the corresponding alkenol *(E)*-2-hepten-1ol was used, the peak areas were clearly higher compared to the aldehyde (Figure 38 C).

5.5.6 Assessment of GST selectivity

As the results in the previous section suggest that the type of expressed GST gene contributes to the bioconversion efficiency, this issue was investigated in more detail. Therefore, substrates for which the single determination of product amounts in the substrate testing data set revealed strong differences between strains with different GST genes were analyzed again in triplicates (Figure 39).

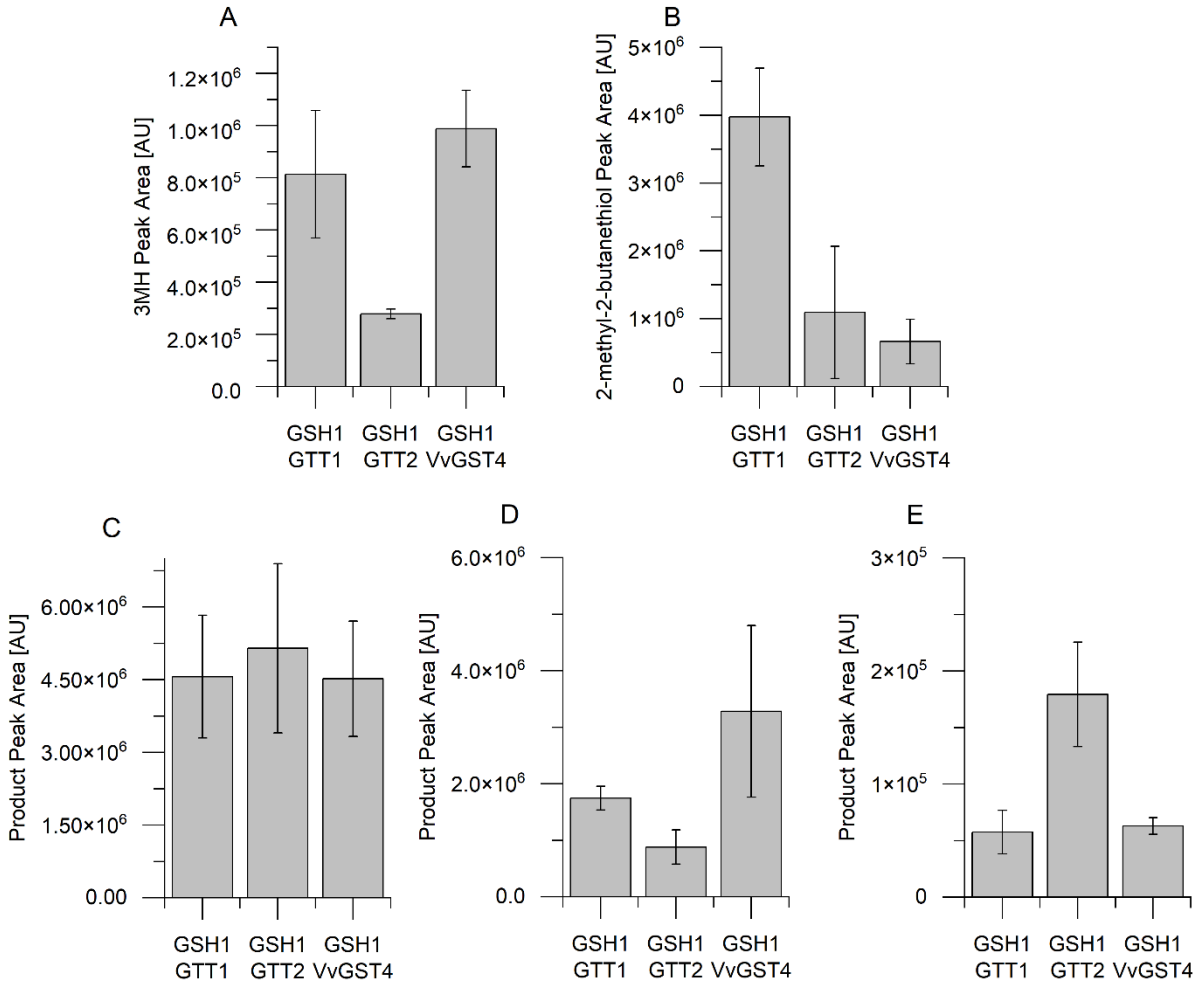

Figure 39: Bioconversion reactions with strong effects of different GST-encoding genes on product amounts. Shown are the peak areas for the products after bioconversion reactions with CEN.PK2-1C strains expressing *tnaA*, *GSH1* and one GST-encoding gene (*GTT1, GTT2* or *VvGST4*). Substrates used were A) *(Z)*-2-hexen-1-ol, B) 3-buten-2-one, C) *(E)*-2-nonenal, D) 1-octen-3-ol or E) *(E)*-3-hexen-1-ol. The substrate concentration used was 100 µg L^{-1} in all experiments. For the bioconversions shown in C), D) and E), the identity of the product structure could not be verified (see Table 2). The data points and error bars represent the mean values and standard deviations for three biological replicates.

The amounts of 3MH synthesized after the addition of *(Z)*-2-hexen-1-ol (Figure 39 A) varied strongly between the strains transformed with the different GST-encoding genes. The bioconversion with the strain expressing *GTT2* resulted in much lower product amounts in comparison to bioconversion reactions with strains expressing *GTT1* or *VvGST4*. In case of the substrate 3-buten-2-one (Figure 39 B), reactions with the strain expressing *GTT1* clearly showed much higher amounts of the product tentatively identified as 2-methyl-2-butanethiol in comparison to bioconversions with strains expressing *GTT2* or *VvGST4*. Figure 39 C-E demonstrate other examples for substrates, for which strains expressing different GST-encoding genes showed clearly different product amounts based on the peak areas. The product identity is however unclear in these cases.

6 Discussion

6.1 Peptidase activities

After analysis of more than 2000 isolates of autochthonous yeasts, only a small proportion of 8.5 % revealed an observable peptidase activity at pH 3. However, it should be noted that strains that grow fast under the selected conditions are more likely to be selected than slow-growing strains. This can lead to false conclusions about peptidase activity.

Further investigation of 30 isolates in grape must and subsequent ITS sequencing of the isolates with the most promising results led to the identification of four *Metschnikowia pulcherrima* and two *Metschnikowia chrysoperlae* isolates.

The yeast *Metschnikowia pulcherrima* occurs ubiquitously, including the surfaces of many fruits, and is therefore frequently found in spontaneous fermentations.[27] It has already been discussed for diverse applications in biotechnology.[268]

Compared to *Saccharomyces cerevisiae* and other non-*Saccharomyces* yeasts, *M. pulcherrima* is characterized by higher robustness to the composition of nitrogen-containing nutrients.[269] In addition to reducing ethanol content in wine,[270] this yeast is also associated with a variety of extracellular enzymes such as *β*-glycosidases, *β*-lyases, and also peptidases.[21] For this reason, the identification of *Metschnikowia* strains in the performed screening is not surprising. In previous screenings of oenological isolates, *M. pulcherrima* isolates that could hydrolyze casein have already been determined.[271,272]

Moreover, the aspartic peptidase MpAPr1 of *M. pulcherrima* has already been identified using sequence similarities to known aspartic peptidases[273] and was further characterized.[274] In addition, its activity towards wine proteins and thus the reduction of turbidity in wine was demonstrated[275] and the response of the production of this peptidase to available nitrogen sources was investigated.[276] Since MpAPr1 is currently the only identified aspartic peptidase of *M. pulcherrima*, this or a closely related enzyme is a potential candidate for the observed enzyme activity. Since it has been observed that different strains of the same genus can exhibit different peptidase activities and several different peptidases,[277] the observed differences in protein signal reduction are also conclusive.

Although peptidase activity has already been described for *M. pulcherrima*, the partly strong reductions in protein concentrations are remarkable. In contrast to the partially described peptidases of *M. pulcherrima*, which showed activity only in model solutions at neutral pH values,[278] strains could apparently be identified during the screening at low pH values, which are also active in wine conditions. The demonstrated stronger effect on protein signals

after must fermentation compared to the commercially available Flavia MP346 strain confirms that the identified *M. pulcherrima* strains are interesting candidates for co-fermentations. However, when considering these results, it must also be noted that the differences in the measured protein concentrations could also be partly due to different growth rates during the incubation period. The two identified *M. chrysoperlae* isolates are also noteworthy because this strain is uncharacterized so far.

Since the genus *Metschnikowia* is also associated with major influences on the aroma composition of wines, for example the increase of 2-phenylethanol and esters,[16,279] an analysis of the aroma composition of fermented wines is reasonable in the future.

6.2 Pectinase activities

The screening for pectinase activity led to the identification of 161 isolates that showed significant growth in the presence of high amounts of pectin and the associated low pH values. The ability for strong growth is essential for the initial approach of reducing pectin concentrations, for example in pomace and cocoa beans, prior to pressing by fermentation with one of these yeasts. Unfortunately, the subsequent screening for polygalacturonase activity did not reveal any pronounced signals for these isolates. This finding is not surprising, since only a small percentage of yeasts are known to exhibit this enzyme activity to a high extent and therefore rather pectinases of higher fungi are used in the industry.[280]

6.3 *β*-Glycosidase activities

6.3.1 Comparative investigations on different *β*-glycosidase surrogate substrates

In the comparative study of the most commonly used surrogate substrates, 4-MUG turned out to be most suitable for the photometric identification of *β*-glycosidase activities.

Photometric measurements of liquid assays additionally enable precise activity quantification and are feasible in a high-throughput format using 96-well plates. The described differences in solid and liquid assay conditions can be caused, for example, by the different availabilities of oxygen. Since the possible application of such strains takes place in a liquid environment (for example in must fermentation) and the liquid culture approach simplifies activity quantification, liquid assay conditions are most appropriate for screening, which has been recently stated also by two other studies.[281,282]

Although arbutin and esculin were so far mainly used for the qualitative determination of *β*-glycosidic activities on agar plates, photometric determination and quantification is also possible under liquid assay conditions. While the detected compounds of 4-MUG and pNPG

derive from products of the enzymatic reaction (4-MU and pNP), the hydrolysis of arbutin and esculin can be followed photometrically via the reduction of the substrate's fluorescence. Whereas the slow hydrolysis of arbutin is clearly a drawback for its potential use in a screening, esculin revealed to be suitable for this purpose.

Although the detection of fluorescence intensity decrease during *β*-glycosidase-mediated esculin hydrolysis represents a suitable assay, the detection of increasing absorbance or fluorescence signal intensities during conversion of pNPG or 4-MUG is less error-prone. This is due to the fact that many parameters can lead to the decrease of absorbance or fluorescence signals, for example precipitation phenomena or pH changes, whereas an increase of signal intensity is rarely caused by artifacts. In conclusion, photometric detection of the substrate is more amenable to artifacts if compared to the detection of hydrolysis products in case of pNPG or 4-MUG.

A comparison of these two surrogate substrates and the respective photometric measurements revealed, that the fluorescence-based assay is much more sensitive and apparently does not show saturation effects with the used enzyme concentrations. The possibility of adjusting the strength of the fluorescence signal amplification after the transformation from light into electricity (gain setting) in the case of more strongly deviating enzyme activities also leads to a considerable expansion of the measurable enzyme activities. In addition, the measurement of a fluorescent molecule is less influenced by cells and other sample ingredients compared to absorbance-based assays. Although pNPG has been commonly used as substrate for *β*-glycosidase characterization in previous studies,[173,283–285] 4-MUG represents a highly suitable alternative surrogate substrate for screenings and kinetic investigations of *β*-glycosidase activities.

The detected changes in the spectral properties of 4-MU due to the variation of pH or the addition of ethanol should be taken into account, but do not prevent the use of 4-MUG as a surrogate substrate for *β*-glycosidase assays. To determine the amount of surrogate converted, separate calibration curves can be established for each tested condition. Therefore, 4-MUG assays were proven to be sufficiently robust against changes in the pH value and the addition of glucose or ethanol.

So far, 4-MUG has been frequently used in the context of Gaucher's disease[160,286] to detect the lack of *β*-glycosidase activity in human cells.[287,288] Few reports exist about its use for the characterization of *β*-glycosidases in bacteria[235] and yeast[289] or for the staining of functional *β*-glycosidases in native polyacrylamide gels.[290] The use of 4-MUG for quantitative photometric *β*-glycosidase activity assays during a screening was reported by only two groups.[162,291]

After addition of the surrogate substrate, *A. pullulans* cells clearly accumulated 4-MU in the cytoplasm which indicates a cytoplasmic localization of the responsible *β*-glycosidase enzymes. In the case of *I. terricola*, 4-MU fluorescence could be detected in the cells and in the culture medium. This observation is consistent with the previously described secretion of significant amounts of *β*-glycosidase by this strain.[176] These experiments suggest 4-MUG to be a useful probe for microscopic assessment of the potential enzyme localization. However, it should be noted that direct conclusions concerning the subcellular localization of the enzymes are difficult to draw. Although preliminarily conducted experiments (data not shown) reveiled no indication for transport processes, it is also possible that the aglycon is transported into or out of the cells. However, 4-MUG might be useful for future investigations of subcellular *β*-glycosidase localization.

6.3.2 Investigation of non-*Saccharomyces* yeasts with intracellular *β*-glycosidase activity for wine aroma modification

The performed screening led to the discovery of several interesting non-*Saccharomyces* yeast strains with relevant *β*-glycosidase activity. Strains with activity in cell lysates showed no activity at low pH and glucose or ethanol concentrations usually present during must fermentations. Whole cells, however, were at least partly able to hydrolyze terpene-glycosides at low pH values, most probably after import in the cells. The observed differences of *β*-glycosidase properties in the investigated yeast cultures confirms the high diversity of this enzyme activity in non-*Saccharomyces* yeasts.

Possible explanations for the decrease of *β*-glycosidase activity in the disrupted cell samples are incomplete cell disruption or partial inactivation of the respective enzymes.

The described rare appearance of *β*-glycosidase activity in the supernatant clearly indicates a strong cell association of the enzymes in most of the screened candidates. Since only a few strains showed high activity after disruption, an intact cell seems to be furthermore essential for the hydrolysis of 4-MUG. These conclusions are in line with the hypothesis of beneficial effects of whole cell systems on the pH tolerance of the conversion system.

Further investigation of the *β*-glycosidase activities in the supernatant revealed comparable activities in the supernatant and the untreated culture samples. As the culture samples used for the measurements included the supernatant, this result is not surprising. The strain with high *β*-glycosidase activities in the supernatant at wine conditions was identified as *Rhodotorula mucolaginosa*. *R. mucolaginosa* is known for extracellular *β*-glycosidic activity and has already been successfully tested for the possible application in wine aroma enhancement.[139] Currently, four genes in the genome of *R. mucolaginosa* in the NCBI database (NCBI:txid5537) are associated with *β*-glycosidases, but none of them has been

clearly identified. Further investigations could clarify, if one of these entries is responsible for the extracellular enzyme activity described above.

The strains with high activities after cell disruption showed only marginal activity in the culture samples. Therefore, it is likely that 4-MUG was not transported into the intact cells, at least under the conditions used in these experiments. The detailed investigation of the activities in cell lysates illustrates the adaptation of the so far overlooked intracellular *β*-glycosidases to intracellular conditions. The high activities are therefore not directly applicable and would require additional protection by the intact cell.

ITS sequencing of the twelve strains with the highest activity of whole cell samples at pH 3 revealed, that 4 strains belonged to the genus *Wickerhamomyces*, which is well known for its *β*-glycosidase activity.[292] For this genus, intra- and extracellular *β*-glycosidase activity was described[94] and in 14 genomes deposited in the NCBI taxonomy browser (NCBI:txid599737), 20 proteins were found to be associated with *β*-glycosidases. 7 of the named proteins are classified as *β*-glycosidases, whereas three were identified in *Wickerhamomyces anomalus* and four in *Wickerhamomyces ciferri*.

Another yeast was identified as *Issatchenkia terricola*, for which an extracellular *β*-glycosidase is described in wine context.[176] The gene coding for this *β*-glycosidase activity was recently identified as *g4180*. Furthermore, the authors were able to identify ten additional genes for putative *β*-glycosidases which could also be responsible for the described enzyme activity.[293] Surprisingly, the screening results suggested higher cell-associated activities than in the supernatant for this strain. This could be reasoned by the fact, that different surrogate substrates (which might be transported into the cell to different extents) were used. A search for *Issatchenkia terricola* *β*-glycosidases using the NCBI taxonomy browser (NCBI:txid4909) yielded 30 hits related to *β*-glycosidases. Three of these enzymes are described as possible *β*-glycosidases and were identified in a strain isolated from fermented masau fruits. Two of these proteins (SUN4 and ADG3) are described as secreted enzymes, while the remaining protein could be responsible for the observed intracellular activity.

Two strains with high activity were the yeast-like basidiomycete A*ureobasidium pullulans*, which is already well known for *β*-glycosidase activity in the cell supernatant,[141] while cell-associated activity has not been studied. The in-depth characterization of the *β*-glycosidase activities of these species is confirmed by 1012 entries for *β*-glycosidases in the NCBI taxonomy browser (NCBI:txid5580). However, as mentioned before, the identification of an intracellular activity has not been described yet. The fact that strains with high cell-associated activities in the screening have been already described for their extracellular activities reinforces the assumption that many cell-associated activities could have been overlooked so

far. The described *β*-glycosidases may also be capable of even higher activities at low pH values before secretion.

Two strains associated with high *β*-glycosidase activity could be identified as *Nakazawaea ishiwadae*, which was recently described to occur in wine fermentations.[294] A search with the NCBI taxonomy browser led to a genome sequence (NCBI:txid1538179) for which only 13 proteins are annotated. None of these sequences was identified as *β*-glycosidase. Recently, whole-genome sequencing analysis of *Nakazawaea ishiwadae* strain GDMCC 60786 revealed, that this strain expresses phosphoglucomutases, phosphofructokinases, phosphoglycerate kinases, phosphoglycerate mutases, pyruvate decarboxylases, and pyruvate dehydrogenases.[295] However, *β*-glycosidases were not described in this study. Based on the available genome sequence and the confirmed relevance for wine fermentation, a more detailed investigation of the responsible *β*-glycosidases, for example by purification of the enzyme activity and subsequent sequencing, could be interesting for future studies.

Additionally, one strain each of *Hanseniaspora occidentalis*, *Candida railenensis* and *Bulleromyces albus* could be associated with high cell-related activity at lower pH values. These species are well known to occur in wine fermentations.[296–298]

For *Hanseniaspora occidentalis*, the deposited genome sequence (NCBI:txid56407) in the NCBI taxonomy browser contains 20 annotations for proteins, none of which is associated with *β*-glycosidase activity. In a more detailed examination of the genome sequence of the closely related non-conventional wine yeast *Hanseniaspora guilliermondii* Strain UTAD222 and a comparison with two strains of the same genus, 879 '*Hanseniaspora*-specific' proteins were identified. Three of these proteins (HGUI_02084, HGUI_02647 and HGUI_02781) were identified as β-glycosidases.[299] Although these enzymes have not been characterized in detail, it is possible that a structurally related enzyme is responsible for the observed activity.

A genome sequence for *Candida railenensis* has also been deposited in the NCBI taxonomy browser (NCBI:txid45579). 5972 proteins are annotated for this sequence, two of which (Sun41p and Sim1p) have been identified as secreted *β*-glycosidases. Furthermore, there is one ergosteryl-*β*-glycosidase identified and two possible *β*-glycosidases with the accession numbers CAH2352108.1 and CAH2353540.1, which originate from a draft genome of the *Candida railenensis* strain CLIB 1423. Since the enzyme activities described in the context of this study are rather cell-associated, only the latter two putative enzymes can be considered to be responsible for the observed *β*-glycosidase activity.

The genome sequence deposited for *Bulleromyces albus* (NCBI:txid157611) contains only seven protein annotations, none of which has been identified as *β*-glycosidase.

There is no further evidence in the literature for possible enzymes of this strain capable of the identified *β*-glycosidase reaction. This further emphasizes the novelty of the identified strain.

The described effects of the investigated substrates on *β*-glycosidase activity revealed strongly different influences of the added substrates on the different organisms. Although increased *β*-glycosidase activity can be partially achieved with supplementation of the culture medium, negative effects may also result. Before application, the influences of potential substrates during cultivation should therefore be investigated in detail. However, the results are consistent with previously published results. The positive effect of cellobiose in the culture medium on the *β*-glycosidic activity, which was observed for *B. albus*, has been described for several other organisms.[141–143] The extracellular *β*-glycosidase activity in the *Issatchenkia terricola* culture was not affected after the cultivation with naringin and hesperidin.[140]

Further investigation of *β*-glycosidase localization after the addition of the surrogate substrate using a confocal laser scanning microscope revealed additional indications for an intracellular or at least cell-associated localization of the hydrolytic enzymes of *N. ishiwadae* and *C. railenensis*. For *B. albus*, indications of cell-associated *β*-glycosidase activity localized at the cell membrane were observed. The described observations for *H. occidentalis* cells could either be caused by a specific location of the responsible enzymes or by transport of the cleaved surrogate substrate into certain parts of the cell, for example the vacuole.

The described observations are supported by the fact, that no significant activity could be detected in the investigation of cell lysates of *B. albus*. This is probably due to inefficient cell disruption or enzyme inactivation. Additionally, the potential membrane localization might be causal for the activity loss, as cells and membrane compartments were separated before the cell lysate measurements. Looking at the activity of the cell lysates of *N. ishiwadae*, *H. occidentalis* and *C. railenensis*, it could be concluded that intact cells protect the enzymes and thereby maintain their activity. After the cells were disrupted, activity at low pH values was clearly decreased. This observation is in line with the general opinion that whole cells provide the best known environment for enzymes under harsh reaction conditions.[300]

The measured profiles of selected terpenes in the sample headspaces after the incubation of a must-derived glycoside mixture with whole cells or corresponding cell lysates revealed clear differences, especially for *N. ishiwadae*. These results are either an indication of the filter function of the membrane, or the organisms are able to further metabolize or modify substances. The proposed filter function can be explained by the fact that glycosides must be transported across the cell membrane to get in contact with intracellular enzymes. This would be a decisive difference to extracellular *β*-glycosidases, which have direct access to all aroma-glycosides present in the must. The frequently described transformation of aglycones after glycosidase-catalyzed release has been well reviewed.[301]

For example, geraniol can be partially transformed into citronellol by microbial cells after precursor hydrolysis. It must be considered that these transformations could also be partly responsible for the observed differences.

The observed changes of *β*-glycosidase activity of *B. albus* in must and citrate-phosphate buffer supplemented with glucose and ethanol could be related to the previously postulated membrane association, as enzymes on the surface of the cell are more exposed to exogenous additives than intracellular enzymes. In addition, the *β*-glycosidase activity of *H. occidentalis* seems to be highly inhibited by glucose. The measured activity decrease for *N. ishiwadae* and *C. railenensis* in must furthermore suggests the presence of other inhibiting factors in addition to glucose and sugar.

Although the determined activities of the strains strongly decreased under conditions related to wine production, a significant influence of *N. ishiwadae* and *C. railenensis* on the terpene concentrations after mixed fermentations with *Saccharomyces cerevisiae* was already demonstrated after transfer of the selected strains with respective data to the HGU.[302] This confirms the potential of the investigated strains to influence aroma compositions and is a proof for the use of strains with intracellular or cell-associated *β*-glycosidase activity.

Therefore, the described strains can be used as aroma liberation catalysts at low pH values, whereby a filter function of the cell membrane is conceivable and could yield selectivity benefits. This might be a first indication that intracellular *β*-glycosidases can represent an attractive alternative to the so far mainly investigated extracellular *β*-glycosidases and might enable more selective aroma release applications.

The described studies showed that the screening approach using 4-MUG as a surrogate substrate can deliver strains with specific *β*-glycosidase properties, for example in whole cultures measured at pH 3. The obtained results strongly suggested that the responsible enzymes are located intracellularly or at least cell-associated. This assumption was in line with the observation of a protective effect of the whole cell catalyst against low pH values via the cellular pH homeostasis. From this property and the selectivity of aroma molecule release indicated by the respective experimental data, it can be concluded that strains with intracellular *β*-glycosidase activity have strong application potential during fruit juice processing.

6.4 *β*-Lyase activities

6.4.1 Engineering yeast strains for high thiol release activity by a directed evolution approach using SMC

Due to the importance of several volatile thiols for the aroma impression of wine and other beverages, the aim of the following experiments was the use of SMC as a screening and selection tool for the identification and optimization of microorganisms with high capability to convert precursor compounds into thiols. Due to the fact that SMC must be cleaved by a *β*-lyase enzyme to provide nitrogen for cell growth, the compound had been promoted to be useful for linking growth to the *β*-lyase activity,[256] which is the key reaction for thiol release.

The initial attempt of screening a collection of wine-related non-*Saccharomyces* yeasts for efficient growth in medium with SMC as sole nitrogen source first revealed that only few strains showed cell densities which were considerably above the average value. Although two consecutive growth phases in SMC medium were used, most strains either had some nitrogen reserves available or a basal SMC cleavage rate seems to be present in all cells. As a high *β*-lyase activity was assumed for the strains with highest cell density values, they were selected for further investigation using the DTNB assay. In general, the SMC-based screening approach in liquid medium also allows a rapid quantification of cell densities achieved and is thus advantageous compared to the previously published procedure with agar plates.[256] However, as the thiol synthesis pathways as well as the SMC degradation route in yeast cells have not been investigated in detail, efficient SMC usage should not be equated with high 4MMP or 3MH release activity and *vice versa*.

Other previously published methods for *β*-lyase activity assessment often rely on the conversion of Cys-4MMP and, in some cases, the subsequent detection of the resulting pyruvate after further conversion with lactate dehydrogenase.[193,303] Since these assays are relatively laborious, a growth-independent quantitative assay, which is also based on SMC as substrate was established. It furthermore uses DTNB, which forms a pigment after reaction with thiols and is very similar to a recently published method: Li *et al.* also applied DTNB in similar assays, but in combination with other thiol precursors such as L-cystathionine, L-cystine, L-methionine, or Cys-4MMP instead of SMC.[237] Although using Cys-4MMP is closer to reality, this molecule is very expensive and therefore not suitable for large-scale pre-screenings like conducted in this work.

Two consecutive rounds with a photometric DTNB assay for SMC cleavage product detection and a headspace GC-MS assay for direct detection of SMC cleavage products finally led to the selection of six candidates, for which high cleavage activity was assumed. Whereas in the growth-based initial screening organisms with low nitrogen demand yield unjustified

advantages, the SMC cleavage assays should correlate better with *β*-lyase activity or SMC conversion in general, respectively. The fact that only small amounts of methanethiol and dimethyl disulfide were detected in the headspace of the assays including DTNB suggests that all thiols formed during the assay react with DTNB and could be quantified by the absorbance of TNB^{2-}. The top six strains could be assigned to *P. kudriavzevii* and *W. anomalus*.

P. kudriavzevii is known in the wine sector for several positive effects such as deacidification.[4] *W. anomalus* is known for a variety of different enzyme activities, which can also influence the aroma composition of wines.[292,304] Interestingly, both species could be isolated from Chinese sesame-flavored Baijiu, in which 2-furfurylthiol seems to be responsible for the characteristic sesame flavor.[305] In case of *W. anomalus*, a 2-furfurylthiol release activity could be indeed observed for some of the isolated strains of this species.[305]

Although the SMC-based thiol release properties for the two identified species could not compete with the commercial strain X-thiol, the potential of using SMC for optimization of thiol release properties in a directed evolution approach was evaluated. The optimization of yeast strains with evolutionary approaches has been described in several studies,[e.g. 254,306–308] also in the beer[309] and wine environment.[249,253] In these experiments, a selective pressure is applied to the cultures, resulting in cells that have randomly undergone mutations conferring fitness advantages under the selective conditions applied. These cells have a growth advantage and therefore accumulate in the culture.

Different tests were performed to assess the improvement potential for growth in SMC medium and the influence of high *β*-lyase activity on the ability of a yeast strain to grow with SMC as sole nitrogen source. Comparative growth studies with SMC or different amounts of $(NH_4)_2SO_4$ as nitrogen source showed that the available nitrogen limits growth, mainly the reachable cell density. While this observation was consistent for *P. kudriavzevii*, X-thiol and VIN13, the longer lag phases of *W. anomalus* in medium with $(NH_4)_2SO_4$ concentrations of 0.4 mmol L^{-1} and 0.5 mmol L^{-1} indicated, that high concentrations have negative influences on the growth of this strain. The significantly reduced growth rates and longer lag phases of all cultures during growth in SMC medium furthermore proved that utilization of nitrogen from SMC strongly limits cell growth, which indicated improvement potential within the evolutionary approach. The possibility that growth in SMC medium is limited due to strong toxic effects of SMC was also ruled out. In comparison to other potential *β*-lyase substrates, a relatively low toxicity has been already described for SMC.[256]

Unexpectedly, it was observed that although X-thiol has been noted for the highest release of methanethiol and dimethyl disulfide in the SMC cleavage assay, this strain grew poorly in SMC medium. Furthermore, the effect of *tnaA* expression in AWRI1631 showed weaker effects than expected. The increase in *β*-lyase activity after transformation[193] should have led to

significantly increased growth rates, if *β*-lyase-catalyzed SMC cleavage limits its utilization, but the observed effects were only moderate. An explanation could be that, at least in this strain, not only *β*-lyase activity limits nitrogen release from SMC, but also other mechanisms such as transport of SMC into the cells. Since *β*-lyases are mainly located intracellularly, transport is an important aspect of this reaction.[310]

Examination of the evolved strain´s growth rates indicated significant and specific changes in the ability to utilize nitrogen from SMC after the 25 sequential batch cultivations in SMC medium. For X-thiol and VIN13 in most cases clearly increased growth rates were observed, indicating an improved utilization of nitrogen from SMC. While the observed growth difference between mutated and wild type cells were comparable for all three selected clones of *P. kudriavzevii*, X-thiol and VIN13, the examined clones of the evolved *W. anomalus* population showed slightly different growth curves, some of which showed no or only a slight improvement to that of the starting strain. As the growth improvement in SMC medium even for the finally selected clone *W. anomalus* 25-2 is minor, the evolved population was probably not homogeneous with regard to this trait after the evolution procedure.

The previously discussed differences in the growth curves suggested possible advantages of the evolved cells with regard to the release of 4MMP and 3MH from their precursors. To further investigate the strain´s thiol release properties with regard to respective aroma-relevant molecules with importance in wine, the strains could be cultured in a must with low natural precursor concentrations (for example Müller-Thurgau) supplemented with the natural precursors Cys-4MMP and Glut-3MH in the future.

However, it has to be considered that the structures of SMC and the aroma thiol precursors have marked differences and the involved uptake factors or *β*-lyases in the evolved strains might accept SMC, but not the glutathione and cysteine conjugates. This fact might result in more efficient flux of SMC through this pathway but is not necessarily a prove for differences in the conversion of the aroma thiol precursors. In this context it has to be kept in mind that several other enzymes, for example *γ*-glutamyltranspeptidase and carboxypeptidase are essential for conversion of these precursors, but not necessary for the utilization of SMC. Such factors might still limit flux through the aroma thiol release pathway without limiting higher SMC conversion. Recently, it was also indicated that the growth ability in SMC medium does not correlate well with *β*-lyase activity or aroma thiol release improvement, respectively.[311]

Since the observed growth differences of the cells transformed with *tnaA* and the associated strong increase in *β*-lyase activity turned out to be much smaller than the effects after the evolution experiments, a sole increase in *β*-lyase activity as a consequence of random mutations of natural *β*-lyases such as STR3[207] and *IRC7*[303] is unlikely.

Much more probable, a transporter for SMC and the thiol precursors such as OPT1 for import[213] or GEX1 for export[312] from the cell, or YBT1 for transport into the vacuole[213] is also affected.

Genetically modified *S. cerevisiae* strains overexpressing *β*-lyases like *IRC7* or *tnaA* have been developed for wine aroma improvement[193,257] and also for application in the craft beer sector by the US companies Omega Yeast and Berkeley Yeast. Direct comparisons in future will show if the strains developed via adaptive laboratory evolution might be even more efficient than those GMO yeasts due to altered enzymes of the aforementioned classes.

To further investigate the causes of the observed enhancement in growth and thiol release, the obtained strains of X-thiol and VIN13 were sent for genome sequencing. Analysis of genome sequence data and testing of sequence-phenotype relationships are addressed in ongoing work and detailed analysis of the thiol liberation properties will be conducted in the future.

Especially when combined with grape varieties rich in thiol precursors, application of strains evolved by this way could probably lead to a significant increase of thiol levels. In addition, the directed evolution approach can also be applied in a more selective way by using not SMC, but a specific thiol precursor. Such procedures, maybe even combined with counter selection steps, could enable a variety of specific thiol release properties that can be introduced in strains without genetic engineering. As thiol release is furthermore important also for preparation of beer, liquor and juices, the application of the directed evolution principle presented here allows a much more efficient use of the plant-derived aroma precursors and facilitates the development of many novel beverage variants.

6.5 Engineering volatile thiol formation in yeast

Within the described experiments, yeast strains and bioconversion conditions were established and optimized for the synthesis of thiols from a number of respective substrates via a natural biosynthetic route. To assess the synthesized 3MH quantities, an external calibration line was created, on the basis of which the produced 3MH quantities were estimated. The first engineering step towards whole cell catalysts with high flux through the whole pathway was the expression of the *tnaA* gene from *E. coli*, which has been described to lead to high *β*-lyase activity.[193] Comparison of the two different yeast strains AWRI1631 and CEN.PK2-1C showed increased values in *β*-lyase activity in an indirect assay after genomic integration of a *tnaA* expression construct. Although the CEN.PK2-1C transformants exhibited much higher activities in this assay, first tests for bioconversion of added *(E)*-2-hexenal into 3MH showed comparable productivities of both strains. The discrepancy between the *β*-lyase assay and the 3MH production experiments with regard to differences between the two strains might be the

result of for example a lower *(E)*-2-hexenal uptake capability of AWRI1631. Another explanation might be the possibility of different H_2S production levels in the strains investigated, which can also contribute to thiol formation. Although unlikely, this could be true also for some of the conditions tested and should be evaluated in future experiments.

To test whether conversion of *(E)*-2-hexenal to 3MH was enabled after genome integration of *tnaA* and the concomitant strong *β*-lyase activity of the cells, the selected transformants were incubated on a 10 mL scale in 100 mmol L^{-1} citrate-phosphate buffer and synthesized 3MH was quantified. The data suggests, that 3MH formation from added *(E)*-2-hexenal is probably not the result of a spontaneous reaction with cysteine at low pH values to form a precursor molecule,[266] which is subsequently hydrolyzed by the yeast cells. The increase of produced 3MH amount at neutral pH rather indicates an enzymatic reaction that takes place to higher extent at pH 7.

The absence of the product 3MH in reactions without the addition of *(E)*-2-hexenal or *(E)*-2-hexen-1-ol confirms that these substances act as substrates of the described thiol biosynthesis pathway. Higher amounts of substrate, however, led to higher product amounts only up to a substrate concentration of 100 µg L^{-1}. Although the mechanism behind is unclear, one can assume that both substrates have an inhibitory effect on the enzymes involved in thiol formation or on the cells´ fitness in general. As *(E)*-2-hexenal and *(E)*-2-hexen-1-ol can be interconverted by endogenous yeast alcohol dehydrogenases,[313] it is unclear, if one of them or both are actually responsible for the inhibition of product formation at elevated substrate concentration. Although in the described experiments, *(E)*-2-hexen-1-ol yielded higher 3MH levels, a higher thiol conversion was found for *(E)*-2-hexenal during must fermentation.[219] Although it has not been experimentally proven to which extent the aldehyde or the alkenol or both can be converted to their respective glutathionylated forms by GSTs, a higher activity for the aldehyde due to its high electrophilicity is expected. The latter is a general property of substrates of GSTs, which show a high level of substrate promiscuity apart from that.[314] In case the aldehyde is in fact the main converted substrate, the higher product levels obtained with the alkenol substrate would point to a higher inhibitory or destructive action of the alkenol, which might be partly prevented by the *in situ* aldehyde production. The comparisons of the product peak areas after the use of C_5-, C_6- and C_7- aldehydes and respective alkenols clearly demonstrated the generality of higher thiol product levels obtained with alkenol substrates.

The pronounced decrease in the product levels at higher reaction volumes in the 10 mL vials suggests, that probably the lack of oxygen limits the conversion efficiency due to lower cell capacity. Although oxygen is not directly involved in the described reaction, oxygen availability can also affect the synthesis of enzymes necessary in the thiol synthesis pathway, such as oxidoreductases and peptidases. In addition, older cells seem to be unable to perform the

bioconversion towards the thiols, since longer cultivation times in the cell preparation step also led to a strong decrease of measurable product concentrations. After the assays were supplemented with pyridoxal-5-phosphate, no change in the amounts of the produced 3MH was detected. This suggests that pyridoxal-5-phosphate, although it is the essential co-factor for *β*-lyases,[315,316] is either not taken up or is not limiting product formation under the selected conditions. In order to provide the cells with nutrients to support the maintenance metabolism or even enable growth, addition of glucose and complex media like YPD and YCB containing a variety of supplements were tested. However, these conditions led to clearly decreased productivities, which suggests that only resting cells have the ability to produce 3MH. Since GSH is involved in the cell´s response to oxidative stress,[317,318] attempts were also made to increase the amount of GSH contained in the cells by causing oxidative stress in form of Zn_2Cl[318,319] and H_2O_2. However, at least under the conditions tested, these additions almost abolished the synthesis of measurable amounts of 3MH.

The productivity of the biocatalyst was strongly improved by the overexpression of one of the two enzymes γ-glutamylcysteine synthetase or GST. The overexpression of *GSH1* and the proposed associated increase in the intracellular GSH concentration led to a strong improvement in contrast to the external addition of GSH. Limitations of GSH uptake for example through the high affinity glutathione transporter Hgt1p[320] might explain these differences.

Positive effects of overexpression of a GST-encoding gene on product concentration were different depending on the specific gene. These enzymes are probably part of the thiol synthesis pathway by catalyzing the transfer of *(E)*-2-hexen-1-ol to glutathione. Moreover, for specific substrates specific GSTs were optimal with regard to high product levels. Thus, a specificity of the transformed enzymes for the used substrate is likely. The simultaneous overexpression of *GSH1* and a GST-encoding gene led to higher product concentrations, if compared to the reference strain only expressing a GST-encoding gene. However, only the *GSH1*/*GTT1* and *GSH1*/*VvGST4* co-expression strains yielded higher product levels compared to the strain only overexpressing *GSH1*. As no determination of enzyme levels in the individual strains was performed, it is unclear, how the presence of two plasmids influenced the expression levels. Therefore, additional conclusions about pathway flux limitations in the strains cannot be drawn.

After the sequential optimization of reaction conditions and catalyst engineering towards higher 3MH productivity, expansion of the product portfolio was examined by the use of a number of alternative substrates. Some of the identified peaks could probably not be assigned to a possible product based on their mass spectra as respective spectra are not contained in the NIST database. However, based on the calculated molecular mass and the fact that the peaks

were only found in reactions with cells overexpressing genes encoding TnaAp, a GST and Gsh1p, some of the products could be tentatively identified with high probability.

For seven of the 18 substrates used, the predicted product could not be detected. This is true for example for the applied terpenes and *(Z)*-6-nonenal, which confirmed the assumption that the substrate for the described reaction needs to be unsaturated in the α,β-position. In addition, this applies to *(Z)*-3-hexenyl acetate, a green leaf fragrance that occurs in the leaves and berries of many plants[236] and to furfural, the thiol equivalent of which, 2-furfurylthiol, is one of the main components of the roast aroma in coffee and is therefore of great economic interest.[236] Despite a report about the formation of 2-furfurylthiol from cysteine-furfural conjugates[239] and L-cysteine and furfural[240] by yeasts, this product could not be identified. Although a possible product was identified for *(E)*-2-nonenal, no product was detected for *(Z)*-6-nonenal. This additionally confirms that the position of the double bond is important for the conversion of linear substrates. Since a standard was available for 3MH, it was possible to clearly identify this product on the basis of the retention time and the similarity in the mass spectra measured after the bioconversions of either *(Z)*-2-hexen-1-ol or *(E)*-2-hexen-1-ol although the comparison with the collected data to the calculated expected mass ratios did not give any additional indications for this product. In these cases, glutathione is obviously conjugated to the same carbon atom in both molecules. The use of *(E)*-3-hexen-1-ol instead resulted in a potential product peak, in whose mass spectrum the molecular ion of the expected products could not be found. The detected ion with *m/z* 124 may be a fragment ion of the compound synthesized from *(E)*-3-hexen-1-ol. The compound´s retention time and its mass spectrum showed clear differences to the values obtained for 3MH, which is one possible product for this substrate. Instead, this peak might be caused by 4-mercaptohexan-1-ol. However, the examination of the natural occuring isotope distribution revealed no indication for a sulfur group. Therefore, the identification as a possible product peak will require further investigation in the future.

The incubation with *(E)*-2-pentenal, *(E)*-2-pentenol, *(E)*-2-heptenal and *(E)*-2-hepten-1-ol led to the identification of product peaks, for which the predicted products could be tentatively identified by their expected molecular mass and the mass intensity distribution. In bioconversion tests with terpenoids, except for (R)-(+)-pulegone no conversion products could be detected in the described approach. This observation is in line with the assumption, that these substances are weak electrophiles because they do not have the respective arrangement of double bond and alcohol/carbonyl. The conversion of 3-methyl-2-buten-1-ol, on the other hand, led to the tentative identification of the expected product 3-mercapto-3-methylbutan-1-ol based on the comparison of the mass spectra to a reference database and identification of the molecular ion.

This molecule is known as an aroma component in Sauvignon Blanc wines.[321] Investigation of the possible product peak after incubation with 3-buten-2-one revealed a fragment of the expected molecular ion, as well as the expected distribution of mass intensities for a sulfur containing molecule. Based on these observations, it is very likely that the identified peak is caused by one of the two expected products 4-mercaptobutane-2-one or 3-mercaptobutane-2-one.

For the bioconversion reactions with 3-penten-2-one, three possible product peaks were identified, two of which showed identical mass spectra. Since the calculated mass intensity distribution for the predicted sulfur containing products was only matching for the peak at 6.6 min, this is most probably the sought molecule containing a thiol group. After incubation with (R)-(+)-pulegone, two peaks with very similar mass spectra were identified which most probably contain a thiol group. These are most probably the expected product 8-mercapto-*p*-menthan-3-one and its enol form or two different 8-mercapto-*p*-menthan-3-on isomers.[322] Due to the similar mass spectra, no more precise statements can be made based on the described measurements. In the future, further investigations of the synthesized molecules will be necessary to clarify their identity. After the conversion of 1-octen-3-ol, one of the key aromas of fungi,[236] efficient synthesis of a product could be observed, but it was not possible to identify the expected molecular ion mass or an indication for sulfur isotope patterns in its mass spectrum. Even the conversion of *(E)*-2-nonenal, an aldehyde with nine C-atoms, could be proven by identification of a putative product. This shows the high general substrate promiscuity of the whole pathway, which might be further expanded by the use of other GSTs. Moreover, nearly no knowledge exists so far on the substrate specificity of other factors involved in the pathway – transporters, dehydrogenases or reductases, γ-glutamyltranspeptidases, carboxypeptidases and β-lyases. Although more detailed studies are necessary to identify the flux-limiting steps in the whole pathway with respect to certain substrates, the platform can be extremely useful for the synthesis of many different thiol compounds.

The biosynthetic route engineered in the yeast strains within this work resembles the pathway which contributes strongly to the formation of volatile thiols during the production of wine and other beverages. Therefore, the established system also allows testing for example the activities of specific GSTs from certain *Vitis vinifera* varieties or the activities of specific β-lyases or other pathway enzymes from wine yeast strains towards certain substrates. Furthermore, it enables the simple preparation of small amounts of thiols for example for olfactory tests in flavour research. However, if the system should be used for biotechnological production in future, considerable optimization of productivity will be necessary.

7 Supplementary information

7.1 Plasmid maps

7.1.1 BKD_*tnaA*

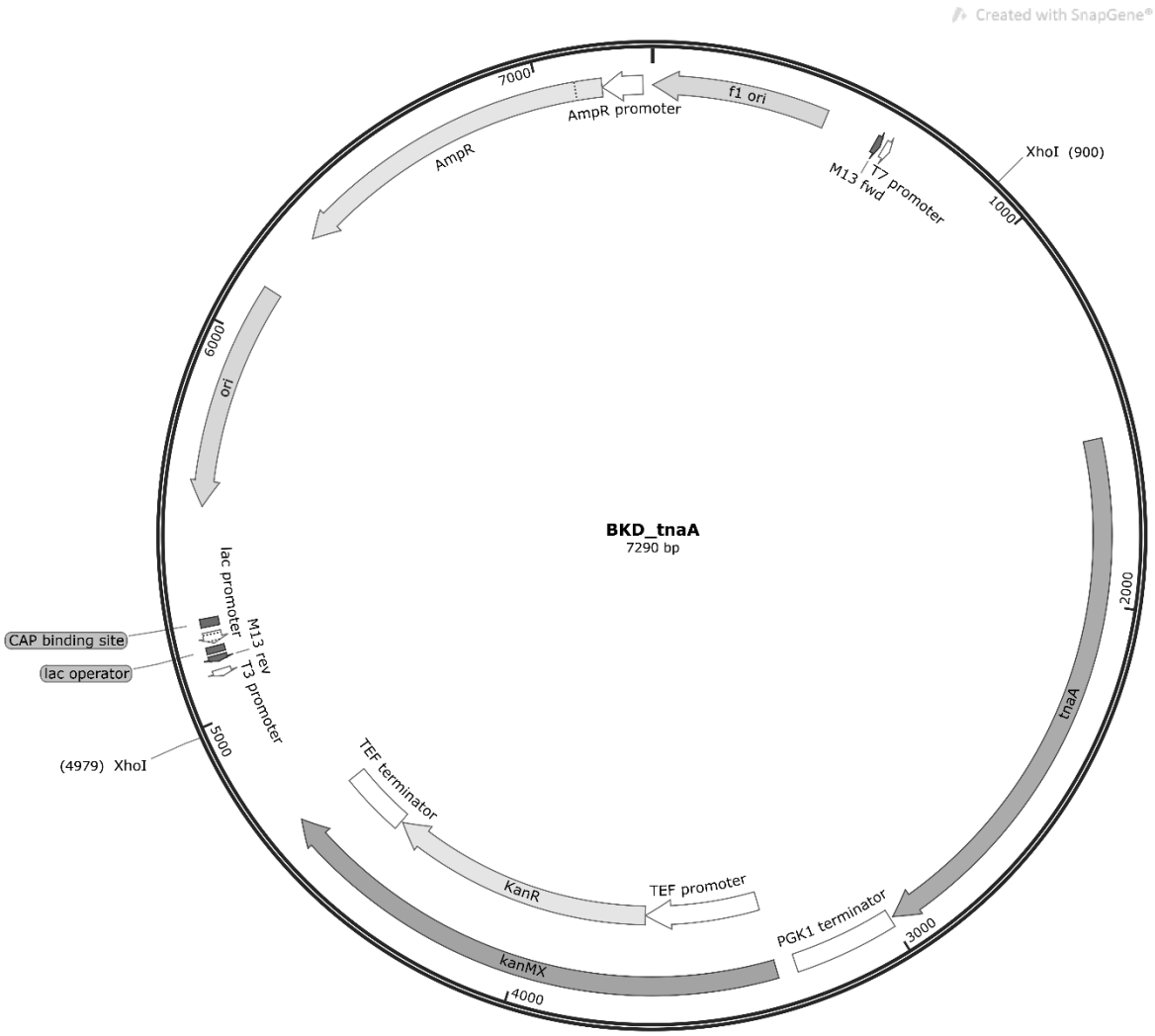

Figure S 1: Map of the BKD_*tnaA* plasmid used for *tnaA* integration into the delta sequences of yeast cells.

7.1.2 pPK-Plasmids

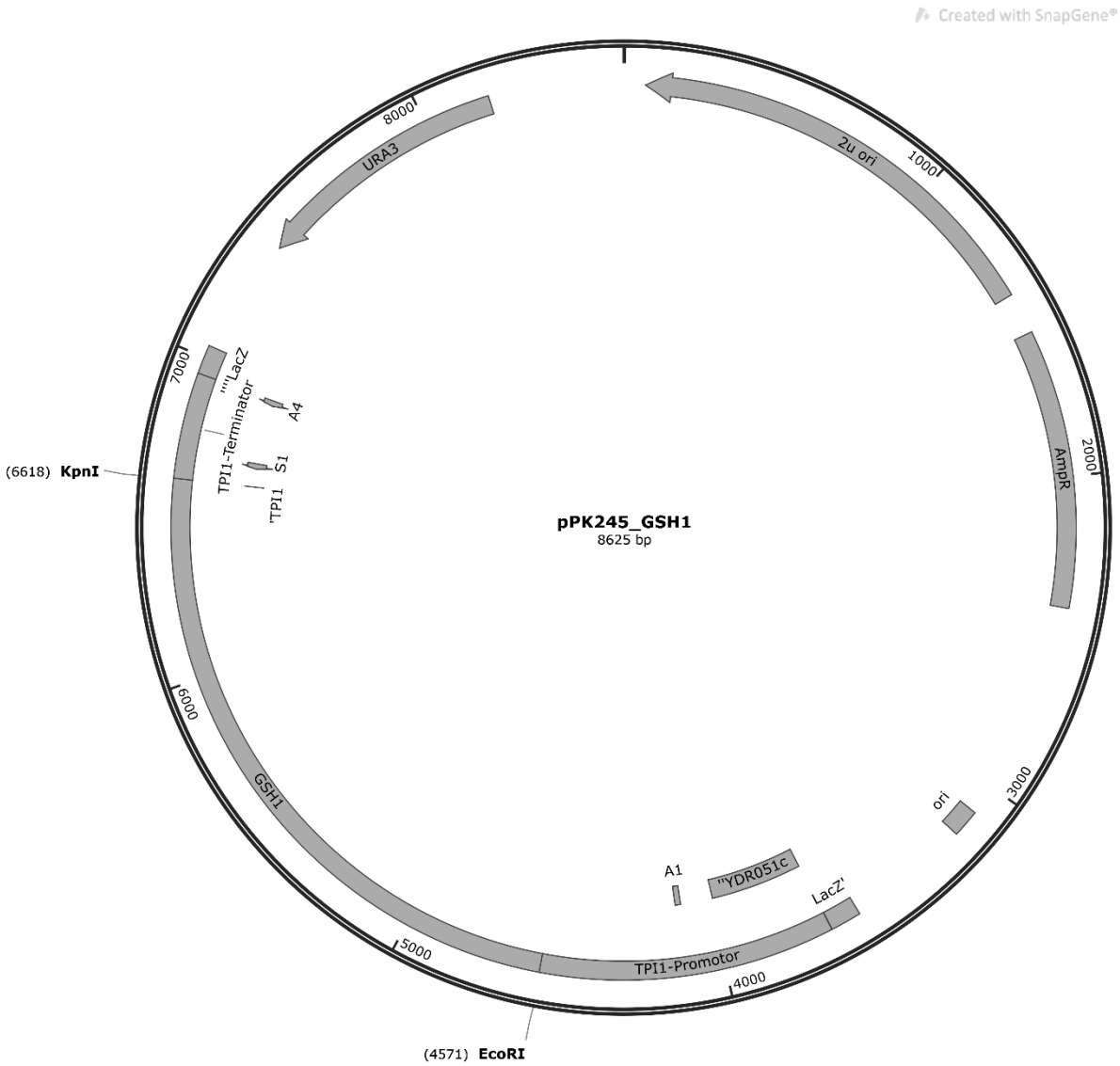

Figure S 2: Map of the pPk245_GSH1 plasmid used for GSH1 overexpression in CEN-PK2-1C cells.

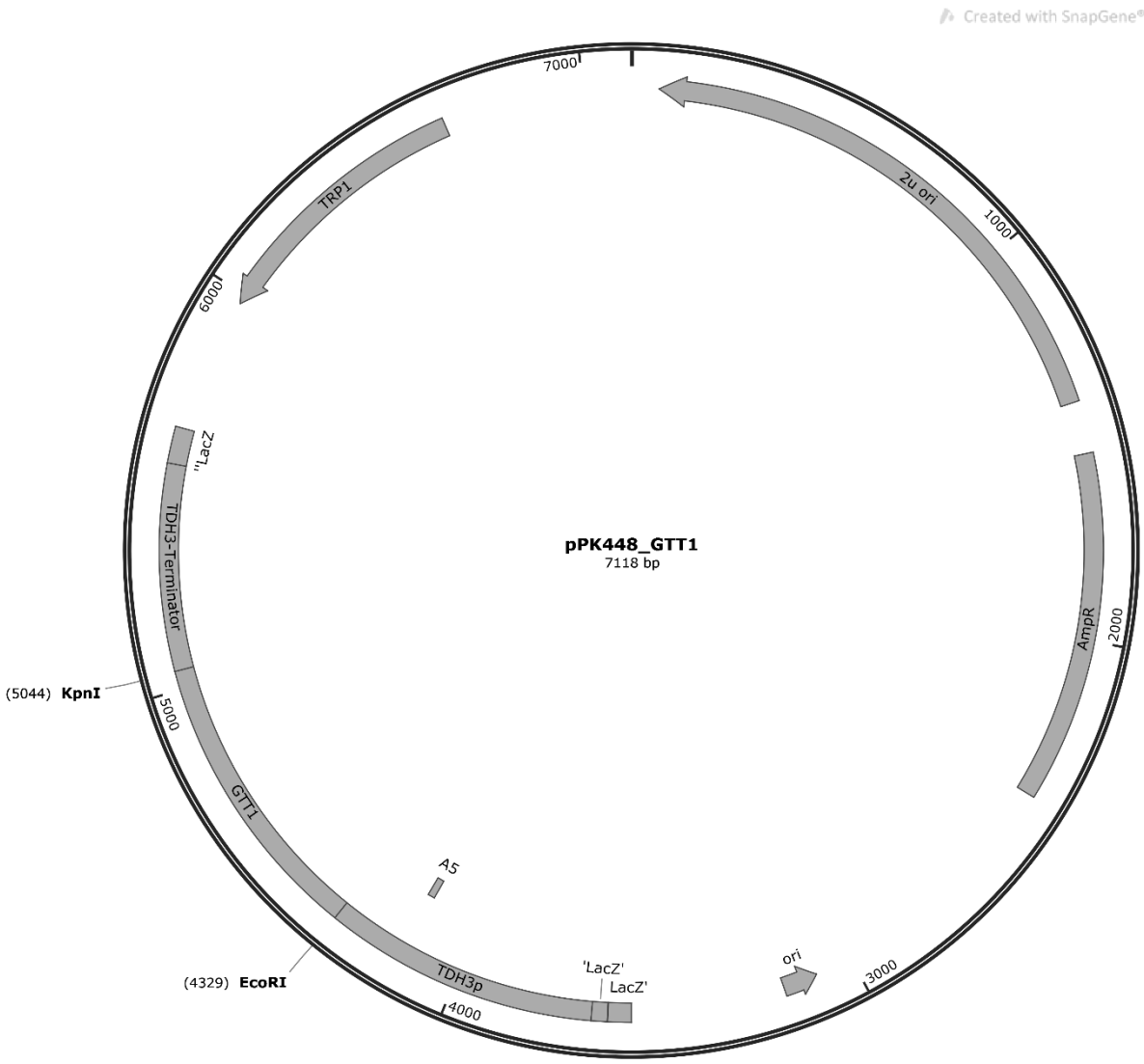

Figure S 3: Map of the pPk448_GTT1 plasmid used for GTT1 overexpression in CEN-PK2-1C cells.

Figure S 4: Map of the pPk448_GTT2 plasmid used for GTT2 overexpression in CEN-PK2-1C cells.

Figure S 5: Map of the pPk448_VvGST4 plasmid used for VvGST4 overexpression in CEN-PK2-1C cells.

7.2 β-Glycosidase activities

7.2.1 Comparative investigations on different β-glycosidase surrogate substrates

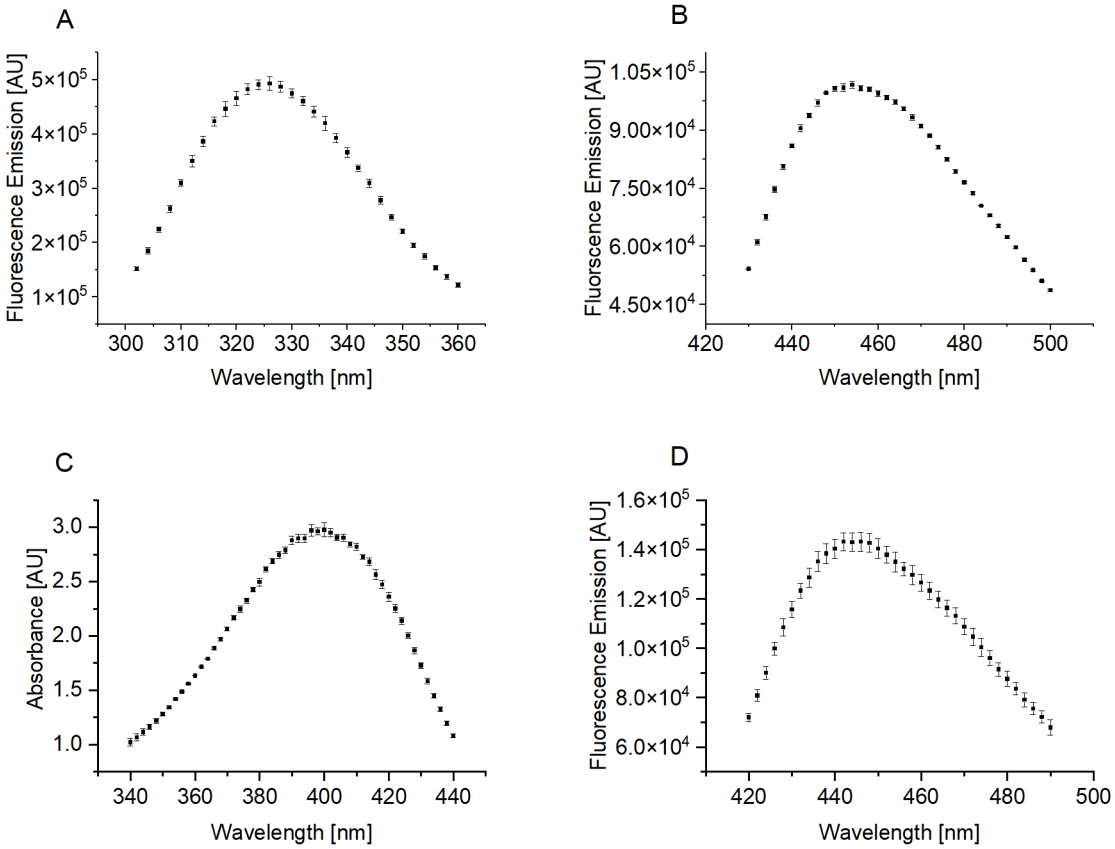

Figure S 6: Fluorescence emission and absorbance spectra of the investigated surrogate substrates in case of arbutin (A) and esculin (B) or the conversion products pNP (C) and 4-MU (D). Fluorescence was measured after excitation at the excitation maximum wavelength determined in the experiments. Experiments were conducted in triplicates. The values represent the mean values of three experiments and the respective standard deviations.

7.2.2 Investigation of non-*Saccharomyces* yeasts with intracellular *β*-glycosidase activity for wine aroma modification

Table S 1: Calculated values for the increase in fluorescence over time of the 50 isolates with the highest values for the conditions studied. The results are illustrated in Figure 25 and the calculation of the values is described in section 4.4.2.1.

Position	Isolate ID	Culture pH 7 [AU]	Culture pH 3 [AU]	Supernatant pH 7 [AU]	Cell Lysis pH 7 [AU]
Top 50 whole culture pH 7					
1	26b / 8	4943.22459	5121.77005	67.0211216	4319.10732
2	26b / 4	4820.19343	4198.86479	244.556518	629.760562
3	25b / 75	4168.31451	3761.12159	328.713709	646.175369
4	1bGspbN91	4002.30222	2207.9234	222.075356	1755.31474
5	Gk-bN-13	3558.94922	47.1168291	1039.69377	748.956138
6	1bTspoaN1	3501.27044	1303.52757	1683.92464	834.72098
7	40b / 70	3030.15166	2306.6642	-31.733518	908.581463
8	Gk-bN-11	2868.07786	17.2276201	559.771476	252.941146
9	1bGspbN31	2838.94354	1877.0895	328.933316	1670.40022
10	Gk-bN-15	2829.79868	30.7120393	883.220677	667.178883
11	1bGspbN43	2821.17824	1234.8009	286.657985	1532.32073
12	1bGsaN79	2793.71174	77.6699835	2007.82117	706.035714
13	1bGsaN1	2766.67917	422.518514	1774.07987	533.852646
14	1bGshcN4	2732.55322	342.509641	1487.93443	626.864179
15	1bGspcN4	2670.68506	847.355198	746.881254	305.93438
16	26b / 2	2432.26558	1585.19918	-44.80417	1617.78978
17	1bGshaN32	2405.73786	1091.88209	506.777552	701.887292
18	Gk-bN-8	2268.19571	6.16265575	820.488233	180.293635
19	1bGspbN23	2115.85291	965.630838	73.7853126	664.173521
20	1bGspbN78	2100.84656	1271.97424	32.8674862	1798.68107
21	1bGspbN26	2092.10085	822.759408	947.591118	1516.11774
22	1bGshcN7	2031.52009	983.197167	342.590177	1190.53452
23	13b / 60	1993.71246	4059.7104	78.0314336	310.881868
24	1bGshaN18	1932.99488	1533.14314	397.082543	1162.35365
25	1bGshcN6	1888.44516	967.736644	492.270894	1218.15929
26	Gk-bN-12	1827.95155	20.1958666	308.54206	511.386202
27	27b / 29	1785.10266	982.578956	-12.413634	53.9053255
28	1bGshcN67	1717.99493	80.3498293	572.916166	259.847695
29	1bGspbN93	1703.06811	950.296966	169.05414	888.743335
30	Gk-bN-7	1680.32648	-10.480129	625.024004	156.036861
31	34b / 12	1676.03474	1841.27849	316.96895	103.825817
32	33b / 49	1637.70312	2131.07934	91.7160023	173.217654
33	GS-B-9	1607.43136	79.944398	1480.14423	239.068812
34	1bGspbN94	1600.04736	87.2592554	1005.37808	346.150857
35	1bGshcN2	1571.95389	683.18314	113.636872	1012.45879
36	GS-B-43	1567.32815	77.6639756	1464.01023	455.732981
37	1bTA-a13	1554.70926	2620.92308	-468	32.6
38	26b / 74	1521.67591	1089.68321	-43.246678	750.396229

Position	Isolate ID	Culture pH 7 [AU]	Culture pH 3 [AU]	Supernatant pH 7 [AU]	Cell Lysis pH 7 [AU]
39	1bGspbN60	1513.12494	713.460906	218.135532	983.014752
40	GSCN13	1432.4466	170.269108	1299.76841	191.898286
41	35b / 27	1418.59669	772.915806	533.95754	310.35539
42	GS-B-30	1398.95047	76.1069369	1248.0954	258.969893
43	GS-B-26	1370.07809	179.458689	1207.10974	229.410052
44	GSCN10	1366.41703	117.843365	1267.10757	143.641339
45	GS-B-38	1365.00993	174.795672	1157.02863	140.497237
46	GSCN36	1352.39326	154.675153	1269.70949	158.777983
47	28b / 72	1338.98837	1900.5098	98.6030093	50.1461731
48	1bGspbN79	1333.76348	12.5762802	879.175903	514.57845
49	GS-B-6	1329.20324	109.393961	1270.40025	319.847206
50	GSCN5	1316.62834	127.083658	1048.53093	125.089875
Top 50 whole culture pH 3					
1	26b / 8	4943.22459	5121.77005	67.0211216	4319.10732
2	26b / 4	4820.19343	4198.86479	244.556518	629.760562
3	13b / 60	1993.71246	4059.7104	78.0314336	310.881868
4	25b / 75	4168.31451	3761.12159	328.713709	646.175369
5	1bTA-a13	1554.70926	2620.92308	-468	32.6
6	01b / 3	23.4988925	2395.1067	-36.215459	120.668195
7	40b / 68	584.796176	2392.00668	-41.054896	410.409663
8	40b / 70	3030.15166	2306.6642	-31.733518	908.581463
9	1bGspbN91	4002.30222	2207.9234	222.075356	1755.31474
10	1bTA-c42	877.266667	2182.96667	117.5	64.2222222
11	01b / 11	-21.283776	2141.16121	-33.733798	-40.238237
12	33b / 49	1637.70312	2131.07934	91.7160023	173.217654
13	01b / 7	38.1304512	1997.73673	-25.943678	-3.6847256
14	28b / 72	1338.98837	1900.5098	98.6030093	50.1461731
15	1bGspbN31	2838.94354	1877.0895	328.933316	1670.40022
16	01b / 9	178.626463	1847.73438	-21.692545	307.2738
17	34b / 12	1676.03474	1841.27849	316.96895	103.825817
18	1bTA-c56	847.533333	1824.76667	120.822222	26.6222222
19	29b / 1	1297.09945	1702.20239	179.98223	-2.3154188
20	34b / 10	1184.00601	1673.11256	43.3056585	-0.9252127
21	26b / 2	2432.26558	1585.19918	-44.80417	1617.78978
22	28b / 76	1155.84317	1576.67596	101.188837	7.39873589
23	1bGshaN18	1932.99488	1533.14314	397.082543	1162.35365
24	35b / 25	1111.78903	1512.23199	-13.568548	181.759996
25	28b / 78	1140.3263	1496.57181	103.929067	30.27444
26	34b / 6	812.164626	1312.48326	10.5524126	-28.576989
27	1bTspoaN1	3501.27044	1303.52757	1683.92464	834.72098
28	1bGspbN78	2100.84656	1271.97424	32.8674862	1798.68107
29	1bGspbN43	2821.17824	1234.8009	286.657985	1532.32073
30	23b / 41	104.527409	1210.50812	-58.770371	2005.53153
31	25b / 41	938.04428	1199.21839	-31.027049	1094.38524
32	35b / 35	926.85813	1187.61354	90.2254746	353.829547

Position	Isolate ID	Culture pH 7 [AU]	Culture pH 3 [AU]	Supernatant pH 7 [AU]	Cell Lysis pH 7 [AU]
33	35b / 41	953.275504	1185.43081	202.893432	74.8707218
34	16b / 52	1240.64218	1147.48823	-43.063681	12517.3766
35	26b / 50	1077.92555	1131.37468	-27.07344	1085.77807
36	1bGshaN32	2405.73786	1091.88209	506.777552	701.887292
37	26b / 74	1521.67591	1089.68321	-43.246678	750.396229
38	42b / 12	406.137006	1047.53145	-46.047864	356.094446
39	1bGshaN35	143.223659	1035.15513	-8.5104714	87.874467
40	35b / 33	798.464082	1025.15179	66.8145835	87.5242179
41	1bGshcN7	2031.52009	983.197167	342.590177	1190.53452
42	27b / 29	1785.10266	982.578956	-12.413634	53.9053255
43	35b / 31	508.692937	970.838651	40.5810195	-8.1910064
44	1bGshcN6	1888.44516	967.736644	492.270894	1218.15929
45	1bGspbN23	2115.85291	965.630838	73.7853126	664.173521
46	1bGspbN93	1703.06811	950.296966	169.05414	888.743335
47	25b / 77	353.640145	907.491619	-40.924268	1153.63324
48	25b / 25	183.93179	879.418198	-26.396699	1230.03962
49	1bGspcN4	2670.68506	847.355198	746.881254	305.93438
50	24b / 78	693.074923	841.258651	-35.366719	347.206303
Top 50 supernatant pH 7					
1	1bGsaN79	2793.71174	77.6699835	2007.82117	706.035714
2	1bGsaN1	2766.67917	422.518514	1774.07987	533.852646
3	1bTspoaN1	3501.27044	1303.52757	1683.92464	834.72098
4	1bGshcN4	2732.55322	342.509641	1487.93443	626.864179
5	GS-B-9	1607.43136	79.944398	1480.14423	239.068812
6	GS-B-43	1567.32815	77.6639756	1464.01023	455.732981
7	GSCN13	1432.4466	170.269108	1299.76841	191.898286
8	GS-B-6	1329.20324	109.393961	1270.40025	319.847206
9	GSCN36	1352.39326	154.675153	1269.70949	158.777983
10	GSCN10	1366.41703	117.843365	1267.10757	143.641339
11	GS-B-30	1398.95047	76.1069369	1248.0954	258.969893
12	GS-B-26	1370.07809	179.458689	1207.10974	229.410052
13	GS-B-38	1365.00993	174.795672	1157.02863	140.497237
14	GSCN44	1294.32533	141.437414	1142.75291	199.529406
15	GS-B-27	1234.17273	64.9143841	1117.65352	152.833203
16	GSCN14	1288.09777	152.7512	1102.81941	124.786364
17	1bTHna-46	1195.42708	127.887771	1088.55384	244.572079
18	1bMAna-70	1157.37778	83.1444444	1074.84444	340.644444
19	GSCN43	1224.81916	145.139844	1066.73162	212.204019
20	1bMAna-24	1136.58889	92.9	1062.23333	401.266667
21	GSCN3	1232.60042	124.064989	1054.49965	79.2452605
22	GSCN5	1316.62834	127.083658	1048.53093	125.089875
23	Gk-bN-13	3558.94922	47.1168291	1039.69377	748.956138
24	GSCN12	1171.74357	130.491443	1032.36605	176.126478
25	GSCN1	1164.59322	122.633374	1030.48371	175.758761
26	GSCN40	1160.13544	132.168567	1018.20387	161.292709

Position	Isolate ID	Culture pH 7 [AU]	Culture pH 3 [AU]	Supernatant pH 7 [AU]	Cell Lysis pH 7 [AU]
27	1bGspbN94	1600.04736	87.2592554	1005.37808	346.150857
28	GS-B-15	990.184717	61.6657622	980.215569	196.623163
29	GSCN11	1106.24556	122.203907	975.767919	122.90758
30	1bTHna-43	1078.4103	203.568051	954.141939	154.697252
31	1bTHna-1	1071.14158	89.1821861	948.818161	718.638253
32	1bGspbN26	2092.10085	822.759408	947.591118	1516.11774
33	MspBN24	1030.88689	53.8365178	946.986036	255.614361
34	GS-B-31	1138.84899	133.5363	945.47726	164.327229
35	GSCN9	1128.59499	107.898717	921.982011	138.285794
36	1bMAna-25	1051.32222	76.6222222	920.966667	303.544444
37	MspBN57	1017.49843	39.3629086	917.046748	124.802888
38	GS-B-44	1098.15439	157.333799	909.982201	290.788778
39	1bMAna-49	1033.64444	100.044444	904.011111	507.677778
40	GS-B-17	983.318952	74.9661795	894.454103	416.226866
41	GS-B-21	981.127732	84.7816056	886.925492	200.785049
42	GSCN48	1013.93115	82.4766393	884.179259	180.831738
43	GS-B-39	972.812811	41.3489303	884.030165	75.4829821
44	Gk-bN-15	2829.79868	30.7120393	883.220677	667.178883
45	1bGspbN79	1333.76348	12.5762802	879.175903	514.57845
46	1bMAna-10	1025.46667	116.288889	871.888889	74.1666667
47	GS-B-37	1032.61531	61.2932974	864.425756	121.898268
48	GS-B-8	912.383819	26.6998717	853.556413	163.585466
49	1bTHna-56	1011.63399	191.08156	851.910507	212.702699
50	1bTHna-100	977.565244	168.217489	841.211748	303.898086
Top 50 cell Lysis pH 7					
1	16b / 52	1240.64218	1147.48823	-43.063681	12517.3766
2	16b / 46	379.578912	651.982219	-42.22421	6201.78228
3	26b / 8	4943.22459	5121.77005	67.0211216	4319.10732
4	1bTmaN23	18.0664955	35.7089111	-45.179807	3594.91064
5	1bGkdN-14	278.504164	94.082087	49.1322321	3008.06247
6	01b / 1	237.939085	-153.35977	-43.967262	2661.2173
7	1bGkdN-57	313.333304	111.207793	54.0479859	2657.70846
8	16b / 60	-0.6314651	226.397943	-49.98042	2312.32395
9	13b / 21	-45.53086	-47.963323	-51.141463	2286.25722
10	16b / 58	-1.0866457	208.945697	-46.429622	2164.41642
11	15b / 4	99.1481158	373.823694	-51.443539	2012.44829
12	23b / 41	104.527409	1210.50812	-58.770371	2005.53153
13	16b / 68	89.6537275	241.721963	-39.488828	1979.7135
14	1bGeaN-15	278.600535	112.737028	43.0223457	1909.39417
15	1bGkdN-63	294.350911	111.584223	2.11138237	1880.5051
16	1bGkdN-68	273.017344	102.982363	39.9229281	1845.99876
17	26b / 76	23.2409204	117.64726	-53.679727	1812.48663
18	1bGspbN78	2100.84656	1271.97424	32.8674862	1798.68107
19	16b / 66	-10.372384	37.3485239	-41.145222	1784.51515
20	1bGspbN91	4002.30222	2207.9234	222.075356	1755.31474

Position	Isolate ID	Culture pH 7 [AU]	Culture pH 3 [AU]	Supernatant pH 7 [AU]	Cell Lysis pH 7 [AU]
21	13b / 66	893.717249	260.514521	14.7843172	1741.19463
22	1bTspobN1	583.527485	165.315777	158.510222	1703.18678
23	1bGspbN31	2838.94354	1877.0895	328.933316	1670.40022
24	15b / 1	-5.2246385	279.262224	-45.449791	1641.38262
25	26b / 2	2432.26558	1585.19918	-44.80417	1617.78978
26	1bGkdN-13	327.168745	135.966754	82.4511874	1600.14211
27	1bGkdN-65	240.515491	59.6313516	20.5155812	1552.8092
28	1bGspbN43	2821.17824	1234.8009	286.657985	1532.32073
29	1bGkdN-60	262.324474	98.5242796	30.9451475	1525.19326
30	1bGkdN-55	297.09908	136.371936	50.1583414	1523.7594
31	1bGspbN26	2092.10085	822.759408	947.591118	1516.11774
32	1bGkdN-11	266.997151	107.081937	82.0770094	1506.80021
33	1bGsbN8	208.346097	105.537969	52.7022908	1485.55207
34	1bGkdN-58	322.603066	120.390903	109.72605	1483.32231
35	1bGkdN-53	371.06384	159.186301	77.5299749	1459.29621
36	09b / 67	9.38517998	178.659167	-49.186883	1440.73954
37	1bGsbN18	285.084368	101.683374	-41.99095	1413.03325
38	NC8	-15.891786	395.442812	-50.567341	1386.88574
39	17b / 51	74.9186442	133.657777	-42.263151	1368.35044
40	1bTspub85	739.668312	150.239694	572.641096	1342.15346
41	1bGkdN-10	344.841053	152.277708	51.4920571	1326.21912
42	1bGsbN7	223.905481	99.4169626	47.9259364	1314.50749
43	1bGkdN-3	235.531812	71.050546	57.5580453	1313.82169
44	14b / 76	20.7546417	49.5131951	-45.386629	1285.12475
45	1bGkdN-39	298.089977	97.6771252	-14.848867	1246.20554
46	24b / 14	1247.56143	628.75859	-27.278349	1233.14158
47	25b / 25	183.93179	879.418198	-26.396699	1230.03962
48	17b / 37	44.3134646	178.156596	-50.052622	1222.49745
49	1bGshcN6	1888.44516	967.736644	492.270894	1218.15929
50	15b / 35	93.6213811	212.286784	-44.912765	1213.89813

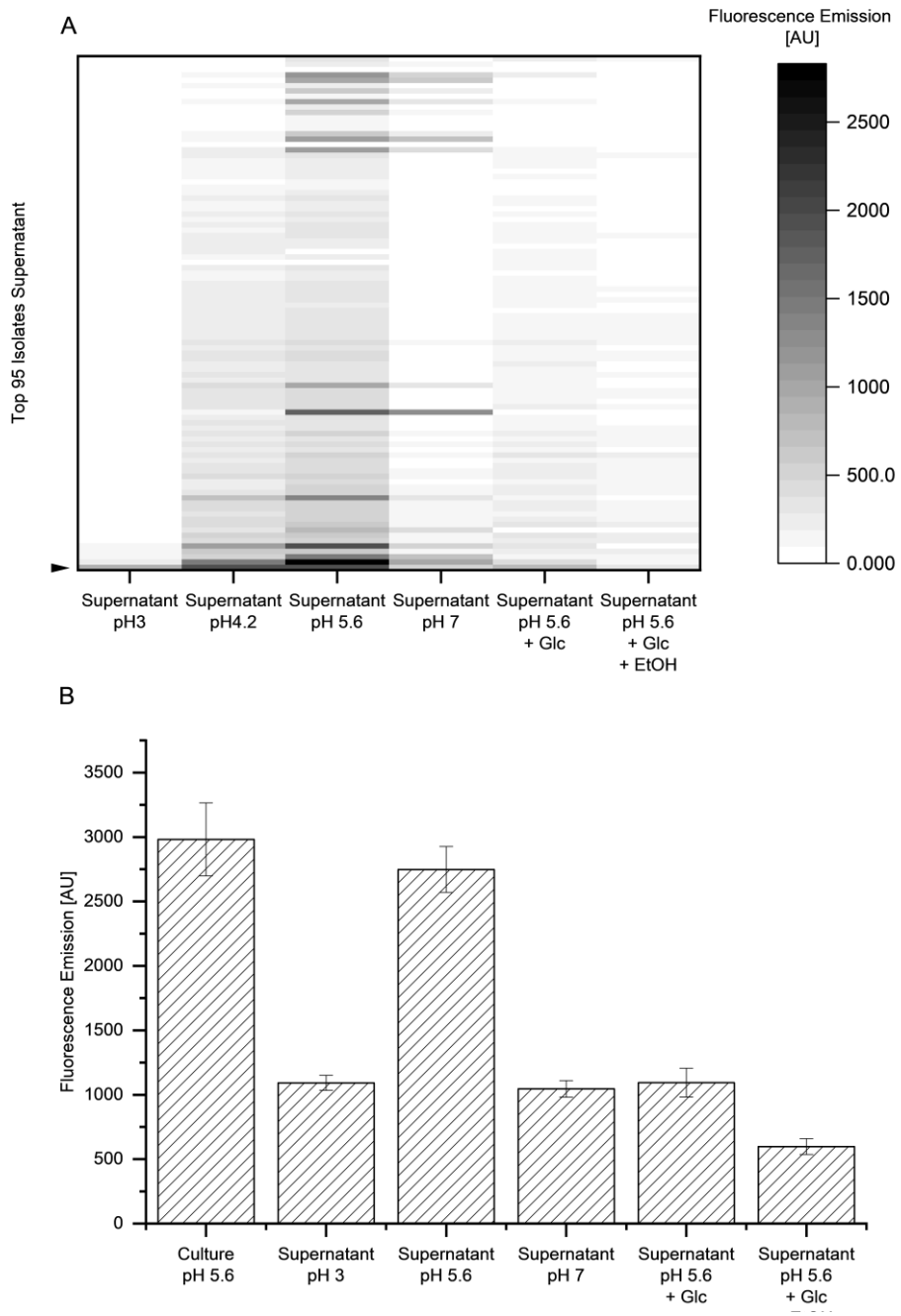

Figure S 7: Comparison of the *β*-glycosidase properties of the 96 strains with the highest activity from the screening for high culture supernatant activity. The strains with the highest activity in the supernatant at pH 7 were examined under conditions similar to those encountered in wine fermentation, using lower pH values and the addition of glucose and ethanol. A) One strain, which was later identified as *R. mucolaginosa*, showed measurable activity at pH 3 and in the presence of glucose and ethanol (arrow), B) Detailed characterization of the enzyme activity in *R. mucolaginosa* supernatant. The values for fluorescence increase per minute are given in arbitrary units and were calculated as described in paragraph 4.4.2.1.

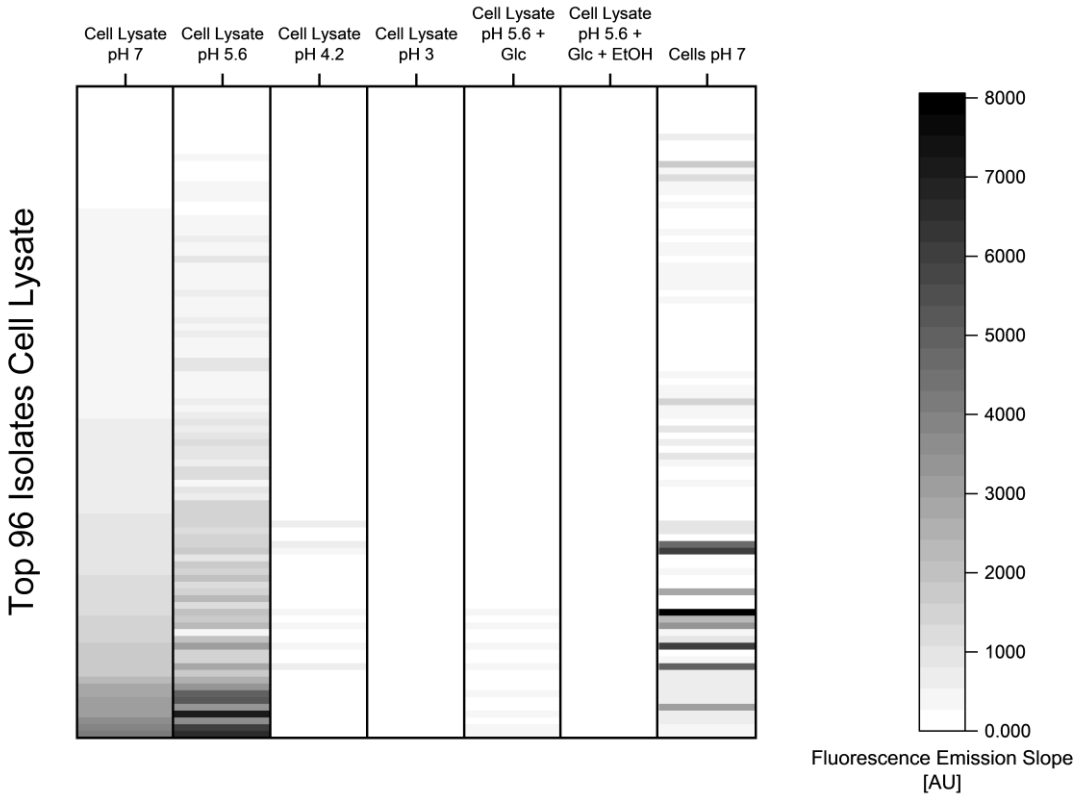

Figure S 8: Comparison of the *β*-glycosidase properties of the 96 strains with the highest activity from the screening for high activity in the cell lysate. The strains with the highest activity in the supernatant at pH 7 were examined under conditions similar to those encountered in wine fermentation, using lower pH values and the addition of glucose and ethanol. Decreasing pH values strongly influenced the measured activities, none of the tested strains showed activity at pH 3. Some strains showed activity at pH 5.6 after the addition of sugar while the addition of ethanol led to a sharp decrease of the measured enzyme activities. The values for fluorescence increase per minute are given in arbitrary units and were calculated as described in paragraph 4.4.2.1.

7.3 *β*-Lyase activities

7.3.1 Engineering yeast strains for high thiol release activity by a directed evolution approach using SMC

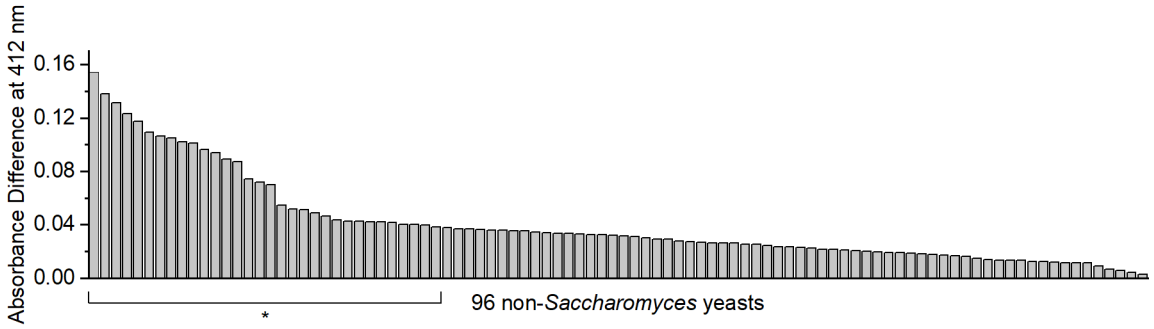

Figure S 9: Comparison of SMC cleavage activity of the 96 yeast strains selected from the SMC-based growth screenings. The DNTB assay was used for activity determination. The whole experimental setup is described in the material and methods section. Asterisk: 32 selected yeast strains for the assessment of methanethiol release in triplicates.

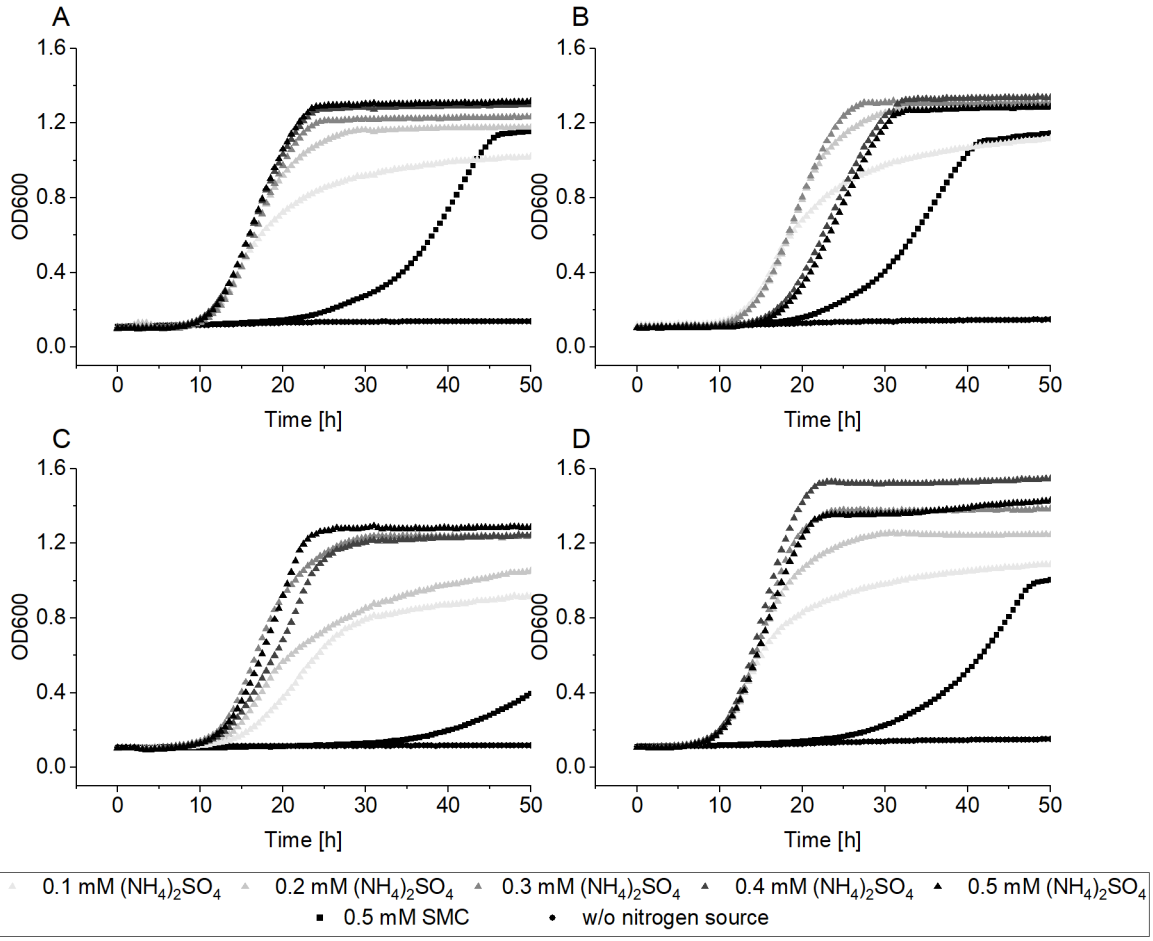

Figure S 10: Growth of the selected strains in synthetic medium without nitrogen source, with SMC as nitrogen source or with varying $(NH_4)_2SO_4$ amounts. A) *P. kudriavzevii*, B) *W. anomalus*, C) X-thiol, D) VIN13. The tested media resulted in strongly different growth patterns. The cell density of *P. kudriavzevii* cells raised at comparable rates for all $(NH_4)_2SO_4$ concentrations tested. In addition, the maximum cell density achieved increased with increasing amounts of $(NH_4)_2SO_4$. The observations were similar for *W. anomalus* with prolonged lag phases to approximately 15 h at higher $(NH_4)_2SO_4$ concentrations of 0.5 and 0.6 mmol L^{-1}. However, comparable growth rates and maximum optical density are achieved even at these concentrations. The growth of X-thiol shows a higher increase in optical density during the exponential phase with increasing $(NH_4)_2SO_4$ concentrations. At the lower $(NH_4)_2SO_4$ concentrations (0.2 mmol L^{-1} and 0.1 mmol L^{-1}), the maximum cell density was not reached within 50 h. Similar patterns to *P. kudriavzevii* are observed for VIN13, where the amount of $(NH_4)_2SO_4$ used appears to have a strong influence on the maximum cell density achieved. When SMC was used as sole nitrogen source, a longer lag phase and strongly reduced growth rates were observed. Precultures were grown in 600 µL synthetic medium with 0.1 mmol L^{-1} $(NH_4)_2SO_4$ for 24 h at 30 °C, 600 rpm and 80 % humidity.

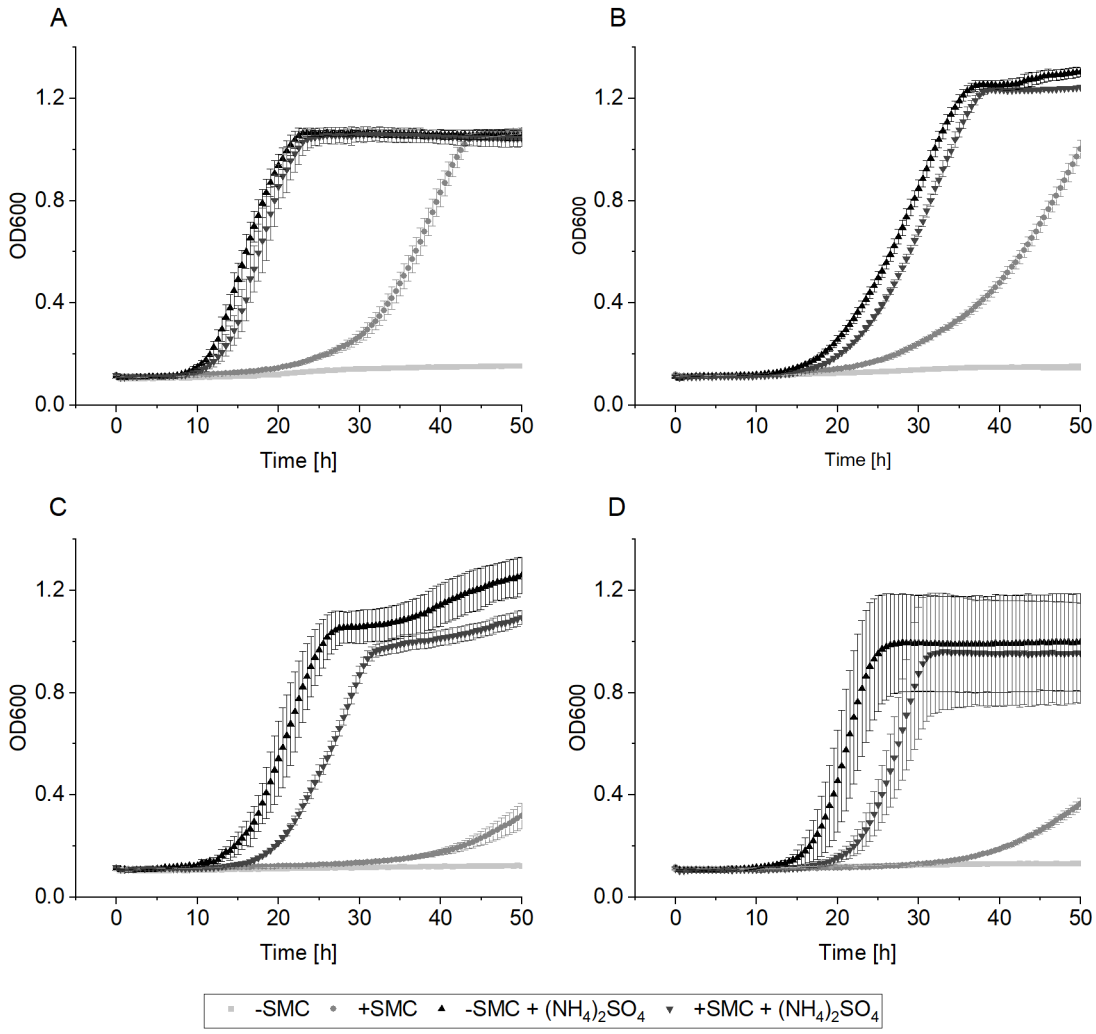

Figure S 11: Comparison of the cell growth of the selected strains on synthetic medium with different nitrogen sources to investigate potential growth inhibition effects of SMC. A) *P. kudriavzevii*, B) *W. anomalus*, C) X-thiol, D) VIN13. Addition of SMC to the medium containing $(NH_4)_2SO_4$ caused a growth inhibition effect in all cultures. However, the growth in the medium containing SMC and $(NH_4)_2SO_4$ was only slightly compromised, whereas growth in medium with SMC as sole nitrogen source was strongly inhibited. Precultures were grown in 600 µL synthetic medium with 0.1 mmol L^{-1} $(NH_4)_2SO_4$ for 24 h at 30 °C, 600 rpm and 80 % humidity.

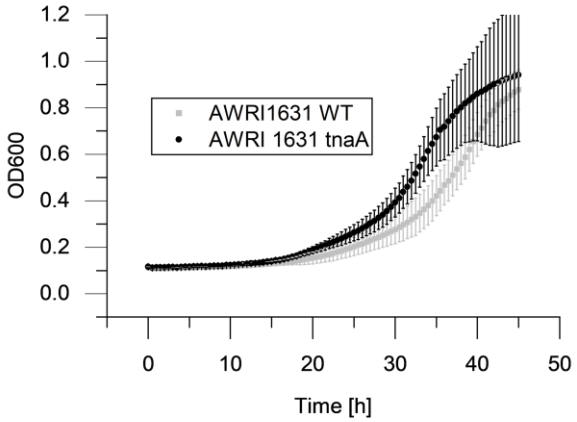

Figure S 12: Comparison of the growth of the AWRI1631 wild type strain with the AWRI1631 *tnaA* strain in SMC medium. After genomic integration of a *tnaA* expression construct, the AWRI1631 cells showed slightly faster growth characteristics in SMC medium. Precultures were grown in 600 µL synthetic medium with 0.1 mmol L^{-1} $(NH_4)_2SO_4$ for 24 h at 30 °C, 600 rpm and 80 % humidity.

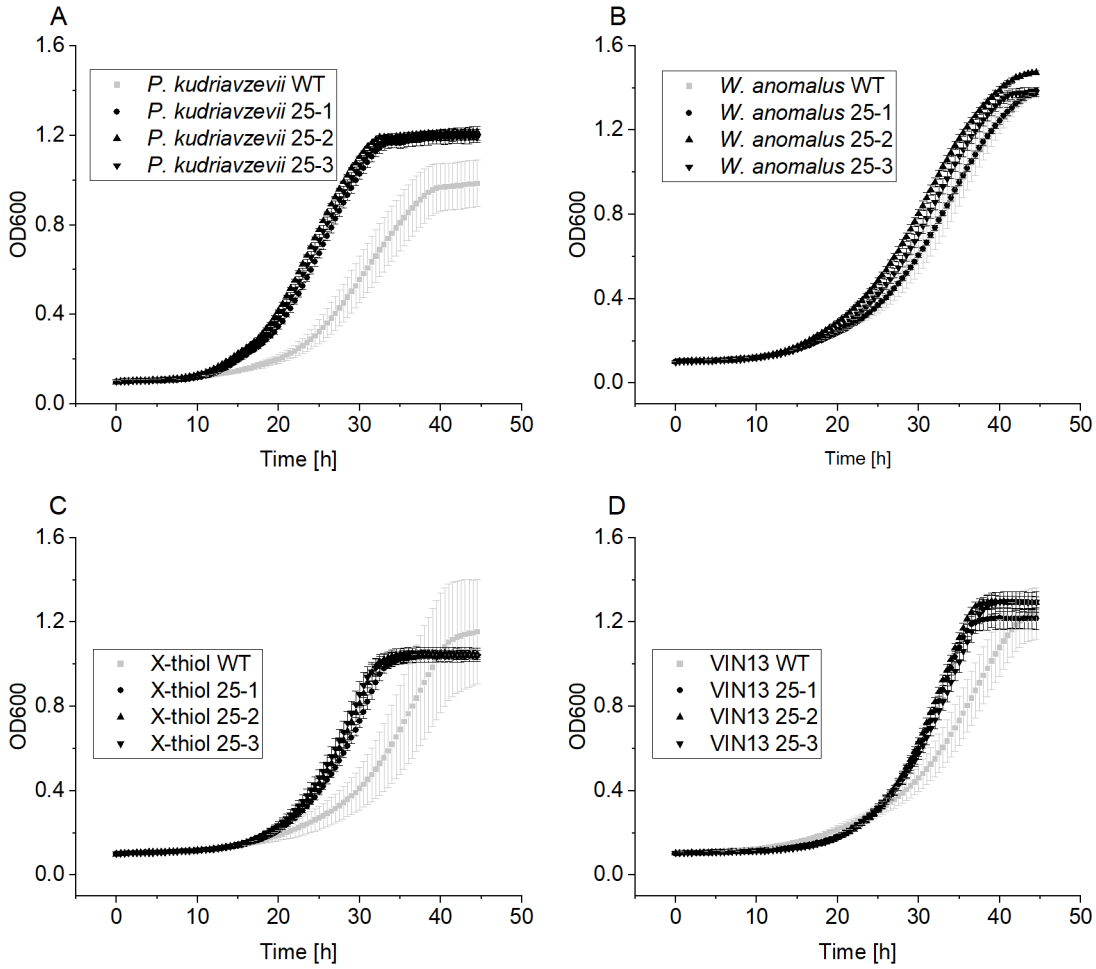

Figure S 13: Detailed illustration of the growth curves of three individual clones from the evolved populations in SMC medium. While the selected colonies of *P. kudriavzevii*, X-thiol and VIN13 showed relatively comparable results with distinctive differences to the starting strain, the growth curves of the selected *W. anomalus* cultures were more diverse and transformant 1 did not show improved growth compared to the wild type strain. Precultures were grown in 600 µL synthetic medium with 0.1 mmol L^{-1} $(NH_4)_2SO_4$ for 24 h at 30 °C, 600 rpm and 80 % humidity.

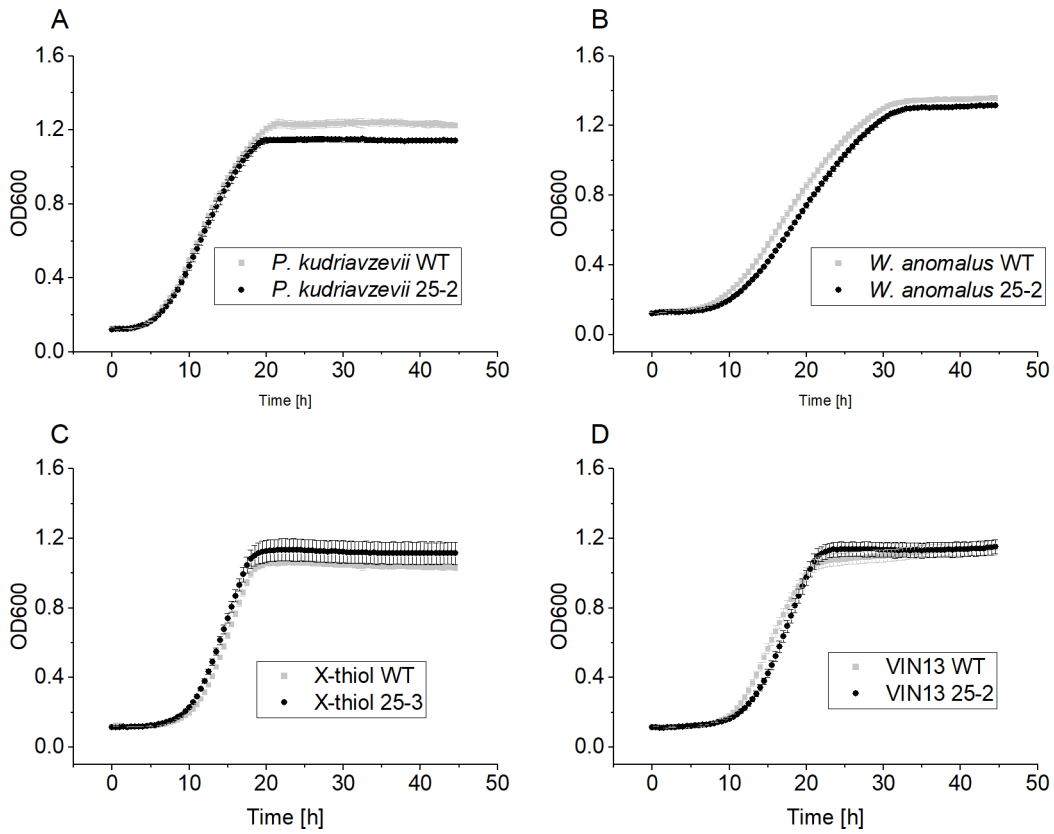

Figure S 14: Comparison of the cell growth before and after the evolutionary experiments on synthetic medium with 0.5 mmol L^{-1} $(NH_4)_2SO_4$. The growth curves of the evolved strains and the respective wild type strains exhibited only minor differences. Precultures were grown in 600 µL synthetic medium with 0.1 mmol L^{-1} $(NH_4)_2SO_4$ for 24 h at 30 °C, 600 rpm and 80 % humidity.

7.4 Engineering volatile thiol formation in yeast

Table S 2: Overview of the DNA sequences used in this work to enhance thiol formation in yeasts. The selected sequences were flanked with the corresponding digestion sites of the enzymes used for cloning (grey). An additional restriction site in the sequence of *GSH1* was replaced with a different codon encoding the same amino acid, while *VvGST4* was codon-optimized for the overexpression in *S. cerevisieae* (red).

Protein	Sequence
GSH1	GAATTCATGGGACTCTTAGCTTTGGGCACGCCTTTGCAGTGGTTTGAG TCTAGGACGTACAATGAACACATAAGGGATGAAGGTATCGAGCAGTTG TTGTATATTTTCCAAGCTGCTGGTAAAAGAGACAATGACCCTCTTTTTTG GGGAGACGAGCTTGAGTACATGGTTGTAGATTTTGATGATAAGGAGAG AAATTCTATGCTCGACGTTTGCCATGACAAGATACTCACTGAGCTTAAT ATGGAGGATTCGTCCCTTTGTGAGGCTAACGATGTGAGTTTTCACCCT GAGTATGGCCGGTATATGTTAGAGGCAACACCAGCTTCTCCATATTTGA ATTACGTGGGTAGTTACGTTGAGGTTAACATGCAAAAAAGACGTGCCAT TGCAGAATATAAGCTATCTGAATATGCGAGACAAGATAGTAAAAATAAC TTGCATGTGGGCTCCAGGTCTGTCCCTTTGACGCTGACTGTCTTCCCG AGGATGGGATGCCCCGACTTTATTAACATTAAGGATCCGTGGAATCATA AAAATGCCGCTTCCAGGTCTCTGTTTTTACCCGATGAAGTCATTAACAG ACATGTCAGGTTTCCTAACTTGACAGCATCCATCAGGACCAGGCGTGG TGAAAAAGTTTGCATGAATGTTCCCATGTATAAAGATATAGCTACTCCA GAAACGGATGACTCCATCTACGATCGAGATTGGTTTTTACCAGAAGACA AAGAGGCGAAACTGGCTTCCAAACCGGGTTTCATTTATATGGATTCCAT GGGTTTTGGCATGGGCTGTTCGTGCTTACAAGTGACCTTTCAGGCACC CAATATCAACAAGGCACGTTACCTGTACGATGCATTAGTGAATTTTGCA CCTATAATGCTAGCCTTCTCTGCCGCTGCGCCTGCTTTTAAAGGTTGG CTAGCCGACCAAGATGTTCGTTGGAATGTGATATCTGGTGCGGTGGAC GACCGTACTCCGAAGGAAAGAGGTGTTGCGCCATTACTACCCAAATAC AACAAGAACGGATTTGGAGGCATTGCCAAAGACGTACAAGATAAAGTC CTTGAAATACCAAAGTCAAGATATAGTTCGGTTGATCTTTTCTTGGGTG GGTCGAAATTTTTCAATAGGACTTATAACGACACAAATGTACCTATTAAT GAAAAAGTATTAGGACGACTACTAGAGAATGATAAGGCGCCACTGGAC TATGATCTTGCTAAACATTTTGCGCATCTCTACATAAGAGATCCAGTATC TACATTCGAAGAACTGTTGAATCAGGACAACAAAACGTCTTCAAATCAC TTTGAAAACATCCAAAGTACAAATTGGCAGACATTACGTTTTAAACCCC CCACACAACAAGCAACCCCGGACAAAAAGGATTCTCCTGGTTGGAGAG TGGAGTTCAGACCATTTGAAGTGCAACTATTAGATTTTGAGAACGCTGC

	GTATTCCGTGCTCATATACTTGATTGTCGATAGCATTTTGACCTTTTCCG ATAATATTAACGCATATATTCATATGTCCAAAGTATGGGAAAATATGAAG ATAGCCCATCACAGAGATGCTATCCTATTTGAAAAATTTCATTGGAAAA AATCATTTCGCAACGACACCGATGTGGAAACTGAAGATTATTCTATAAG CGAGATTTTCCATAATCCAGAGAATGGTATATTTCCTCAATTTGTTACGC CAATCCTATGCCAAAAAGGGTTTGTAACCAAAGATTGGAAAGAATTAAA GCATTCTTCCAAACACGAGAGACTATACTATTATTTAAAGCTAATTTCTG ATAGAGCAAGCGGTGAATTGCCAACAACAGCAAAATTCTTTAGAAATTT TGTACTACAACATCCAGATTACAAACATGATTCAAAAATTTCAAAGTCGA TCAATTATGATTTGCTTTCTACGTGTGATAGACTTACCCATTTAGACGAT TCAAAAGGTGAATTGACATCCTTTTTAGGAGCTGAAATTGCAGAATATG TAAAAAAAAATAAGCCTTCAATAGAAAGCAAATGTTAAGGTACC
GTT1	GAATTCATGTCGTTGCCAATTATCAAAGTCCATTGGTTGGACCATTCCA GAGCGTTCAGACTTTTGTGGTTATTAGACCATTTGAACCTTGAATATGA AATTGTCCCTTATAAAAGAGATGCTAACTTCCGTGCTCCACCAGAATTA AAGAAAATTCACCCATTAGGAAGATCTCCATTGTTAGAAGTTCAAGACA GAGAAACTGGTAAGAAGAAGATACTTGCCGAGTCCGGTTTCATCTTCC AATATGTCTTGCAGCATTTTGATCATTCACACGTTTTAATGAGCGAAGAT GCTGATATTGCAGACCAGATTAACTATTATCTGTTTTATGTAGAAGGTTC CTTGCAACCACCTTTAATGATTGAGTTCATTCTTTCAAAGGTGAAGGAT TCTGGTATGCCCTTCCCTATTTCGTACTTGGCAAGAAAAGTGGCAGACA AGATCAGTCAGGCATACTCTAGTGGTGAAGTTAAGAACCAGTTCGACTT TGTGGAGGGTGAAATTTCCAAAAATAACGGCTACCTGGTTGATGGGAA GTTGAGCGGTGCCGATATCTTGATGTCTTTCCCTTTGCAGATGGCGTTT GAAAGAAAGTTTGCCGCACCAGAGGATTATCCTGCCATTTCCAAATGG TTAAAGACCATAACCTCAGAGGAGTCGTATGCTGCTTCTAAGGAAAAG GCGCGTGCTTTAGGTAGCAATTTCTAAGGTACC
GTT2	GAATTCATGAATGGCAGAGGTTTCCTGATTTACAATGGAGGTGAAAAGA TGAAACAAAAAATGATAATATATGACACACCCGCAGGGCCTTATCCGG CCCGAGTCCGCATTGCCTTGGCTGAGAAGAACATGCTATCAAGTGTGC AATTTGTGAGGATCAACCTCTGGAAGGGAGAGCACAAGAAGCCTGAAT TTCTTGCCAAGAACTATTCAGGCACAGTGCCAGTGCTTGAACTTGATGA CGGGACTTTAATCGCTGAATGCACAGCCATTACTGAATACATTGATGCA CTTGATGGTACACCCACTCTTACCGGCAAAACACCGCTGGAAAAAGGC GTAATCCACATGATGAACAAACGCGCAGAGTTGGAACTGCTCGACCCT GTTAGTGTTTATTTTCACCATGCTACACCTGGATTGGGGCCTGAAGTCG AGCTTTACCAAAACAAAGAGTGGGGACTTCGCCAGCGCGACAAAGCCC

	TACATGGAATGCATTATTTTGATACCGTTCTCAGAGAACGCCCATATGT TGCTGGTGATTCATTCTCAATGGCTGACATCACAGTAATAGCTGGTCTA ATATTTGCTGCAATTGTAAAACTACAAGTGCCGGAAGAGTGCGAGGCG CTTCGAGCTTGGTATAAGAGAATGCAACAGCGCCCCAGCGTGAAGAAA CTGCTAGAAATCCGTTCAAAATCCTCGTAAGGTACC
VvGST4 (optimized for expression in *S. cerevisiae*)	GAATTCATGGTTATGAAGGTTTACGGTCCAGTTAGAGCTGCTTGTCCAC AAAGAGTTTTGGCTTGTTTAGTTGAAAAAGGTGTTGAATTTGAGGTTGT TCATGTTGATTTGGATTCTGGTGAACAAAAAAGACCAGATTTTCTATTAA GGCAACCATTTGGTCAAGTTCCAGTTGTTGAAGATGGTGACTTTAGATT GTTTGAATCTAGAGCTATTGTCAGATATATCGCTGCTAAATATGCTGAA CAAGGTCCAGATTTGTTAGGTAAATCTTTAGAAGAAAAGGCTGTTGTTG ATCAATGGTTGGAAGTTGAAGCTCATAATTTTAATGAGTTGGTTTACAC ACTGGTTATGCAATTAGTTATTTTGCCAAGAATGGGTGAAAGAGGTGAC TTGGCTTTGGCTCATACTTGTGAACAAAAATTAGAAAAGGTCTTCGATG TTTACGAACAAAGATTGTCTAAATCTAGATACTTGGCTGGTGACTCTTTT ACTTTAGCTGATTTGTCTCATTTGCCAGCTATTAGATATTTGGTTAAAGA AGCTGGTATGGCTCATTTGGTTACTGAAAGAAAATCTGTTTCTGCTTGG TGGGAAGATATTTCTAATAGAGCTGCTTGGAAAAAAGTTATGGAATTGG CTGCTTAAGGTACC

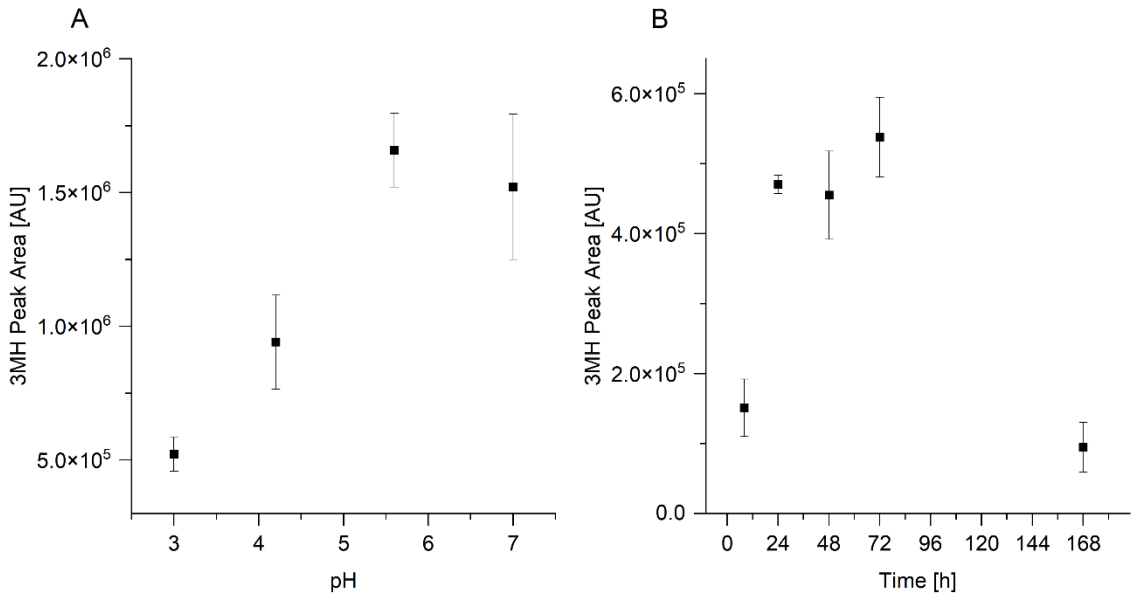

Figure S 15: Determination of 3MH peak area at different pH values (A) and after different bioconversion times of CEN.PK2.1C *tnaA* cells (B). The pH assays were conducted with a cell density corresponding to OD_{600nm} of 10, the bioconversion time experiments with a cell density corresponding to OD_{600nm} of 5. The data points and error bars represent the mean values and standard deviations for three biological replicates

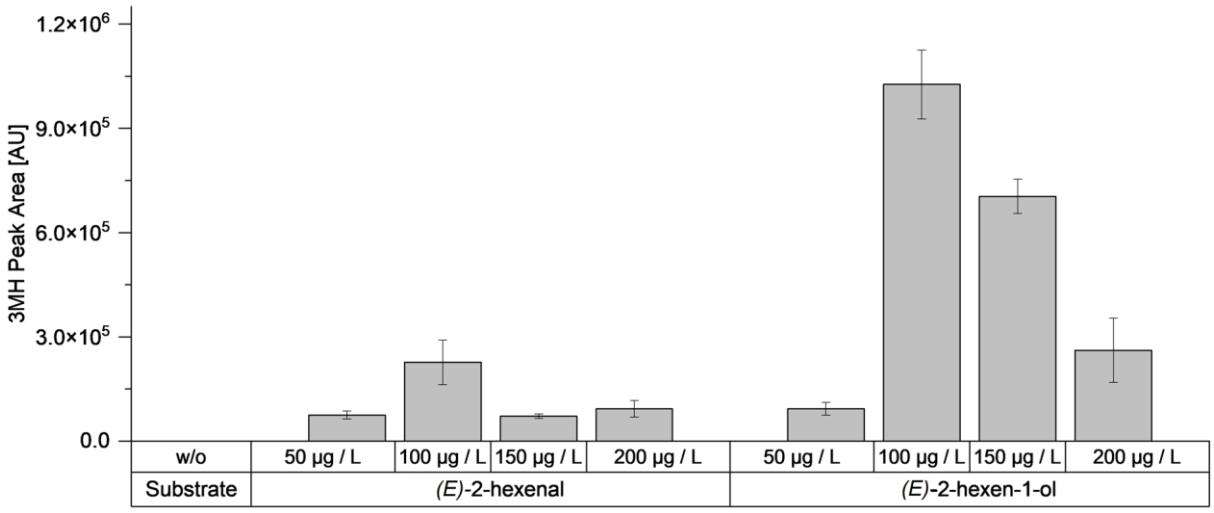

Figure S 16: Substrate concentrations and type highly affect the efficiency of 3MH production. Different amounts of either *(E)*-2-hexenal or *(E)*-2-hexen-1-ol were added as substrate for the biotransformation with a cell density corresponding to OD_{600nm} of 7.5 with CEN.PK2.1C *tnaA* cells. The data points and error bars represent the mean values and standard deviations for three biological replicates.

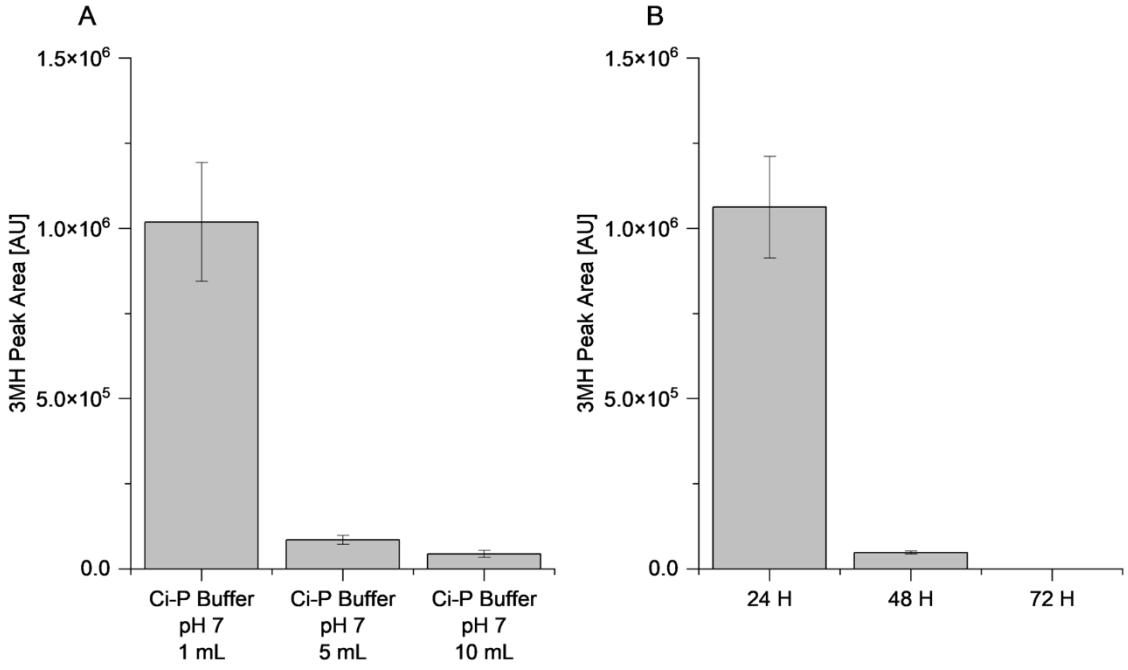

Figure S 17: Influences of different reaction volumes (A) and different cell growth phase times before the reaction (B) with CEN.PK2.1C *tnaA* cells. The cell density (OD_{600nm}) was set to 7.5. 100 µg *(E)*-2-hexen-1-ol per L was used as substrate. The data points and error bars represent the mean values and standard deviations for three biological replicates.

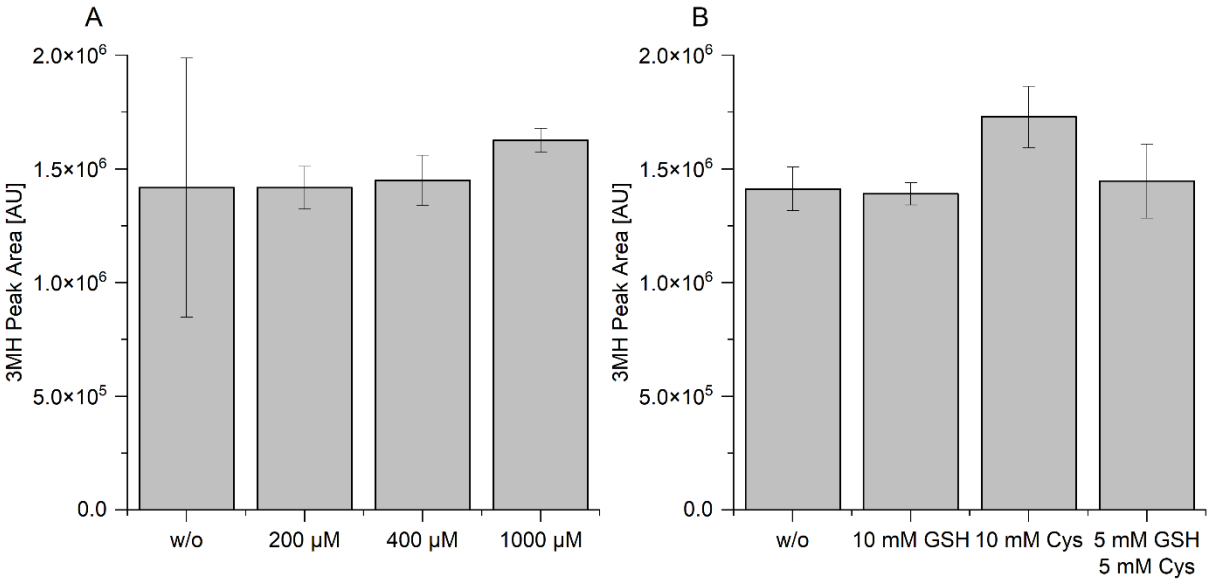

Figure S 18: Effects of CEN.PK2.1C *tnaA*-based bioconversion reaction supplementation with different amounts of pyridoxal-5-phosphate (A) and cysteine or glutathione (B). The cell density (OD_{600nm}) was set to 10. 100 µg L^{-1} *(E)*-2-hexen-1-ol was used as substrate. The data points and error bars represent the mean values and standard deviations for three biological replicates.

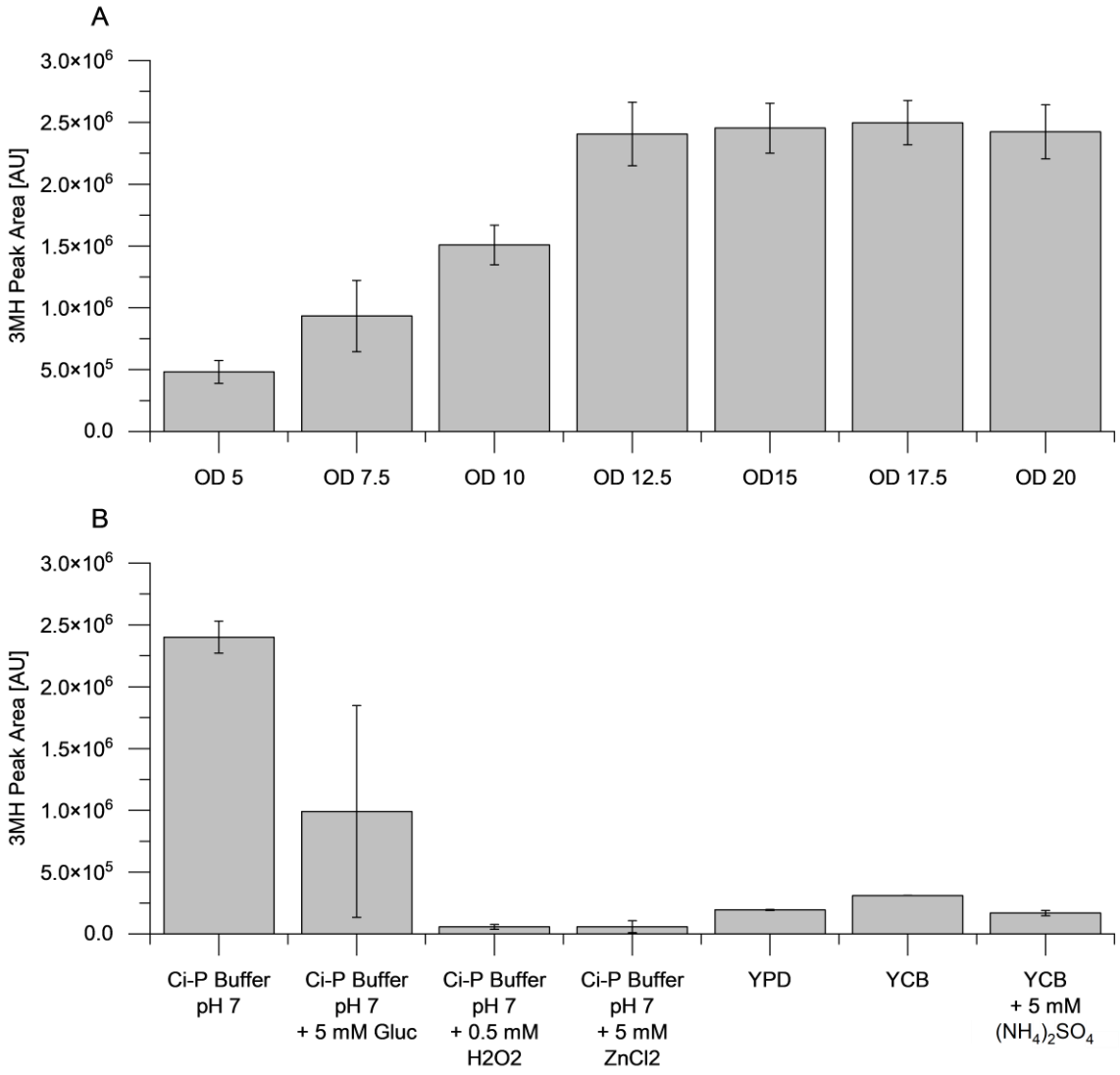

Figure S 19: Assessment of the effects of different cell densities of CEN.PK2.1C *tnaA* cells (A) and various reaction media (B) on 3MH production. In (B) a cell density corresponding to an OD_{600nm} of 15 was used. 100 µg L^{-1} *(E)*-2-hexen-1-ol was used as substrate. The data points and error bars represent the mean values and standard deviations for three biological replicates.

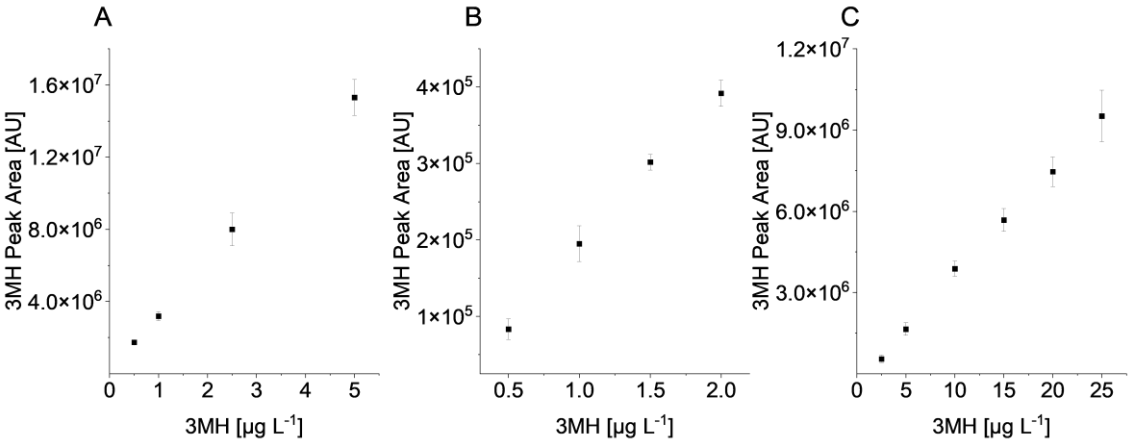

Figure S 20: Calibration curves for quantification of 3MH concentrations in the assays. Determination of the correlating 3MH peak area at a split value of 5 (A), as well as at a split value of 60 (B and C).

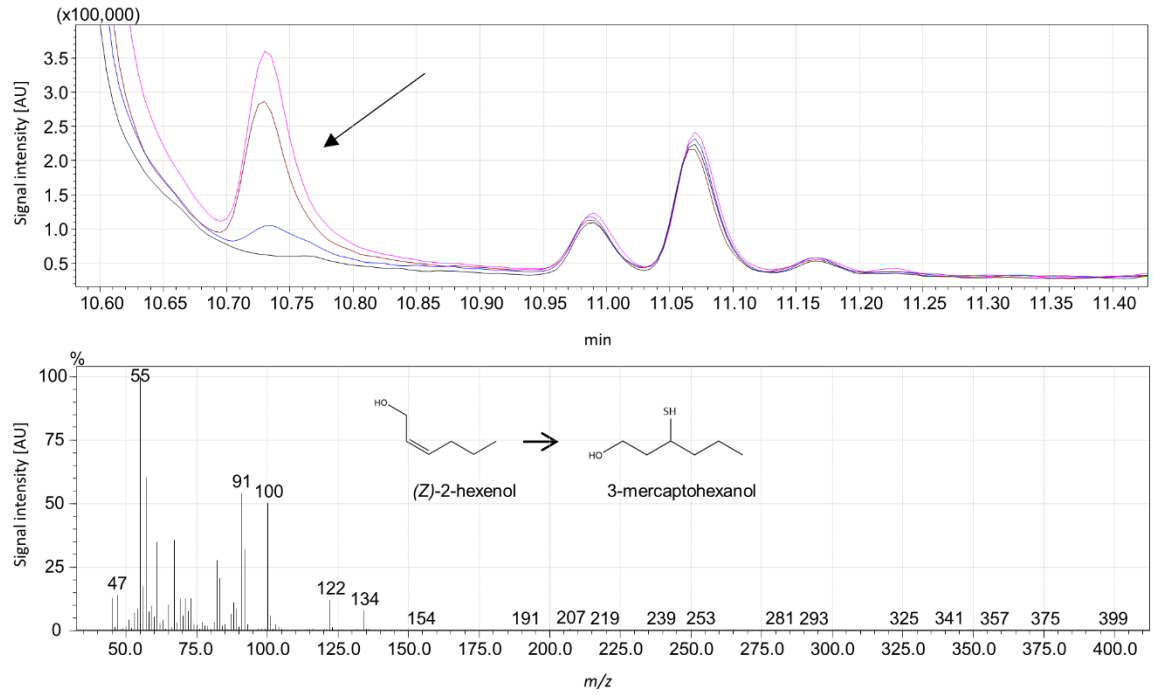

Figure S 21: GC-MS chromatograms of bioconversion reaction samples with CEN.PK2.1C empty vector control (black), CEN.PK2.1C *tnaA* GSH1-GTT1 (pink), GSH1-GTT2 (blue), and GSH1-VvGST4 (red) after 24 h incubation with the substrate *(Z)*-2-hexen-1-ol. The chromatogram section, in which a possible product peak was identified, is shown. Arrow: Identified product peak. Below: Mass spectrum of the identified peak after conversion with GSH1-GTT1. The mass spectra of the peaks were identical for all three strains.

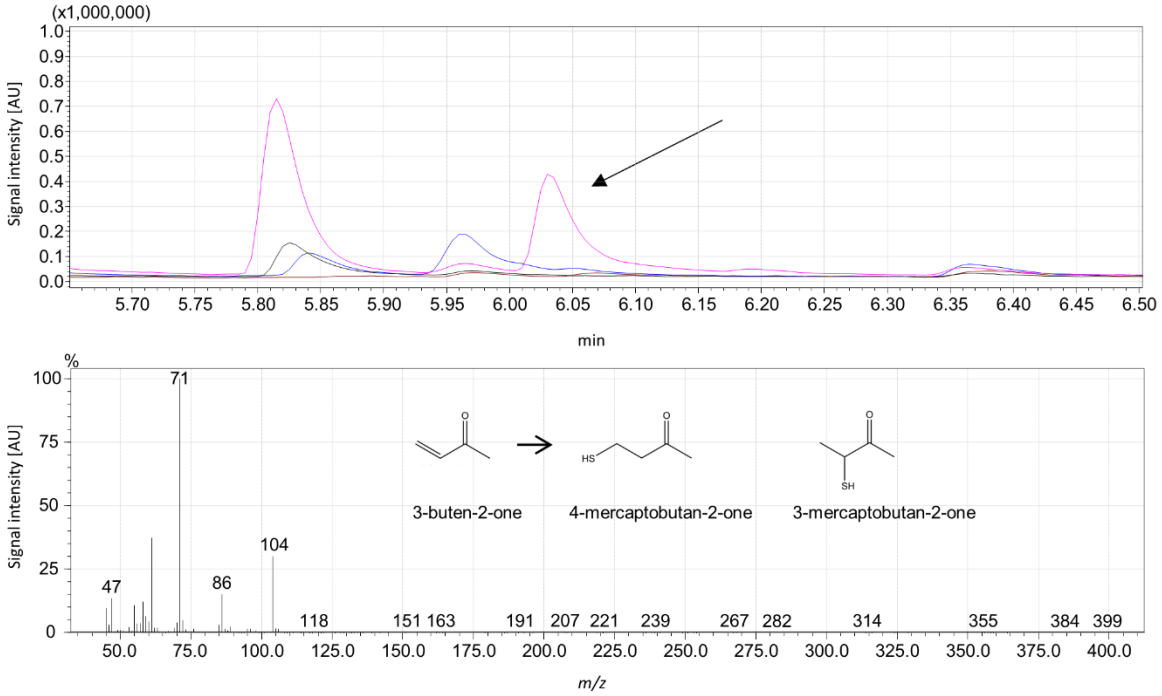

Figure S 22: GC-MS chromatograms of bioconversion reaction samples with CEN.PK2.1C empty vector control (black), CEN.PK2.1C *tnaA* GSH1-GTT1 (pink), GSH1-GTT2 (blue), and GSH1-VvGST4 (red) after 24 h incubation with the substrate 3-buten-2-one. The chromatogram section, in which a possible product peak was identified, is shown. Arrow: Identified product peak. Below: Mass spectrum of the identified peak after conversion with GSH1-GTT1. The mass spectra of the peaks were identical for all three strains.

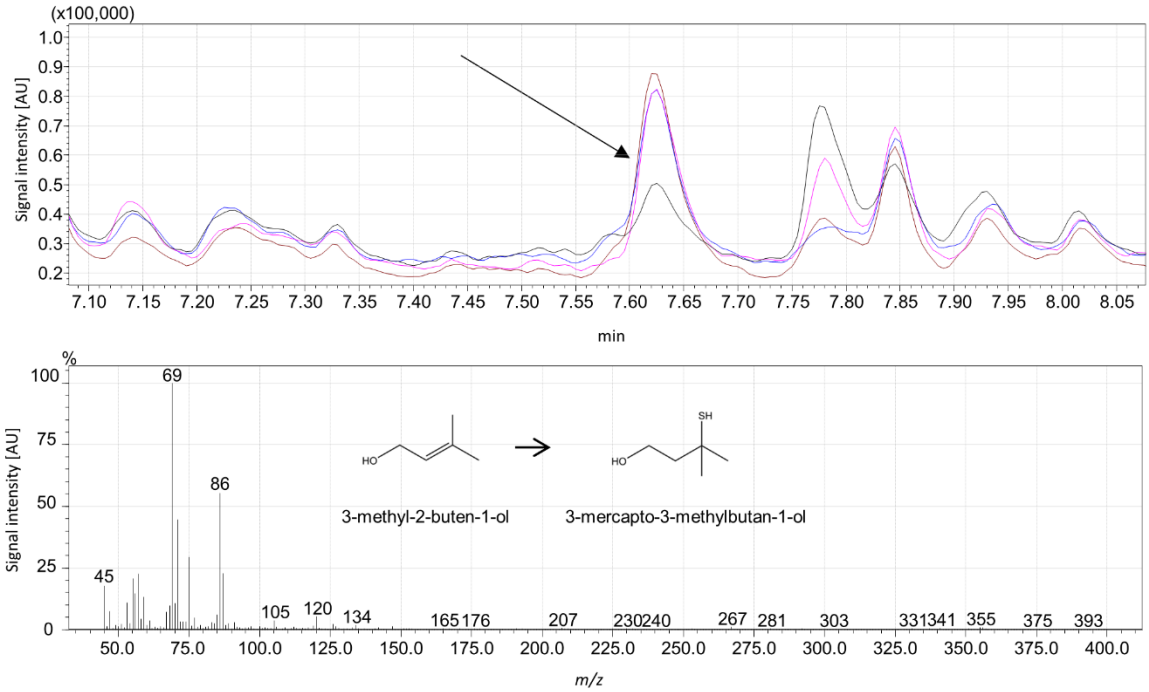

Figure S 23: GC-MS chromatograms of bioconversion reaction samples with CEN.PK2.1C empty vector control (black), CEN.PK2.1C *tnaA* GSH1-GTT1 (pink), GSH1-GTT2 (blue), and GSH1-VvGST4 (red) after 24 h incubation with the substrate 3-methyl-2-buten-1-ol. The chromatogram section, in which a possible product peak was identified, is shown. Arrow: Identified product peak. Below: Mass spectrum of the identified peak after conversion with GSH1-GTT1. The mass spectra of the peaks were identical for all three strains.

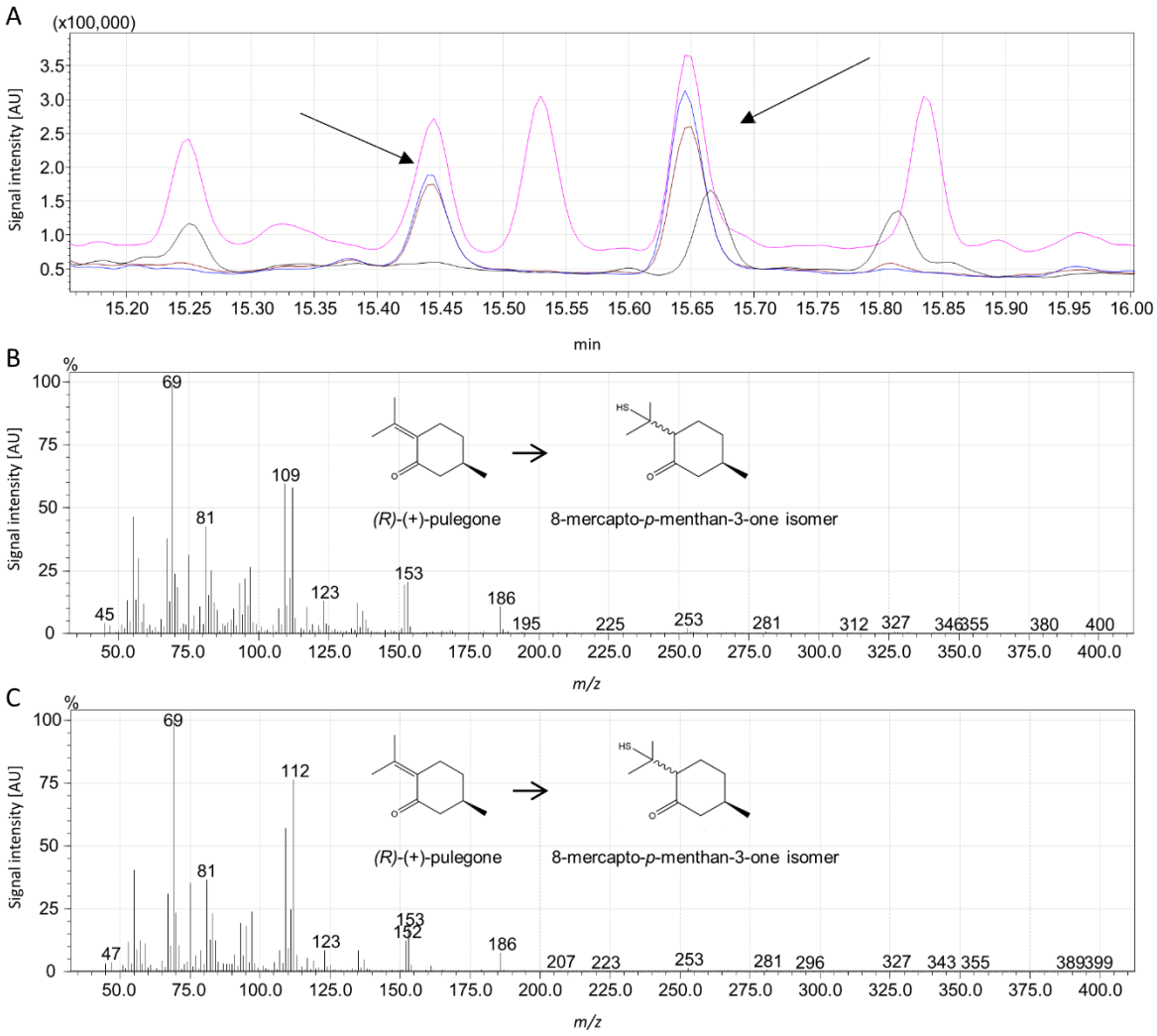

Figure S 24: A) GC-MS chromatograms of bioconversion reaction samples with CEN.PK2.1C empty vector control (black), CEN.PK2.1C *tnaA* GSH1-GTT1 (pink), GSH1-GTT2 (blue), and GSH1-VvGST4 (red) after 24 h incubation with the substrate (R)-(+)-pulegone. The chromatogram section, in which possible product peaks were identified, is shown. Arrows: Identified product peaks. B) Mass spectrum of the peak at 15.45 min, C) Mass spectrum of the peak at 15.65 min. Below: Mass spectrum of the identified peaks after conversion with GSH1-GTT1. The mass spectra of the peaks were identical for all three strains.

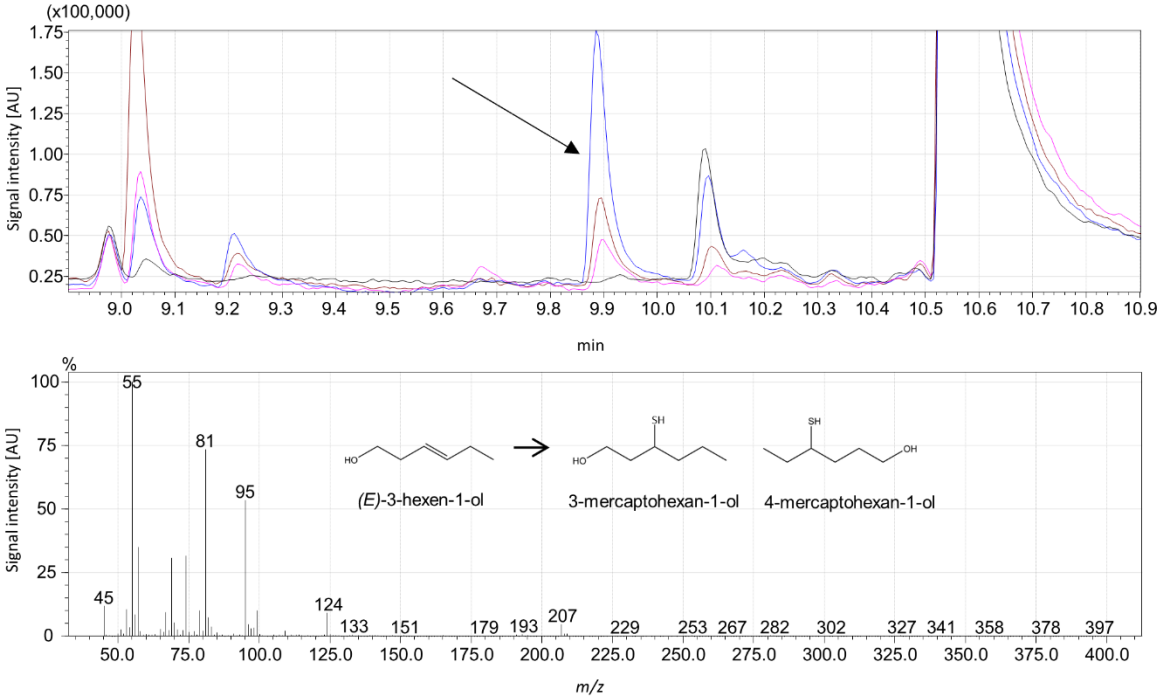

Figure S 25: GC-MS chromatograms of bioconversion reaction samples with CEN.PK2.1C empty vector control (black), CEN.PK2.1C *tnaA* GSH1-GTT1 (pink), GSH1-GTT2 (blue), and GSH1-VvGST4 (red) after 24 h incubation with the substrate *(E)*-3-hexen-1-ol. The chromatogram section, in which a possible product peak was identified, is shown. Arrow: Identified product peak. Below: Mass spectrum of the identified peak after conversion with GSH1-GTT1. The mass spectra of the peaks were identical for all three strains.

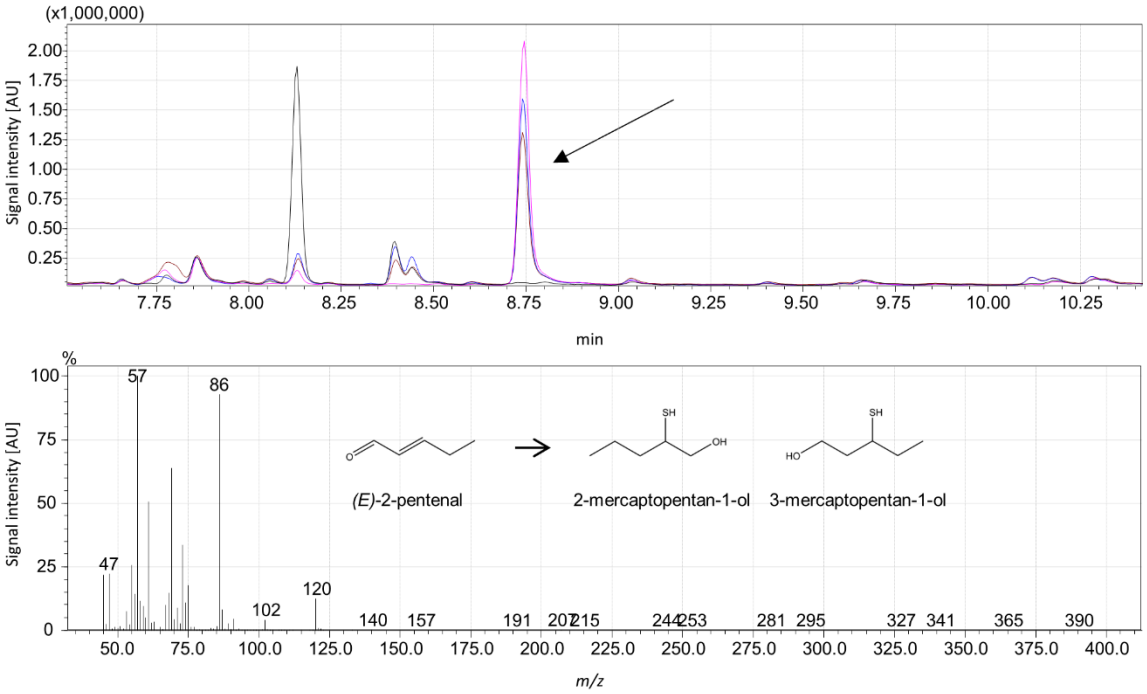

Figure S 26: GC-MS chromatograms of bioconversion reaction samples with CEN.PK2.1C empty vector control (black), CEN.PK2.1C *tnaA* GSH1-GTT1 (pink), GSH1-GTT2 (blue), and GSH1-VvGST4 (red) after 24 h incubation with the substrate *(E)*-2-pentenal. The chromatogram section, in which a possible product peak was identified, is shown. Arrow: Identified product peak. Below: Mass spectrum of the identified peak after conversion with GSH1-GTT1. The mass spectra of the peaks were identical for all three strains.

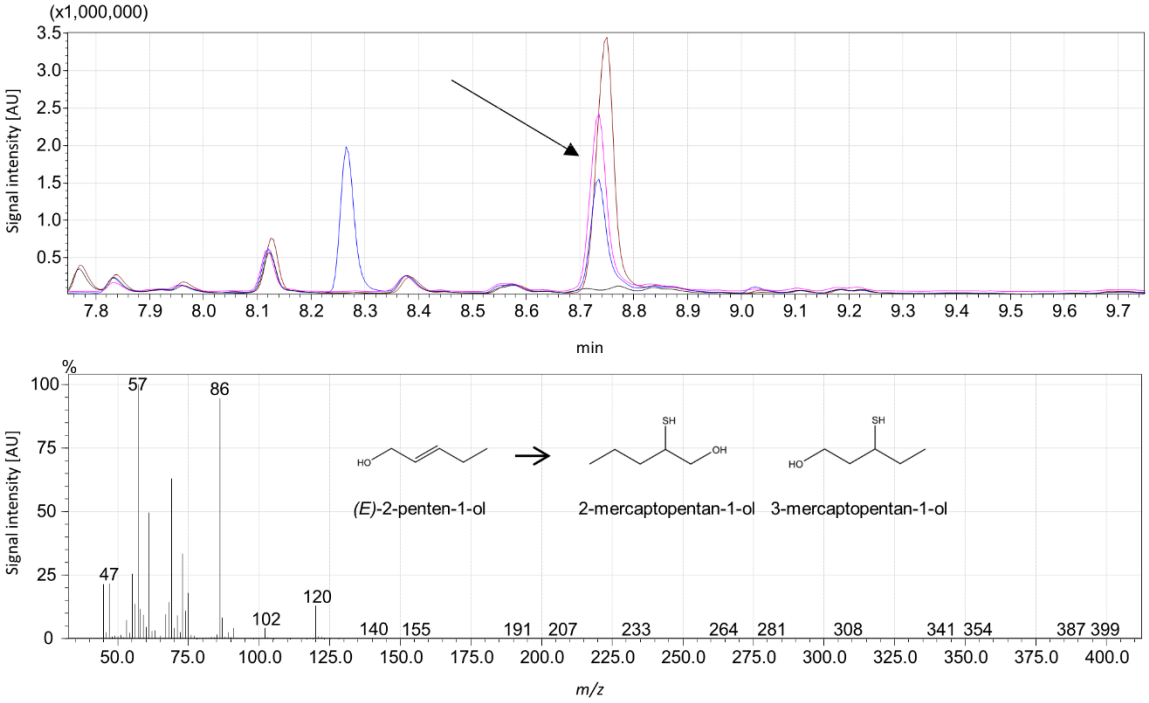

Figure S 27: GC-MS chromatograms of bioconversion reaction samples with CEN.PK2.1C empty vector control (black), CEN.PK2.1C *tnaA* GSH1-GTT1 (pink), GSH1-GTT2 (blue), and GSH1-VvGST4 (red) after 24 h incubation with the substrate *(E)*-2-penten-1-ol. The chromatogram section, in which a possible product peak was identified, is shown. Arrow: Identified product peak. Below: Mass spectrum of the identified peak after conversion with GSH1-GTT1. The mass spectra of the peaks were identical for all three strains.

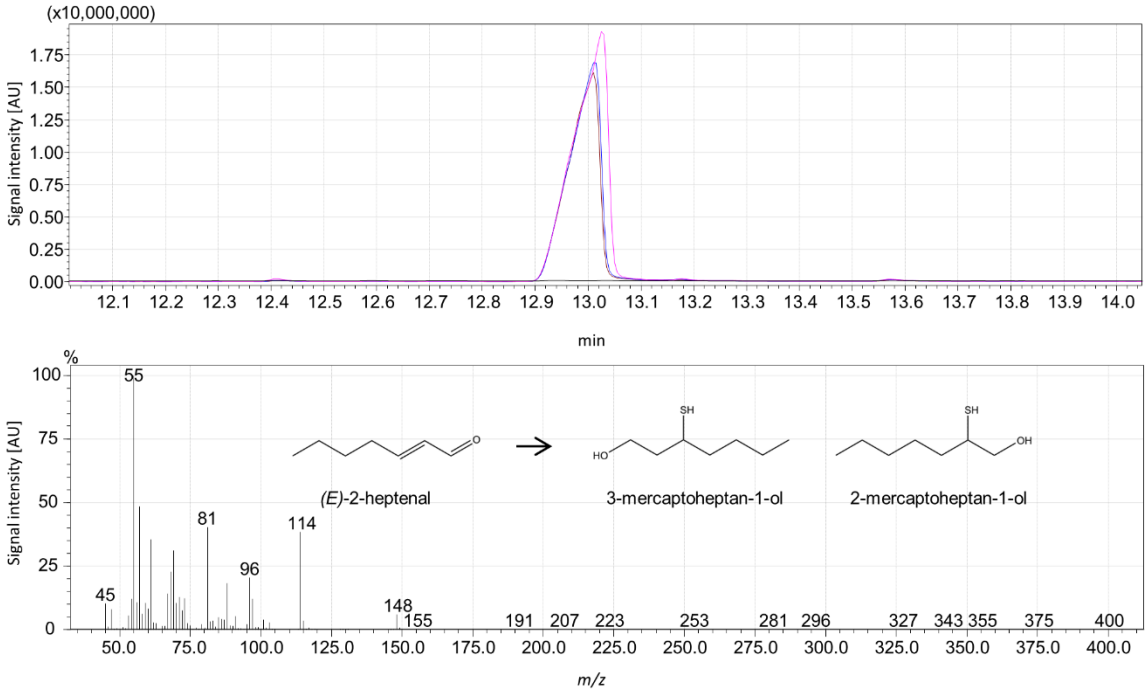

Figure S 28: GC-MS chromatograms of bioconversion reaction samples with CEN.PK2.1C empty vector control (black), CEN.PK2.1C *tnaA* GSH1-GTT1 (pink), GSH1-GTT2 (blue), and GSH1-VvGST4 (red) after 24 h incubation with the substrate *(E)*-2-heptenal. The chromatogram section, in which a possible product peak was identified, is shown. Below: Mass spectrum of the identified peak after conversion with GSH1-GTT1. The mass spectra of the peaks were identical for all three strains.

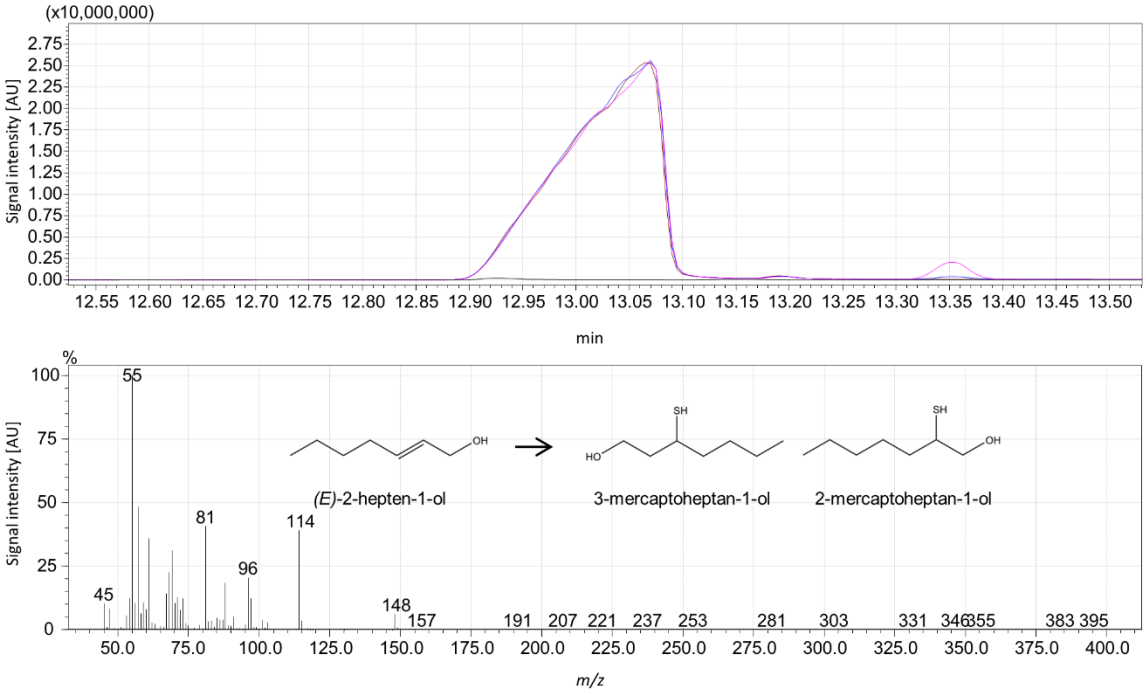

Figure S 29: GC-MS chromatograms of bioconversion reaction samples with CEN.PK2.1C empty vector control (black), CEN.PK2.1C *tnaA* GSH1-GTT1 (pink), GSH1-GTT2 (blue), and GSH1-VvGST4 (red) after 22 h incubation with the substrate *(E)*-2-heptenol. The chromatogram section, in which a possible product peak was identified, is shown. Below: Mass spectrum of the identified peak after conversion with GSH1-GTT1. The mass spectra of the peaks were identical for all three strains.

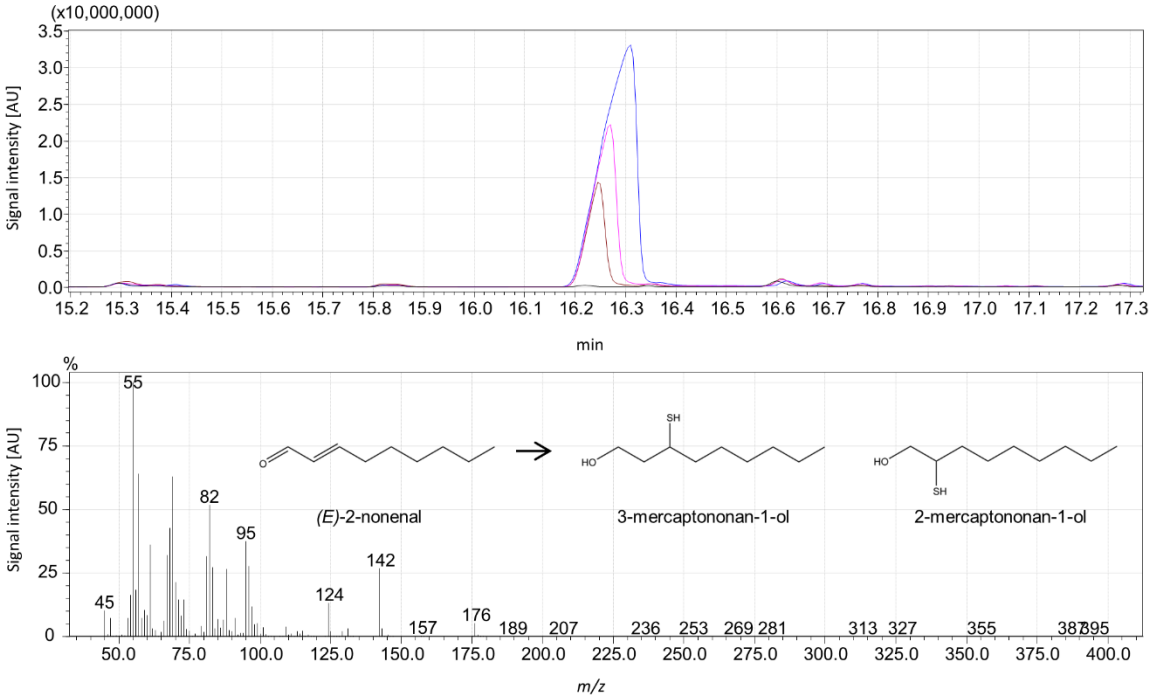

Figure S 30: GC-MS chromatograms of bioconversion reaction samples with CEN.PK2.1C empty vector control (black), CEN.PK2.1C *tnaA* GSH1-GTT1 (pink), GSH1-GTT2 (blue), and GSH1-VvGST4 (red) after 24 h incubation with the substrate *(E)*-2-nonenal. The chromatogram section, in which a possible product peak was identified, is shown. Below: Mass spectrum of the identified peak after conversion with GSH1-GTT1. The mass spectra of the peaks were identical for all three strains.

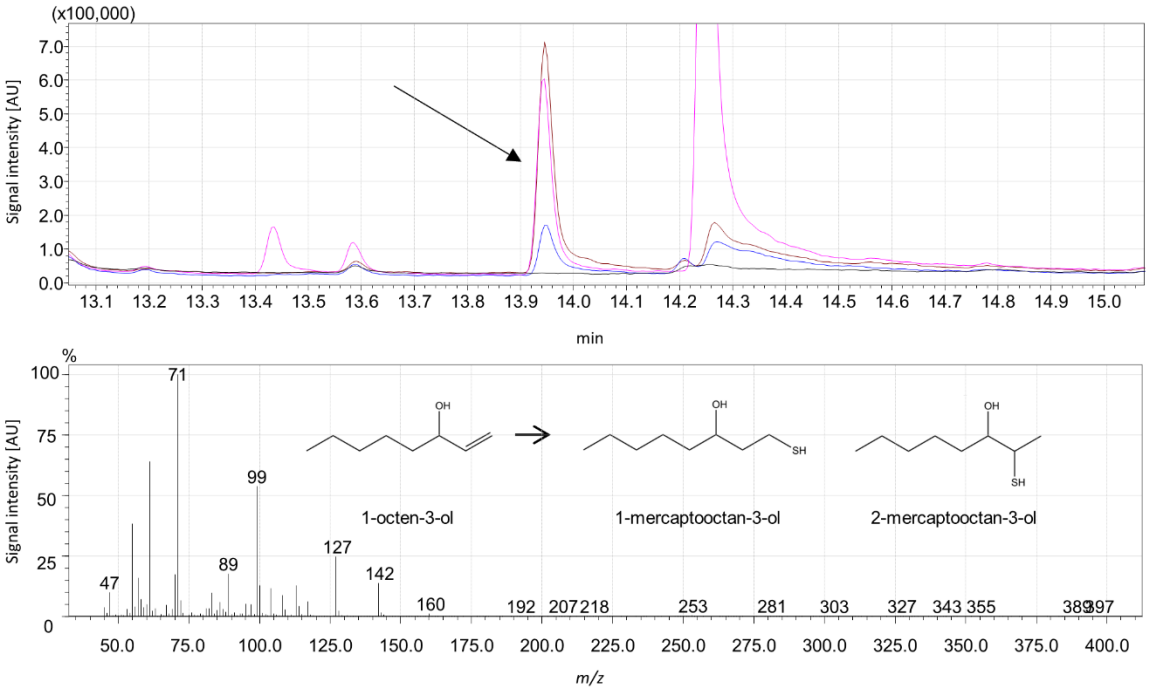

Figure S 31: GC-MS chromatograms of bioconversion reaction samples with CEN.PK2.1C empty vector control (black), CEN.PK2.1C *tnaA* GSH1-GTT1 (pink), GSH1-GTT2 (blue), and GSH1-VvGST4 (red) after 24 h incubation with the substrate 1-octen-3-ol. The chromatogram section, in which a possible product peak was identified, is shown. Arrow: Identified product peak. Below: Mass spectrum of the identified peak after conversion with GSH1-GTT1. The mass spectra of the peaks were identical for all three strains.

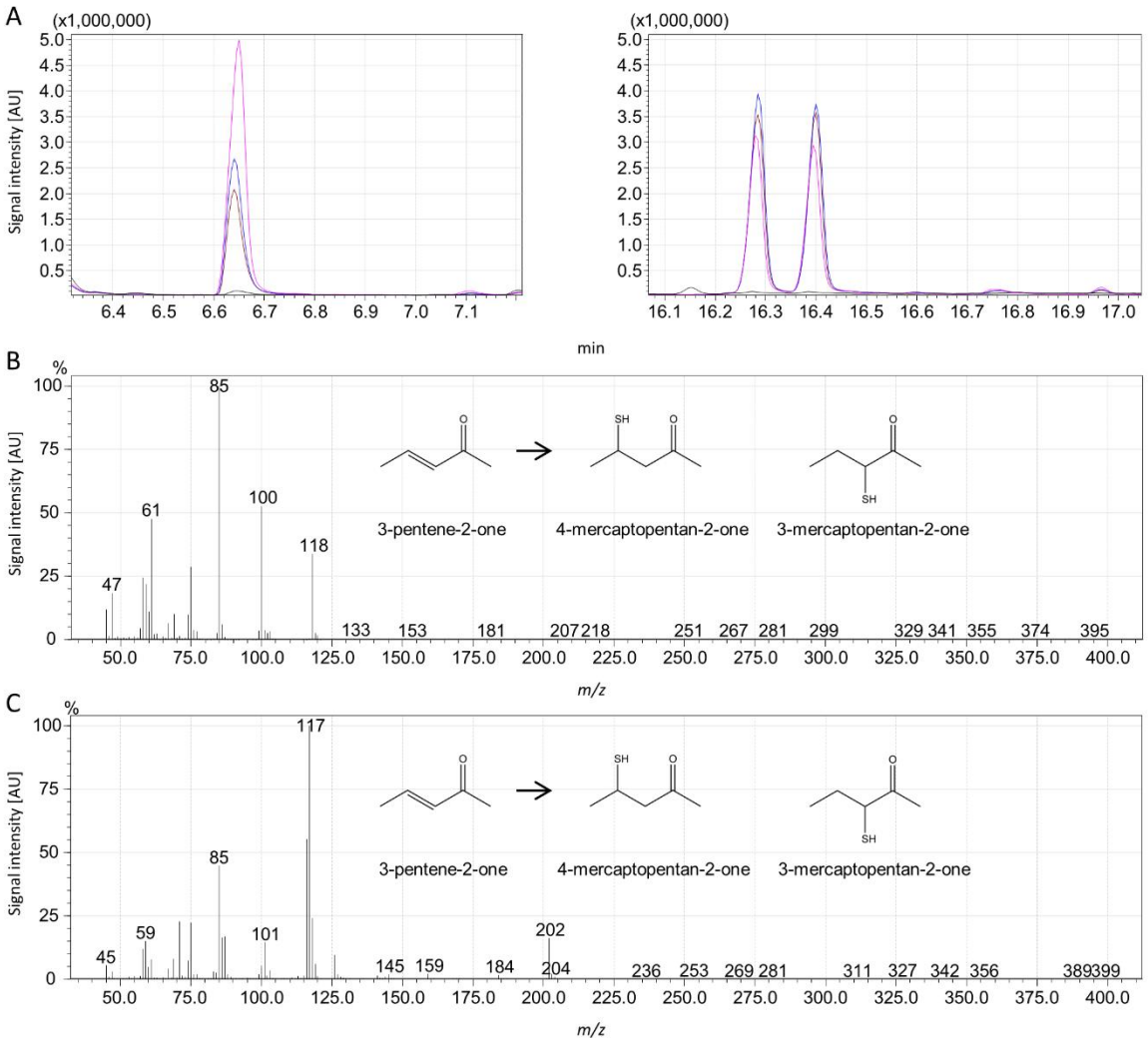

Figure S 32: A) GC-MS chromatograms of bioconversion reaction samples with CEN.PK2.1C empty vector control (black), CEN.PK2.1C *tnaA* GSH1-GTT1 (pink), GSH1-GTT2 (blue), and GSH1-VvGST4 (red) after 24 h incubation with the substrate 3-pentene-2-one. The chromatogram sections, in which possible product peaks were identified, are shown. B) Mass spectrum of the peak at 6.6 min, C) Mass spectrum of the peaks at 16.25 and 16.4 min. Below: Mass spectra of the identified peaks after conversion with GSH1-GTT1. The mass spectra of the peaks were identical for all three strains.

Table S 3: Chemical formulae and calculated isotopic distributions of the tentatively identified product peaks. The calculated mass intensity values stated were calculated with ChemDraw Prime based on the chemical formulae and the natural occurring isotope distribution. The mean values of the measured mass intensities were calculated based on the GC-MS measurements of the three CEN.PK2.1C *tnaA* transformants GSH1-GTT1, GSH1-GTT2 and GSH1-VvGST4. Asterisk: Since a product peak could only be identified after the incubation of 3-methyl-2-buten-1-ol with CEN.PK2.1C *tnaA* GSH1-GTT1, no mean value was calculated for this product.

Substrate(s)	Expected product(s)	Chemical formula of product (s)	Calculated mass of product(s) [u]	Calculated mass intensity ratios (%)	Measured mass intensity ratios (%)
3-Methyl-2-buten-1-ol	3-Mercapto-3-methylbutan-1-ol, 2-Mercapto-3-methylbutan-1-ol	$C_5H_{12}OS$	120.06	100	
			121.06	6.2	16.4 ± 2.6
			122.06	4.6	9.9 % ± 1.6
3-Buten-2-one	4-Mercaptobutan-2-one, 3-Mercaptobutan-2-one	C_4H_8OS	104.03	100	
			105.03	5.2	5.8*
			106.03	4.8	4.8*
(R)-(+)-Pulegone (Peak at 14.45 min)	8-Mercapto-*p*-menthan-3-one derivate	$C_{10}H_{18}OS$	186.11	100	
			187.11	11.9	8.3 ± 7.4
			188.1	4.5	4.4 ± 3.7
(R)-(+)-Pulegone (Peak at 15.65 min)	8-Mercapto-*p*-menthan-3-one derivate		186.11	100	
			187.11	11.9	7.0 ± 6.0
			188.1	4.5	3.0 ± 2.8
(Z)-2-Hexen-1-ol	2-Mercaptohexan-1-ol, 3-Mercaptohexan-1-ol	$C_6H_{14}OS$	134.08	100	
			135.08	7.5	13.3 ± 6.3
			136.07	4.5	8.1 ± 3.7
(E)-3-Hexen-1-ol	3-Mercaptohexan-1-ol, 4-Mercaptohexan-1-ol		134.08	100	
			135.08	7.5	156.8 ± 49.9
			136.07	4.5	99.4 ± 11.8
(E)-2-Pentenal,	3-Mercaptopentan-1-ol, 2-Mercaptopentan-1-ol	$C_5H_{12}OS$	120.06	100	
			121.06	6.2	6.3 ± 0.2
			122.06	4.6	5.7 ± 1.3
(E)-2-Penten-1-ol			120.06	100	
			121.06	6.2	6.3 ± 0.2
			122.06	4.6	5.0 ± 0.1
(E)-2-Heptenal,	3-Mercaptoheptan-1-nol, 2-Mercaptoheptan-1-ol	$C_7H_{16}OS$	148.09	100	
			149.1	7.8	9.7 ± 0.4

Substrate(s)	Expected product(s)	Chemical formula of product (s)	Calculated mass of product(s) [u]	Calculated mass intensity ratios (%)	Measured mass intensity ratios (%)
			150.09	4.6	5.0 ± 0.2
(E)-2-Hepten-1-nol			148.09	100	
			149.1	7.8	10 ± 0.0
			150.09	4.6	5.5 ± 0.1
(E)-2-Nonenal	3-Mercaptononan-1-ol, 2-Mercaptononan-1-ol	$C_9H_{20}OS$	176.12	100	
			177.13	10	12.6 ± 1.2
			178.12	4.5	5.5 ± 0.1
1-Octen-3-ol	1-Mercaptooctan-3-ol, 2-Mercaptooctan-3-ol	$C_8H_{18}OS$	162.11	100	
			163.11	9.7	108.6 ± 82.4
			164.1	4.5	135.2 ± 146.4
3-Pentene-2-one (Peak at 6.6 min)	4-Mercaptopentan-2-one 3-Mercaptopentan-2-one	$C_5H_{10}OS$	118.05	100	
			119.05	5.6	6.6 ± 0.2
			120.04	4.5	4.8 ± 0.1
3-Pentene-2-one (Peak at 16.25 min)			118.05	100	
			119.05	5.6	24.1 ± 0.3
			120.04	4.5	4.2 ± 0.2
3-Pentene-2-one (Peak at 16.4 min)			118.05	100	
			119.05	5.6	24.0 ± 0.4
			120.04	4.5	4.2 ± 0.1

7.5 Copyright

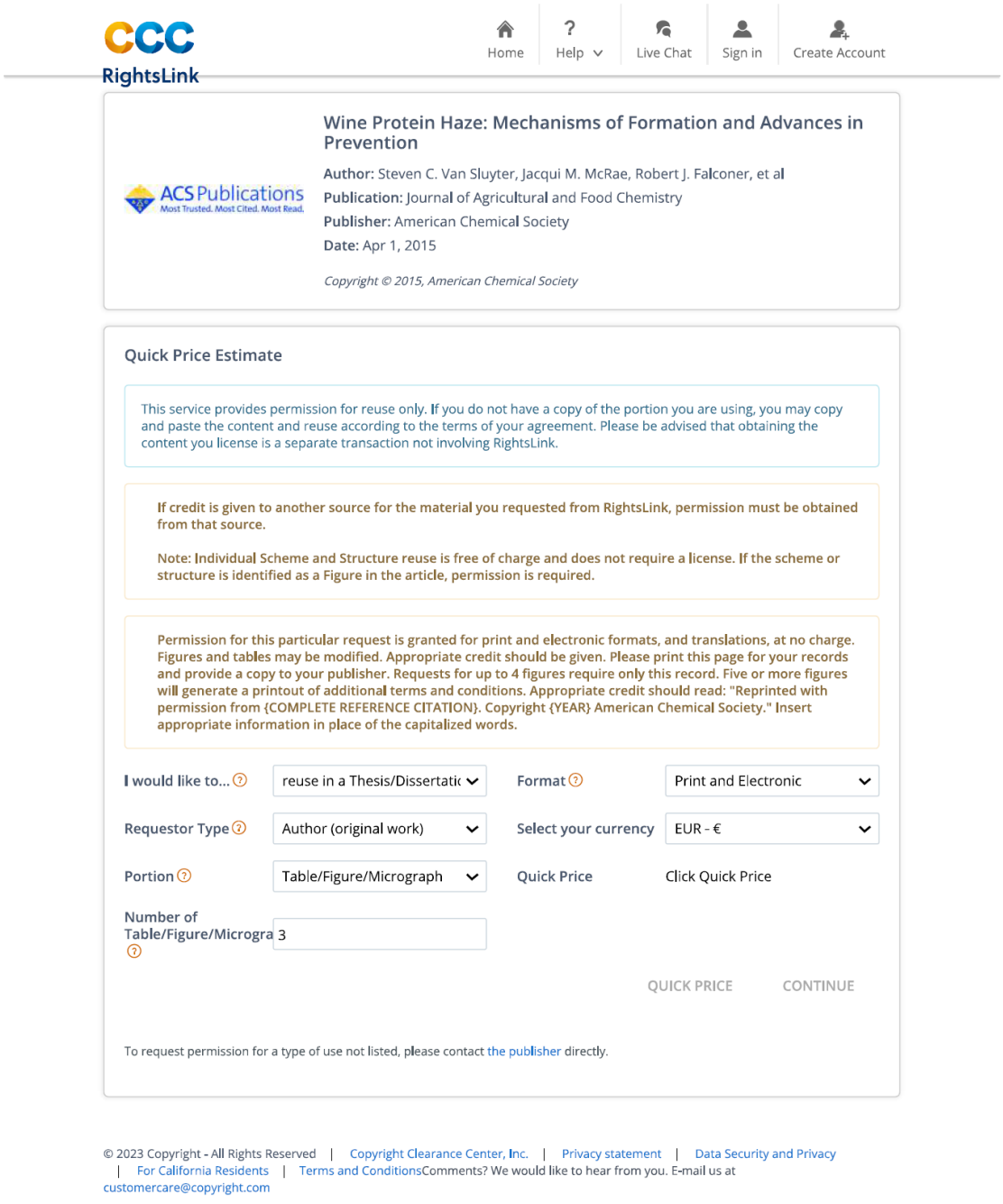

RightsLink

Home | Help | Live Chat | Sign in | Create Account

Wine Protein Haze: Mechanisms of Formation and Advances in Prevention

Author: Steven C. Van Sluyter, Jacqui M. McRae, Robert J. Falconer, et al
Publication: Journal of Agricultural and Food Chemistry
Publisher: American Chemical Society
Date: Apr 1, 2015

Copyright © 2015, American Chemical Society

Quick Price Estimate

This service provides permission for reuse only. If you do not have a copy of the portion you are using, you may copy and paste the content and reuse according to the terms of your agreement. Please be advised that obtaining the content you license is a separate transaction not involving RightsLink.

If credit is given to another source for the material you requested from RightsLink, permission must be obtained from that source.

Note: Individual Scheme and Structure reuse is free of charge and does not require a license. If the scheme or structure is identified as a Figure in the article, permission is required.

Permission for this particular request is granted for print and electronic formats, and translations, at no charge. Figures and tables may be modified. Appropriate credit should be given. Please print this page for your records and provide a copy to your publisher. Requests for up to 4 figures require only this record. Five or more figures will generate a printout of additional terms and conditions. Appropriate credit should read: "Reprinted with permission from {COMPLETE REFERENCE CITATION}. Copyright {YEAR} American Chemical Society." Insert appropriate information in place of the capitalized words.

I would like to...	reuse in a Thesis/Dissertatic	Format	Print and Electronic
Requestor Type	Author (original work)	Select your currency	EUR - €
Portion	Table/Figure/Micrograph	Quick Price	Click Quick Price
Number of Table/Figure/Micrograp	3		

QUICK PRICE CONTINUE

To request permission for a type of use not listed, please contact the publisher directly.

8 References

(1) Lambrechts, M. G.; Pretorius, I. S. Yeast and Its Importance to Wine Aroma - a Review, *SAJEV.* **2019**, *21*.

(2) Rogerson; S, F. S.; Vale; E; Grande; J, H.; Silva; M, M. C. Alternative Processing of Port-Wine Using Pectolytic Enzymes, *Cienc. Tecnol. Aliment.* **2000,** pp. 222–227.

(3) Maturano, Y. P.; Rodríguez Assaf, L. A.; Toro, M. E.; Nally, M. C.; Vallejo, M.; Castellanos de Figueroa, L. I.; Combina, M.; Vazquez, F. Multi-Enzyme Production by Pure and Mixed Cultures of *Saccharomyces* and Non-*Saccharomyces* Yeasts During Wine Fermentation, *Int. J. Food Microbiol.* **2012**, *155,* pp. 43–50.

(4) Padilla, B.; Gil, J. V.; Manzanares, P. Past and Future of Non-*Saccharomyces* Yeasts: From Spoilage Microorganisms to Biotechnological Tools for Improving Wine Aroma Complexity, *Front. Microbiol.* **2016**, *7,* p. 411.

(5) Roland, A.; Schneider, R.; Razungles, A.; Cavelier, F. Varietal Thiols in Wine: Discovery, Analysis and Applications, *Chem. Rev.* **2011**, *111,* pp. 7355–7376.

(6) Swiegers, J. H.; Francis, I. L.; Herderich, M. J. Meeting Consumer Expectations Through Management in Vineyard and Winery, *AWRI Report.* **2006,** pp. 34–42.

(7) Howell, K. S.; Klein, M.; Swiegers, J. H.; Hayasaka, Y.; Elsey, G. M.; Fleet, G. H.; Høj, P. B.; Pretorius, I. S.; Barros Lopes, M. A. de Genetic Determinants of Volatile-Thiol Release by *Saccharomyces Cerevisiae* During Wine Fermentation, *Appl. Environ. Microbiol.* **2005**, *71,* pp. 5420–5426.

(8) Howell, K. S.; Swiegers, J. H.; Elsey, G. M.; Siebert, T. E.; Bartowsky, E. J.; Fleet, G. H.; Pretorius, I. S.; Barros Lopes, M. A. de Variation in 4-Mercapto-4-Methyl-Pentan-2-One Release by *Saccharomyces Cerevisiae* Commercial Wine Strains, *FEMS Microbiol. Lett.* **2004**, *240,* pp. 125–129.

(9) Swiegers, J. H.; Bartowsky, E. J.; Henschke, P. A.; Pretorius Yeast and Bacterial Modulation of Wine Aroma and Flavour, *Aust. J. Grape Wine Res.* **2005**, *11,* pp. 139–173.

(10) Sturm, J.; Grossmann, M.; Schnell, S. Influence of Grape Treatment on the Wine Yeast Populations Isolated from Spontaneous Fermentations, *Appl. Environ. Microbiol.* **2006**, *101,* pp. 1241–1248.

(11) Beltran, G.; Torija, M. J.; Novo, M.; Ferrer, N.; Poblet, M.; Guillamón, J. M.; Rozès, N.; Mas, A. Analysis of Yeast Populations During Alcoholic Fermentation: A Six Year Follow-up Study, *Syst. Appl. Microbiol.* **2002**, *25,* pp. 287–293.

(12) Escribano, R.; González-Arenzana, L.; Garijo, P.; Berlanas, C.; López-Alfaro, I.; López, R.; Gutiérrez, A. R.; Santamaría, P. Screening of Enzymatic Activities Within Different Enological Non-*Saccharomyces* Yeasts, *J. Food Sci. Technol.* **2017**, *54,* pp. 1555–1564.

(13) Andorrà, I.; Berradre, M.; Rozès, N.; Mas, A.; Guillamón, J. M.; Esteve-Zarzoso, B. Effect of Pure and Mixed Cultures of the Main Wine Yeast Species on Grape Must Fermentations, *Eur. Food Res. Technol.* **2010**, *231,* pp. 215–224.

(14) Mendes Ferreira, A.; Clímaco, M. C.; Mendes Faia, A. The Role of Non-*Saccharomyces* Species in Releasing Glycosidic Bound Fraction of Grape Aroma Components - a Preliminary Study, *J. Appl. Microbiol.* **2001**, *91,* pp. 67–71.

(15) Rodríguez, M. E.; Lopes, C. A.; Barbagelata, R. J.; Barda, N. B.; Caballero, A. C. Influence of *Candida Pulcherrima* Patagonian Strain on Alcoholic Fermentation Behaviour and Wine Aroma, *Int. J. Food Microbiol.* **2010**, *138,* pp. 19–25.

(16) Zhang, B.-Q.; Shen, J.-Y.; Duan, C.-Q.; Yan, G.-L. Use of Indigenous *Hanseniaspora Vineae* and *Metschnikowia Pulcherrima* Co-Fermentation with *Saccharomyces Cerevisiae* to Improve the Aroma Diversity of Vidal Blanc Icewine, *Front. Microbiol.* **2018**, *9,* p. 2303.

(17) Contreras, A.; Hidalgo, C.; Henschke, P. A.; Chambers, P. J.; Curtin, C.; Varela, C. Evaluation of Non-*Saccharomyces* Yeasts for the Reduction of Alcohol Content in Wine, *Appl. Environ. Microbiol.* **2014**, *80,* pp. 1670–1678.

(18) Lleixà, J.; Martín, V.; Del Portillo, M. C.; Carrau, F.; Beltran, G.; Mas, A. Comparison of Fermentation and Wines Produced by Inoculation of *Hanseniaspora Vineae* and *Saccharomyces Cerevisiae*, *Front. Microbiol.* **2016**, *7,* p. 338.

(19) Renault, P.; Coulon, J.; Revel, G. de; Barbe, J.-C.; Bely, M. Increase of Fruity Aroma During Mixed *T. Delbrueckii*/*S. Cerevisiae* Wine Fermentation Is Linked to Specific Esters Enhancement, *Int. J. Food Microbiol.* **2015**, *207,* pp. 40–48.

(20) Gobbi, M.; Comitini, F.; Domizio, P.; Romani, C.; Lencioni, L.; Mannazzu, I.; Ciani, M. *Lachancea Thermotolerans* and *Saccharomyces Cerevisiae* in Simultaneous and Sequential Co-Fermentation: A Strategy to Enhance Acidity and Improve the Overall Quality of Wine, *Food Microbiol.* **2013**, *33,* pp. 271–281.

(21) Morata, A.; Escott, C.; Bañuelos, M. A.; Loira, I.; Del Fresno, J. M.; González, C.; Suárez-Lepe, J. A. Contribution of Non-*Saccharomyces* Yeasts to Wine Freshness. A Review, *Biomolecules.* **2019**, *10*.

(22) Buerth, C.; Heilmann, C. J.; Klis, F. M.; Koster, C. G. de; Ernst, J. F.; Tielker, D. Growth-Dependent Secretome of *Candida Utilis*, *Microbiology.* **2011**, *157,* pp. 2493–2503.

(23) van Rensberg, P.; Pretorius, I. S. Enzymes in Winemaking: Harnessing Natural Catalysts for Efficient Biotransf Ormations - a Review, *SAJEV.* **2019**, *21*.

(24) Claus, H. Exoenzymes of Wine Microorganisms. In *Biology of Microorganisms on Grapes, in Must and in Wine;* König, H.; Unden, G.; Fröhlich, J., Eds.; Springer Berlin Heidelberg: Berlin, Heidelberg, 2009, pp. 259–271.

(25) Sadoudi, M.; Tourdot-Maréchal, R.; Rousseaux, S.; Steyer, D.; Gallardo-Chacón, J.-J.; Ballester, J.; Vichi, S.; Guérin-Schneider, R.; Caixach, J.; Alexandre, H. Yeast-Yeast Interactions Revealed by Aromatic Profile Analysis of Sauvignon Blanc Wine Fermented by Single or Co-Culture of Non-*Saccharomyces* and *Saccharomyces* Yeasts, *Food Microbiol.* **2012**, *32,* pp. 243–253.

(26) Ciani, M.; Comitini, F. Non-*Saccharomyces* Wine Yeasts Have a Promising Role in Biotechnological Approaches to Winemaking, *Ann. Microbiol.* **2011**, *61,* pp. 25–32.

(27) Morata, A.; Loira, I.; Escott, C.; Del Fresno, J. M.; Bañuelos, M. A.; Suárez-Lepe, J. A. Applications of *Metschnikowia Pulcherrima* in Wine Biotechnology, *Fermentation.* **2019**, *5,* p. 63.

(28) Fleet, G. H. Wine Yeasts for the Future, *FEMS Yeast Res.* **2008**, *8,* pp. 979–995.

(29) Claus, H.; Mojsov, K. Enzymes for Wine Fermentation: Current and Perspective Applications, *Fermentation.* **2018**, *4,* p. 52.

(30) Sahay, S.; Hamid, B.; Singh, P.; Ranjan, K.; Chauhan, D.; Rana, R. S.; Chaurse, V. K. Evaluation of Pectinolytic Activities for Oenological Uses from Psychrotrophic Yeasts, *Lett. Appl. Microbiol.* **2013**, *57,* pp. 115–121.

(31) Vos, A. *Preclinical studies on the immune-modulatory effects of dietary oligosaccharides,* Maastricht University, the Netherlands, ISBN/EAN: 9789064642425. **2008**.

(32) Da Silva, E. G.; Fátima Borges, M. de; Medina, C.; Piccoli, R. H.; Schwan, R. F. Pectinolytic Enzymes Secreted by Yeasts from Tropical Fruits, *FEMS Yeast Res.* **2005**, *5,* pp. 859–865.

(33) Heidarizadeh, M.; Fathi Rezaei, P.; Shahabivand, S. Novel Pectinase from *Piriformospora Indica*, Optimization of Growth Parameters and Enzyme Production in Submerged Culture Condition, *Turk. J. Biochem.* **2018**, *43,* pp. 289–295.

(34) Gognies, S.; Gainvors, A.; Aigle, M.; Belarbi, A. Cloning, Sequence Analysis and Overexpression of a *Saccharomyces Cerevisiae* Endopolygalacturonase-Encoding Gene (PGL1), *Yeast.* **1999**, *15,* pp. 11–22.

(35) Merín, M. G.; Morata de Ambrosini, V. I. Highly Cold-Active Pectinases Under Wine-Like Conditions from Non-*Saccharomyces* Yeasts for Enzymatic Production During Winemaking, *Lett. Appl. Microbiol.* **2015**, *60,* pp. 467–474.

(36) Belda, I.; Conchillo, L. B.; Ruiz, J.; Navascués, E.; Marquina, D.; Santos, A. Selection and Use of Pectinolytic Yeasts for Improving Clarification and Phenolic Extraction in Winemaking, *Int. J. Food Microbiol.* **2016**, *223,* pp. 1–8.

(37) Alimardani-Theuil, P.; Gainvors-Claisse, A.; Duchiron, F. Yeasts: An Attractive Source of Pectinases - from Gene Expression to Potential Applications: A Review, *Process Biochem.* **2011**, *46,* pp. 1525–1537.

(38) Merín, M. G.; Mendoza, L. M.; Morata de Ambrosini, V. I. Pectinolytic Yeasts from Viticultural and Enological Environments: Novel Finding of *Filobasidium Capsuligenum* Producing Pectinases, *J. Basic Microbiol.* **2014**, *54,* pp. 835–842.

(39) Blanco, P.; Sieiro, C.; Villa, T. G. Production of Pectic Enzymes in Yeasts, *FEMS Microbiol. Lett.* **1999**, *175,* pp. 1–9.

(40) Fernández-González, M.; Ubeda, J. F.; Vasudevan, T. G.; Otero, R. C.; Briones, A. I. Evaluation of Polygalacturonase Activity in *Saccharomyces Cerevisiae* Wine Strains, *FEMS Microbiol. Lett.* **2004**, *237,* pp. 261–266.

(41) Luh, B. S.; Phaff, H. J. Properties of Yeast Polygalacturonase, *Arch. Biochem. Biophys.* **1954**, *48,* pp. 23–37.

(42) Barnett, J. A.; Payne, R. W.; Yarrow, D. Yeasts: Characteristics and Identification, 3rd Edition, *Pediatr. Dermatol.* **2001**, *18,* p. 547.

(43) Jia, J.; Wheals, A. Endopolygalacturonase Genes and Enzymes from *Saccharomyces Cerevisiae* and *Kluyveromyces Marxianus*, *Curr. Genet.* **2000**, *38,* pp. 264–270.

(44) Radoi, F.; Kishida, M.; Kawasaki, H. Endo-Polygalacturonase in *Saccharomyces* Wine Yeasts: Effect of Carbon Source on Enzyme Production, *FEMS Yeast Res.* **2005**, *5,* pp. 663–668.

(45) Oliveira, K. F.; Malavolta, L.; Souza, C. S.; Vicente, E. J.; Laluce, C. Pectinolytic Activity Secreted by Yeasts Isolated from Fermented Citrus Molasses, *J. Appl. Microbiol.* **2006**, *100,* pp. 633–640.

(46) Bayly, F. C.; Berg, H. W. Grape and Wine Proteins of White Wine Varietals, *Am. J. Enol. Vitic.*, *1967,* pp. 18–32.

(47) Batista, L.; Monteiro, S.; Loureiro, V. B.; Teixeira, A. R.; Ferreira, R. B. The Complexity of Protein Haze Formation in Wines, *Food Chem.* **2009**, *112,* pp. 169–177.

(48) Santoro, M. Fractionation and Characterization of Must and Wine Proteins, *Am. J. Enol. Vitic.*, *1995,* pp. 250–254.

(49) Ferreira, R. B.; Piçarra-Pereira, M. A.; Monteiro, S.; Loureiro, V. B.; Teixeira, A. R. The Wine Proteins, *Trends Food Sci. Technol.* **2001**, *12,* pp. 230–239.

(50) Sarmento, M. R.; Oliveiraz, J. C.; Slatner, M.; Boulton, R. B. Effect of Ion-Exchange Adsorption on the Protein Profiles of White Wines, *Food Sci. Technol. Int.* **2001**, *7,* pp. 217–224.

(51) Cosme, F.; Fernandes, C.; Ribeiro, T.; Filipe-Ribeiro, L.; Nunes, F. M. White Wine Protein Instability: Mechanism, Quality Control and Technological Alternatives for Wine Stabilisation—An Overview, *Beverages.* **2020**, *6,* p. 19.

(52) Ferreira, R.; Monteiro, S.; Picarra-Pereira, M. A.; Tanganho, M. C.; Loureiro, V. B.; Teixiera, A. R. Characterization of the Proteins from Grapes and Wines by Immunological Methods, *Am. J. Enol. Vitic.*, *2000,* pp. 22–28.

(53) Ferreira, R. B.; Monteiro, S. S.; Piçarra-Pereira, M. A.; Teixeira, A. R. Engineering Grapevine for Increased Resistance to Fungal Pathogens Without Compromising Wine Stability, *Trends Biotechnol.* **2004**, *22,* pp. 168–173.

(54) Cilindre, C.; Castro, A. J.; Clément, C.; Jeandet, P.; Marchal, R. Influence of *Botrytis Cinerea* Infection on Champagne Wine Proteins (Characterized by Two-Dimensional Electrophoresis/immunodetection) And Wine Foaming Properties, *Food Chem.* **2007**, *103,* pp. 139–149.

(55) van Sluyter, S. C.; McRae, J. M.; Falconer, R. J.; Smith, P. A.; Bacic, A.; Waters, E. J.; Marangon, M. Wine Protein Haze: Mechanisms of Formation and Advances in Prevention, *J. Agric. Food Chem.* **2015**, *63,* pp. 4020–4030.

(56) Monteiro, S.; Piçarra-Pereira, M. A.; Mesquita, P. R.; Loureiro, V. B.; Teixeira, A.; Ferreira, R. B. The Wide Diversity of Structurally Similar Wine Proteins, *J. Agric. Food. Chem.* **2001**, *49,* pp. 3999–4010.

(57) Dufrechou, M.; Vernhet, A.; Roblin, P.; Sauvage, F.-X.; Poncet-Legrand, C. White Wine Proteins: How Does the PH Affect Their Conformation at Room Temperature?, *J. Colloids Surf.* **2013**, *29,* pp. 10475–10482.

(58) Tattersall, D. B.; Pocock, K. F.; Hayasaka, Y.; Adams, K.; van Heeswijck, R.; Waters, E. J.; Høj, P. B. Pathogenesis Related Proteins — Their Accumulation in Grapes During Berry Growth and Their Involvement in White Wine Heat Instability. Current Knowledge and Future Perspectives in Relation to Winemaking Practices. In *Molecular Biology & Biotechnology of the Grapevine;* Roubelakis-Angelakis, K. A., Ed.; Springer Netherlands: Dordrecht, 2001, pp. 183–201.

(59) Falconer, R. J.; Marangon, M.; van Sluyter, S. C.; Neilson, K. A.; Chan, C.; Waters, E. J. Thermal Stability of Thaumatin-Like Protein, Chitinase, and Invertase Isolated from Sauvignon Blanc and Semillon Juice and Their Role in Haze Formation in Wine, *J. Agric. Food. Chem.* **2010**, *58,* pp. 975–980.

(60) Marangon, M.; van Sluyter, S. C.; Neilson, K. A.; Chan, C.; Haynes, P. A.; Waters, E. J.; Falconer, R. J. Roles of Grape Thaumatin-Like Protein and Chitinase in White Wine Haze Formation, *J. Agric. Food. Chem.* **2011**, *59,* pp. 733–740.

(61) Esteruelas, M.; Poinsaut, P.; Sieczkowski, N.; Manteau, S.; Fort, M. F.; Canals, J. M.; Zamora, F. Characterization of Natural Haze Protein in Sauvignon White Wine, *Food Chem.* **2009**, *113,* pp. 28–35.

(62) Waters, E. J.; Shirley, N. J.; Williams, P. J. Nuisance Proteins of Wine Are Grape Pathogenesis-Related Proteins, *J. Agric. Food. Chem.* **1996,** pp. 3–5.

(63) Waters, E. J.; Wallace, W.; Tate, M. E.; Williams, P. J. Isolation and Partial Characterization of a Natural Haze Protective Factor from Wine, *J. Agric. Food Chem.* **1993**, *41,* pp. 724–730.

(64) Marangon, M.; Sauvage, F.-X.; Waters, E. J.; Vernhet, A. Effects of Ionic Strength and Sulfate Upon Thermal Aggregation of Grape Chitinases and Thaumatin-Like Proteins in a Model System, *J. Agric. Food. Chem.* **2011**, *59,* pp. 2652–2662.

(65) Peng, Z.; Pocock, K. F.; Waters, E. J.; Francis, I. L.; Williams, P. J. Taste Properties of Grape (*Vitis Vinifera*) Pathogenesis-Related Proteins Isolated from Wine, *J. Agric. Food Chem.* **1997**, *45,* pp. 4639–4643.

(66) Charpentier, C.; Escot, S.; Gonzalez, E.; Dulau, L.; Feuillat, M. The Influence of Yeast Glycosylated Proteins on Tannins Aggregation in Model Solution, *OENO One.* **2016**, *38,* p. 209.

(67) Pocock, K. F.; Alexander, G. M.; Hayasaka, Y.; Jones, P. R.; Waters, E. J. Sulfate - a Candidate for the Missing Essential Factor That Is Required for the Formation of Protein Haze in White Wine, *J. Agric. Food. Chem.* **2007**, *55,* pp. 1799–1807.

(68) Pashova, V.; Güell, C.; López, F. White Wine Continuous Protein Stabilization by Packed Column, *J. Agric. Food. Chem.* **2004**, *52,* pp. 1558–1563.

(69) Marangon, M.; Luchetta, M.; Waters, E. J. Protein Stabilisation of White Wines Using Zirconium Dioxide Enclosed in a Metallic Cage, *Aust. J. Grape Wine Res.* **2011**, *17,* pp. 28–35.

(70) Mierczynska-Vasilev, A.; Wahono, S. K.; Smith, P. A.; Bindon, K.; Vasilev, K. Using Zeolites to Protein Stabilize White Wines, *Sustainable Chem. Eng.* **2019**.

(71) Ribéreau-Gayon, P.; Glroies, Y.; Maujean, A.; Dubourdieu, D., Eds. *Handbook of Enology. Volume 2: The Chemistry of Wine Stabilization and Treatments;* John Wiley & Sons Inc.: Hoboken, NJ, USA, 2006.

(72) Brown, S. L.; Stockdale, V. J.; Pettolino, F.; Pocock, K. F.; Barros Lopes, M. de; Williams, P. J.; Bacic, A.; Fincher, G. B.; Høj, P. B.; Waters, E. J. Reducing Haziness in White Wine by Overexpression of *Saccharomyces Cerevisiae* Genes YOL155c and YDR055w, *Appl. Microbiol. Biotechnol.* **2007**, *73,* pp. 1363–1376.

(73) *Dossier des OIV-Kodex der önologischen Verfahren (2019/C 409/01), OENO 4/01; 15/05: Behandlung von Wein mit Mannoproteinen aus Hefen,* 2019.

(74) Vincenzi, S.; Plesani, M.; Curioni, A. Removal of Specific Protein Components by Chitin Enhances Protein Stability in a White Wine, *Am. J. Enol. Vitic.*, *2005,* pp. 246–254.

(75) Ndlovu, T.; Divol, B.; Bauer, F. F. Yeast Cell Wall Chitin Reduces Wine Haze Formation, *Appl. Environ. Microbiol.* **2018**, *84*.

(76) Tyndall, J. D. A.; Nall, T.; Fairlie, D. P. Proteases Universally Recognize Beta Strands in Their Active Sites, *Chem. Rev.* **2005**, *105,* pp. 973–999.

(77) Borelli, C.; Ruge, E.; Lee, J. H.; Schaller, M.; Vogelsang, A.; Monod, M.; Korting, H. C.; Huber, R.; Maskos, K. X-Ray Structures of Sap1 and Sap5: Structural Comparison of the Secreted Aspartic Proteinases from *Candida Albicans*, *Proteins.* **2008**, *72,* pp. 1308–1319.

(78) Suguna, K.; Padlan, E. A.; Smith, C. W.; Carlson, W. D.; Davies, D. R. Binding of a Reduced Peptide Inhibitor to the Aspartic Proteinase from *Rhizopus Chinensis*: Implications for a Mechanism of Action, *PNAS.* **1987**, *84,* pp. 7009–7013.

(79) Badgujar, S. B.; Mahajan, R. T. Biological Aspects of Proteolytic Enzymes: A Review, *J. Pharm. Res.* **2010,** pp. 2048–2068.

(80) Hervé, A. Aging on Lees and Their Alternatives: Impact on Wine. In *Managing Wine Quality;* Alexandre Herve, Ed.; Elsevier, 2022, pp. 213–244.

(81) Schlander, M.; Distler, U.; Tenzer, S.; Thines, E.; Claus, H. Purification and Properties of Yeast Proteases Secreted by *Wickerhamomyces Anomalus* 227 and *Metschnikovia Pulcherrima* 446 During Growth in a White Grape Juice, *Fermentation.* **2017**, *3,* p. 2.

(82) Dizy, M.; Bisson, L. F. Proteolytic Activity of Yeast Strains During Grape Juice Fermentation, *Am. J. Enol. Vitic.*, *2000,* pp. 155–167.

(83) Cramer, A. C.; Vlassides, S.; Block, D. E. Kinetic Model for Nitrogen-Limited Wine Fermentations, *Biotechnol. Bioeng.* **2002**, *77,* pp. 49–60.

(84) Marangon, M.; van Sluyter, S. C.; Robinson, E. M. C.; Muhlack, R. A.; Holt, H. E.; Haynes, P. A.; Godden, P. W.; Smith, P. A.; Waters, E. J. Degradation of White Wine Haze Proteins by Aspergillopepsin I and II During Juice Flash Pasteurization, *Food Chem.* **2012**, *135,* pp. 1157–1165.

(85) van Sluyter, S. C.; Warnock, N. I.; Schmidt, S.; Anderson, P.; van Kan, J. A. L.; Bacic, A.; Waters, E. J. Aspartic Acid Protease from *Botrytis Cinerea* Removes Haze-Forming Proteins During White Winemaking, *J. Agric. Food. Chem.* **2013**, *61,* pp. 9705–9711.

(86) Benucci, I.; Esti, M.; Liburdi, K. Effect of Free and Immobilised Stem Bromelain on Protein Haze in White Wine, *Aust. J. Grape Wine Res.* **2014**, *20,* pp. 347–352.

(87) Maicas, S.; Mateo, J. J. Hydrolysis of Terpenyl Glycosides in Grape Juice and Other Fruit Juices: A Review, *Appl. Microbiol. Biotechnol.* **2005**, *67,* pp. 322–335.

(88) Gunata, Y. Z.; Bayonove, C. L.; Baumes, R. L.; Cordonnier, R. E. The Aroma of Grapes I. Extraction and Determination of Free and Glycosidically Bound Fractions of Some Grape Aroma Components, *J. Chromatogr. A.* **1985**, *331,* pp. 83–90.

(89) Krammer, G.; Winterhalter, P.; Schwab, M.; Schreier, P. Glycosidically Bound Aroma Compounds in the Fruits of *Prunus* Species: Apricot (*P. Armeniaca*, L.), Peach (*P. Persica*, L.), Yellow Plum (*P. Domestica*, L. Ssp. Syriaca), *J. Agric. Food Chem.* **1991**, *39,* pp. 778–781.

(90) Hjelmeland, A. K.; Ebeler, S. E. Glycosidically Bound Volatile Aroma Compounds in Grapes and Wine: A Review, *Am. J. Enol. Vitic.* **2015**, *66,* pp. 1–11.

(91) Jones, P.; Vogt, T. Glycosyltransferases in Secondary Plant Metabolism: Tranquilizers and Stimulant Controllers, *Planta.* **2001**, *213,* pp. 164–174.

(92) Park, S. K.; Morrison, J. C.; Adams, D. O.; Noble, A. C. Distribution of Free and Glycosidically Bound Monoterpenes in the Skin and Mesocarp of Muscat of Alexandria Grapes During Development, *J. Agric. Food Chem.* **1991**, *39,* pp. 514–518.

(93) Ebeler, S. E. Analytical Chemistry: Unlocking the Secrets of Wine Flavour, *Food Rev. Int.* **2001**, *17,* pp. 45–64.

(94) Sabel, A.; Martens, S.; Petri, A.; König, H.; Claus, H. *Wickerhamomyces Anomalus* AS1: A New Strain with Potential to Improve Wine Aroma, *Ann. Microbiol.* **2014**, *64,* pp. 483–491.

(95) Stahl-Biskup, E.; Intert, F.; Holthuijzen, J.; Stengele, M.; Schulz, G. Glycosidically Bound Volatiles - a Review 1986–1991, *Flavour Fragr. J.* **1993**, *8,* pp. 61–80.

(96) Mateo, J.; Jiménez, M. Monoterpenes in Grape Juice and Wines, *J. Chromatogr. A.* **2000**, *881,* pp. 557–567.

(97) Schober, D. *Freisetzung glycosidisch gebundener Aromastoffe während der Wein- und Sektbereitung: Chemische, Sensorische und Molekularbiologische Untersuchungen:* Kaiserslautern, 2016.

(98) Meng, X.; Maliakal, P.; Lu, H.; Lee, M.-J.; Yang, C. S. Urinary and Plasma Levels of Resveratrol and Quercetin in Humans, Mice, and Rats After Ingestion of Pure Compounds and Grape Juice, *J. Agric. Food Chem.* **2004**, *52,* pp. 935–942.

(99) Ferner, M. J. *Untersuchungen und Charakterisierung ausgewählter Glucosidase-Varietäten mit dem Ziel einer Weinaromaverbesserung:* Hamburg, 2012.

(100) Fernández-Pacheco, P.; García-Béjar, B.; Briones Pérez, A.; Arévalo-Villena, M. Free and Immobilised *β*-Glucosidases in Oenology: Biotechnological Characterisation and Its Effect on Enhancement of Wine Aroma, *Front. Microbiol.* **2021**, *12,* p. 723815.

(101) Bhatia, Y.; Mishra, S.; Bisaria, V. S. Microbial *β*-Glucosidases: Cloning, Properties, and Applications, *Crit. Rev. Biotechnol.* **2002**, *22,* pp. 375–407.

(102) Alem, H.; Rigou, P.; Schneider, R.; Ojeda, H.; Torregrosa, L. Impact of Agronomic Practices on Grape Aroma Composition: A Review, *J. Sci. Food Agric.* **2019**, *99,* pp. 975–985.

(103) Wüst, M. Wein — Qualität Entscheidet Sich in Nanogramm: Zur Biochemie Des Sortentypischen Weinaromas, *Chemie Unserer Zeit.* **2003**, *37,* pp. 8–17.

(104) Ilc, T.; Parage, C.; Boachon, B.; Navrot, N.; Werck-Reichhart, D. Monoterpenol Oxidative Metabolism: Role in Plant Adaptation and Potential Applications, *Front. Plant. Sci.* **2016**, *7,* p. 509.

(105) Michlmayr, H. *Glykosidasen für die Aromastoff-Freisetzung in Wein und Fruchtsäften: Isolierung aus kommerziellen Starterkulturen für die malolactische Fermentation und partielle Charakterisierung:* Wien, 2008.

(106) Rapp, A. Aromastoffe Des Weines, *Chemie Unserer Zeit.* **1992**, *26,* pp. 273–284.

(107) Dziadas, M.; Jeleń, H. H. Comparison of Enzymatic and Acid Hydrolysis of Bound Flavor Compounds in Model System and Grapes, *Food Chem.* **2016**, *190,* pp. 412–418.

(108) Fischer, U.; Ganss, S.; Schmarr, H. G. Intensivierung Des Weinaromes, *Kuratorium für Technik und Bauwesen in der Landwirtschaft e.V.*, *2001*.

(109) Hernandez-Orte, P.; Concejero, B.; Astrain, J.; Lacau, B.; Cacho, J.; Ferreira, V. Influence of Viticulture Practices on Grape Aroma Precursors and Their Relation with Wine Aroma, *J. Sci. Food Agric.* **2015**, *95,* pp. 688–701.

(110) Palomo, E. S.; Pérez-Coello, M. S.; Díaz-Maroto, M. C.; González Viñas, M. A.; Cabezudo, M. D. Contribution of Free and Glycosidically-Bound Volatile Compounds to the Aroma of Muscat “A Petit Grains” Wines and Effect of Skin Contact, *Food Chem.* **2006**, *95,* pp. 279–289.

(111) Winterhalter, P.; Skouroumounis, G. K. Glycoconjugated Aroma Compounds: Occurrence, Role and Biotechnological Transformation, *Biotech. Aroma Comp.* **1997**, *55,* pp. 73–105.

(112) Gachon, C. M. M.; Langlois-Meurinne, M.; Saindrenan, P. Plant Secondary Metabolism Glycosyltransferases: The Emerging Functional Analysis, *Trends Plant. Sci.* **2005**, *10,* pp. 542–549.

(113) Sarry, J.; Gunata, Z. Plant and Microbial Glycoside Hydrolases: Volatile Release from Glycosidic Aroma Precursors, *Food Chem.* **2004**, *87,* pp. 509–521.

(114) Stanitzek, S. *Monoterpenylglucosyltransferasen aus Vitis vinifera: Funktionelle Charakterisierung und Analytik der Produkte mittels LC-MS/MS:* Bonn, 2014.

(115) Bowles, D.; Lim, E.-K. Glycosyltransferases of Small Molecules: Their Roles in Plant Biology, *eLS.* **2010**.

(116) Schwab, W.; Fischer, T.; Wüst, M. Terpene Glucoside Production: Improved Biocatalytic Processes Using Glycosyltransferases, *Eng. Life Sci.* **2015**, *15,* pp. 376–386.

(117) Loscos, N.; Hernández-Orte, P.; Cacho, J.; Ferreira, V. Evolution of the Aroma Composition of Wines Supplemented with Grape Flavour Precursors from Different Varietals During Accelerated Wine Ageing, *Food Chem.* **2010**, *120,* pp. 205–216.

(118) Park, S. K.; Noble, A. C. Monoterpenes and Monoterpene Glycosides in Wine Aromas, *In Beer and Wine Production. ACS Sypmosium Series*, *1993,* pp. 98–109.

(119) Zhang, P.; Zhang, R.; Sirisena, S.; Gan, R.; Fang, Z. *β*-Glucosidase Activity of Wine Yeasts and Its Impacts on Wine Volatiles and Phenolics: A Mini-Review, *Food Microbiol.* **2021**, *100,* p. 103859.

(120) Ahmed, A.; Nasim, F. -H.; Batool, K.; Bibi, A. Microbial *β*-Glucosidase: Sources, Production and Applications, *Sci. Educ.*, *2017,* pp. 31–46.

(121) Vasserot, Y.; Arnaud, A.; Galzy, P. Monoterpenol Glycosides in Plants and Their Biotechnological Transformation, *Acta Biotechnol.* **1995**, *15,* pp. 77–95.

(122) Lecas, M.; Gunata, Z. Y.; Sapis, J.-C.; Bayonove, C. L. Purification and Partial Characterization of *β* -Glucosidase from Grape, *Phytochemistry.* **1991**, *30,* pp. 451–454.

(123) Maicas, S.; Mateo, J. J. Enzyme Contribution of Non-*Saccharomyces* Yeasts to Wine Production, *UJMR.* **2015**, *3,* pp. 17–25.

(124) Loscos, N.; Hernandez-Orte, P.; Cacho, J.; Ferreira, V. Release and Formation of Varietal Aroma Compounds During Alcoholic Fermentation from Nonfloral Grape Odorless Flavor Precursors Fractions, *J. Agric. Food. Chem.* **2007**, *55,* pp. 6674–6684.

(125) Villena, M. A.; Iranzo, J. F. Ú.; Pérez, A. I. B. *β*-Glucosidase Activity in Wine Yeasts: Application in Enology, *Enzyme Microb. Technol.* **2007**, *40,* pp. 420–425.

(126) Zhang, J.; Zhao, N.; Xu, J.; Qi, Y.; Wei, X.; Fan, M. Homology Analysis of 35 *β*-Glucosidases in *Oenococcus Oeni* and Biochemical Characterization of a Novel *β*-Glucosidase BGL0224, *Food Chem.* **2021**, *334,* p. 127593.

(127) Tofalo, R.; Patrignani, F.; Lanciotti, R.; Perpetuini, G.; Schirone, M.; Di Gianvito, P.; Pizzoni, D.; Arfelli, G.; Suzzi, G. Aroma Profile of Montepulciano D'abruzzo Wine Fermented by Single and Co-Culture Starters of Autochthonous *Saccharomyces* and Non-*Saccharomyces* Yeasts, *Front. Microbiol.* **2016**, *7,* p. 610.

(128) Oliveira, I.; Ferreira, V. Modulating Fermentative, Varietal and Aging Aromas of Wine Using Non-*Saccharomyces* Yeasts in a Sequential Inoculation Approach, *Microorganisms.* **2019**, *7*.

(129) Madrigal, T.; Maicas, S.; Mateo Tolosa, J. J. Glucose and Ethanol Tolerant Enzymes Produced by *Pichia* (*Wickerhamomyces*) Isolates from Enological Ecosystems, *Am. J. Enol. Vitic.* **2013**, *64,* pp. 126–133.

(130) Grossmann, M.; Rapp, A.; Rieth, W. Enzymatische Freisetzung Gebundener Aromastoffe in Wein., *Dtsch. Lebensm. Rdsch.*, *1987,* pp. 7–12.

(131) Barbagallo, R. N.; Spagna, G.; Palmeri, R.; Restuccia, C.; Giudici, P. Selection, Characterization and Comparison of *β*-Glucosidase from Mould and Yeasts Employable for Enological Applications, *Enzyme Microb. Technol.* **2004**, *35,* pp. 58–66.

(132) Spagna, G.; Barbagallo, R. N.; Palmeri, R.; Restuccia, C.; Giudici, P. Properties of Endogenous *β*-Glucosidase of a *Pichia Anomala* Strain Isolated from Sicilian Musts and Wines, *Enzyme Microb. Technol.* **2002**, *31,* pp. 1036–1041.

(133) Swangkeaw, J.; Vichitphan, S.; Butzke, C. E.; Vichitphan, K. The Characterisation of a Novel *Pichia Anomala β*-Glucosidase with Potentially Aroma-Enhancing Capabilities in Wine, *Ann. Microbiol.* **2009**, *59,* pp. 335–343.

(134) Zhang, Y.; Min, Z.; Qin, Y.; Ye, D.-Q.; Song, Y.-Y.; Liu, Y.-L. Efficient Display of Aspergillus Niger *β*-Glucosidase on *Saccharomyces Cerevisiae* Cell Wall for Aroma Enhancement in Wine, *J. Agric. Food Chem.* **2019**, *67,* pp. 5169–5176.

(135) Ketudat Cairns, J. R.; Esen, A. *β*-Glucosidases, *Cell. Mol. Life Sci.* **2010**, *67,* pp. 3389–3405.

(136) Mateo, J. J.; Di Stefano, R. Description of the *β*-Glucosidase Activity of Wine Yeasts, *Food Microbiol.* **1997**, *14,* pp. 583–591.

(137) López, M. C.; Mateo, J. J.; Maicas, S. Screening of *β*-Glucosidase and *B*-Xylosidase Activities in Four Non-*Saccharomyces* Yeast Isolates, *J. Food Sci.* **2015**, *80,* C1696-704.

(138) Wang, Y.; Xu, Y.; Li, J. A Novel Extracellular *β*-Glucosidase from *Trichosporon Asahii*: Yield Prediction, Evaluation and Application for Aroma Enhancement of Cabernet Sauvignon, *J. Food Sci.* **2012**, *77,* M505-15.

(139) Hu, K.; Zhu, X. L.; Mu, H.; Ma, Y.; Ullah, N.; Tao, Y. A Novel Extracellular Glycosidase Activity from *Rhodotorula Mucilaginosa* : Its Application Potential in Wine Aroma Enhancement, *Lett. Appl. Microbiol.* **2016**, *62,* pp. 169–176.

(140) Ovalle, S. de; Cavello, I.; Brena, B. M.; Cavalitto, S.; González-Pombo, P. Production and Characterization of a *β*-Glucosidase from *Issatchenkia Terricola* and Its Use for Hydrolysis of Aromatic Precursors in Cabernet Sauvignon Wine, *LWT.* **2017**.

(141) Baffi, M. A.; Tobal, T.; Lago, J. H. G.; Boscolo, M.; Gomes, E.; Da-Silva, R. Wine Aroma Improvement Using a *β*-Glucosidase Preparation from *Aureobasidium Pullulans*, *Appl. Biochem. Biotechnol.* **2013**, *169,* pp. 493–501.

(142) Rani, V.; Dash, S.; Nain, L.; Arora, A. Expression of Novel Glucose Tolerant *β*-Glucosidase on Cell Surface by *Rhodotorula Glutinis* Isolate, *Biocatal. Agric. Biotechnol.* **2015**, *4,* pp. 380–387.

(143) Maitan-Alfenas, G. P.; A Lage, L. G. de; Almeida, M. N. de; Visser, E. M.; Rezende, S. T. de; Guimarães, V. M. Hydrolysis of Soybean Isoflavones by *Debaryomyces Hansenii* UFV-1 Immobilised Cells and Free *β*-Glucosidase, *Food Chem.* **2014**, *146,* pp. 429–436.

(144) Gondé, P.; Arnaud, A.; Ratomahenina, R.; Galzy, P.; Nicolas, M. The Enzyme Systems in a Strain of *Candida Wickerhamii* Meyer and Yarrow Participating in the Hydrolysis of Cellodextrins, *J. Gen. Appl. Microbiol.* **1984**, *30,* pp. 509–521.

(145) Leclerc, M.; Gondé, P.; Arnaud, A.; Ratomahenina, R.; Galzy, P.; Nicolas, M. The Enzyme Systems in a Strain of *Candida Wickerhamii* Meyer and Yarrow Paricipating in the Hydrolysis of Cellodextrins, *J. Gen. Appl. Microbiol.* **1984,** pp. 509–521.

(146) Arévalo Villena, M.; Ubeda Iranzo, J. F.; Cordero Otero, R. R.; Briones Pérez, A. I. Optimization of a Rapid Method for Studying the Cellular Location of *β*-Glucosidase Activity in Wine Yeasts, *J. Appl. Microbiol.* **2005**, *99,* pp. 558–564.

(147) Hernandez, L. *β*-Glucosidase Activity in a *Saccharomyces Cerevisiae* Wine Strain, *Int J Food Microbiol.* **2003**, *80,* pp. 171–176.

(148) Rosi, I.; Vinella, M.; Domizio, P. Characterization of *β*-Glucosidase Activity in Yeasts of Oenological Origin, *J. Appl. Bacteriol.* **1994**, *77,* pp. 519–527.

(149) Manzanares, P.; Rojas, V.; Genovés, S.; Vallés, S. A Preliminary Search for Anthocyanin- *β*-D-Glucosidase Activity in Non-*Saccharomyces* Wine Yeasts, *Int. J. Food Sci Technol.* **2000**, *35,* pp. 95–103.

(150) Ariaeenejad, S.; Nooshi-Nedamani, S.; Rahban, M.; Kavousi, K.; Pirbalooti, A. G.; Mirghaderi, S.; Mohammadi, M.; Mirzaei, M.; Salekdeh, G. H. A Novel High Glucose-Tolerant *β*-Glucosidase: Targeted Computational Approach for Metagenomic Screening, *Front. Bioeng. Biotechnol.* **2020**, *8,* p. 813.

(151) Zang, X.; Liu, M.; Fan, Y.; Xu, J.; Xu, X.; Li, H. The Structural and Functional Contributions of *β*-Glucosidase-Producing Microbial Communities to Cellulose Degradation in Composting, *Biotechnol. Biofuels.* **2018**, *11,* p. 51.

(152) Godse, R.; Bawane, H.; Tripathi, J.; Kulkarni, R. Unconventional *β*-Glucosidases: A Promising Biocatalyst for Industrial Biotechnology, *Appl. Biochem. Biotechnol.* **2021**, *193,* pp. 2993–3016.

(153) Gaensly, F.; Agustini, B. C.; Da Silva, G. A.; Picheth, G.; Bonfim, T. M. B. Autochthonous Yeasts with *β*-Glucosidase Activity Increase Resveratrol Concentration During the Alcoholic Fermentation of *Vitis Labrusca* Grape Must, *J. Funct. Foods.* **2015**, *19,* pp. 288–295.

(154) Hayasaka, Y.; Baldock, G. A.; Parker, M.; Pardon, K. H.; Black, C. A.; Herderich, M. J.; Jeffery, D. W. Glycosylation of Smoke-Derived Volatile Phenols in Grapes as a Consequence of Grapevine Exposure to Bushfire Smoke, *J. Agric. Food Chem.* **2010**, *58,* pp. 10989–10998.

(155) Härtl, K.; Huang, F.-C.; Giri, A. P.; Franz-Oberdorf, K.; Frotscher, J.; Shao, Y.; Hoffmann, T.; Schwab, W. Glucosylation of Smoke-Derived Volatiles in Grapevine (*Vitis Vinifera*) Is Catalyzed by a Promiscuous Resveratrol/Guaiacol Glucosyltransferase, *J. Agric. Food Chem.* **2017**, *65,* pp. 5681–5689.

(156) Aizawa, K. Studien Über Carbohydrase. Die fermentative Hydrolyse der p-Nitrophenol-glukoside, *J. Biochem.* **1939**.

(157) Miskin, A.; Edberg, S. C. Esculin Hydrolysis Reaction by *Escherichia Coli*, *J. Clin. Microbiol.* **1978**, *7,* pp. 251–254.

(158) Pérez, G.; Fariña, L.; Barquet, M.; Boido, E.; Gaggero, C.; Dellacassa, E.; Carrau, F. A Quick Screening Method to Identify *β*-Glucosidase Activity in Native Wine Yeast Strains: Application of Esculin Glycerol Agar (EGA) Medium, *World J. Microbiol. Biotechnol.* **2011**, *27,* pp. 47–55.

(159) Oftedal, L.; Maple-Grødem, J.; Førland, M. G. G.; Alves, G.; Lange, J. Validation and Assessment of Preanalytical Factors of a Fluorometric in Vitro Assay for Glucocerebrosidase Activity in Human Cerebrospinal Fluid, *Sci. Rep.* **2020**, *10,* p. 22098.

(160) Peters, S. P.; Lee, R. E.; Glew, R. H. A Microassay for Gaucher's Disease, *Clin. Chim. Acta.* **1975**, *60,* pp. 391–396.

(161) Charoenchai, C.; Fleet, G. H.; Henschke, P. A.; Todd, B. E. N. Screening of Non-*Saccharomyces* Wine Yeasts for the Presence of Extracellular Hydrolytic Enzymes, *Aust. J. Grape Wine Res.* **1997,** 2-8.

(162) Fia, G.; Giovani, G.; Rosi, I. Study of *β*-Glucosidase Production by Wine-Related Yeasts During Alcoholic Fermentation. A New Rapid Fluorimetric Method to Determine Enzymatic Activity, *J. Appl. Microbiol.* **2005**, *99,* pp. 509–517.

(163) Carrau, F. M.; Medina, K.; Boido, E.; Farina, L.; Gaggero, C.; Dellacassa, E.; Versini, G.; Henschke, P. A. De Novo Synthesis of Monoterpenes by *Saccharomyces Cerevisiae* Wine Yeasts, *FEMS Microbiol. Lett.* **2005**, *243,* pp. 107–115.

(164) Riccio, P.; Rossano, R.; Vinella, M.; Domizio, P.; Zito, F.; Sansevrino, F.; D'Elia, A.; Rosi, I. Extraction and Immobilization in One Step of Two *β*-Glucosidases Released from a Yeast Strain of *Debaryomyces Hansenii*, *Enzyme Microb. Technol.* **1999**, *24,* pp. 123–129.

(165) Gunata, Z.; Bayonove, C.; Baumes, R.; Cordonnier, R. Stability of Free and Bound Fractions of Some Aroma Components of Grapes Cv. Muscat During the Wine Processing: Preliminary Results, *Am. J. Enol. Vitic.*, *1986,* pp. 112–114.

(166) Delcroix, A.; Gunata, Z.; Sapis, J. C.; Salmon, J.-M.; Bayonove, C. Glycosidase Activities of Three Enological Yeast Strains During Winemaking: Effect on the Terpenol Content of Muscat Wine, *Am. J. Enol. Vitic.*, *1994,* pp. 291–296.

(167) Zoecklein, B. W.; Marcy, J. E.; Williams, J. M.; Jasinski, Y. Effect of Native Yeasts and Selected Strains of *Saccharomyces Cerevisiae* on Glycosyl Glucose, Potential Volatile Terpenes and Selected Aglycones of White Riesling (*Vitis Vinifera*) Wines, *J. Food Compos. Anal.*, *1997,* pp. 55–65.

(168) Ubeda Iranzo, J.; Briones Pérez, A.; Izquierdo Cañas, P. Study of the Oenological Characteristics and Enzymatic Activities of Wine Yeasts, *Food Microbiol.* **1998**, *15,* pp. 399–406.

(169) Chassagne, D.; Vernizeau, S.; Nedjma, M.; Alexandre, H. Hydrolysis and Sorption by *Saccharomyces Cerevisiae* Strains of Chardonnay Grape Must Glycosides During Fermentation, *Enzyme Microb. Technol.*, *2005,* pp. 212–217.

(170) Eglinton, J. M.; McWilliam, S. J.; Fogarty, M. W.; Francis, I. L.; Kwiatkowski, M. J.; Høj, P. B.; Henschke, P. A. The Effect of *Saccharomyces Bayanus*-Mediated Fermentation on the Chemical Composition and Aroma Profile of Chardonnay Wine, *Aust. J. Grape Wine Res.* **2000**, *6,* pp. 190–196.

(171) Ugliano, M.; Bartowsky, E. J.; McCarthy, J.; Moio, L.; Henschke, P. A. Hydrolysis and Transformation of Grape Glycosidically Bound Volatile Compounds During Fermentation with Three *Saccharomyces* Yeast Strains, *J. Agric. Food Chem.* **2006**, *54,* pp. 6322–6331.

(172) Gil, J. V.; Manzanares, P.; Genovés, S.; Vallés, S.; González-Candelas, L. Over-Production of the Major Exoglucanase of *Saccharomyces Cerevisiae* Leads to an Increase in the Aroma of Wine, *Int. J. Food Microbiol.* **2005**, *103,* pp. 57–68.

(173) Schmidt, S.; Rainieri, S.; Witte, S.; Matern, U.; Martens, S. Identification of a *Saccharomyces Cerevisiae* Glucosidase That Hydrolyzes Flavonoid Glucosides, *Appl. Environ. Microbiol.* **2011**, *77,* pp. 1751–1757.

(174) Bozoudi, D.; Tsaltas, D. The Multiple and Versatile Roles of *Aureobasidium Pullulans* in the Vitivinicultural Sector, *Fermentation.* **2018**, *4,* p. 85.

(175) Badal C. Saha; Shelby N. Freer; Rodney J. Bothast Production, Purification, and Properties of a Thermostable *β*-Glucosidase from a Color Variant Strain of *Aureobasidium Pullulans*, *Appl. Environ. Microbiol.* **1994,** pp. 3774–3780.

(176) González-Pombo, P.; Fariña, L.; Carrau, F.; Batista-Viera, F.; Brena, B. M. A Novel Extracellular *β*-Glucosidase from *Issatchenkia Terricola*: Isolation, Immobilization and

Application for Aroma Enhancement of White Muscat Wine, *Process. Biochem.* **2011**, *46,* pp. 385–389.

(177) Li, Y.; Wang, Y.; Fan, L.; Wang, F.; Liu, X.; Zhang, H.; Zhou, J. Assessment of *β*-D-Glucosidase Activity and Bgl Gene Expression of *Oenococcus Oeni* SD-2a, *PloS one.* **2020**, *15,* e0240484.

(178) Maicas, S.; Mateo, J. Microbial Glycosidases for Wine Production, *Beverages.* **2016**, *2,* p. 20.

(179) Gueguen, Y.; Chemardin, P.; Pien, S.; Arnaud, A.; Galzy, P. Enhancement of Aromatic Quality of Muscat Wine by the Use of Immobilized *β*-Glucosidase, *J. Biotechnol.* **1997**, *55,* pp. 151–156.

(180) Capone, D. L.; Barker, A.; Williamson, P. O.; Francis, I. L. The Role of Potent Thiols in Chardonnay Wine Aroma, *Aust. J. Grape Wine Res.* **2018**, *24,* pp. 38–50.

(181) Marais, J. Sauvignon Blanc Cultivar Aroma - a Review, *S. Afr. J. Enol. Vitic.* **1994,** pp. 41–45.

(182) Rajchl, A.; Čížková, H.; Voldřich, M.; Lukešová, D.; Panovská, Z. Methoxypyrazines in Sauvignon Blanc Wines, Detection of Addition of Artificial Aroma, *Czech J. Food Sci.* **2009**, *27,* pp. 259–266.

(183) Coetzee, C.; Du Toit, W. J. A Comprehensive Review on Sauvignon Blanc Aroma with a Focus on Certain Positive Volatile Thiols, *Int. Food Res. J.* **2012**, *45,* pp. 287–298.

(184) Müller, N.; Rauhut, D. Recent Developments on the Origin and Nature of Reductive Sulfurous Off-Odours in Wine, *Fermentation.* **2018**, *4,* p. 62.

(185) Masneuf-Pomarède, I.; Mansour, C.; Murat, M.-L.; Tominaga, T.; Dubourdieu, D. Influence of Fermentation Temperature on Volatile Thiols Concentrations in Sauvignon Blanc Wines, *Int. J. Food Microbiol.* **2006**, *108,* pp. 385–390.

(186) McGorrin, R. J. The Significance of Volatile Sulfur Compounds in Food Flavors. In *Volatile Sulfur Compounds in Food;* Qian, M. C.; Fan, X.; Mahattanatawee, K., Eds.; J. Am. Chem. Soc.: Washington, DC, 2011, pp. 3–31.

(187) Tominaga, T.; Niclass, Y.; Frérot, E.; Dubourdieu, D. Stereoisomeric Distribution of 3-Mercaptohexan-1-Ol and 3-Mercaptohexyl Acetate in Dry and Sweet White Wines Made from *Vitis Vinifera* (Var. Sauvignon Blanc and Semillon), *J. Agric. Food Chem.* **2006**, *54,* pp. 7251–7255.

(188) Nikolantonaki, M.; Chichuc, I.; Teissedre, P.-L.; Darriet, P. Reactivity of Volatile Thiols with Polyphenols in a Wine-Model Medium: Impact of Oxygen, Iron, and Sulfur Dioxide, *Anal. Chim. Acta.* **2010**, *660,* pp. 102–109.

(189) Tominaga, T.; Masneuf, I.; Dubourdieu, D. Powerful Aromatic Volatile Thiols in Wines Made from Several *Vitis Vinifera* L. Cv. Sauvignon Blan., *ACS Symposium Series*, *2004,* pp. 314–337.

(190) Tominaga, T.; Baltenweck-Guyot, R.; Des Gachons, C. P.; Dubourdieu, D. Contribution of Volatile Thiols to the Aromas of White Wines Made from Several *Vitis Vinifera* Grape Varieties, *Am. J. Enol. Vitic.*, *2000,* pp. 178–181.

(191) Murat, M. L.; Tominaga, T.; Dubourdieu, D. Assessing the Aromatic Potential of Cabernet Sauvignon and Merlot Musts Used to Produce Rose Wine by Assaying the Cysteinylated Precursor of 3-Mercaptohexan-1-Ol, *J. Agric. Food Chem.* **2001**, *49,* pp. 5412–5417.

(192) Roland, A.; Schneider, R.; Charrier, F.; Cavelier, F.; Rossignol, M.; Razungles, A. Distribution of Varietal Thiol Precursors in the Skin and the Pulp of Melon B. And Sauvignon Blanc Grapes, *Food Chem.* **2011**, *125,* pp. 139–144.

(193) Swiegers, J. H.; Capone, D. L.; Pardon, K. H.; Elsey, G. M.; Sefton, M. A.; Francis, I. L.; Pretorius, I. S. Engineering Volatile Thiol Release in *Saccharomyces Cerevisiae* for Improved Wine Aroma, *Yeast.* **2007**, *24,* pp. 561–574.

(194) Dubourdieu, D.; Tominaga, T.; Masneuf, I.; Des Peyrot Gachons, C.; Murat, M.-L. The Role of Yeasts in Grape Flavor Development During Fermentation: The Example of Sauvignon Blanc, *Am. J. Enol. Vitic.*, *2006,* pp. 81–88.

(195) Lilly, M.; Bauer, F. F.; Lambrechts, M. G.; Swiegers, J. H.; Cozzolino, D.; Pretorius, I. S. The Effect of Increased Yeast Alcohol Acetyltransferase and Esterase Activity on the Flavour Profiles of Wine and Distillates, *Yeast.* **2006**, *23,* pp. 641–659.

(196) van Wyk, N.; Michling, F.; Bergamo, D.; Brezina, S.; Pretorius, I. S.; Wallbrunn, C. von; Wendland, J. Effect of Isomixing on Grape Must Fermentations of ATF1-Overexpressing Wine Yeast Strains, *Foods.* **2020**, *9*.

(197) Keusgen, M.; Schulz, H.; Glodek, J.; Krest, I.; Krüger, H.; Herchert, N.; Keller, J. Characterization of Some *Allium* Hybrids by Aroma Precursors, Aroma Profiles, and Alliinase Activity, *J. Agric. Food Chem.* **2002**, *50,* pp. 2884–2890.

(198) Starkenmann, C.; Troccaz, M.; Howell, K. The Role of Cysteine and Cysteine-S Conjugates as Odour Precursors in the Flavour and Fragrance Industry, *Flavour Fragr. J.* **2008**, *23,* pp. 369–381.

(199) Capone, D. L.; Jeffery, D. W. Effects of Transporting and Processing Sauvignon Blanc Grapes on 3-Mercaptohexan-1-Ol Precursor Concentrations, *J. Agric. Food Chem.* **2011**, *59,* pp. 4659–4667.

(200) Fuentes, S.; Sullivan, W.; Tilbrook, J.; Tyerman, S. A Novel Analysis of Grapevine Berry Tissue Demonstrates a Variety-Dependent Correlation Between Tissue Vitality and Berry Shrivel, *Aust. J. Grape Wine Res.* **2010**, *16,* pp. 327–336.

(201) Gunata, Z.; Biron, C.; Sapis, J. C.; Bayonove, C. Glycosidase Activities in Sound and *Botrytis* Infected Grapes in Relation to Hydrolysis of Grape Monoterpenyl Glycosides, *Vitis*, *1989*.

(202) Maggu, M.; Winz, R.; Kilmartin, P. A.; Trought, M. C. T.; Nicolau, L. Effect of Skin Contact and Pressure on the Composition of Sauvignon Blanc Must, *J. Agric. Food Chem.* **2007**, *55,* pp. 10281–10288.

(203) Tominaga, T.; Masneuf-Pomarède, I.; Dubourdieu, D. A S-Cysteine Conjugate, Precursor of Aroma of White Sauvignon, *OENO One.* **1995,** pp. 227–232.

(204) Wakabayashi, H.; Wakabayashi, M.; Eisenreich, W.; Engel, K.-H. Stereochemical Course of the Generation of 3-Mercaptohexanal and 3-Mercaptohexanol by *β*-Lyase-Catalyzed Cleavage of Cysteine Conjugates, *J. Agric. Food Chem.* **2004**, *52,* pp. 110–116.

(205) Thibon, C.; Marullo, P.; Claisse, O.; Cullin, C.; Dubourdieu, D.; Tominaga, T. Nitrogen Catabolic Repression Controls the Release of Volatile Thiols by *Saccharomyces Cerevisiae* During Wine Fermentation, *FEMS Yeast Res.* **2008**, *8,* pp. 1076–1086.

(206) Cordente, A. G.; Borneman, A. R.; Bartel, C.; Capone, D.; Solomon, M.; Roach, M.; Curtin, C. D. Inactivating Mutations in Irc7p Are Common in Wine Yeasts, Attenuating Carbon-Sulfur *β*-Lyase Activity and Volatile Sulfur Compound Production, *Appl. Environ. Microbiol.* **2019**, *85*.

(207) Holt, S.; Cordente, A. G.; Curtin, C. *Saccharomyces Cerevisiae* STR3 and Yeast Cystathionine *β*-Lyase Enzymes: The Potential for Engineering Increased Flavor Release, *Bioeng. Bugs.* **2012**, *3,* pp. 178–180.

(208) Winter, G.; van der Westhuizen, T.; Higgins, V. J.; Curtin, C.; Ugliano, M. Contribution of Cysteine and Glutathione Conjugates to the Formation of the Volatile Thiols 3-Mercaptohexan-1-Ol (3MH) And 3-Mercaptohexyl Acetate (3MHA) During Fermentation by *Saccharomyces Cerevisiae*, *Aust. J. Grape Wine Res.* **2011**, *17,* pp. 285–290.

(209) Capone, D. L.; Sefton, M. A.; Hayasaka, Y.; Jeffery, D. W. Analysis of Precursors to Wine Odorant 3-Mercaptohexan-1-Ol Using HPLC-MS/MS: Resolution and Quantitation of Diastereomers of 3-S-Cysteinylhexan-1-Ol and 3-S-Glutathionylhexan-1-Ol, *J. Agric. Food Chem.* **2010**, *58,* pp. 1390–1395.

(210) Schneider, R.; Charrier, F.; Razungles, A.; Baumes, R. Evidence for an Alternative Biogenetic Pathway Leading to 3-Mercaptohexanol and 4-Mercapto-4-Methylpentan-2-One in Wines, *Anal. Chim. Acta.* **2006**, *563,* pp. 58–64.

(211) Subileau, M.; Schneider, R.; Salmon, J.-M.; Degryse, E. New Insights on 3-Mercaptohexanol (3MH) Biogenesis in Sauvignon Blanc Wines: Cys-3MH and (E)-Hexen-2-Al Are Not the Major Precursors, *J. Agric. Food Chem.* **2008**, *56,* pp. 9230–9235.

(212) Grant-Preece, P. A.; Pardon, K. H.; Capone, D. L.; Cordente, A. G.; Sefton, M. A.; Jeffery, D. W.; Elsey, G. M. Synthesis of Wine Thiol Conjugates and Labeled Analogues: Fermentation of the Glutathione Conjugate of 3-Mercaptohexan-1-Ol Yields the Corresponding Cysteine Conjugate and Free Thiol, *J. Agric. Food Chem.* **2010**, *58,* pp. 1383–1389.

(213) Cordente, A. G.; Capone, D. L.; Curtin, C. D. Unravelling Glutathione Conjugate Catabolism in *Saccharomyces Cerevisiae*: The Role of Glutathione/dipeptide Transporters and Vacuolar Function in the Release of Volatile Sulfur Compounds 3-Mercaptohexan-1-Ol and 4-Mercapto-4-Methylpentan-2-One, *Appl. Microbiol. Biotechnol.* **2015**, *99,* pp. 9709–9722.

(214) Santiago, M.; Gardner, R. C. Yeast Genes Required for Conversion of Grape Precursors to Varietal Thiols in Wine, *FEMS Yeast Res.* **2015**, *15,* fov034.

(215) Ganguli, D.; Kumar, C.; Bachhawat, A. K. The Alternative Pathway of Glutathione Degradation Is Mediated by a Novel Protein Complex Involving Three New Genes in *Saccharomyces Cerevisiae*, *Genetics.* **2007**, *175,* pp. 1137–1151.

(216) Des Peyrot Gachons, C.; Tominaga, T.; Dubourdieu, D. Sulfur Aroma Precursor Present in S-Glutathione Conjugate Form: Identification of S-3-(Hexan-1-Ol)-Glutathione in Must from *Vitis Vinifera* L. Cv. Sauvignon Blanc, *J. Agric. Food Chem.* **2002**, *50,* pp. 4076–4079.

(217) Roland, A.; Schneider, R.; Razungles, A.; Le Guernevé, C.; Cavelier, F. Straightforward Synthesis of Deuterated Precursors to Demonstrate the Biogenesis of Aromatic Thiols in Wine, *J. Agric. Food Chem.* **2010**, *58,* pp. 10684–10689.

(218) Subileau, M.; Schneider, R.; Salmon, J.-M.; Degryse, E. Nitrogen Catabolite Repression Modulates the Production of Aromatic Thiols Characteristic of Sauvignon Blanc at the Level of Precursor Transport, *FEMS Yeast Res.* **2008**, *8,* pp. 771–780.

(219) Harsch, M. J.; Benkwitz, F.; Frost, A.; Colonna-Ceccaldi, B.; Gardner, R. C.; Salmon, J.-M. New Precursor of 3-Mercaptohexan-1-Ol in Grape Juice: Thiol-Forming Potential and Kinetics During Early Stages of Must Fermentation, *J. Agric. Food Chem.* **2013**, *61,* pp. 3703–3713.

(220) Roland, A.; Vialaret, J.; Razungles, A.; Rigou, P.; Schneider, R. Evolution of S-Cysteinylated and S-Glutathionylated Thiol Precursors During Oxidation of Melon B. And Sauvignon Blanc Musts, *J. Agric. Food Chem.* **2010**, *58,* pp. 4406–4413.

(221) Kalua, C. M.; Boss, P. K. Comparison of Major Volatile Compounds from Riesling and Cabernet Sauvignon Grapes (*Vitis Vinifera* L.) From Fruitset to Harvest, *Aust. J. Grape Wine Res.* **2010**, *16,* pp. 337–348.

(222) Thibon, C.; Böcker, C.; Shinkaruk, S.; Moine, V.; Darriet, P.; Dubourdieu, D. Identification of S-3-(Hexanal)-Glutathione and Its Bisulfite Adduct in Grape Juice from *Vitis Vinifera* L. Cv. Sauvignon Blanc as New Potential Precursors of 3SH, *Food Chem.* **2016**, *199,* pp. 711–719.

(223) Bonnaffoux, H.; Delpech, S.; Rémond, E.; Schneider, R.; Roland, A.; Cavelier, F. Revisiting the Evaluation Strategy of Varietal Thiol Biogenesis, *Food Chem.* **2018**, *268,* pp. 126–133.

(224) Renault, P.; Coulon, J.; Moine, V.; Thibon, C.; Bely, M. Enhanced 3-Sulfanylhexan-1-Ol Production in Sequential Mixed Fermentation with *Torulaspora Delbrueckii*/*Saccharomyces Cerevisiae* Reveals a Situation of Synergistic Interaction Between Two Industrial Strains, *Front. Microbiol.* **2016**, *7,* p. 293.

(225) Choné, X.; Lavigne-Cruège, V.; Tominaga, T.; van Leeuwen, C.; Castagnède, C.; Saucier, C.; Dubourdieu, D. Effect of Vine Nitrogen Status on Grape Aromatic Potential: Flavor Precursors (S-Cysteine Conjugates), Glutathione and Phenolic Content in *Vitis Vinifera* L. Cv Sauvignon Blanc Grape Juice, *OENO One.* **2016**, *40,* p. 1.

(226) Brajkovich, M.; Tibbits, N.; Peron, G.; Lund, C. M.; Dykes, S. I.; Kilmartin, P. A.; Nicolau, L. Effect of Screwcap and Cork Closures on SO2 Levels and Aromas in a Sauvignon Blanc Wine, *J. Agric. Food Chem.* **2005**, *53,* pp. 10006–10011.

(227) Ochiai, N.; Sasamoto, K.; Kishimoto, T. Development of a Method for the Quantitation of Three Thiols in Beer, Hop, and Wort Samples by Stir Bar Sorptive Extraction with in Situ Derivatization and Thermal Desorption-Gas Chromatography-Tandem Mass Spectrometry, *J. Agric. Food. Chem.* **2015**, *63,* pp. 6698–6706.

(228) Dennenlöhr, J.; Thörner, S.; Rettberg, N. Analysis of Hop-Derived Thiols in Beer Using on-Fiber Derivatization in Combination with HS-SPME and GC-MS/MS, *J. Agric. Food Chem.* **2020**, *68,* pp. 15036–15047.

(229) Chen, L.; Capone, D. L.; Jeffery, D. W. Analysis of Potent Odour-Active Volatile Thiols in Foods and Beverages with a Focus on Wine, *Molecules.* **2019**, *24*.

(230) Vanzo, A.; Janeš, L.; Požgan, F.; Velikonja Bolta, Š.; Sivilotti, P.; Lisjak, K. UHPLC-MS/MS Determination of Varietal Thiol Precursors in Sauvignon Blanc Grapes, *Sci. Rep.* **2017**, *7,* p. 13122.

(231) Des Peyrot Gachons, C.; Tominaga, T.; Dubourdieu, D. Measuring the Aromatic Potential of *Vitis Vinifera* L. Cv. Sauvignon Blanc Grapes by Assaying S-Cysteine Conjugates, Precursors of the Volatile Thiols Responsible for Their Varietal Aroma, *J. Agric. Food Chem.* **2000**, *48,* pp. 3387–3391.

(232) Ouellette, R. J.; Rawn, J. D. *Organic chemistry;* Elsevier: Amsterdam, Boston, 2014.

(233) Hofmann; Schieberle Quantitative Model Studies on the Effectiveness of Different Precursor Systems in the Formation of the Intense Food Odorants 2-Furfurylthiol and 2-Methyl-3-Furanthiol, *J. Agric. Food Chem.* **1998**, *46,* pp. 235–241.

(234) Tominaga, T.; Blanchard, L.; Darriet, P.; Dubourdieu, D. A Powerful Aromatic Volatile Thiol, 2-Furanmethanethiol, Exhibiting Roast Coffee Aroma in Wines Made from Several *Vitis Vinifera* Grape Varieties, *J. Agric. Food Chem.* **2000**, *48,* pp. 1799–1802.

(235) Setlow, B.; Cabrera-Hernandez, A.; Cabrera-Martinez, R. M.; Setlow, P. Identification of Aryl-Phospho-*β*-Glucosidases in *Bacillus Subtilis*, *Arch. Microbiol.* **2004**, *181,* pp. 60–67.

(236) Surburg, H.; Panten, J. *Common Fragrance and Flavor Materials: Preparation, Properties and Uses*, 6th ed., 2016.

(237) Li, H.-K.; Chang, C.-F.; Lin, H.-J.; Lin, J.-L.; Lee, Y.-T.; Wu, Y.-H.; Liu, C.-Y.; Lin, T.-C.; Hsu, P.-H.; Lin, H.-T. V. Conversion of a Thiol Precursor into Aroma Compound 4-Mercapto-4-Methyl-2-Pentanone Using Microbial Cell Extracts, *Fermentation.* **2021**, *7,* p. 129.

(238) Kerkenaar, A.; Schmedding, D. J.; Berg, J. Method for Preparing Thiol Compounds with Bacterial *β*-Lyase.

(239) Huynh-Ba, T.; Matthey-Doret, W.; Fay, L. B.; Bel Rhlid, R. Generation of Thiols by Biotransformation of Cysteine-Aldehyde Conjugates with Baker's Yeast, *J. Agric. Food Chem.* **2003**, *51,* pp. 3629–3635.

(240) Zha, M.; Sun, B.; Yin, S.; Mehmood, A.; Cheng, L.; Wang, C. Generation of 2-Furfurylthiol by Carbon-Sulfur Lyase from the Baijiu Yeast *Saccharomyces Cerevisiae* G20, *J. Agric. Food. Chem.* **2018**, *66,* pp. 2114–2120.

(241) Allocati, N.; Masulli, M.; Di Ilio, C.; Federici, L. Glutathione Transferases: Substrates, Inihibitors and Pro-Drugs in Cancer and Neurodegenerative Diseases, *Oncogenesis.* **2018**, *7,* p. 8.

(242) Conn, S.; Curtin, C.; Bézier, A.; Franco, C.; Zhang, W. Purification, Molecular Cloning, and Characterization of Glutathione S-Transferases (GSTs) From Pigmented *Vitis Vinifera* L. Cell Suspension Cultures as Putative Anthocyanin Transport Proteins, *J. Exp. Bot.* **2008**, *59,* pp. 3621–3634.

(243) Wu, A.-L.; Moye-Rowley, W. S. GSH1, Which Encodes *Γ*-Glutamylcysteine Synthetase, Is a Target Gene for YAP-1 Transcriptional Regulation, *Mol. Cell. Biol.* **1994,** pp. 5832–5839.

(244) Franklin, C. C.; Backos, D. S.; Mohar, I.; White, C. C.; Forman, H. J.; Kavanagh, T. J. Structure, Function, and Post-Translational Regulation of the Catalytic and Modifier Subunits of Glutamate Cysteine Ligase, *Mol. Asp. Med.* **2009**, *30,* pp. 86–98.

(245) Njälsson, R.; Norgren, S. Physiological and Pathological Aspects of GSH Metabolism, *Acta Paediatr.* **2005**, *94,* pp. 132–137.

(246) Lu, S. C. Regulation of Glutathione Synthesis, *Mol. Asp. Med.* **2009**, *30,* pp. 42–59.

(247) Jaworski, A. F.; Aitken, S. M. Exploration of the Six Tryptophan Residues of *Escherichia Coli* Cystathionine *β*-Lyase as Probes of Enzyme Conformational Change, *Arch. Biochem. Biophys.* **2013**, *538,* pp. 138–144.

(248) Phillips, R. S.; Demidkina, T. V.; Faleev, N. G. Structure and Mechanism of Tryptophan Indole-Lyase and Tyrosine Phenol-Lyase, *Biochim. Biophys. Acta.* **2003**, *1647,* pp. 167–172.

(249) Tilloy, V.; Ortiz-Julien, A.; Dequin, S. Reduction of Ethanol Yield and Improvement of Glycerol Formation by Adaptive Evolution of the Wine Yeast *Saccharomyces Cerevisiae* Under Hyperosmotic Conditions, *Appl. Environ. Microbiol.* **2014**, *80,* pp. 2623–2632.

(250) Kutyna, D. R.; Varela, C.; Stanley, G. A.; Borneman, A. R.; Henschke, P. A.; Chambers, P. J. Adaptive Evolution of *Saccharomyces Cerevisiae* to Generate Strains with Enhanced Glycerol Production, *Appl. Microbiol. Biotechnol.* **2012**, *93,* pp. 1175–1184.

(251) Stanley, D.; Fraser, S.; Chambers, P. J.; Rogers, P.; Stanley, G. A. Generation and Characterisation of Stable Ethanol-Tolerant Mutants of *Saccharomyces Cerevisiae*, *J. Ind. Microbiol. Biotechnol.* **2010**, *37,* pp. 139–149.

(252) McBryde, C.; Gardner, J. M.; Barros Lopes, M. de; Jiranek, V. Generation of Novel Wine Yeast Strains by Adaptive Evolution, *Am. J. Enol. Vitic.*, *2006,* pp. 423–430.

(253) Cadière, A.; Ortiz-Julien, A.; Camarasa, C.; Dequin, S. Evolutionary Engineered *Saccharomyces Cerevisiae* Wine Yeast Strains with Increased in Vivo Flux Through the Pentose Phosphate Pathway, *Metab. Eng.* **2011**, *13,* pp. 263–271.

(254) Patzschke, A.; Steiger, M. G.; Holz, C.; Lang, C.; Mattanovich, D.; Sauer, M. Enhanced Glutathione Production by Evolutionary Engineering of *Saccharomyces Cerevisiae* Strains, *Biotechnol. J.* **2015**, *10,* pp. 1719–1726.

(255) Cakar, Z. P.; Seker, U. O. S.; Tamerler, C.; Sonderegger, M.; Sauer, U. Evolutionary Engineering of Multiple-Stress Resistant *Saccharomyces Cerevisiae*, *FEMS Yeast Res.* **2005**, *5,* pp. 569–578.

(256) Belda, I.; Ruiz, J.; Navascués, E.; Marquina, D.; Santos, A. Improvement of Aromatic Thiol Release Through the Selection of Yeasts with Increased *β*-Lyase Activity, *Int. J. Food Microbiol.* **2016**, *225,* pp. 1–8.

(257) Kiene, F.; Pretorius, I. S.; Rauhut, D.; Wallbrunn, C. von; van Wyk, N. Construction and Analysis of a Yeast for the Simultaneous Release and Esterification of the Varietal Thiol 3-Sulfanylhexan-1-Ol, *J. Agric. Food Chem.* **2021**, *69,* pp. 11919–11925.

(258) Gietz, R. D.; Schiestl, R. H. Quick and Easy Yeast Transformation Using the LiAc/SS Carrier DNA/PEG Method, *Nat. Protoc.* **2007**, *2,* pp. 35–37.

(259) Nieri, P.; Carpi, S.; Fogli, S.; Polini, B.; Breschi, M. C.; Podestà, A. Cholinesterase-Like Organocatalysis by Imidazole and Imidazole-Bearing Molecules, *Sci. Rep.* **2017**, *8,* p. 45760.

(260) Ciriminna, R.; Fidalgo, A.; Meneguzzo, F.; Presentato, A.; Scurria, A.; Nuzzo, D.; Alduina, R.; Ilharco, L. M.; Pagliaro, M. Pectin: A Long-Neglected Broad-Spectrum Antibacterial, *ChemMedChem.* **2020**, *15,* pp. 2228–2235.

(261) Piñeiro, Z.; Palma, M.; Barroso, C. G. Determination of Terpenoids in Wines by Solid Phase Extraction and Gas Chromatography, *Anal. Chim. Acta.* **2004**, *513,* pp. 209–214.

(262) Bowers, G. N.; McComb, R. B.; Christensen, R. G.; Schaffer, R. High-Purity 4-Nitrophenol: Purification, Characterization, and Specifications for Use as a Spectrophotometric Reference Material, *Clin. Chem.* **1980,** pp. 724–729.

(263) Lee, B.; Pometto, A. L.; Demicri, A.; Hinz, P. N. Media Evaluation for the Production of Microbial Enzymes, *J. Agric. Food. Chem.* **1998**.

(264) Tofalo, R.; Perpetuini, G.; Battistelli, N.; Tittarelli, F.; Suzzi, G. Correlation Between IRC7 Gene Expression and 4-Mercapto-4-Methylpentan-2-One Production in *Saccharomyces Cerevisiae* Strains, *Yeast.* **2020**, *37,* pp. 487–495.

(265) Collier, H. A Note on the Molar Absorptivity of Reduced Ellman's Reagent, 3-Carboxylato-4-Nitrothiophenolate, *Anal. Biochem.* **1973**, *56,* pp. 310–311.

(266) Clark, A. C.; Deed, R. C. The Chemical Reaction of Glutathione and *Trans*-2-Hexenal in Grape Juice Media to Form Wine Aroma Precursors: The Impact of PH, Temperature, and Sulfur Dioxide, *J. Agric. Food Chem.* **2018**, *66,* pp. 1214–1221.

(267) Ask, M.; Mapelli, V.; Höck, H.; Olsson, L.; Bettiga, M. Engineering Glutathione Biosynthesis of *Saccharomyces Cerevisiae* Increases Robustness to Inhibitors in Pretreated Lignocellulosic Materials, *Microb. Cell Factories.* **2013**, *12,* p. 87.

(268) Pawlikowska, E.; Kręgiel, D. Non Conventional Yeast *Metschnikowia Pulcherrima* and Its Application in Biotechnology, *Adv. Microbiol.* **2019**, *56,* pp. 405–415.

(269) Roca-Mesa, H.; Sendra, S.; Mas, A.; Beltran, G.; Torija, M.-J. Nitrogen Preferences During Alcoholic Fermentation of Different Non-*Saccharomyces* Yeasts of Oenological Interest, *Microorganisms.* **2020**, *8*.

(270) Puškaš, V. S.; Miljić, U. D.; Djuran, J. J.; Vučurović, V. M. The Aptitude of Commercial Yeast Strains for Lowering the Ethanol Content of Wine, *Food Sci. Nutr.* **2020**, *8,* pp. 1489–1498.

(271) Fernández-González, M.; Úbeda, J.; Briones, A. Typing of Non-*Saccharomyces* Yeasts with Enzymatic Activities of Interest in Wine-Making, *Int. J. Food Microbiol.* **2000**, *59,* pp. 29–36.

(272) Mateo, J. J.; Maicas, S.; Thieβen, C. Biotechnological Characterisation of Exocellular Proteases Produced by Enological *Hanseniaspora* Isolates, *Int. J. Food Sci. Technol.* **2015**, *50,* pp. 218–225.

(273) Reid, V. J.; Theron, L. W.; Du Toit, M.; Divol, B. Identification and Partial Characterization of Extracellular Aspartic Protease Genes from *Metschnikowia Pulcherrima* IWBT Y1123 and Candida Apicola IWBT Y1384, *Appl. Environ. Microbiol.* **2012**, *78,* pp. 6838–6849.

(274) Theron, L. *Investigating the impact of MpAPr1, an aspartic protease from the yeast Metschnikowia pulcherrima, on wine properties:* Bordeaux, 2017.

(275) Theron, L. W.; Bely, M.; Divol, B. Monitoring the Impact of an Aspartic Protease (MpAPr1) On Grape Proteins and Wine Properties, *Appl. Microbiol. Biotechnol.* **2018**, *102,* pp. 5173–5183.

(276) Snyman, C.; Theron, L. W.; Divol, B. The Expression, Secretion and Activity of the Aspartic Protease MpAPr1 in *Metschnikowia Pulcherrima* IWBT Y1123, *JIMB.* **2019**, *46,* pp. 1733–1743.

(277) Ni-orn, C. *Impact of protease activity of yeasts on wine fermentation and formation of volatile and non-volatile metabolites:* Gießen, 2008.

(278) Ganga, M. A.; Martínez, C. Effect of Wine Yeast Monoculture Practice on the Biodiversity of Non-*Saccharomyces* Yeasts, *J. Appl. Microbiol.* **2004**, *96,* pp. 76–83.

(279) Vicente, J.; Ruiz, J.; Belda, I.; Benito-Vázquez, I.; Marquina, D.; Calderón, F.; Santos, A.; Benito, S. The Genus *Metschnikowia* in Enology, *Microorganisms.* **2020**, *8*.

(280) Suhaimi, H.; Dailin, D. J.; Malek, R. A.; Hanapi, S. Z.; Ambehabati, K. K.; Keat, H. C.; Prakasham, S.; Elsayed, E. A.; Misson, M.; El Enshasy, H. Fungal Pectinases: Production and Applications in Food Industries. In *Fungi in sustainable food production,* pp. 85–115.

(281) Liu, J.; Bao, H.; Liu, C.; Wu, F.; Gao, F. “Turn-on” Fluorescence Determination of *β*-Glucosidase Activity Using Fluorescent Polymer Nanoparticles Formed from Polyethylenimine Cross-Linked with Hydroquinone, *Appl. Polym. Mater.* **2019**, *1,* pp. 3057–3063.

(282) Sapkota, A. Bile Esculin Test- Principle, Procedure, Results, Uses, Limitations, 2020. https://microbenotes.com/bile-esculin-test/. Thursday, September 16, 2021.

(283) Karnchanatat, A.; Petsom, A.; Sangvanich, P.; Piaphukiew, J.; Whalley, A. J. S.; Reynolds, C. D.; Sihanonth, P. Purification and Biochemical Characterization of an Extracellular *β*-Glucosidase from the Wood-Decaying Fungus *Daldinia Eschscholzii*, *FEMS Microbiol. Lett.* **2007**, *270,* pp. 162–170.

(284) Larue, K.; Melgar, M.; Martin, V. J. J. Directed Evolution of a Fungal *β*-Glucosidase in *Saccharomyces Cerevisiae*, *Biotechnol. Biofuels.* **2016**, *9,* p. 52.

(285) Kuo, H.-P.; Wang, R.; Huang, C.-Y.; Lai, J.-T.; Lo, Y.-C.; Huang, S.-T. Characterization of an Extracellular *β*-Glucosidase from *Dekkera Bruxellensis* for Resveratrol Production, *J. Food. Drug. Anal.* **2018**, *26,* pp. 163–171.

(286) van Smeden, J.; Dijkhoff, I. M.; Helder, R. W. J.; Al-Khakany, H.; Boer, D. E. C.; Schreuder, A.; Kallemeijn, W. W.; Absalah, S.; Overkleeft, H. S.; Aerts, J. M. F. G.; Bouwstra, J. A. In Situ Visualization of Glucocerebrosidase in Human Skin Tissue: Zymography Versus Activity-Based Probe Labeling, *J. Lipid Res.* **2017**, *58,* pp. 2299–2309.

(287) Takahashi, T.; Nishio, H.; Kodama, S.; Nakamura, H. *β*-Glucosidase Activity in Liver, Spleen and Brain in Acute Neuropathic Gaucher Disease, *Brain. Dev.* **1990**, *12,* pp. 202–205.

(288) Fleury, D.; Domaingue, P.; Gillard, C.; Touitou, R.; Mollat, P. Expression, Purification, Characterization and Crystallization of a Recombinant Human Cytosolic *β*-Glucosidase Produced in Insect Cells, *Protein. Expr. Purif.* **2007**, *52,* pp. 96–103.

(289) Turan, Y.; Zheng, M. Purification and Characterization of an Intracellular *β*-Glucosidase from the Methylotrophic Yeast *Pichia Pastoris*, *Biochem.* **2005**, *70,* pp. 1363–1368.

(290) Michlmayr, H.; Schümann, C.; Barreira Braz Da Silva, Nuno M.; Kulbe, K. D.; Del Hierro, A. M. Isolation and Basic Characterization of a *β*-Glucosidase from a Strain of *Lactobacillus Brevis* Isolated from a Malolactic Starter Culture, *J. Appl. Microbiol.* **2010**, *108,* pp. 550–559.

(291) Bell, C. W.; Fricks, B. E.; Rocca, J. D.; Steinweg, J. M.; McMahon, S. K.; Wallenstein, M. D. High-Throughput Fluorometric Measurement of Potential Soil Extracellular Enzyme Activities, *J. Vis. Exp.* **2013,** e50961.

(292) Padilla, B.; Gil, J.; Manzanares, P. Challenges of the Non-Conventional Yeast *Wickerhamomyces Anomalus* in Winemaking, *Fermentation.* **2018**, *4,* p. 68.

(293) Dourron, J.; de Ovalle, S.; González-Pombo, P.; Villarino, A.; Ramón, A.; Costábile, A. Genome Sequencing and Oenologically Relevant Traits of the Uruguayan Native Yeast *Issatchenkia Terricola*, *OENO One.* **2022**.

(294) Ruiz, J.; Ortega, N.; Martín-Santamaría, M.; Acedo, A.; Marquina, D.; Pascual, O.; Rozès, N.; Zamora, F.; Santos, A.; Belda, I. Occurrence and Enological Properties of Two New Non-Conventional Yeasts (*Nakazawaea Ishiwadae* and *Lodderomyces Elongisporus*) In Wine Fermentations, *Int. J. Food Microbiol.* **2019**, *305,* p. 108255.

(295) Ma, W.; Yu, J.; Zhang, X.; Guo, S.; Zhang, F.; Jin, W.; Dong, J.; Jia, S.; Zhong, C.; Xue, J. Whole-Genome Sequencing Exploitation Analysis of Non-Saccharomyces Yeast Nakazawaea Ishiwadae GDMCC 60786 and Its Physiological Characterizations, *Food Bioscience.* **2021**, *41,* p. 100982.

(296) Drumonde-Neves, J.; Franco-Duarte, R.; Lima, T.; Schuller, D.; Pais, C. Association Between Grape Yeast Communities and the Vineyard Ecosystems, *PloS one.* **2017**, *12,* e0169883.

(297) Jolly, N. P.; Varela, C.; Pretorius, I. S. Not Your Ordinary Yeast: Non-*Saccharomyces* Yeasts in Wine Production Uncovered, *FEMS Yeast Res.* **2014**, *14,* pp. 215–237.

(298) Kosel, J.; Raspor, P.; Čadež, N. Maximum Residue Limit of Fungicides Inhibits the Viability and Growth of Desirable Non- *Saccharomyces* Wine Yeasts, *Aust. J. Grape Wine Res.* **2019**, *25,* pp. 43–52.

(299) Seixas, I.; Barbosa, C.; Mendes-Faia, A.; Güldener, U.; Tenreiro, R.; Mendes-Ferreira, A.; Mira, N. P. Genome Sequence of the Non-Conventional Wine Yeast *Hanseniaspora Guilliermondii* UTAD222 Unveils Relevant Traits of This Species and of the *Hanseniaspora* Genus in the Context of Wine Fermentation, *DNA research : an international journal for rapid publication of reports on genes and genomes.* **2019**, *26,* pp. 67–83.

(300) Carvalho, C. C. C. R. de Whole Cell Biocatalysts: Essential Workers from Nature to the Industry, *Microb. Biotechnol.* **2017**, *10,* pp. 250–263.

(301) Ugliano, M.; Henschke, P. A. Yeasts and Wine Flavour. In *Wine Chemistry and Biochemistry;* Moreno-Arribas, M. V.; Polo, M. C., Eds.; Springer New York: New York, NY, 2009, pp. 313–392.

(302) van Wyk, N.; Pretorius, I. S.; Wallbrunn, C. von Assessing the Oenological Potential of *Nakazawaea Ishiwadae*, *Candida Railenensis* and *Debaryomyces Hansenii* Strains in Mixed-Culture Grape Must Fermentation with *Saccharomyces Cerevisiae*, *Fermentation.* **2020**, *6,* p. 49.

(303) Roncoroni, M.; Santiago, M.; Hooks, D. O.; Moroney, S.; Harsch, M. J.; Lee, S. A.; Richards, K. D.; Nicolau, L.; Gardner, R. C. The Yeast IRC7 Gene Encodes a *β*-Lyase Responsible for Production of the Varietal Thiol 4-Mercapto-4-Methylpentan-2-One in Wine, *Food Microbiol.* **2011**, *28,* pp. 926–935.

(304) Belda, I.; Ruiz, J.; Alastruey-Izquierdo, A.; Navascués, E.; Marquina, D.; Santos, A. Unraveling the Enzymatic Basis of Wine "Flavorome": A Phylo-Functional Study of Wine Related Yeast Species, *Front. Microbiol.* **2016**, *7,* p. 12.

(305) Zha, M.; Yin, S.; Sun, B.; Wang, X.; Wang, C. STR3 and CYS3 Contribute to 2-Furfurylthiol Biosynthesis in Chinese Sesame-Flavored Baijiu Yeast, *J. Agric. Food. Chem.* **2017**, *65,* pp. 5503–5511.

(306) Portnoy, V. A.; Bezdan, D.; Zengler, K. Adaptive Laboratory Evolution--Harnessing the Power of Biology for Metabolic Engineering, *Curr. Opin. Biotechnol.* **2011**, *22,* pp. 590–594.

(307) Paramasivan, K.; A, A.; Gupta, N.; Mutturi, S. Adaptive Evolution of Engineered Yeast for Squalene Production Improvement and Its Genome-Wide Analysis, *Yeast.* **2021**, *38,* pp. 424–437.

(308) Baldi, N.; Valk, S. C. de; Sousa-Silva, M.; Casal, M.; Soares-Silva, I.; Mans, R. Evolutionary Engineering Reveals Amino Acid Substitutions in Ato2 and Ato3 That Allow Improved Growth of *Saccharomyces Cerevisiae* on Lactic Acid, *FEMS Yeast Res.* **2021**, *21*.

(309) Ekberg, J.; Rautio, J.; Mattinen, L.; Vidgren, V.; Londesborough, J.; Gibson, B. R. Adaptive Evolution of the Lager Brewing Yeast *Saccharomyces Pastorianus* for Improved Growth Under Hyperosmotic Conditions and Its Influence on Fermentation Performance, *FEMS Yeast Res.* **2013**, *13,* pp. 335–349.

(310) Bonnaffoux, H.; Roland, A.; Schneider, R.; Cavelier, F. Spotlight on Release Mechanisms of Volatile Thiols in Beverages, *Food Chem.* **2021**, *339,* p. 127628.

(311) Michel, M.; Haslbeck, K.; Ampenberger, F.; Meier-Dörnberg, T.; Stretz, D.; Hutzler, M.; Coelhan, M.; Jacov, F.; Liu, Y. Screening of Brewing Yeast *β*-Lyase Activity and Release of Hop Volatile Thiols from Precursors During Fermentation, *Br. Sc.* **2019,** pp. 179–186.

(312) Dhaoui, M.; Auchère, F.; Blaiseau, P.-L.; Lesuisse, E.; Landoulsi, A.; Camadro, J.-M.; Haguenauer-Tsapis, R.; Belgareh-Touzé, N. Gex1 Is a Yeast Glutathione Exchanger That Interferes with PH and Redox Homeostasis, *Mol. Biol. Cell.* **2011**, *22,* pp. 2054–2067.

(313) Buchhaupt, M.; Guder, J. C.; Etschmann, M. M. W.; Schrader, J. Synthesis of Green Note Aroma Compounds by Biotransformation of Fatty Acids Using Yeast Cells Coexpressing Lipoxygenase and Hydroperoxide Lyase, *Appl. Microbiol. Biotechnol.* **2012**, *93,* pp. 159–168.

(314) Armstrong, R. N. Structure, Catalytic Mechanism, and Evolution of the Glutathione Transferases, *Chem. Res. Toxicol.* **1997**, *10,* pp. 2–18.

(315) Clausen, T.; Huber, R.; Laber, B.; Pohlenz, H. D.; Messerschmidt, A. Crystal Structure of the Pyridoxal-5′ -Phosphate Dependent Cystathionine *β*-Lyase from *Escherichia Coli* at 1.83 a, *J. Mol. Biol.* **1996**, *262,* pp. 202–224.

(316) Bertoldi, M.; Cellini, B.; Laurents, D. V.; Borri Voltattorni, C. Folding Pathway of the Pyridoxal 5′ -Phosphate C-S Lyase MalY from *Escherichia Coli*, *Biochem. J.* **2005**, *389,* pp. 885–898.

(317) Polona, J.; Petra, M.; Peter, R. Increased Glutathione Content in Yeast *Saccharomyces Cerevisiae* Exposed to NaCl, *Ann. Microbiol.* **2006,** pp. 175–178.

(318) Jamnik, P.; Medved, P.; Raspor, P. Increased Glutathione Content in Yeast *Saccharomyces Cerevisiae* Exposed to NaCl, *Ann. Microbiol.* **2006**, *56,* pp. 175–178.

(319) Steiger, M. G.; Patzschke, A.; Holz, C.; Lang, C.; Causon, T.; Hann, S.; Mattanovich, D.; Sauer, M. Impact of Glutathione Metabolism on Zinc Homeostasis in *Saccharomyces Cerevisiae*, *FEMS Yeast Res.* **2017**, *17*.

(320) Bourbouloux, A.; Shahi, P.; Chakladar, A.; Delrot, S.; Bachhawat, A. K. Hgt1p, a High Affinity Glutathione Transporter from the Yeast *Saccharomyces Cerevisiae*, *J. Biol. Chem.* **2000**, *275,* pp. 13259–13265.

(321) Tominaga, T.; Furrer, A.; Henry, R.; Dubourdieu, D. Identification of New Volatile Thiols in the Aroma of *Vitis Vinifera* L. Var. Sauvignon Blanc Wines, *Flavour Fragr. J.* **1998**, *13,* pp. 159–162.

(322) Mosandl, A.; Köpke, T.; Benish, W. Stereoisomeric Flavour Compounds LXII. Structure Elucidation of 8-Mercapto-P-Menthan-3-One Isomers, *Tetrahedron: Asymmetry.* **1993**, *4,* pp. 651–654.

I declare that I have completed this dissertation single-handedly without the unauthorized help of a second party and only with the assistance acknowledged therein. I have appropriately acknowledged and cited all text passages that are derived verbatim from or are based on the content of published work of others, and all information relating to verbal communications. I consent to the use of an anti-plagiarism software to check my thesis. I have abided by the principles of good scientific conduct laid down in the charter of the Justus Liebig University Giessen „Satzung der Justus-Liebig-Universität Gießen zur Sicherung guter wissenschaftlicher Praxis“ in carrying out the investigations described in the dissertation.

_____ _____

Date Felix Marcel Rainer Graf